

METHODS OF ENERGY RECOVERY IN THE IRON AND STEEL INDUSTRY:  
EVALUATION OF NEW POSSIBILITIES AND  
DESIGN STUDIES FOR SLAB COOLING

- BY -

GULCHARAN SINGH BRAINCH

A thesis submitted in fulfilment of the requirements for the degree of Doctor of Philosophy

Awarded the degree of M.Phil.

---

THE UNIVERSITY OF ASTON IN BIRMINGHAM

JANUARY 1980

17 NOV 1980

271148

THESIS  
669.1  
BRA



# GULCHARAN SINGH BRAINCH

M.PHIL. THESIS

1980

## SUMMARY

The world energy crisis was brought to a head by the formation of the oil cartel (OPEC) and its collective action in 1973/1974 to quadruple oil prices. The days of cheap and abundant energy sources came to an abrupt end. The immediate energy crisis was absorbed by the strong economies of the major energy consumers, hence the ever-increasing demand for non-renewable energy resources continues almost unabated.

In contrast to most manufacturing industry, the direct energy costs of material manufacturers are a significant proportion of their total production costs. Therefore, in the forefront of the list of priorities at the British Steel Corporation was to consider and evaluate every possible method of reducing its energy bill. The present study was initiated to review the present state-of-the-art in the energy recovery equipment field and to evaluate new areas and novel techniques for the British Steel Corporation.

A breakdown of energy usage and losses for an integrated iron and steel works was obtained. The possible areas for future energy recovery are highlighted. The existing energy recovery methods are briefly discussed and their advantages and disadvantages listed. New developments, currently under investigation in the UK and overseas iron and steel industry are considered and their advantages and disadvantages discussed.

Three methods of using fluidisation for recovering energy from gaseous combustion products are evaluated and their potential mathematically assessed. Of the three methods considered, the falling-cloud heat exchanger offers promise for the iron and steel industry and is recommended for further in-depth consideration. A procedure for the selection of a refrigerant for use in low temperature turbines was thoroughly examined. The final choice was between R-114 and R-11 and on the basis of relative costs R-11 was selected. The advantages of the refrigerant turbine and a possible application and potential saving are discussed.

A source of high grade thermal energy, currently wasted, is highlighted. Steel ingots are soaked at a high temperature in soaking pits and then passed through primary rolling mills and formed into slabs at a temperature in excess of 1000°C. Due to production scheduling difficulties and the need to examine its surface for imperfections i.e. impurities, slag, cracks, etc., the slabs are cooled to ambient conditions prior to finishing processes.

A technique for energy recovery from slabs to raise steam for power generation or process use was mathematically evaluated. Then an experimental model was designed and built to verify the theoretical model. The results are encouraging and a preliminary study concludes that a potential investment of £3M is justified on the basis of 1975 production rates and costs at Llanwern iron and steel works. (Note: In 1975 soaking pits and rolling mills were working at below 50% of their full capacity).

ENERGY RECOVERY

FLUIDISATION

SLAB COOLING

LOW TEMPERATURE TURBINES

ECONOMIC ASSESSMENT

## ACKNOWLEDGEMENTS

The author wishes to express his gratitude and sincere thanks to the following:

The members of the supervisory team, Mr. D.C. Hickson, Dr. D.R. Dugwell, Mr. S.A. Gregory and Mr. G.A. Montgomerie, particularly Mr. Hickson for his help, enthusiasm, encouragement and many hours spent reading drafts.

British Steel Corporation, his employer, and the Science Research Council for financial support.

The staff of the Department of Mechanical Engineering, particularly Mr. N. Moss for his help with the experimental rig and experiments.

GEC Gas Turbines Limited for the use of their typing and Xerox copying facilities.

Last by no means least Chris Bakewell for diligently typing this thesis.



# CONTENTS

PAGE  
NUMBER

SUMMARY	I
ACKNOWLEDGEMENTS	II
LIST OF TABLES	VI
LIST OF FIGURES	VII
NOMENCLATURE	XI
CHAPTER 1	INTRODUCTION
	1
1.1	Introduction
	2
1.2	The energy crisis and its implication
	3
1.3	UK energy situation
	7
1.4	Energy and the British iron and steel industry
	8
1.5	Energy uses/losses in an integrated iron and steelworks
	10
1.6	Characteristics of flue gases
	13
1.7	Methods of energy recovery
	15
FIGURES	18-27
CHAPTER 2	ENERGY RECOVERY : EXISTING METHODS
	28
2.1	Waste-heat boilers
	29
2.2	Fixed regenerators
	29
2.3	Ceramic recuperators
	32
2.4	Metallic recuperators
	35
2.4.1	Convective recuperators
	36
	(A) Cast tubular
	36
	(B) Multi-tube steel
	37
	(C) Hazen metallic
	38
2.4.2	Radiative recuperators
	39
FIGURES	41-55
CHAPTER 3	ENERGY RECOVERY : NEW DEVELOPMENTS
	56
3.1	Ceramic recuperator
	57
3.2	Rotary regenerator
	60
3.3	Evaporative cooling of blast furnace
	62
3.4	Dry-coke quenching
	66
FIGURES	67-75
CHAPTER 4	ENERGY RECOVERY : NOVEL TECHNIQUES
	76
4.1	Fluidised bed recuperator
	77
4.2	Fluidised bed regenerator
	78
4.2.1	Fluidised bed regenerator - first type
	79
4.2.2	Fluidised bed regenerator - second type
	82
4.3	Refrigerant turbine cycle
	86
4.3.1	Application of refrigerant turbine to recover energy from blast furnace stoves No. 1,2,3,4 and 5 at Port Talbot works
	89
4.3.2	Conclusions and recommendations
	90
FIGURES	91-100

# CONTENTS

(Continued)

	<u>PAGE NUMBER</u>	
CHAPTER 5	THEORETICAL AND ECONOMIC FEASIBILITY OF SLAB COOLING	101
5.1	Introduction	102
5.2	Hot slab details	103
5.3	The energy recovery system	104
5.4	Criteria for optimisation of slab cooling system	106
5.5	Capital investment appraisal	107
5.6	Heat exchanger design - assumptions	108
5.7	Discussion and results	109
5.8	Conclusions of preliminary theoretical study	112
FIGURES		113-118
CHAPTER 6	DESIGN OF AN EXPERIMENTAL RIG FOR SLAB COOLING	119
6.1	Plate heaters	120
6.2	Heat exchanger	121
6.3	Selection of heating elements	122
6.4	Convective vs radiative heat transfer	123
FIGURES		124-134
CHAPTER 7	RESULTS AND DISCUSSION ON SLAB COOLING	135
7.1	Water flow measurements	136
7.2	Heat exchanger cooling calculations	138
7.3	Air cooling of a plate heater	140
7.4	Results and discussion on energy recovery	141
FIGURES		150-165
CHAPTER 8	CONCLUSIONS AND RECOMMENDATIONS	166
8.1	Conclusions and recommendations on slab cooling	167
8.2	General conclusions	168

## APPENDICES

	<u>PAGE NUMBER</u>
APPENDIX I      FLUID BEDS AND HEAT PIPE	170
I.1      Fluidised beds	171
I.1.1      Fluidisation technique	171
I.1.2      Verification of assumption 1 in fluidised bed regenerator	176
I.1.3      Mathematical model of multi-stage fluidised bed regenerator	178
I.2      Heat pipe	181
FIGURES	183-199
APPENDIX II     SLAB COOLING - THERMAL DESIGN	200
II.1     One dimensional transient conduction with cooling at surface by radiation and convection	201
II.2     Heat transfer : general equations	202
II.2.1     Natural convection : vertical plate	202
II.2.2     Free convection in enclosed spaces between vertical walls	202
II.3     Simulated heat exchanger	203
FIGURE	204
APPENDIX III    TABLES OF DATA	205
APPENDIX IV     REFERENCES	221



## LIST OF TABLES

TABLE 1	Pressure drop across a 6.35 mm ID x 0.9 m plain copper tube
TABLE 2	Pressure drop across a 6.35 mm ID x 1.0 m formed copper tube
TABLE 3	Flow distribution in the heat exchanger
TABLE 4	Heat losses from the water circuit with heating load = 2 kW and overall water rate of 30 litres per minute
TABLE 5	Atmospheric cooling of a plate heater with all sides insulated using 76 mm thick refractory
TABLE 6	Energy recovery data with both heaters 'on' using a 100 mm spacer and no reflector
TABLE 7	Energy recovery data with both heaters 'on' using a 100 mm spacer and a reflector leaving 24.5 mm gap at top and bottom
TABLE 8	Energy recovery data using 100 mm spacers and no reflectors
TABLE 9	Energy recovery data using 100 mm spacers and no reflectors
TABLE 10	Energy recovery data using 100 mm spacers and reflectors leaving 38 mm gap at top and bottom
TABLE 11	Energy recovery data using 100 mm spacers and reflectors leaving 25.4 mm gap at top and bottom
TABLE 12	Energy recovery data using 100 mm spacers and leaving 19 mm gap at top and bottom
TABLE 13	Energy recovery data using 100 mm spacers and reflectors leaving 12.7 mm gap at top and bottom



## LIST OF TABLES

TABLE 1	Pressure drop across a 6.35 mm ID x 0.9 m plain copper tube
TABLE 2	Pressure drop across a 6.35 mm ID x 1.0 m formed copper tube
TABLE 3	Flow distribution in the heat exchanger
TABLE 4	Heat losses from the water circuit with heating load = 2 kW and overall water rate of 30 litres per minute
TABLE 5	Atmospheric cooling of a plate heater with all sides insulated using 76 mm thick refractory
TABLE 6	Energy recovery data with both heaters 'on' using a 100 mm spacer and no reflector
TABLE 7	Energy recovery data with both heaters 'on' using a 100 mm spacer and a reflector leaving 24.5 mm gap at top and bottom
TABLE 8	Energy recovery data using 100 mm spacers and no reflectors
TABLE 9	Energy recovery data using 100 mm spacers and no reflectors
TABLE 10	Energy recovery data using 100 mm spacers and reflectors leaving 38 mm gap at top and bottom
TABLE 11	Energy recovery data using 100 mm spacers and reflectors leaving 25.4 mm gap at top and bottom
TABLE 12	Energy recovery data using 100 mm spacers and leaving 19 mm gap at top and bottom
TABLE 13	Energy recovery data using 100 mm spacers and reflectors leaving 12.7 mm gap at top and bottom

## LIST OF FIGURES

- FIGURE 1.1 World energy consumption
- FIGURE 1.2 World energy reserves
- FIGURE 1.3 World energy consumption by source
- FIGURE 1.4 UK energy consumption by source
- FIGURE 1.5 Metallic content of home and foreign iron ore
- FIGURE 1.6 Trends in iron ore consumption
- FIGURE 1.7 Fuel substitution in iron and steelmaking
- FIGURE 1.8 Overall energy diagram for an iron and steelworks
- FIGURE 1.9 Energy use/loss in an integrated iron and steelworks
- FIGURE 1.10 Overall energy flow diagram for an integrated iron and steelworks
- 
- FIGURE 2.1 UK steel production by process
- FIGURE 2.2 Number and type of steel furnaces in use in UK
- FIGURE 2.3 Temperature cycle of surface of regenerator brick
- FIGURE 2.4 Various designs of tile recuperators
- FIGURE 2.5 Short tube recuperator designs
- FIGURE 2.6 Gas Council recuperator construction
- FIGURE 2.7 Stookey recuperator
- FIGURE 2.8 Lackenby Works ceramic recuperator
- FIGURE 2.9 Typical cast tube recuperator
- FIGURE 2.10 Pendant tube recuperator
- FIGURE 2.11 Flue tube recuperator
- FIGURE 2.12 A guide to heat resisting ferrous alloys
- FIGURE 2.13 Tube construction for Hazen recuperator
- FIGURE 2.14 A typical layout of Hazen recuperator
- FIGURE 2.15 Radiation recuperator
- FIGURE 2.16 Combined convection and radiation recuperator
- 
- FIGURE 3.1 Installation of prototype cel ceramic recuperator at Llanwern
- FIGURE 3.2 A cross-section view of ceramic recuperator
- FIGURE 3.3 Ceramic cruciform insert
- FIGURE 3.4 Leakage into waste gas v. measured inlet fan flow
- FIGURE 3.5 Types of rotary regenerators



## LIST OF FIGURES

(Continued)

- FIGURE 3.6 A typical metallic rotary regenerator
- FIGURE 3.7 The rotor assembly of CEL ceramic rotary regenerator
- FIGURE 3.8 Comparison of blast furnace cooling systems
- FIGURE 3.9 Typical evaporative-cooling cooler
- FIGURE 3.10 Giprokoks dry-cooling system (Typical working data)
- 
- FIGURE 4.1 Fluidised-bed recuperator
- FIGURE 4.2 (a) Fluidised-bed regenerator - first type  
(b) Fluidised-bed regenerator - second type
- FIGURE 4.3 Moving bed regenerator designs
- FIGURE 4.4 Multi-stage fluidised-bed regenerator with turbo-generator
- FIGURE 4.5 Combined cycle gas-fired turbine (for gas compressor use)
- FIGURE 4.6 List of refrigerants considered for power turbine cycle
- FIGURE 4.7 Critical thermodynamic properties of refrigerants R-11, R-113 and R-114
- FIGURE 4.8 Rankine cycle on P-H chart of R-113
- FIGURE 4.9 Rankine thermal efficiency up to critical pressure for R11, R113 and R114
- FIGURE 4.10 Specific enthalpy of vapourisation at constant pressure for R11, R113 and R114
- 
- FIGURE 5.1 Slab production data for week ending 19.12.75 at Llawern iron and steel works
- FIGURE 5.2 An arrangement for slab cooling
- FIGURE 5.3 Three modes of heat transfer in slab cooling
- FIGURE 5.4 Slab cooling with cold surface at 300 C
- FIGURE 5.5 Slab cooling with cold surface at 500 C
- FIGURE 5.6 Economic investment in slab cooling with 5% maintenance cost
- FIGURE 5.7 Economic investment in slab cooling with 10% maintenance cost
- 
- FIGURE 6.1 Photograph showing overall layout of slab cooling experimental rig
- FIGURE 6.2 Steam/water separating technique
- FIGURE 6.3 (a) Plate heater (side elevation)  
(b) Plate heater (front elevation)

## LIST OF FIGURES

(Continued)

- FIGURE 6.4 Photograph of base of a plate heater showing details of silit heating elements
- FIGURE 6.5 Photograph of rear of a mild steel plate with embedded thermocouples
- FIGURE 6.6(a) Photograph showing details of the heat exchanger and measuring devices
- (b) Photograph of the steam drum
- FIGURE 6.7 Pictorial diagram of the water circuit
- FIGURE 6.8 Photograph showing two flow selector switches for flow distribution measurement
- FIGURE 6.9 Inverted U-tube manometer shown in upright position
- 
- FIGURE 7.1 Pressure drop across a 1m long copper tube (similar to those used in the heat exchanger)
- FIGURE 7.2 Water flow distribution in the heat exchanger
- FIGURE 7.3 Comparison of measured and calculated overall water flow rates
- FIGURE 7.4 Heat losses via natural convection from cooling system
- FIGURE 7.5 Air cooling of a plate heater with all sides insulated using 76 mm thick refractory
- FIGURE 7.6 Energy recovery with both heaters and no reflectors
- FIGURE 7.7 Energy recovery with both heaters and air gap width of 25.4 mm
- FIGURE 7.8 Energy recovery with both heaters and no reflectors
- FIGURE 7.9 Energy recovery with both heaters and air gap width of 38 mm
- FIGURE 7.10 Energy recovery with both heaters and air gap width of 25.4 mm
- FIGURE 7.11 Energy recovery with both heaters and air gap width of 19 mm
- FIGURE 7.12 Energy recovery with both heaters and air gap width of 12.7 mm
- FIGURE 7.13 Correlations of energy recovery system and evaluation of emissivity x view factor ( $\epsilon.F$ )
- FIGURE 7.14 Variation of emissivity x view factor with air gap width



## LIST OF FIGURES

(Continued)

- FIGURE 7.15 Representation of radiative heat transfer in slab cooling
- FIGURE 7.16 Diagrammatic representation of slab cooling
- FIGURE I.1 Typical relationship between heat transfer coefficient and gas velocity
- FIGURE I.2 Fluid-bed composition in terms of particle residence time
- FIGURE I.3 Percentage of particles with residence time  $t < 100\Delta t$  for various flow rates
- FIGURE I.4 Heat transfer characteristics - mild steel particles fluidised at air mass velocity :  $0.35 \text{ kg/m}^2\text{s}$
- FIGURE I.5 Heating characteristics of mild steel particles with air temp :  $800^\circ\text{C}$  and mass vel:  $0.35 \text{ kg/m}^2\text{s}$
- FIGURE I.6 Minimum residence time to reach temperature, T
- FIGURE I.7 Fluidised-bed composition in terms of particle temperature (where mass flow rate is 1% of total mass in bed)
- FIGURE I.8 Fluidised-bed composition in terms of particle temperature (where mass flow rate is 10% of total mass in bed)
- FIGURE I.9 Block diagram of multi-stage fluidised-bed regenerator
- FIGURE I.10 Air preheat chart fluidised-bed regenerator  $[R_A = R_B]$
- FIGURE I.11 Air preheat chart for fluidised-bed regenerator  $[R_A = 2R_B]$
- FIGURE I.12 Single stage fluidised-bed regenerator-effect of ratio of  $R_A : R_B$
- FIGURE I.13 Prediction of maximum air preheat for a multi-stage fluidised-bed regenerator ( $T_{gi} = 1200^\circ\text{C}$ )
- FIGURE I.14 Pressure distribution around fluidised-bed system
- FIGURE I.15 Heat pipe operation envelope
- FIGURE I.16 Fluid characteristics for heat pipe applications
- FIGURE I.17  $\dot{Q}$ -Dot heat exchanger and its application
- FIGURE II.1 Mathematical model for slab cooling

## NOMENCLATURE

SYMBOL	DESCRIPTION	UNITS
A	Fluidised bed area in equation (5) Appendix I	(m <sup>2</sup> )
A	Heat transfer surface area	(m <sup>2</sup> )
A <sub>he</sub>	Heat exchanger surface area	(m <sup>2</sup> )
Ar	Archimedes number $\left[ = \frac{\rho_g \cdot dp^3 g}{\mu^2} \right]$	(dimensionless)
Bi	Biot number $\left[ = \frac{h \cdot \Delta x}{k_m} \right]$	(dimensionless)
C	A constant in section II.2.1	
Cl	Present consumption rate per annum in Chapter 1	(energy units)
C <sub>1</sub>	A constant in Chapter 7	
C <sub>nr</sub>	Consumption rate in year n given r	(energy units)
C <sub>p</sub>	Specific heat at constant pressure	(J/kg k)
C <sub>R</sub>	A constant factor in equation (9) Appendix I	
C <sub>v</sub>	Specific heat at constant volume	(J/kg k)
D	Distance between hot plate and cooling surface in Appendix II and Chapter 7	(m)
dp	Particle diameter	(m)
d <sub>t</sub>	Tube diameter in equation (8) Appendix I	(m)
F	View factor in Appendix II and Chapter 7	(dimensionless)
Fo	Fourier number $\left[ = \frac{\alpha \Delta t}{\Delta x^2} \right]$	(dimensionless)
g	Gravitational acceleration constant (= 9.81 m/s <sup>2</sup> )	
Gr	Grashoff number $\left[ = \frac{\ell^3 \rho^2 g \beta \Delta T}{\mu^2} \right]$	(dimensionless)
h	Convective heat transfer coefficient	(W/m <sup>2</sup> K)
hm	Mean heat transfer coefficient	(W/m <sup>2</sup> K)
k	Thermal conductivity	(W/m K)
ke	Effective thermal conductivity in Appendix II	(W/m K)
k <sub>m</sub>	Material thermal conductivity	(W/m K)
L	Semi-thickness of a slab in Appendix II	(m)



# NOMENCLATURE

(Continued)

SYMBOL	DESCRIPTION	UNITS
L	Fluidised bed height	(m)
$l$	Plate height	(m)
M	Total mass of water in the water circuit	(kg)
m	Index in Section II.2.1	
$\dot{m}$	Mass flow rate	(kg/s)
n	Number of particles flowing into fluid bed per unit time interval, $\Delta t$	
$N_0$	Total number of particles in fluid bed	
NCl	Supply period @ a constant consumption rate of Cl	
Nr	Supply period in years given TR	
Nu	Nusselt number $\left( = \frac{hd}{k} \right)$	(dimensionless)
P	$= \sigma \epsilon F \frac{\Delta x}{k_m}$ in equation (2) Appendix II	
Pr	Prandtl number $\left( = \frac{C_p \mu}{k} \right)$	(dimensionless)
$\Delta P$	Pressure difference	(Pa)
$P_1$	Atmospheric pressure	(Pa)
$P_2$	Supply pressure to a fluidised bed	(Pa)
q	Rate of thermal energy transfer in Appendix II	(W)
r	Growth rate per annum in Chapter I, re-radiative surface	
R	Ratio of mass capacities	(dimensionless)
Re	Reynolds number $\left( = \frac{\rho \cdot u d}{\mu} \right)$	(dimensionless)
$\Delta T$	Temperature difference	(K)
T	Temperature	(K)
$T_f$	Mean temperature in equations (3) and (4) Appendix II	(K)
$\Delta T_w$	Water temperature rise in $\Delta t$	(K)
t	Time elapsed	(s)
$\Delta t$	Time interval	(s)
$T^1$	New temperature in Appendix II	(K)

# NOMENCLATURE

(Continued)

SYMBOL	DESCRIPTION	UNITS
$T_{AB}$	Temperature of solid particles between bed A and bed B	(K)
$T_C$	Cooling surface temperature in Appendix II	(K)
$T_p$	Plate temperature in Appendix II and Chapter 7	(K)
TR	Total reserves	(energy units)
$T_s$	Surface temperature in II.2.1	(K)
$T_\infty$	Ambient temperature	(K)
U	Velocity	(m/s)
$V_2$	Volumetric flow rate at pressure $P_2$	(m <sup>3</sup> /s)
W	Weight of fluidised particles	(N)
$W_{sa}$	Actual power requirement for fluidisation	(W)
$W_{si}$	Ideal power requirement for fluidisation	(W)
X	= $1 - n/(N_0 + n)$ in equation (16) Appendix I	
$\Delta x$	Elemental thickness	(m)
$\gamma$	Gap in radiation shield	(m)
$\alpha$	Thermal diffusivity $\left( = \frac{k}{\rho C_p} \right)$	(dimensionless)
$\gamma$	Ratio of specific heats $(= C_p/C_v)$	(dimensionless)
$\epsilon$	Void fraction in Appendix I	(dimensionless)
$\epsilon$	Radiative emissivity in Chapter 7 and Appendix II	(dimensionless)
$\epsilon$	Effectiveness of fluid bed regenerator	
$\epsilon_{A1}$	New effectiveness of fluid bed A	
$\epsilon_{B1}$	New effectiveness of fluid bed B	
$\epsilon_f$	Voidage fraction in a fluid bed as a whole	
$\eta$	Pumping efficiency in equation (29) Appendix I	(dimensionless)
$\theta$	Water temperature above ambient in Chapter 7	(K)
$\theta$	Temperature difference between fluidising gas and bed	(K)

## NOMENCLATURE

(Continued)

SYMBOL	DESCRIPTION	UNITS
$\mu$	Viscosity of gas	(kg/ms)
$\rho$	Mass density	(kg/m <sup>3</sup> )
$\sigma$	Stefan - Boltzmann constant	(dimensionless)
$\beta$	Reciprocal of ambient temperature (= 1/T)	(K)

### SUBSCRIPTS

a	refers to air
A	refers to bed A in Appendix I
B	refers to bed B in Appendix I
c	refers to cold surface
f	refers to fluidised state, film
g	refers to gas
i	inlet conditions
m	mean conditions, solid material
mf	minimum fluidisation condition
n	refers to nth element
o	exit conditions
p	refers to solid particles, hot plate
s	refers to solids
t	terminal condition, tubes
tb	refers to top and bottom surfaces
v	refers to vertical surfaces
w	refers to water
$\infty$	refers to bulk fluid



CHAPTER 1  
INTRODUCTION

## 1.1 Introduction

The iron and steel industry consumes over nine per cent of the total United Kingdom <sup>primary</sup> energy consumption [Digest of UK Energy Statistics, 1976]. The British Steel Corporation, representing over ninety per cent of the British iron and steel industry, is the largest single consumer of energy next to the Central Electricity Generating Board (CEGB). Hence its operation is greatly influenced by changes in energy price and availability for, in common with other metal manufacturers, over twenty per cent of total product cost is directly attributable to its energy input [Laws, (1974)]. Therefore BSC has been aware of its dependence on energy and has continuously strived to attain the maximum efficiency in its utilisation to reduce cost.

The forecast of the impending energy crisis during the early part of the 1970's significantly influenced BSC's decision to increase the number of research personnel deployed in improving the energy utilisation factor (EUF = energy consumed per tonne of steel produced and for given quality of ore and steel).

The present study reviews the applied and new developments in thermal energy recovery in the iron and steel industry. It also analyses novel techniques both technically and economically. Its initiation in 1974 was in response to the prevailing energy situation. This is a Total Technology project where the optimum requirement is to investigate an area of research of interest to the industry. Towards meeting this aim, the present study seeks to define novel techniques of interest and how these can be successfully employed in meeting the requirements of the iron and steel industry. Also a theoretical and experimental study of steel slab cooling systems was conducted to investigate its potential for reducing the energy requirements of the iron and steel industry.

Before discussing the effects of the energy crisis on the British Steel Corporation and the economics of energy recovery from areas hitherto unexplored, a brief look at the worldwide implications of the energy crisis is presented. Also an explanation of the present predicament attempts to remedy any misconception regarding the energy crisis.

## 1.2 The energy crisis and its implication

An energy crisis was foreseen by some prior to 1974 [Mayer (1970)], but was not generally realised until after the crude oil price was quadrupled by the Organisation of Petroleum Exporting Countries (OPEC). This in itself caused a strong link between the energy crisis and OPEC action. Hence, once the inevitability of higher oil prices was accepted, the threat of an energy crisis was presumed to be abated, yet the energy experts remained adamant in their prediction of energy doom.

This highly undesirable state of affairs arose due to the adoption of an emotive term 'crisis', which under normal circumstances implies that emergency corrective procedures are required. 'Energy crisis' is a classic example of how a misnomer, to represent a well-thought-out idea, can lead to its ruin. The energy crisis of 1973/74 was followed by the enactment of harsh short-term measures by the Government. The eventual restoration of oil supplies, lifting of oil embargoes and subsequent abandonment of Government measures led to the resumption of the pre-crisis situation. What the public at large failed to observe was that there was a crisis within a crisis. Although the threat caused by the former was to an extent absorbed by the economy of industrialised nations, the latter remains intact.

The factors which led to the prediction of an energy crisis are listed below. And it is these factors which require examination before concluding the existence or non-existence of the crisis.



1. Exponentially expanding world energy consumption
2. The increasing use of non-renewable (during human life-cycle) energy resources
3. The growing concern for environmental consequences of 1.
4. The alarming rate of growth in population

The realisation of these factors coupled with the formation of the OPEC oil cartel brought an abrupt end to the era of abundant and cheap energy.

The world energy consumption (Figure 1.1) has been rising steadily for the last one-quarter of a century at the rate of five per cent per annum. This is equivalent to the doubling of annual energy consumption every fourteen years.

Figure 1.2 shows the total reserves of coal, crude oil, natural gas and uranium. It also shows the supply period for each fuel with due allowance for annual increase as per 1969-1973.

Figure 1.3 shows that, despite large reserves of coal compared with other fuels, there has been a consistent and growing trend away from coal. This move from coal to oil and natural gas has brought about the possibility of earlier exhaustion of energy resources. The intrinsic advantages of oil and natural gas, which are on the whole cheap sources of energy, played a major role in bringing about this dramatic substitution. Lately the awareness of environmental impacts of exponentially rising energy consumption has manifestly altered the criteria for the selection of a fuel for a given purpose. The inherent disadvantages and unattractiveness of coal extraction together with non-availability of low-sulphur coal has accelerated the above trend. Public protests have led to the enactment of legislations to stringently control processes that exhaust harmful effluents. This has further reduced economic coal reserves. Unless higher fuel price differentials are introduced to encourage industry to use coal in place of oil and

natural gas the aforementioned trend will continue to worsen. The final exhaustion of the latter energy sources and subsequent return to coal will cause catastrophic environmental impacts.

Some observers [Stoker et al (1975)] forecast that the annual growth in energy consumption will reduce to around one per cent as a direct result of current awareness and the anticipated continual rise in price of dwindling energy resources. However this appears highly optimistic and wishful thinking. The above estimate can only be realised if the major energy consuming nations maintained or even decreased their present levels of energy intake. To what extent this can be achieved remains highly speculative, as the major energy consumers are also the largest shareholders of the world's economic wealth, As such they are unlikely to relinquish their high standard of living, yet the developing countries will suffer most under the present politico-economic system since they are greatly affected by a rise in fuel price and are more likely to be priced out of the market.

When the above observations are linked with the time-scale for major new and complex developments (e.g. in excess of fifty years) the prediction of a major energy crisis becomes almost a reality. The panacea for it is seen as the fast breeder reactor (FBR). The complex nature of FBR and the anticipated major development programme will require expenditure of substantial amounts of energy, manpower and capital resources. Unless positive steps are taken NOW, the FBR may end up as a 'white elephant' of no avail and with insufficient energy for its completion [Chapman (1975)]. To guard against this possibility, efforts should be concentrated to harness renewable energy resources e.g. solar radiation and its derivatives (i.e. ocean waves, wind and hydro-power), tidal waves and geothermal energy.

All of the above factors have brought the realisation of the imminent end of known and anticipated energy resources. In conclusion



the significant question is not whether there is an energy crisis but how to resolve it.

The final decision inevitably rests with the politicians or whoever controls the resources. A comprehensive range of literature is available on the merits of each but their discussion falls outside the scope of this study.

### Special note

Many observers fall into the trap of ascertaining the supply period, using current rates of consumption. The failure to make necessary adjustments for annual growth in consumption leads to an inflated conclusion. However this situation can be rectified by the use of the equations listed below.

Given that:

- r - growth rate per annum (current or assumed),
  - C1 - present consumption rate per annum,
  - Cnr - consumption rate in year n given r,
  - Nr - supply period in years given TR
- and TR - total reserves

$$Cnr = \sum_{n=1}^{Nr} C1 (1+r)^{n-1} \quad (1)$$

$$\begin{aligned} \therefore TR &= \sum_{n=1}^{Nr} C1 (1+r)^{n-1} \\ &= \frac{C1}{r} ((1+r)^{Nr} - 1) \end{aligned} \quad (2)$$

Let  $TR/C1 = NC1$ : supply period @ constant consumption rate = C1

Re-arranging for Nr,

$$Nr = \log (NC1 \cdot r + 1) / \log (1 + r) \quad (3)$$

for  $r = 0$ ,  $Nr = TR/C1 = NC1$

When the total reserves are discounted in this way, a completely different and perhaps an alarming picture emerges as illustrated in the last column of FIGURE 1.2.

### 1.3 UK energy situation

As explained earlier, the overwhelming inherent and economic advantages of oil and natural gas led to their substitution for coal during the 1950's and 1970's respectively. Successive UK governments imposed taxation on cheap imported oil to ensure the survival of the indigenous coal industry and to supplement its revenue. However, despite these measures the consumption of imported oil continued to increase. The considerable reliance on imported oil implied that the economic prosperity of UK, in common with other European countries, was and still is dependent on the ever changing temperament of its oil suppliers. The awareness of this point amongst OPEC nations led to the formation of an oil cartel which eventually resulted in the 'mini' energy crisis of 1973/74.

The arrival in UK of North Sea gas in 1967 (during the era of abundant and cheap energy) caused severe competition amongst energy suppliers. To promote the sale of North Sea gas, the Gas Boards were far too eager to enter into long-term contracts at constant and highly competitive prices. The capital expenditure necessary for equipment conversion to North Sea gas was highly economic even within the lifetime of the contracts, usually between three and five years. This led to a rapid increase in the use of natural gas. The UK energy consumption by source for years 1950, 1960, 1970 and 1975 is given in Figure 1.4. The trend towards oil and natural gas is clearly illustrated. However this trend may be reversed as coal mining becomes economically more attractive with each rise in oil price and when oil and natural gas are scarce.



The prospects for the UK as presented by North Sea gas and oil comes as a welcome relief, particularly during the present economic difficulties. Although the future remains uncertain, short term advantages of indigenous oil and gas and their influence on UK economy are highly desirable. Given that the known and anticipated reserves of North Sea gas and oil are fully realised the UK expects to be self-supporting, if not a net exporter of energy from 1985 to 1995 [Parker (1975)]. The depletion of indigenous resources of energy beyond this period is anticipated to be just as dramatic as its rise. Therefore the efforts to find new and viable alternative sources of energy should continue unhindered and even stepped-up to ensure their success.

#### 1.4 Energy and the British iron and steel industry

The economic survival of every industry depends upon the existence of a market for its products and the availability of raw materials for their manufacture. Energy is a raw material common to all industries, therefore industrial survival depends on its availability. On average, energy cost contributes between 3 and 4 per cent of the total cost of manufactured product. However, metal manufacturing industries are the exception. In the iron and steel industry between 20 and 25 per cent of the total cost is directly attributable to energy. Therefore, to reduce costs the British Steel Corporation has continuously researched into ways and means of improving its energy utilisation factor. Major policy decisions and concentrated research effort has enabled BSC to reduce its energy requirements per tonne of crude steel from 34.2 GJ in 1960 to under 25 GJ in 1974 [Laws (1974) and McChesney (1974)].

This considerable success in reducing energy requirement is owed to many factors, some of which are listed below.

- (a) The increasing use of high grade imported iron ore
- (b) The rationalisation of iron and steelworks

- (c) The substitution of oil and natural gas for coal, particularly in non-coking uses
- (d) The improvements in Blast Furnace technology
- (e) The phasing-out of open-hearth furnaces in favour of basic oxygen steelmaking (BOS)
- (f) The improvements and new developments in energy recovery techniques

On average, imported iron ore has 62 per cent metallic content compared with 28 per cent in domestic iron ore. The trend towards the use of higher grade imported iron ore has been dramatic over the past few years. Both trends are illustrated by Figures 1.5 and 1.6. However the desire to decrease dependency on imported raw materials has led to the initiation of research programmes to develop a process or processes that would at least partially replace blast furnaces as the source of iron for steelmaking. These are referred to as the Direct-Reduction processes [Szekely (1972)] and their functions are one of the following:

1. produce steel directly from iron ore
2. make a product equivalent to blast furnace pig iron for use in existing steelmaking processes
3. produce low-carbon iron as a melting stock (sometimes referred to as synthetic scrap) for making steel in existing processes

In spite of extensive efforts, no commercially available direct-reduction process has been developed which promises to replace the blast-furnace on a large scale although a number of small units are operating, or under construction, in Mexico, New Zealand, Korea, Yugoslavia and other countries. The rationalisation into major iron and steel complexes at Llanwern, Appleby-Frodingham, South Teeside and Ravenscraig has enabled BSC to considerably reduce its labour and energy requirements. However phasing-out of obsolescent open-hearth



furnaces is proving to be a slow and tedious operation, particularly due to the present economic and unemployment situation. Political pressure to retain and continue production at inefficient plants, hence avoiding mass redundancies in high unemployment areas, has had the effect, contrary to BSC policy, of keeping energy consumption at high levels. Lately, BSC policy has begun to be accepted.

The pattern of fuel consumption in the iron and steel industry has changed significantly and is shown in Figure 1.7. The complete substitution of non-coking coal by other energy sources is clearly evident. But the use of metallurgical coke has remained the dominant source of energy because of its dual function as a chemical reactant and a source of energy.

Finally, numerous improvements in blast furnace technology [Szekely (1972)] have been developed and partially implemented to increase production rate, to improve energy utilisation and to reduce labour requirements, some are listed here.

- (a) Beneficiation of blast furnace burdens
- (b) Higher hot blast temperatures
- (c) Improved coke and sinter production
- (d) Tuyere-fuel injection and oxygen enrichment of the blast
- (e) Economy of scale
- (f) Improved refractory linings
- (g) Operating at higher top pressure
- (h) Improved instrumentation and the use of computer control

Existing and new developments in energy recovery techniques are discussed in detail in Chapters 2 and 3 respectively.

## 1.5 Energy uses/losses in an integrated iron and steelworks

In general the iron and steel industry uses energy to raise materials to temperatures suitable for chemical reactions to take place

and to permit mechanical working. Thring (1952) noted that there are three stages in industrial process development, particularly in material manufacture.

1. The manufacture of material is the primary objective in all stages. In the first stage the objective is attained without process optimisation and without any regard for energy or other inputs. Therefore the term 'thermal efficiency' has no meaning at this primitive level of thinking.
2. The process itself remains unquestioned. However the need to minimise energy input causes the formulation of thermal efficiency. No consideration is given to energy recovery. Hence thermal efficiency is defined as the ratio of the minimum energy required and the energy used to complete a given process.

The minimum energy requirement is considered to be the sum of energy inputs per process. This assumes that the process used is the only method of achieving the desired product.

3. The whole problem is re-examined, the objective is to achieve the desired effect with a minimum of energy expenditure and with due consideration of initial and terminal conditions. Therefore in material manufacture the minimum energy requirement is considered to be the energy required for endothermic less exothermic reactions, in addition to any difference in initial and final energy levels of raw and finished products respectively.

Two examples of processes where three stages are apparent are gas and coke making and manufacture of refractories. However despite considerable improvements in energy consumption associated with stage three, these industries are spread across all of the stages. The iron and steel industry has recently progressed to the third stage but the bulk of the processes still remain in the second stage. The integration of iron



and steelworks together with the introduction of basic oxygen steel-making and continuous casting lends itself to stage three. However the thermal energy of solids remains unrecovered and an obstacle in the path of achieving minimum energy consumption.

The British Steel Corporation which represents over 90 per cent of the British iron and steel industry consumes over 9 per cent of the total UK energy consumption. Figure 1.8 shows that only 30 per cent of its energy requirements are directly attributable to chemical reduction of iron ore. Most high grade thermal energy losses occur in the form of hot combustion products, so BSC has concentrated its research efforts in this sector. Despite this it has remained the major area of energy wastage.

The breakdown of energy uses and losses in an integrated iron and steelworks is shown in Figure 1.9. This is better represented by Figure 1.10 which combine individual processes into a single unit. Leaving aside the outgoings which are currently usefully employed and are produced for a specific objective in mind, the balance of the outgoings can be safely categorised under the following headings and sub-headings.

[a] THERMAL

- (i) solids
- (ii) liquids
- (iii) gases

[b] CHEMICAL

- (i) unburnt gas
- (ii) produced gas of low CV

The relative magnitudes of energy losses in each category is given in Figure 1.8. However the recoverability of energy from these require in depth exploration of their characteristics and also methods of energy recovery. The recoverability factor is governed by both economic and technical feasibility of the proposed and existing system. A detailed examination of existing and new developments in energy recovery techniques from high temperature combustion gases is given in other chapters.

Figures 1.9 and 1.10 clearly show that cooling water temperatures are relatively low (approximately 60°C) so its usefulness in iron and steelworks processes is limited. However with the advent of district heating, horticulture and fish farming in association with large industrial complexes, including iron and steelworks, these represent some possible areas of use for low temperature thermal energy. These possibilities are currently investigated by the BSC.

The recovery of energy from hot combustion gases has presented certain difficulties particularly due to high and low temperature corrosion of metallic structures used in the manufacture of recovery systems. Therefore an understanding of corrosive and other undesirable properties of gaseous combustion products and the process limitations imposed by them is of paramount importance.

## 1.6 Characteristics of flue gases

Both high and low temperature corrosion are greatly influenced by sulphur trioxide. In general, high temperature corrosion is due to the low melting ash deposits whereas low temperature corrosion results from the condensation of sulphuric acid on heat exchanger surfaces. Therefore, an understanding of the mechanism involved in the formation of sulphur trioxide would be of a great significance to inhibit catastrophic failure.

Studies of Harlow (1945) and Burnside et. al. (1956) attributed the formation of  $\text{SO}_3$  to the catalytic oxidation of  $\text{SO}_2$  as the flue gases pass over hot metal tubes.

Reid et. al. (1945) identified that complex trisulphates ( $\text{K}_3$  or  $\text{Na}_3 \text{Fe} (\text{SO}_4)_3$ ) were involved in the external corrosion of superheater metal tubes at around 650°C. Corey et. al. (1945) postulated that alkali iron trisulphates are formed by the reaction of  $\text{SO}_3$  and  $\text{Fe}_2\text{O}_3$  and either  $\text{K}_2\text{SO}_4$  or  $\text{Na}_2\text{SO}_4$ . Laboratory experiments showed that for this reaction to take place at 538°C, the  $\text{SO}_3$  level should be at least



250 ppm. The sum total of  $\text{SO}_3$  produced in the flame and that formed by catalytic oxidation of  $\text{SO}_2$  was not sufficient for this mechanism to occur. Krause et. al (1968) probed the boundary layer in a dynamic gas system and showed that a steep  $\text{SO}_3$  gradient existed in a synthetic flue gas containing  $\text{SO}_2$  and  $\text{O}_2$  flowing at moderate velocities over catalytically active surfaces. This led to the conclusion that beneath deposits on a heat exchanger surface, where gas velocities approach stagnation, the  $\text{SO}_3$  concentration is sufficiently high to permit the formation of the alkali iron trisulphates.

In oil-fired systems, the fuel oils with a high content of vanadium pose additional problems. As with sulphates, a liquid film of vanadate speeds up the corrosion rate and proves troublesome when the metal surface temperatures are lower than the melting point of vanadate.

Low-temperature corrosion is generally responsible for keeping stack gas temperatures above  $163^\circ\text{C}$ . Consequently, energy recovery is restricted.

Some methods of corrosion control are given below:

1. Use of low-sulphur fuels [Reid et. al. (1945), Blum et.al. (1959) and Reid (1974)].
2. In oil-fired systems where the ash loading of the flue gas is low, the use of Magnesium [Reid et. al. (1945), Flux et. al. (1971) and Reese et. al. (1964)] has the following effects:
  - (a) neutralise  $\text{SO}_3$  by the formation of  $\text{MgSO}_4$
  - (b) to cover superheater surfaces with a layer of  $\text{MgO}$  to prevent catalytic formation of high  $\text{SO}_3$ .

However, with coal-fired systems, the ash loading is so high that additives are impractical and expensive.

3. Use of low excess air inhibits, to a large extent, the formation of  $\text{SO}_3$  particularly when the combustion products contain under

0.2% oxygen. As a result of this the dew-point is depressed to around 54°C, thus a higher level of energy recovery is practicable.

## 1.7 Methods of energy recovery

The haphazard setting-up of fuel and energy conservation committees as a dramatic response to sudden and steep rises in fuel price led to the formulation of ill-conceived and ill-defined objectives for industrial energy saving projects. Consequently, the failure of most of these committees to meet these objectives is resulting in their role becoming ineffective or, in some cases, them being completely disbanded. [Cheshire and Buckley (1976)]. Similarly, with energy intensive processes, the foremost urgency is given to finding short-term solutions, hence the energy recovery methods were and are prematurely and unconditionally accepted as the best and the only certain course available to improve the process energy utilisation. This fallacy shows the need for a clear objective before embarking on minor or major research and capital projects. The early recognition of the overall objectives and their widest analysis may result in an opportunity to simplify the equipment or the process. Even the possibility of amalgamation of two or more processes or their complete redundancy should not be discarded. Therefore, one of the above is the ideal and the best solution provided all other factors remain unaffected or are not unduly amplified. Hence, the use of energy recovery methods is the last resort and only when all other alternatives are thoroughly ventilated and are found not to be technically or economically feasible. Once the desirability of the combustion process has been established, the next step is to consider and to evaluate the possible areas of usage for the energy recovered using heat exchangers. Therefore, the economics of energy recovery are primarily governed by the use to which it can be put. The use of energy can be either internal or external to the process. Internal use generally improves the fuel



utilisation per unit production and as such is directly attributable to the process itself. This category includes preheating of stock, gas and combustion air. The secondary advantages of this method include the possibility of using low calorific value fuels e.g. blast-furnace gas. The external use is generally in heating water for space heating and producing steam for process or power generation.

The final decision requires rigorous technical and economic analyses as well as weighing the short-term versus the long-term benefits of the available alternatives.

The equipment available for the recovery of energy from hot gaseous combustion products are as follows:

- |                                       |                        |
|---------------------------------------|------------------------|
| 1. INTERNAL                           | 2. EXTERNAL            |
| (a) metallic and ceramic recuperators | (a) waste-heat boilers |
| (b) Regenerators                      | (b) economisers        |

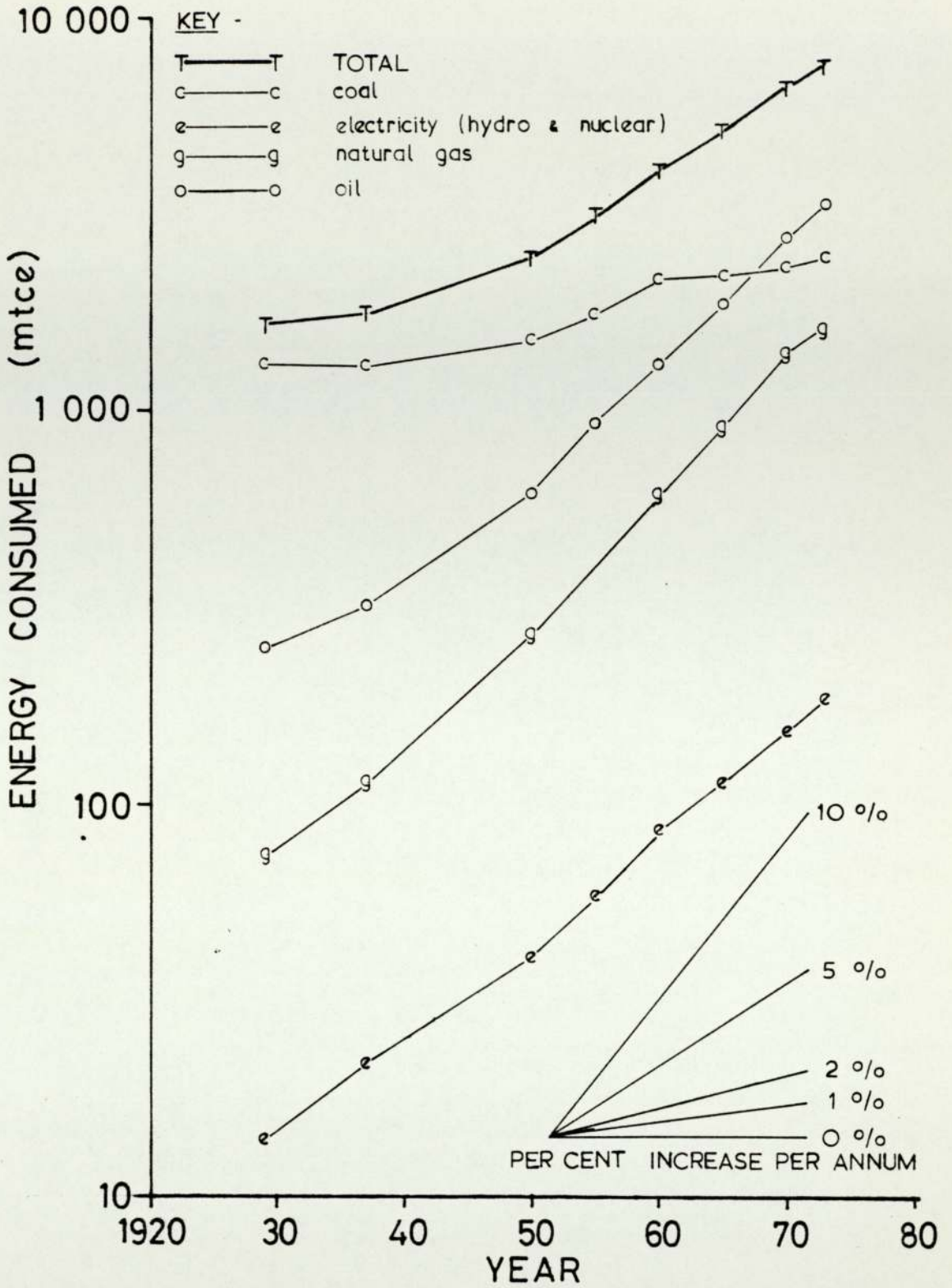
The next three chapters discuss these and other techniques of energy recovery in an order which may appear to be chronological.

Chapter 2 outlines the main energy recovery methods in use at most, if not all of the major iron and steelworks. Chapter 3 gives details of promising energy recovery methods at various stages of development. Finally, Chapter 4 details novel techniques of energy recovery methods investigated during the present study.

In extracting energy from waste gaseous products, the onus is to recover the maximum amount of total energy at the highest feasible temperature. However for the heat to flow the Second Law of thermodynamics requires the existence of a heat source and a heat sink. The lowest conceivable receiving temperature is that of the atmosphere. However, the exhaust gas characteristics, as outlined earlier, impose limitations on both high and low temperatures of energy recovery. Therefore, certain added refinements are necessary in all energy

recovery systems to alleviate these and other difficulties. These are discussed in detail, as and when a particular system is considered.





[ UNITS: mtce = metric tonne coal equivalent ]

Source: UN Statistical Yearbooks  
 Oil and Gas Journal  
 Institute of Petroleum Information Service

FIGURE 1.1 WORLD ENERGY CONSUMPTION

FUEL	KNOWN ECONOMIC RESERVES	POSSIBLE RESERVES UNDER FAVOURABLE CONDITIONS	SUPPLY PERIOD IN YEARS at 1973 RATE OF CONSUMPTION	SUPPLY PERIOD IN YEARS WITH ADJUSTMENT FOR ANNUAL INCREASE [ 1969-1973 ]
COAL	-	$2.6 \times 10^{12}$ TONNE	3200	258
CRUDE OIL	$7.43 \times 10^{10}$ TONNE	$22.3 \times 10^{10}$ TONNE	80	30
NATURAL GAS	$6.3 \times 10^{13}$ m <sup>3</sup>	$18.8 \times 10^{13}$ m <sup>3</sup>	148	41
URANIUM	$9.6 \times 10^5$ TONNE	-	49	34

Source: UN Statistical Yearbooks

FIGURE 1.2 WORLD ENERGY RESERVES



SOURCE	PER CENT		
	1929	1950	1973
COAL	79.7	62.2	32.0
OIL	15.0	25.2	44.2
NATURAL GAS	4.5	11.0	21.4
HYDRO & NUCLEAR	0.8	1.6	2.4

Source: UN Statistical Yearbooks

FIGURE 1.3 WORLD ENERGY CONSUMPTION BY SOURCE

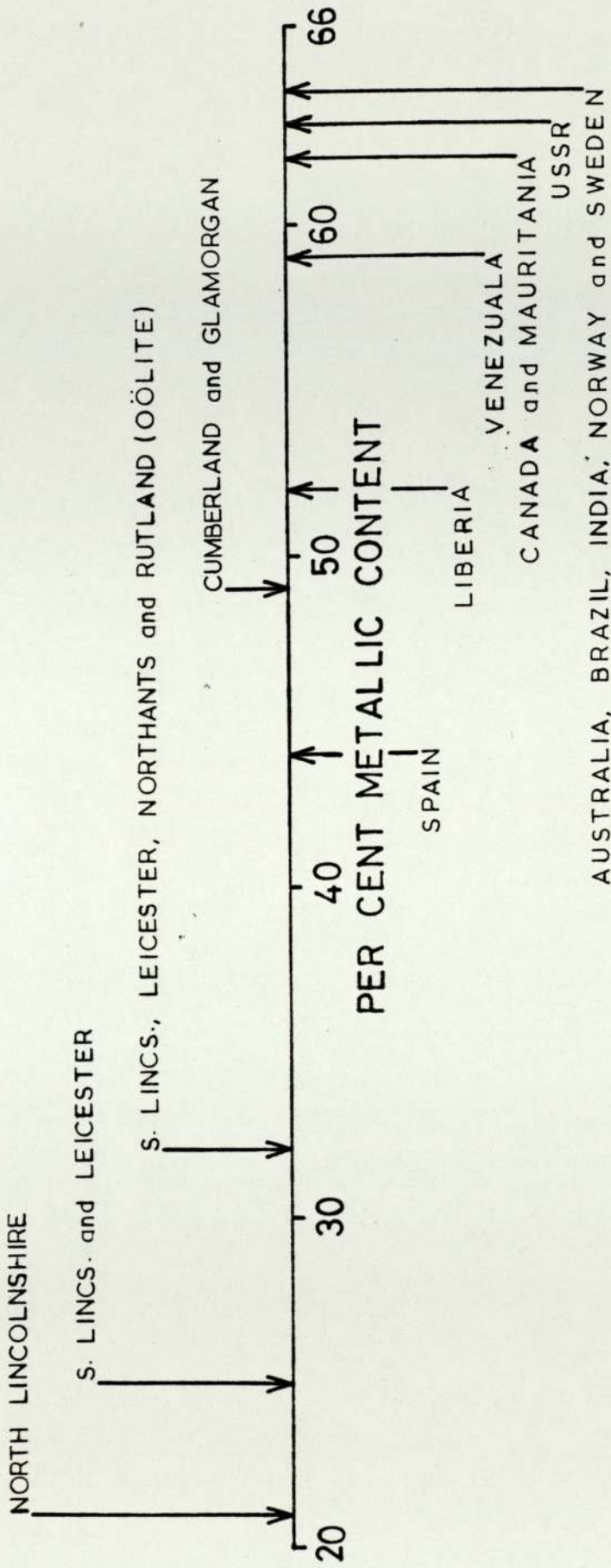
SOURCE	PER CENT			
	1950	1960	1970	1975
COAL	89.8	74.3	46.6	36.9
OIL	9.8	24.7	44.5	42.0
NATURAL GAS	-	-	5.3	17.0
HYDRO & NUCLEAR	0.4	1.0	3.5	4.0

Digest of Energy Statistics 1970, 71 & 76

FIGURE 1.4 UK ENERGY CONSUMPTION BY SOURCE



HOME



FOREIGN

FIGURE 1.5 METALLIC CONTENT OF HOME AND FOREIGN IRON ORE

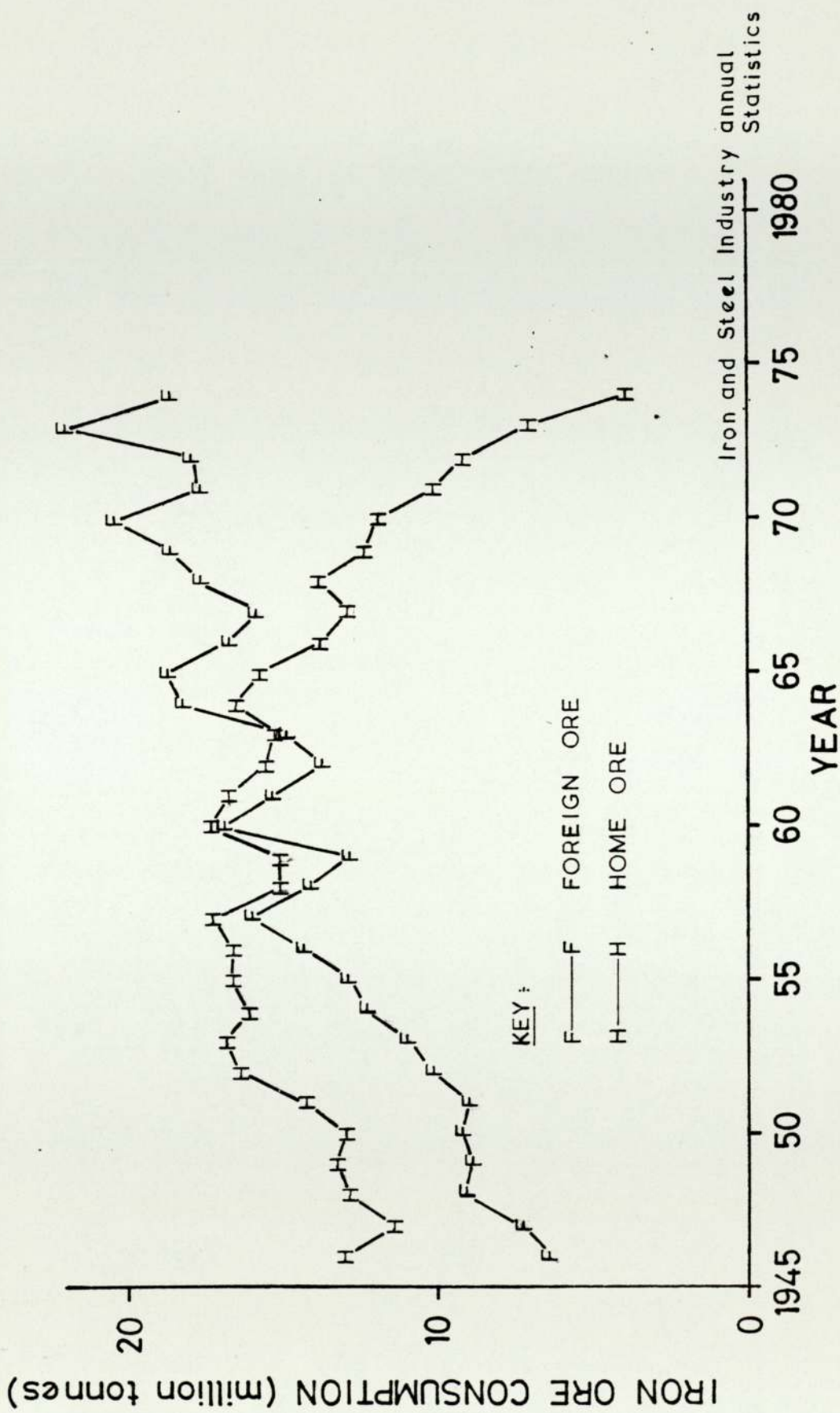


FIGURE 1.6 TRENDS IN IRON ORE CONSUMPTION



SOURCE	PER CENT			
	1955	1960	1965	1972
COKING COAL	61	63	57	52
NON-COKING COAL	23	12	5	0
FUEL OIL	7	13	22	25
ELECTRICITY including overheads	7	10	13	16
GAS [ town and natural ]	2	2	2	7

Source: Iron and Steel Industry Annual Statistics

FIGURE 1.7 FUEL SUBSTITUTION IN IRON AND STEELMAKING

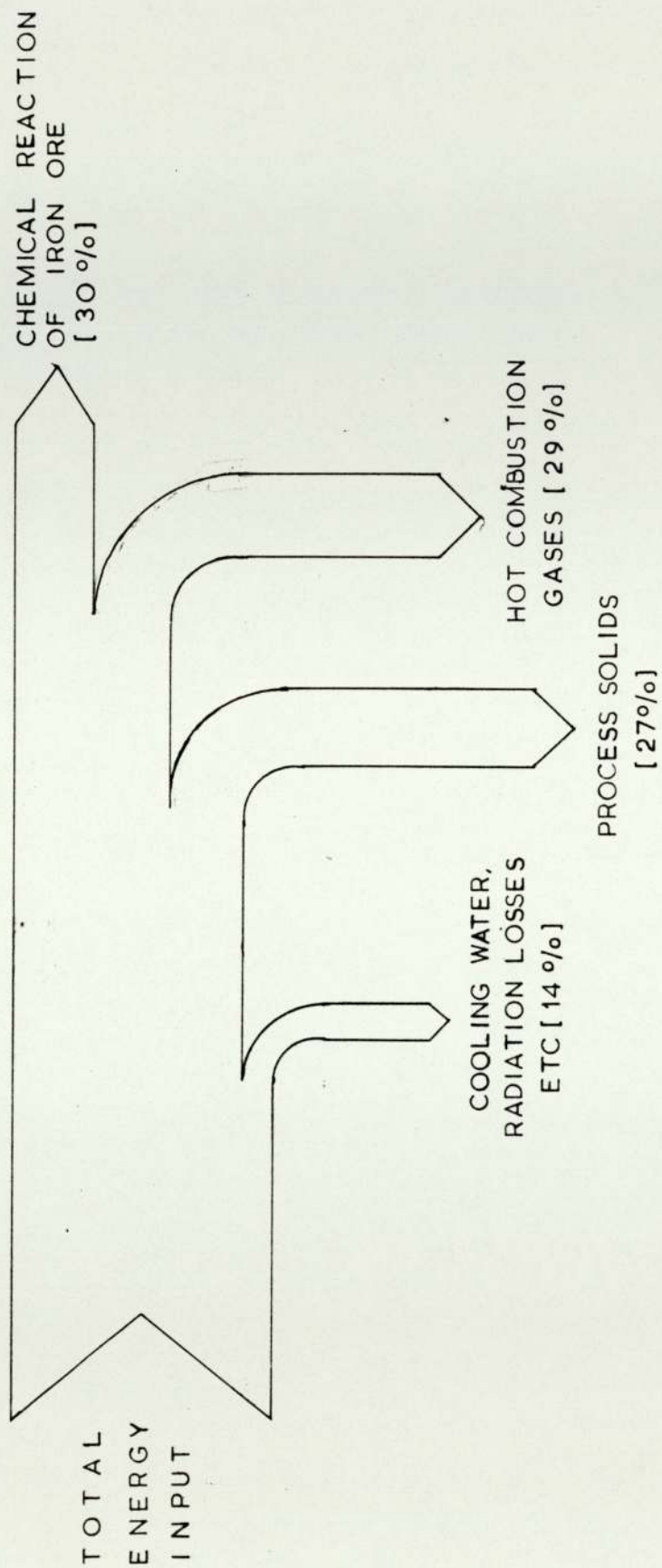


FIGURE 1.8 OVERALL ENERGY DIAGRAM FOR AN IRON AND STEELWORKS



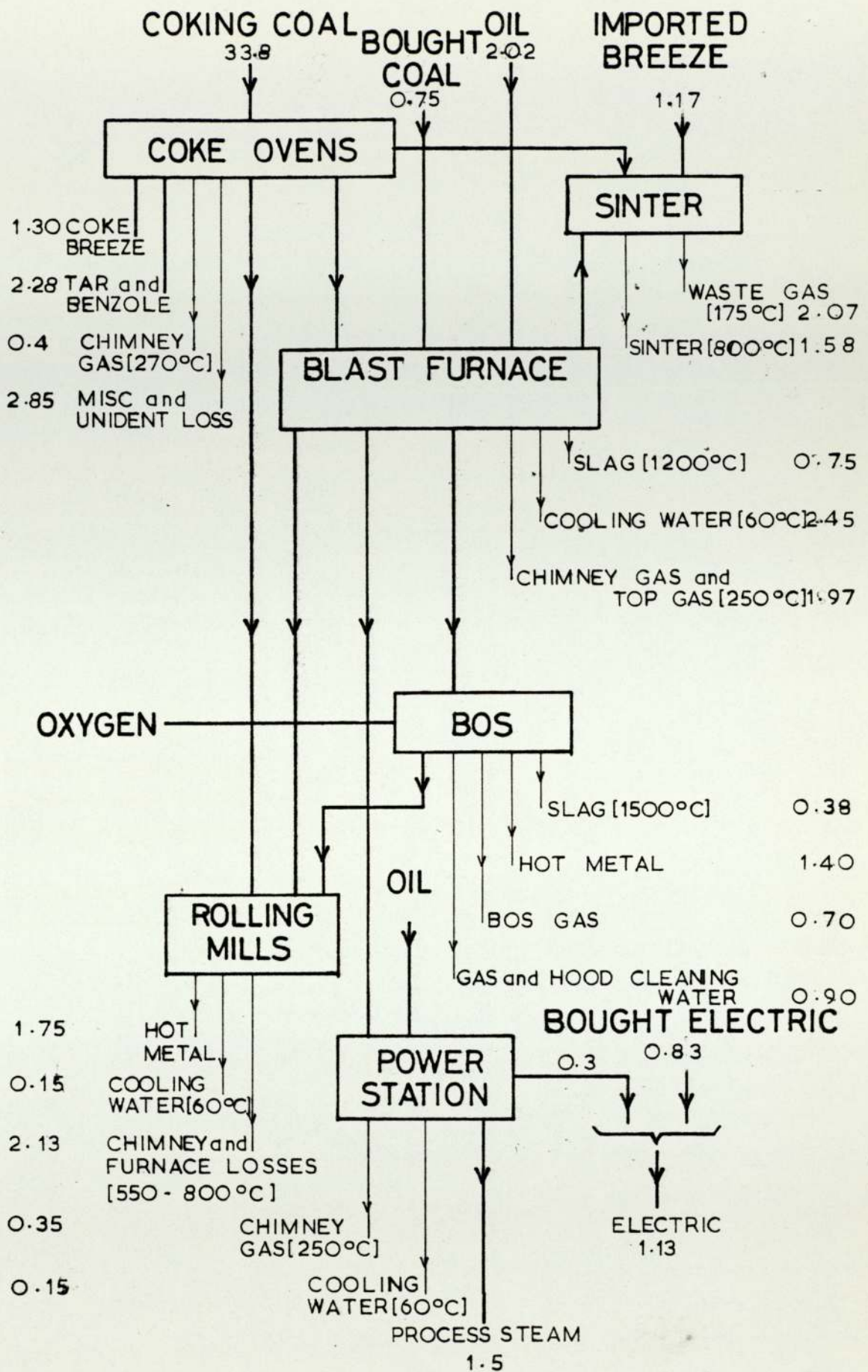


FIGURE 1.9 ENERGY USE / LOSS IN AN INTEGRATED IRON AND STEELWORKS  
( UNITS : GJ per tonne finished steel )

INPUT

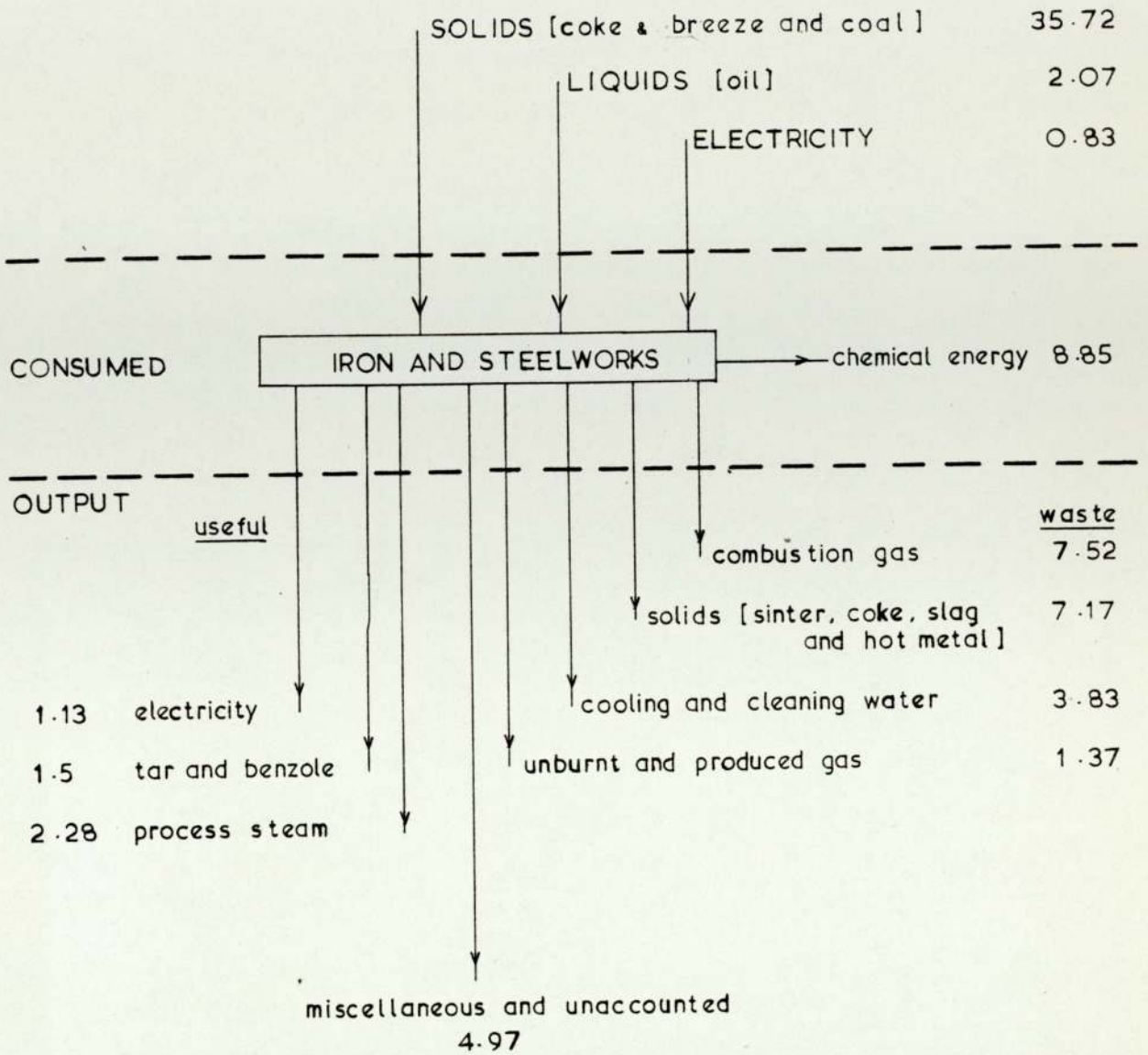


FIGURE 1.10 OVERALL ENERGY FLOW DIAGRAM FOR AN  
 INTEGRATED IRON AND STEELWORKS  
 ( UNITS: GJ per tonne finished steel )



## CHAPTER 2

### ENERGY RECOVERY : EXISTING METHODS

## 2.1 Waste-heat boilers

The application of boilers to produce steam from combustion gases leaving industrial furnaces goes well back to the middle of the last century. These early boilers were inefficient but in many cases produced enough steam to meet a works' own requirements. They operated with flue gas temperatures in excess of 1200 C, hence the accepted designs of fuel-fired boilers were used.

As a result of the increase in fuel price after the First World War more attention was paid to heat recovery equipment. Also the application of regenerative and recuperative principles to preheating of the combustion air and with use of low grade fuel resulted in a significant drop in the waste gas temperature making the fuel-fired boiler designs uneconomic and inefficient at relatively low temperatures, usually below 900 C.

The operation of waste-heat boilers operating in the gas temperature range between 400 C and 900 C is well documented elsewhere.

Interested readers are referred to references under the names of Gregson (1963), Streich et al (1972), Gunn (1976), Csathy (1967), Gibson (1976), Gupton et al (1973), Williams (1969), Antonov et al (1973), Trub et al (1969), and Kunyanskii (1969).

## 2.2 Fixed regenerators

A regenerator is an intricately-woven structure which alternately absorbs and rejects energy from hot to cold fluids respectively. This method was first proposed by Siemens and the history of the regenerative furnace is expounded by Schofield (1961). The preheating of combustion air in open-hearth furnaces, soaking pits, glass-melting tanks, by-product coke ovens, heat-treating furnaces and the like have been carried out, at one stage or another, in regenerators con-



structured of fireclay, chrome or silica bricks. The calculation procedure for the thermal design of regenerators is adequately covered by Jakob (1957), Razelos and Paschkis (1968), Hlinka et al (1961), Berczynski (1968), and the BISRA regenerator group (1958). The use of high efficiency (i.e. high surface area to total volume) bricks improves convective heat transfer [Baab and Blackwood (1968)] and consequently the thermal performance of the regenerator. However, a simultaneous increase in pressure drop is noted. Therefore a thorough investigation into the advantages and disadvantages of using high efficiency bricks must precede a final decision. Generally, most observers have noted a marked savings in both capital and furnace operating costs as a direct result of using high efficiency checkerwork systems especially with 'clean' exhaust gases.

Poletavkin et al (1972) reported satisfactory operation of a regenerator, over a period of 10 000 hours, having zirconium dioxide checkers and giving air preheat temperatures of 1500 - 1700 C. However, despite these undoubted successes, regenerators are continuously in the process of being replaced by recuperators. This trend away from regenerators is attributable to many factors, some of which are discussed below.

In the iron and steel industry, the phasing-out of open hearth furnaces in favour of basic oxygen steelmaking furnaces has drastically reduced the number of O-H furnaces and regenerators in use today. This trend is clearly shown in Figures 2.1 and 2.2.

The major disadvantages of the regenerator can be easily ascertained from a critical analysis of events that occur during reversal of flow direction in the regenerator. At the time of reversal, the products of combustion in the flue, the regenerator and the uptake must be cleared past the burner before the combustion air is able to sustain the process of combustion in front of the burner. The time

required for this process is the sum of the time elements required for throwing the valve, bringing the moving column of combustion products to rest, starting them in the opposite direction and passing them up to the burner. The mixing of products of combustion and air further delays the arrival of pure air in the furnace. Also the passing of gases containing oxygen over the liquid bed results in oxidation of the metal surface. This acts as an insulating barrier between the hot furnace atmosphere and the liquid metal. The whole reversal process takes from 5 to 30 seconds depending on the size of the regenerator. All of the above facts favour long periods of reversal which necessitate the use of a great mass of brickwork in the checkers. This results in a large regenerator with high initial cost. Also, a long period of reversal results in lower average preheat temperatures, hence a reduced fuel economy.

As expected, the temperature change in the regenerator surface is most marked in the first minute after reversal, therefore, the heating and the cooling processes form a cycle and the average temperature during heating is substantially higher than the average temperature during the cooling half of the cycle as shown in Figure 2.3. The original approximation to the cycle was assumed to be that of a thick-wall recuperator. This assumption considerably simplified the calculations for determining the correct size of the regenerator. The BISRA regenerator group (1968), in discussing the paper of Collins, Daws and Taylor (1955), conclude that although their method of deriving approximate equations governing the process is theoretically more accurate, the approximate process method is adequate for most designs. Also the available data on heat transfer is not sufficiently accurate to warrant the use of this accurate approach. Razelos and Paschkis (1968) gives a worked example using the method which approximates to a thick-wall recuperator.



The problem of air infiltration has been studied by most research workers mentioned above. These studies report that the excess air at stack ranges from 30% to 94% causing a drop of 250-300 K in air preheat temperature. Although air leakage can, to an extent, be tolerated in preheating of low calorific value gas the use of the regenerative design is an impossibility due to the danger of carbon monoxide poisoning as well as a possibility of lower efficiency resulting from loss of gas.

The alternation of flame direction in furnaces is often inconvenient and is sometimes impossible as in blast furnaces. For these reasons, some designs have successfully employed the regenerative principle with constant flame direction, the prime example in the iron industry being blast furnace stoves. Also in the furnace where the flame direction alternates from end-to-end, it is difficult, if not impossible to design a port which is equally optimised for both the inlet and exhaust functions.

In comparing regenerative and recuperative soaking pits, Brooks (1959) concludes that the optimal use of space, lower maintenance costs and the improved air port design associated with the recuperative design outweigh the advantages of improved thermal performance experienced in the regenerator design.

All of these factors and the availability of materials, both ceramic and metallic, for high temperature applications led to the consideration of other methods of energy recovery. The first of the new methods of energy recovery from waste gases was the conventional ceramic recuperator.

### 2.3 Ceramic recuperators

A recuperator is a device for exchanging energy between two continuous streams separated by ceramic or metallic material. A continuous heat exchanger offers many advantages.

1. Uninterrupted flow of combustion air.
2. Improved and stable furnace operation.
3. Simplified inlet and exhaust port design compared with a port to serve both inlet and exhaust functions with alternation of flame direction.
4. A single and usually lightweight recuperator in the place of two bulky regenerators.
5. Use of space more effectively.
6. No gas stream switching operation.

The regenerator has its own advantages.

1. High thermal capacity of checkers stabilising air preheat temperature.
2. Simple checkerwork construction.
3. Robustness and reliability.
4. Established heat transfer data.
5. High air preheats.
6. Continuous and uni-directional air flow, i.e. blast furnace stoves.

Despite these many advantages, the interest in ceramic and metallic recuperators flourished well before the open hearth furnace was superseded by the basic oxygen furnace. Recuperators offer a potential reduction in air leakage which was considered so important for preheating of low calorific by-product gases, which were hitherto wasted. In these early days, operating metal temperatures were severely restricted, so the use of ceramic materials was the only alternative available.

The early ceramic recuperators were constructed of ceramic tiles from an alumina fire-brick and were bonded together by cement. Various types of tile recuperators are shown in Figure 2.4. In these designs, the two streams are separated by ceramic tiles. The air leakage is usually high because of porous construction materials and the construction



methods involving numerous joints in the waste gas stream; these crack and open-out with every thermal cycle.

The air leakage varies from 12-25% on a new recuperator to 30-60% after a few months operation. To allow for this increase, oversize air fans are fitted. A method of reducing the air leakage is to use induction fans which lowers the pressure differential between the two streams. However, with air preheat temperatures of 800 C, the fans are required to shift three times more volume of air and are built of high-quality stainless steel to withstand high operating temperatures. Thus initial capital outlay and running costs are substantially increased. The use of steam injectors on soaking pits has been evaluated and an improvement of 30% in soaking pit operating efficiency as well as lowering of fuel consumption by 25-30% is noted. The cost of steam is fully covered by the fuel economy when ingots are charged cold, and when charged hot the steam cost is under a third of the fuel saved. This paragraph is equally applicable to the type of recuperators discussed below.

The material limitations placed severe constraints on the design of ceramic recuperators. Hence the design of ceramic recuperators followed in the footsteps of the advancement in ceramic materials. As ceramic materials became capable of retaining mechanical strength at high temperatures the ceramic element design improved to short length tubes. The Tiesen and the Didier designs Figure 2.5 employed short hexagonal and round tubes respectively having hexagonal flanges at the ends. Although air preheats of around 700 C have been achieved air leakage remained a major problem.

However the use of combined metallic and ceramic air preheaters on a forge furnace has been successful in attaining air preheat temperatures of 700 C with an air leakage of 8-15% at high temperatures.

As the excessive number of joints in the waste gas duct has been largely responsible for high air leakage, the natural progression is to large ceramic tubes. The Gas Council in 1968 Figure 2.6 tried unsuccessfully using the principle of no joints within the waste gas duct by using 450mm silicon carbide tubes spanning the duct. Air preheat temperatures were limited to around 1200 C with inlet waste gas temperatures of around 1800 C. High air leakage in excess of 50 per cent remained a problem.

Stookey recuperators, using large diameter silicon carbide tubes, 178mm ID x 288mm OD x 760mm long have been successful in attaining air preheat temperatures of 870 C with air leakage below 5% at air pressures between 7 and 14 kPa. The tubes are stacked six high and the top of the recuperator has a 'floating head' which allows the tubes to expand without loss of air tightness, as shown in Figure 2.7.

In 1970, two soaking pits at Lackenby Works, British Steel Corporation were installed with part ceramic and part metallic recuperators designed on the basis of Hazen metallic recuperators, (see next section) but proved to be very unreliable. After only 18 months of operation these were dismantled and replaced with metallic recuperators.

New developments in ceramic recuperator design are described in Chapter 3.1.

## 2.4 Metallic recuperators

Metallic recuperators gained widespread interest after the introduction of special alloy steels in their construction during the 1950's. The new materials and better methods of construction improved both air preheat temperatures and leakage rates associated with earlier metallic and ceramic designs. This gave rise to preheating of low calorific value gases i.e. coke oven gas and, in particular, blast furnace gas.



The design of metallic recuperators must take into account all locally prevailing conditions which can be categorised as follows:-

- (a) waste-gas temperature
- (b) composition of the fuel and the waste gas
- (c) construction materials and their maximum operating temperatures
- (d) air and gas preheat required
- (e) maximum allowable pressure drops [both on air and gas sides], and
- (f) economic life

Some of the above factors conflict, such as the requirement to obtain high air and/or gas preheats may lead to overheating of construction materials and consequently a reduced life of recuperator. Therefore the optimum solution is always a compromise which is compatible with desired objectives and the available resources i.e. space, know-how, capital, material and labour.

Metallic recuperators are usually divided into categories based on the prevalent mode of heat transfer, i.e. convective or radiative. Each has its own best temperature domain with a certain degree of overlapping where the rates of heat transfer by convective and radiative modes is of the same order. In this region, economic considerations usually restrict the use of the best mode.

#### **2.4.1 Convective recuperators**

These are used at the lower end of the temperature range upto 1000 C.

The early type of convective recuperator was a simple extension of the conventional 'long tube' ceramic recuperator. This type was referred to as the cast tubular.

##### **2.4.1A Cast tubular**

A typical cast tube recuperator design is shown in Figure 2.9.

It is a 'pure' convection unit in cross-flow. The heat transfer rate is improved by the use of fins integral with the tubes. A number of different types of heating elements are distinguished by the complexity of their fins. The intricacy of fin design is restricted by adverse waste gas composition and its temperature. The latter causes localised hot spots at the ends of the fins which lead to burnout or sintering of dust particles in the vicinity of heat exchanger surfaces. The adhesion of these particles to the cooling surfaces impairs the heat exchanger effectiveness and leads to a reduced economic life. The main disadvantage of this unit for the iron and steel industry is that it cannot be used efficiently with dirty gases. In these cases the fins are blocked by the solids in the waste gas stream which reduces the rate of heat transfer and an increase in pressure drop is inevitable. As with ceramic recuperators employing short-length tubes, air leakage is a major problem. This problem is usually aggravated by poor seal design and faulty installation.

The main advantage of this unit is its compactness and thermal capacity. The latter enables the fluctuations in waste gas temperature to be smoothed-out and an improvement in combustion is noted.

As with all other types of recuperators, the selection of the right material is of utmost importance. Cast-iron is generally employed for high temperature applications where both material strength and resistance to scaling is required. With normal grey iron castings the strength falls rapidly above 500 C.

#### **2.4.1B Multi-tube steel**

Steel tube recuperators, Figure 2.10 are made in many forms to suit site requirements. The tubes, which may be cast or drawn, are grouped in bundles and these are attached at both ends to header boxes. To reduce thermal distortion, the end plates are designed to allow each tube bundle to expand independently.



Either waste gas or combustion air may pass through the tubes, the former is generally preferred with dirty gases, since tubes are easily accessible for cleaning purposes. These recuperators may be installed in the flue or may be free standing above the ground. In a flue tube recuperator (Figure 2.11), the heat transfer is improved by the use of baffle plates to guide air across the tubes.

A comprehensive guide to materials used for steel tube recuperators is given by [Kay (1973)] and is reproduced in Figure 2.12. To reduce costs a tube bundle may be made up of composite tube lengths where 'hot' and 'cold' ends have different material composition to suit designed conditions.

#### 2.4.1C Hazen metallic

The heating element of the Hazen recuperator consists of a concentric tube, as in Figure 2.13. The combustion air enters the cold air chamber and then flows down the inner tube. A formed opening at the lower end of the outer tube directs the air back up between the two tubes. Air velocity in the annular gap is above critical to enhance heat transfer. Banks of these concentric stainless steel tubes are suspended from the air chambers into the flue gas stream. Each tube is free to expand or contract independently. The claimed advantage over a conventional multi-tube steel recuperator is the elimination of air leakage problems as there are no expansion joints. Also heating elements can be replaced without interrupting the furnace operation.

To the author's knowledge, no Hazen metallic recuperator is in operation in the UK but over fifty per cent of the five-zone furnaces built in the USA between 1957 and 1967 were installed with one or more Hazen recuperators. In these installations, the maximum operating air preheat temperature is 470 C. A typical layout of a Hazen recuperator is shown in Figure 2.14.

## 2.4.2 Radiative recuperators

For waste gas temperatures in excess of 900 C, a radiation recuperator of Austeel-Escher design is generally used in UK. This design is best suited to conditions where dirty gases are encountered and pressure drop available on the gas side is severely restricted. This type of recuperator consists of two concentric, large diameter tubes, shown in Figure 2.15. The waste gas stream flows through the inner tube and the combustion air at above critical velocities, passes through the annulus formed by the inner and the outer tube. In the region where low inner tube surface temperature predominates or occasionally for the entire length of the recuperator, longitudinal fins are welded to the inner tube to enhance the heat transfer rate and to strengthen the structure. Another similar design is known as the Schack shell-tube radiation recuperator [Schack (1955)] in which air or gas to be preheated is guided by helical fins in the annulus. The high cost of special heat resisting steels prohibits the use of shell-type radiation recuperators for high pressure applications where thick-walled and large-diameter tubes will be required. For these applications the cage-type of radiation recuperator has been developed which comprises numerous small diameter tubes closely spaced in an upright position around a large diameter circle and are connected to a top and bottom header. To avoid differential expansion which will lead to distortion, the air flow pattern should be uniform in all tubes and hence design of header boxes is critical.

To optimise energy recovery, a combination of radiative and convective recuperators is used. In this way, the use of a radiative recuperator at temperatures below 850 C, where heat transfer by radiation is relatively small, and the use of a convective recuperator at temperatures above 1000 C can be avoided. A design of combined radiation/convection recuperators is shown in Figure 2.16. A comparison of radiative and convective recuperators is given below.



## Radiative

Maximum flue gas temperature

- upto 1600 C

Less sensitive to overheating

Suitable for dirty gases

Heat transfer surfaces are  
easily accessible

Low pressure drop on gas side

- usually natural draught  
is possible

Space requirement is minimum

- can be used as a part  
of the stack

## Convective

Maximum flue gas temperature

- upto 1100 C

coefficient of performance is high

Suitable for high pressure applications

Heat transfer rate is uniform over  
a wide range of temperature

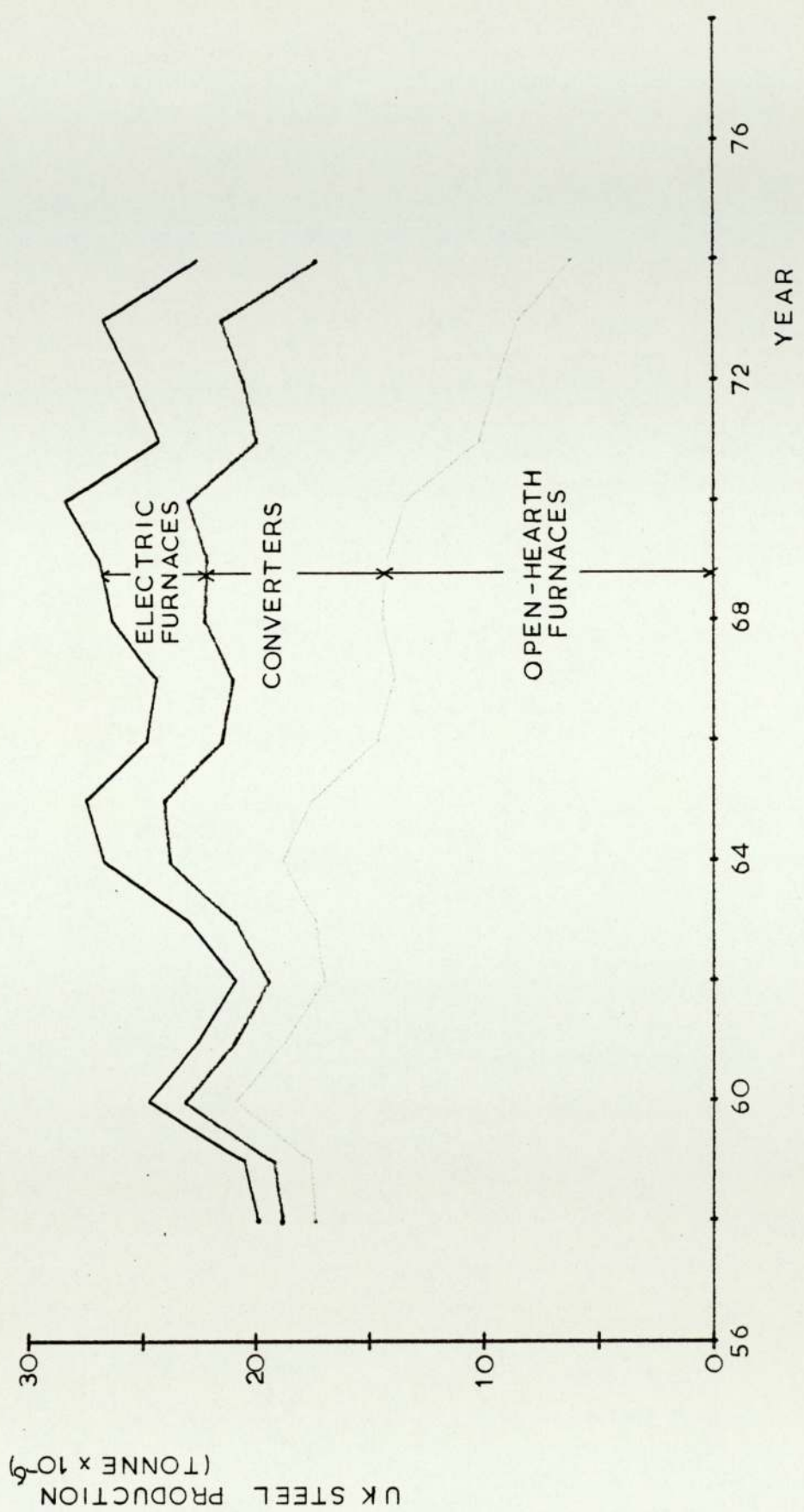


FIGURE 2.1 UK STEEL PRODUCTION BY PROCESS



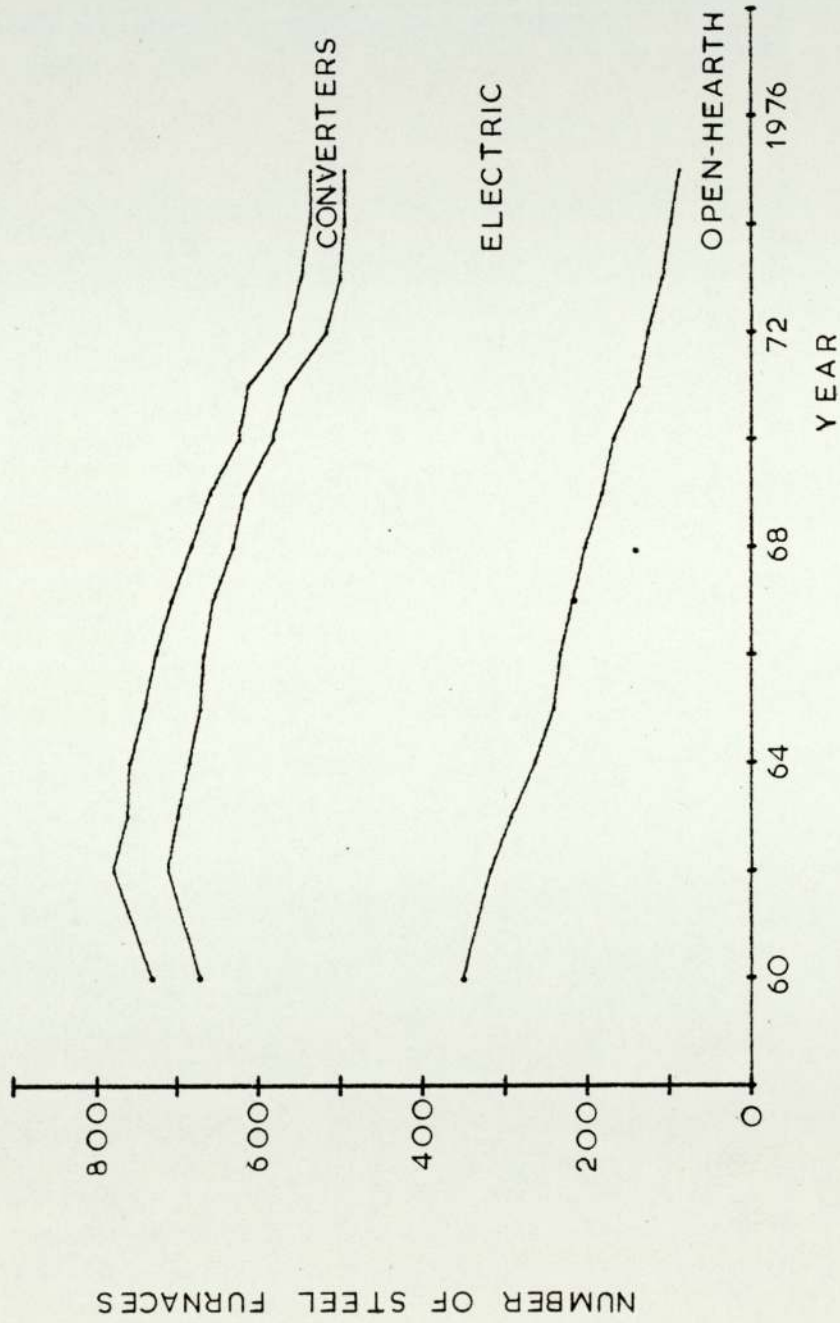


FIGURE 2.2 NUMBER AND TYPE OF STEEL FURNACES IN USE IN U K

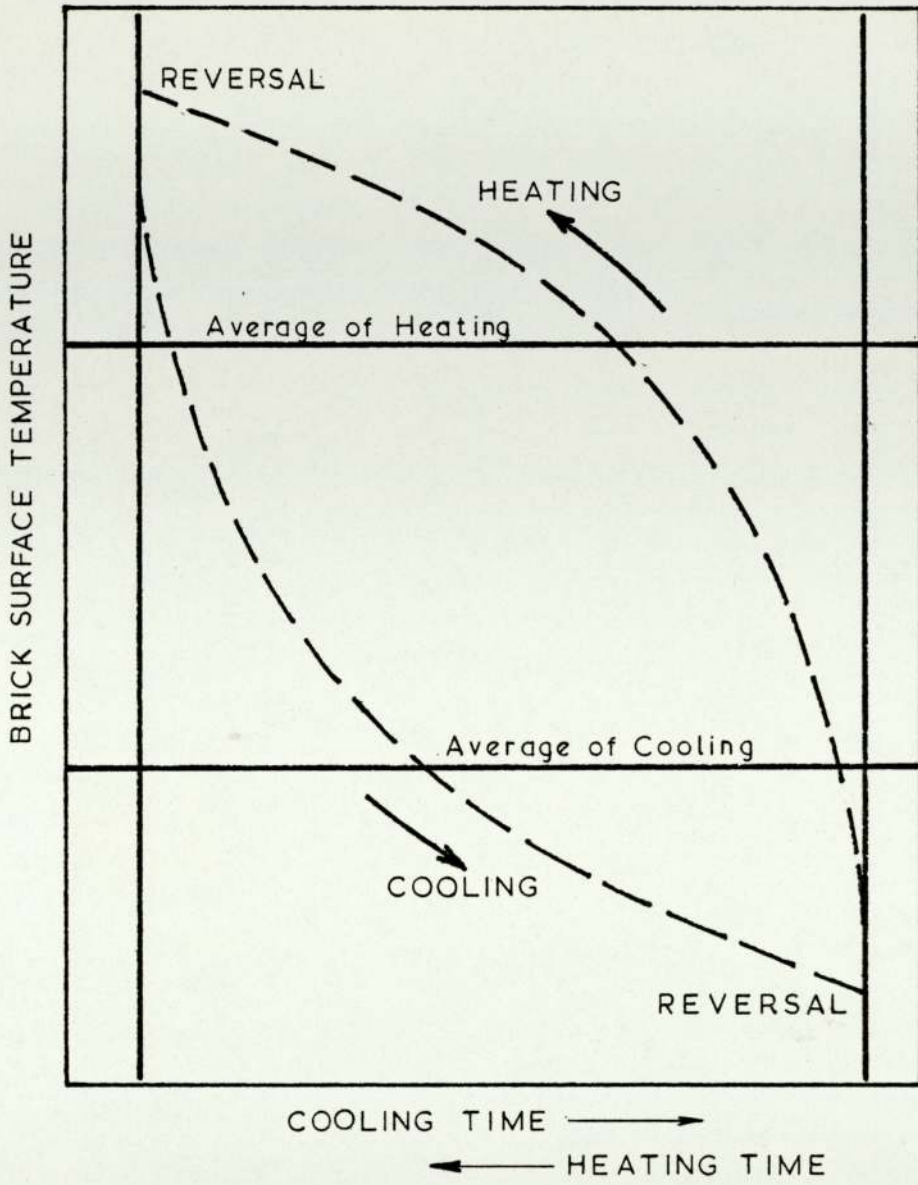


FIGURE 2.3 TEMPERATURE CYCLE OF SURFACE OF REGENERATOR BRICK



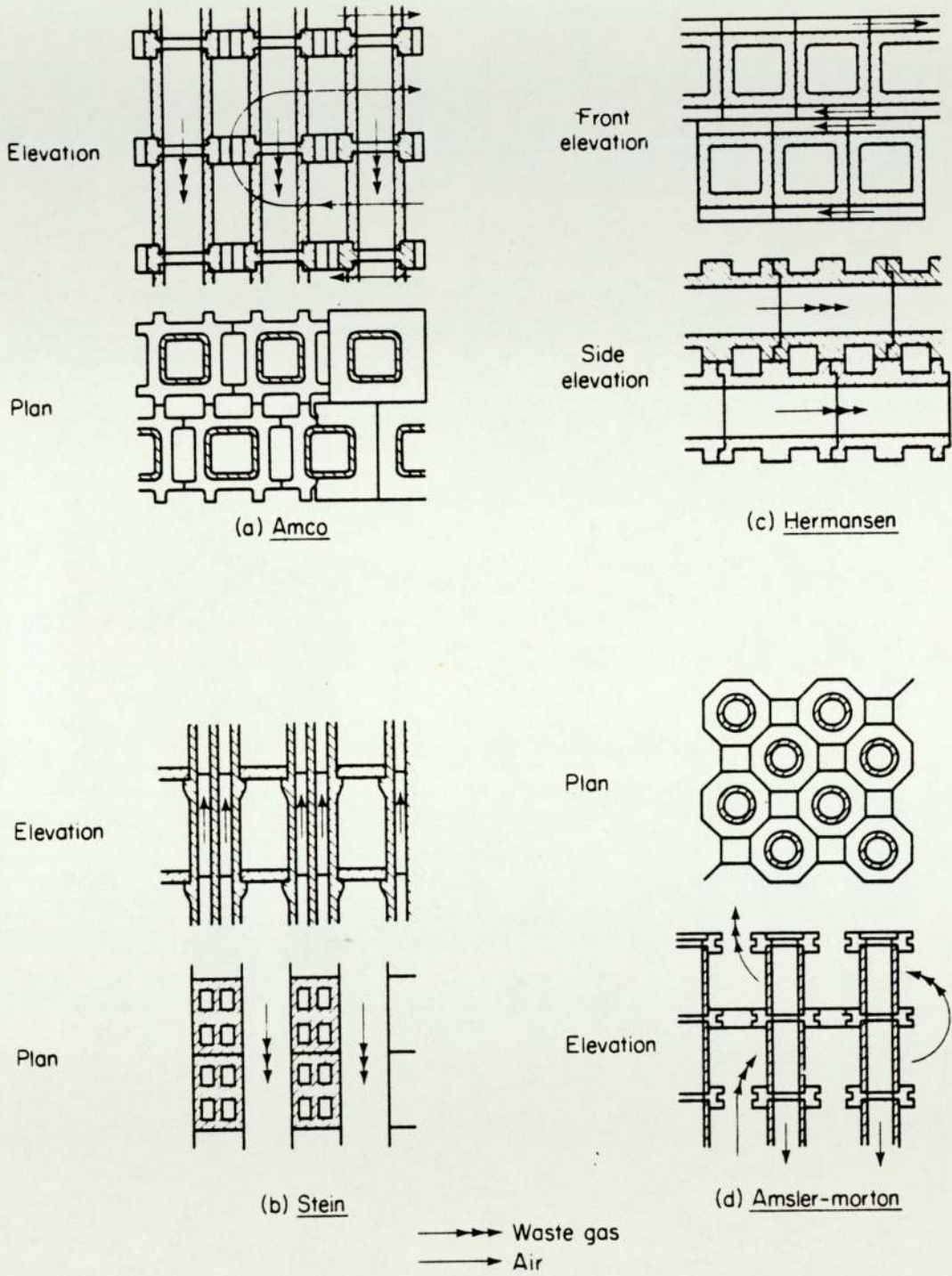
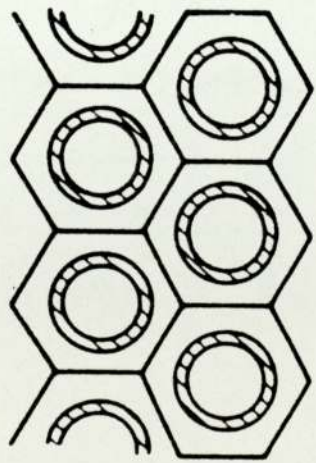
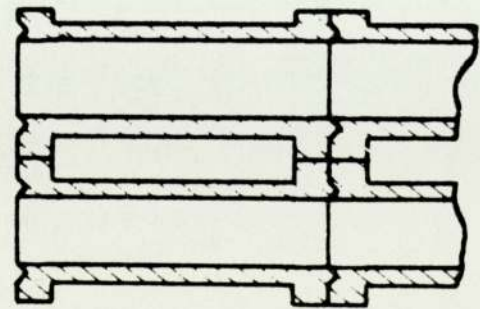
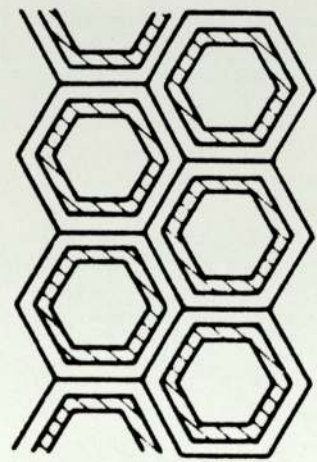


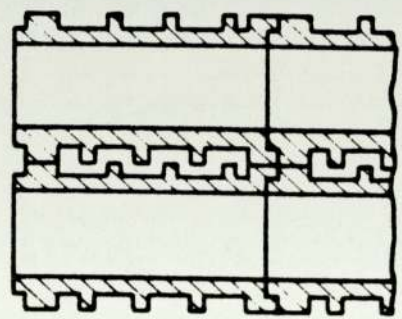
FIGURE 2.4 VARIOUS DESIGNS OF TILE RECUPERATORS



Elevation



Didier



Plan

Teisen

FIGURE 2.5 SHORT TUBE RECUPERATOR DESIGNS



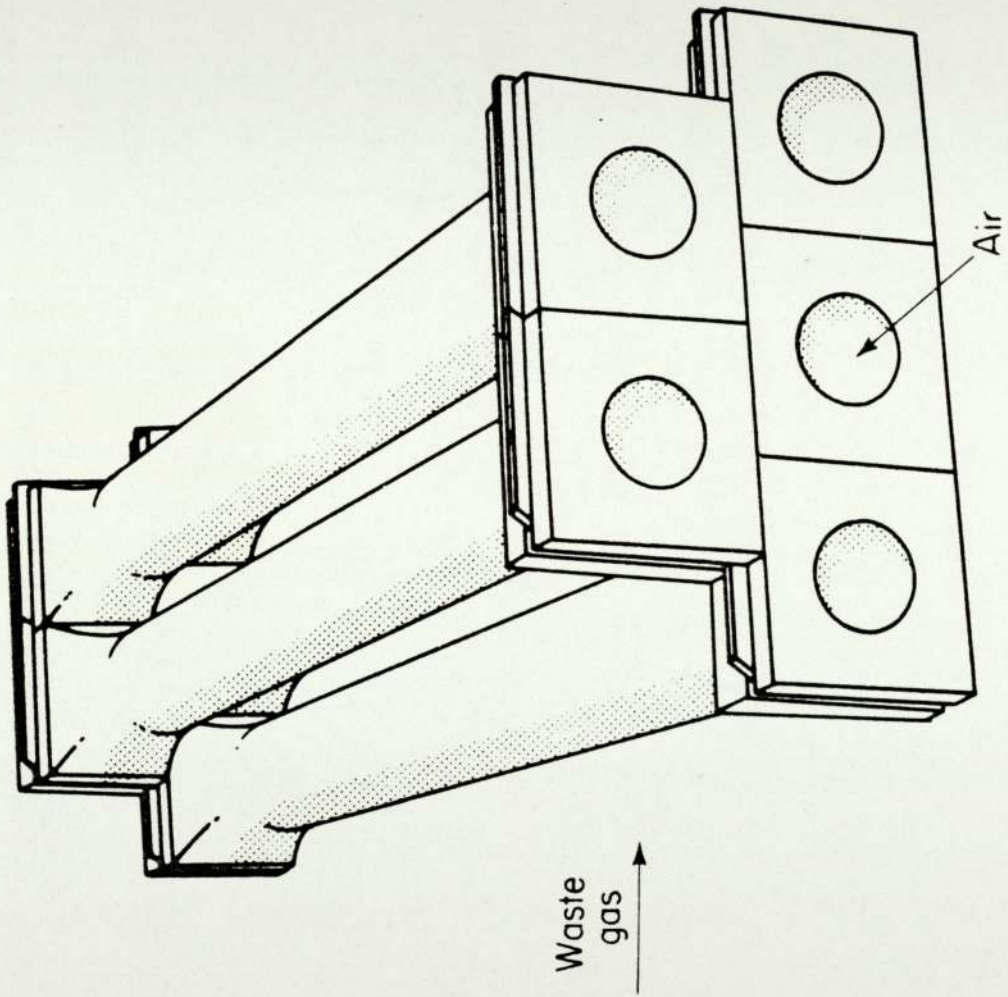


FIGURE 2.6 GAS COUNCIL RECUPERATOR CONSTRUCTION

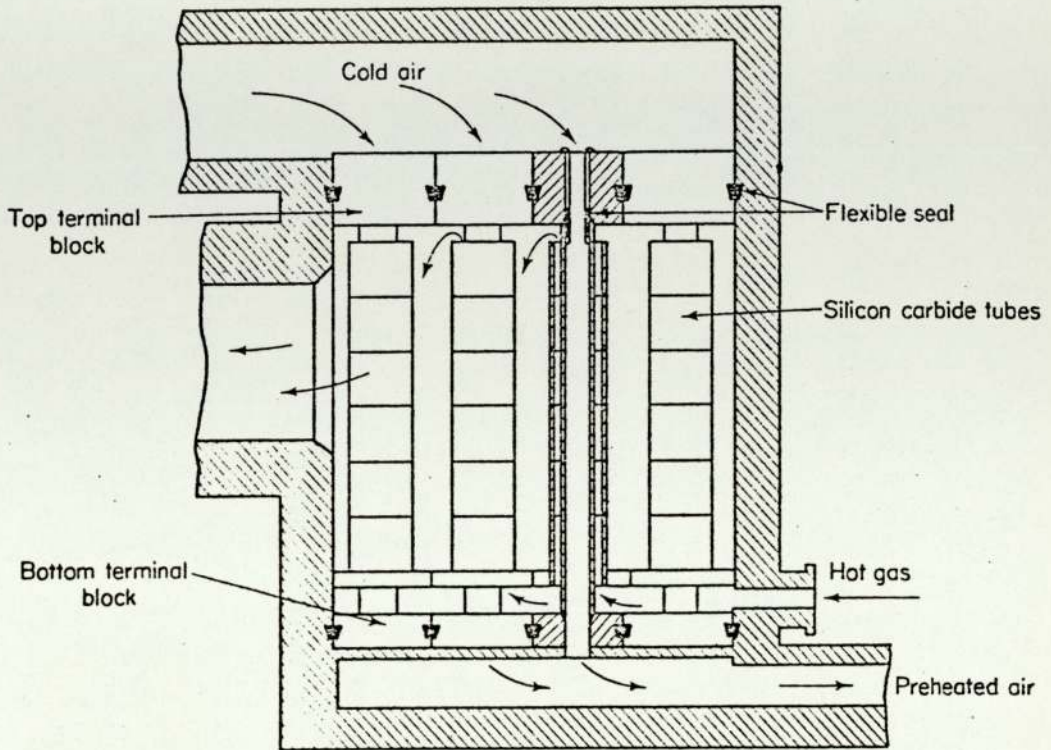


FIGURE 2.7 STOOKEY RECUPERATOR



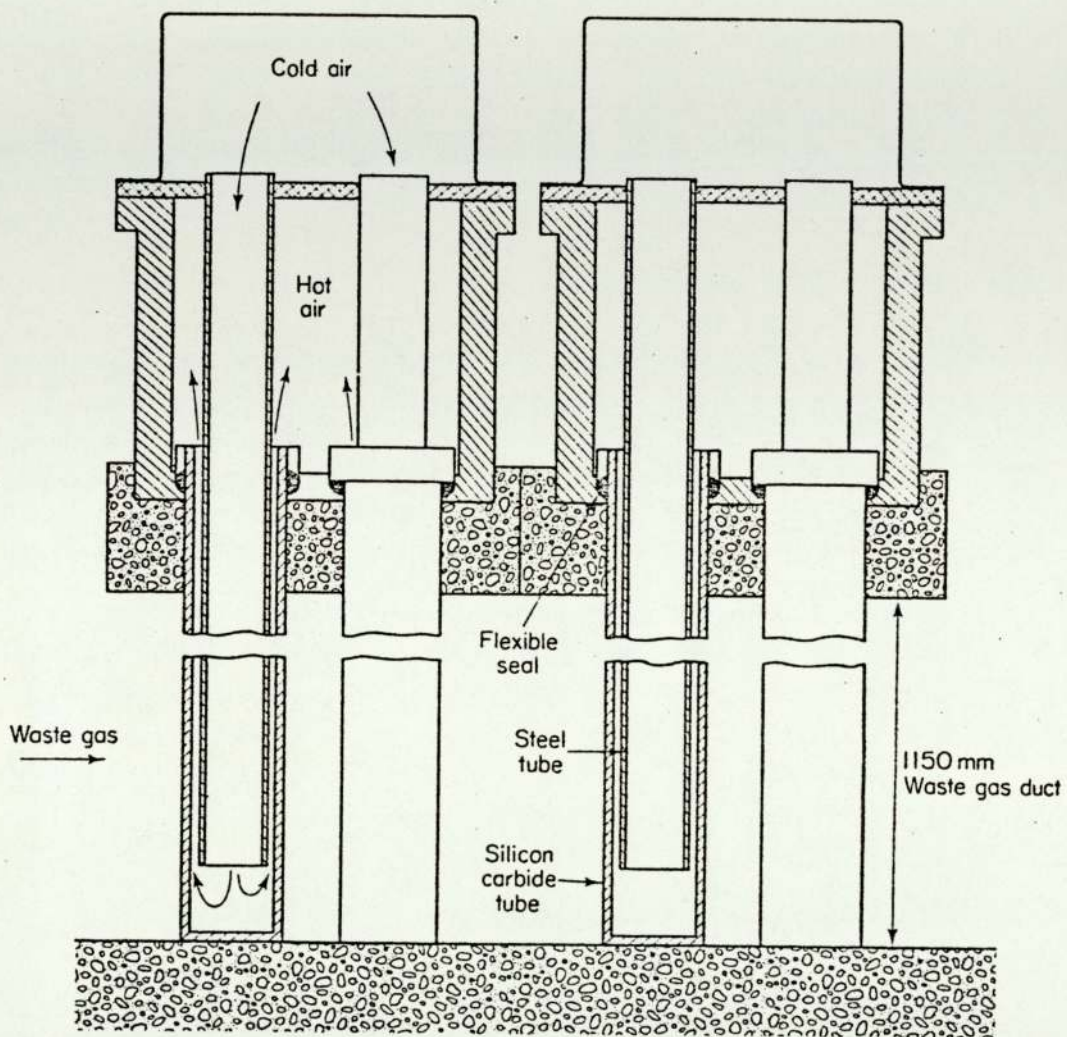


FIGURE 2.8 LACKENBY WORKS CERAMIC RECUPERATOR

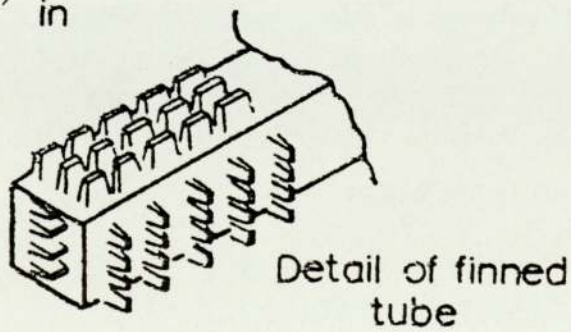
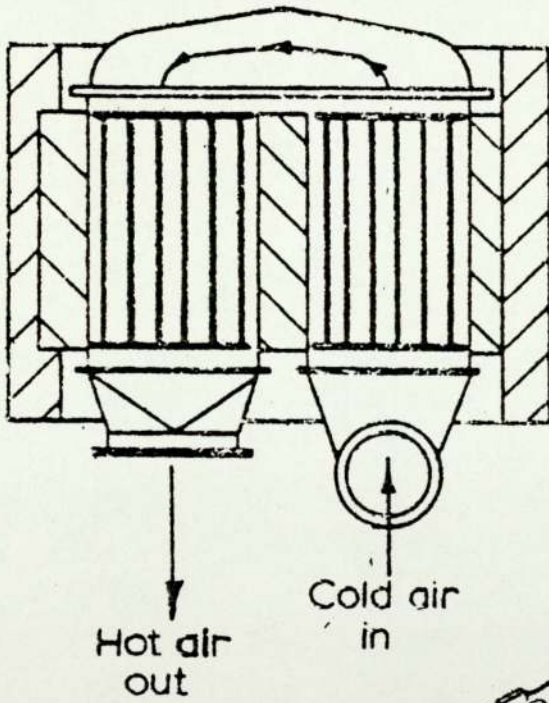
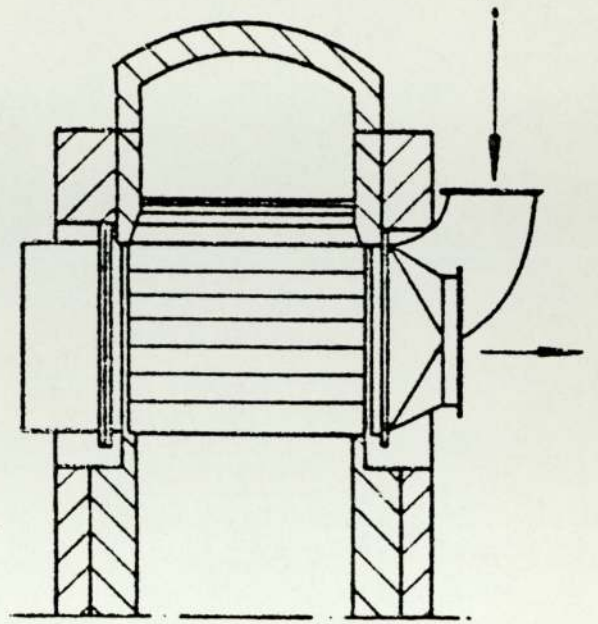
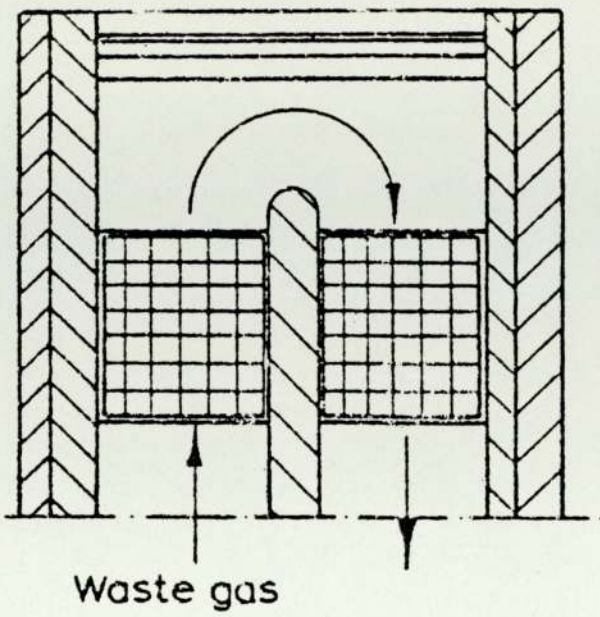


FIGURE 2.9 TYPICAL CAST TUBE RECUPERATOR



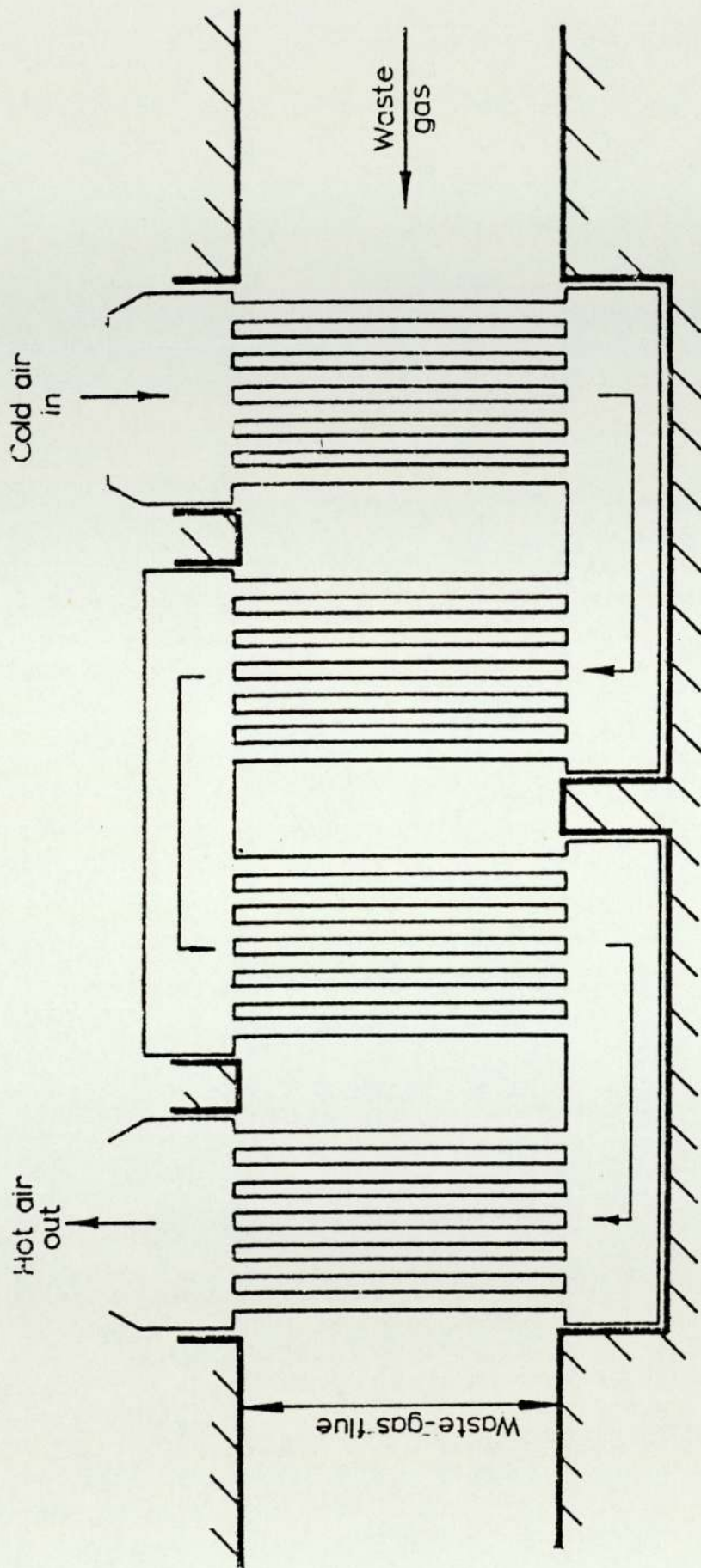


FIGURE 2.10 PENDANT TUBE RECUPERATOR

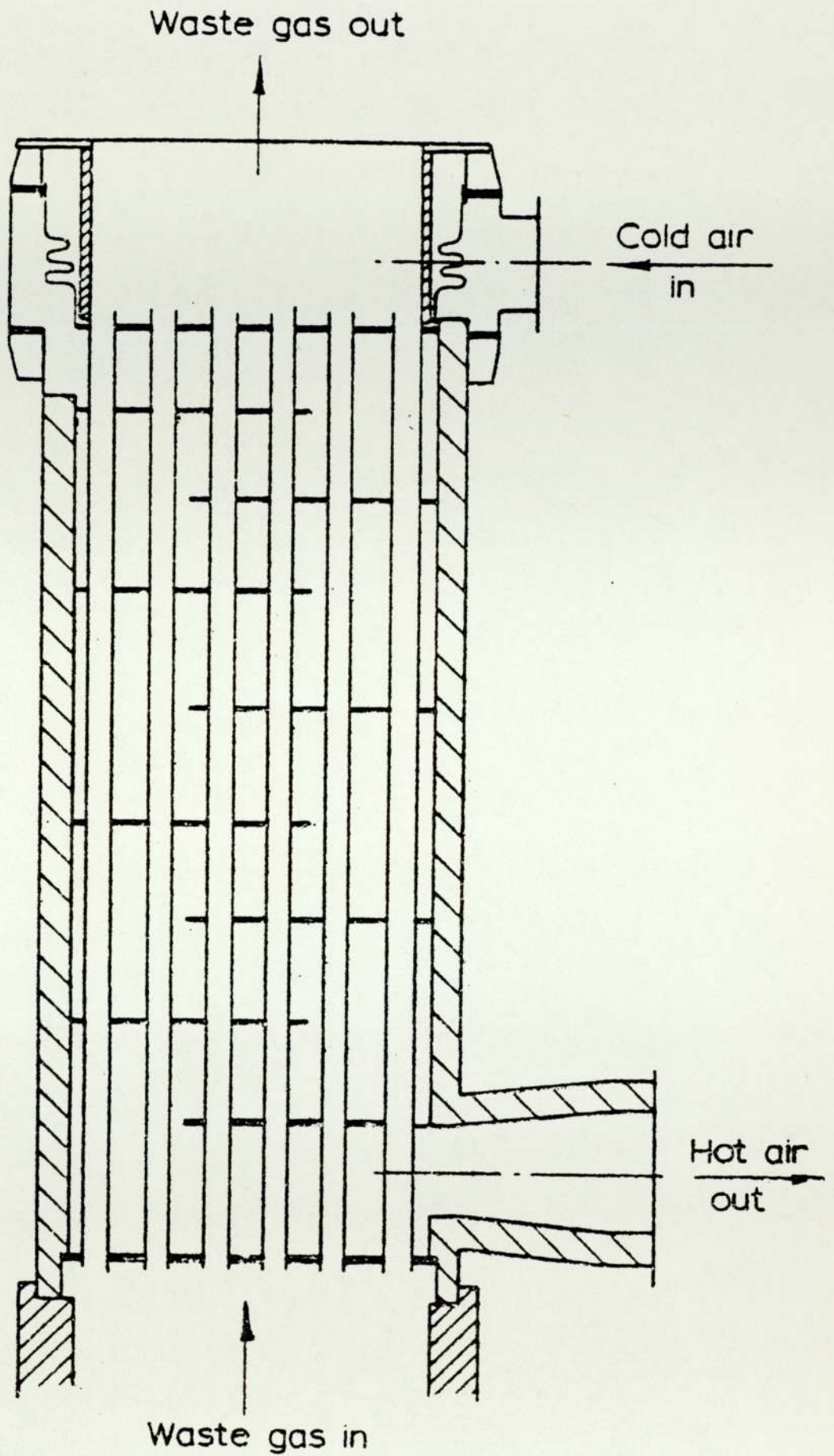


FIGURE 2.11 FLUE TUBE RECUPERATOR



Material	Composition					Max. work. temp	Cracks		Atmosphere slightly				Fuel ash
	C	Si	Cr	Ni	Other elements		Thermal shock	Sigma	H <sub>2</sub>	CO	H <sub>2</sub> S	SO <sub>2</sub>	
<b>Castings</b>													
<b>Irons:</b>													
Grey	3.2	1.5			0.7P 0.2P max	600	B			G	G	F	
Low alloy	3.2	1.8				650	B						
Silicon	2.0	6		30		850	B					FB	
Austenitic	2.0	5	5			900	G						
30% Chrome	1.5	1.0	30			1050	B	B					
<b>Steels:</b>													
Ferritic	0.25	1.0	28	2		1100	B	B		G			
Austenitic	0.4	1.5	25	20		1150	F	F		FG			FB
<b>Fabrications:</b>													
Mild steel	0.23	0.11				450	G	G			FP		
Al-coated MS	0.23	0.11			Al-sprayed	650	G	G			G		
Al-Si steel	0.03	2.5			1.0 Al	750	G	G			G		
PKI*	0.13	0.5	14-18		0.6 Ti	750	G	B	G		G	G	G
18/8 (320)	0.1	0.8	18	8.5		800	G	FG					FG
25/20 (310)	0.12	0.8	25	20		1150	G	FP					FB
20/30 (330)	0.15	2.0	20	35	0.25 Cu, 1 Mn	1100		VG					
Inconel*	0.1	0.7	16	75+	3.75 Al	1200	VG	VG					
Incoloy 800*	0.1	1.0	19/22	30/34	0.5 Cu max	1000	G	G					FB
Nimonic-75*	0.15	1.0	19.5	bal	0.2-0.6 Ti, 0.5 Cu	1200	G	G					FB
Nichrome*			20	80		1150	G	G					VB
Kanthal*			23	-	4.5 Al, 1 Co	1300	F	B					G

\*Trade name. VG = Very Good FB = Fairly Bad VP = Very Poor

SOURCE ; KAY (1973)

FIGURE 2.12 A GUIDE TO HEAT RESISTING FERROUS ALLOYS

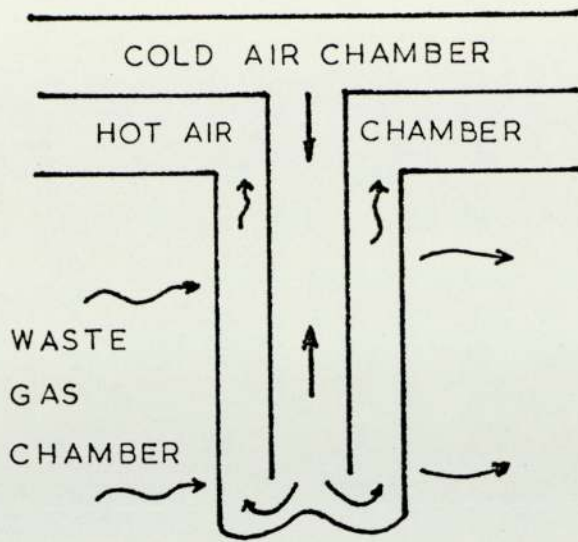


FIGURE 2.13 TUBE CONSTRUCTION FOR HAZEN RECUPERATOR

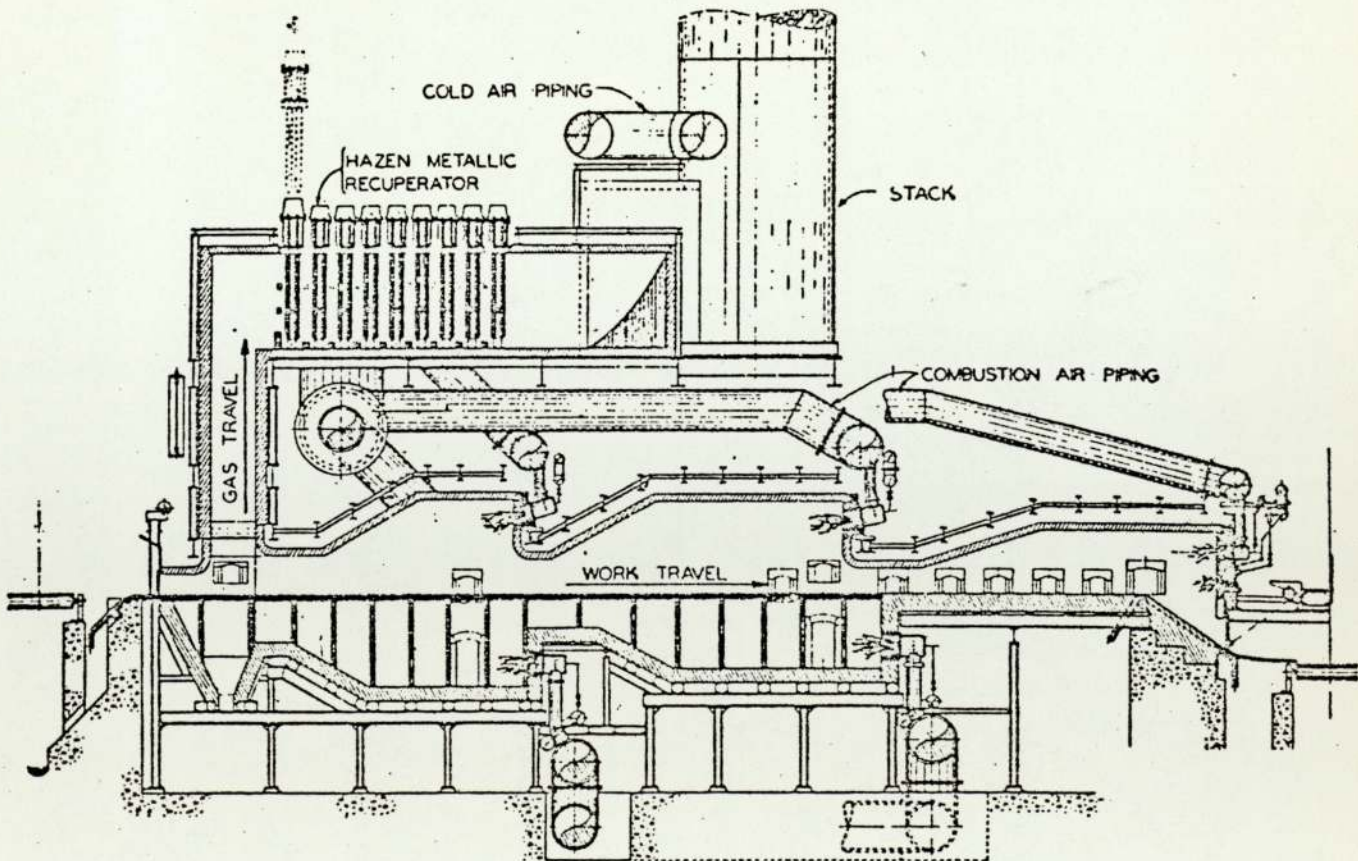


FIGURE 2.14 A TYPICAL LAYOUT OF HAZEN RECUPERATOR



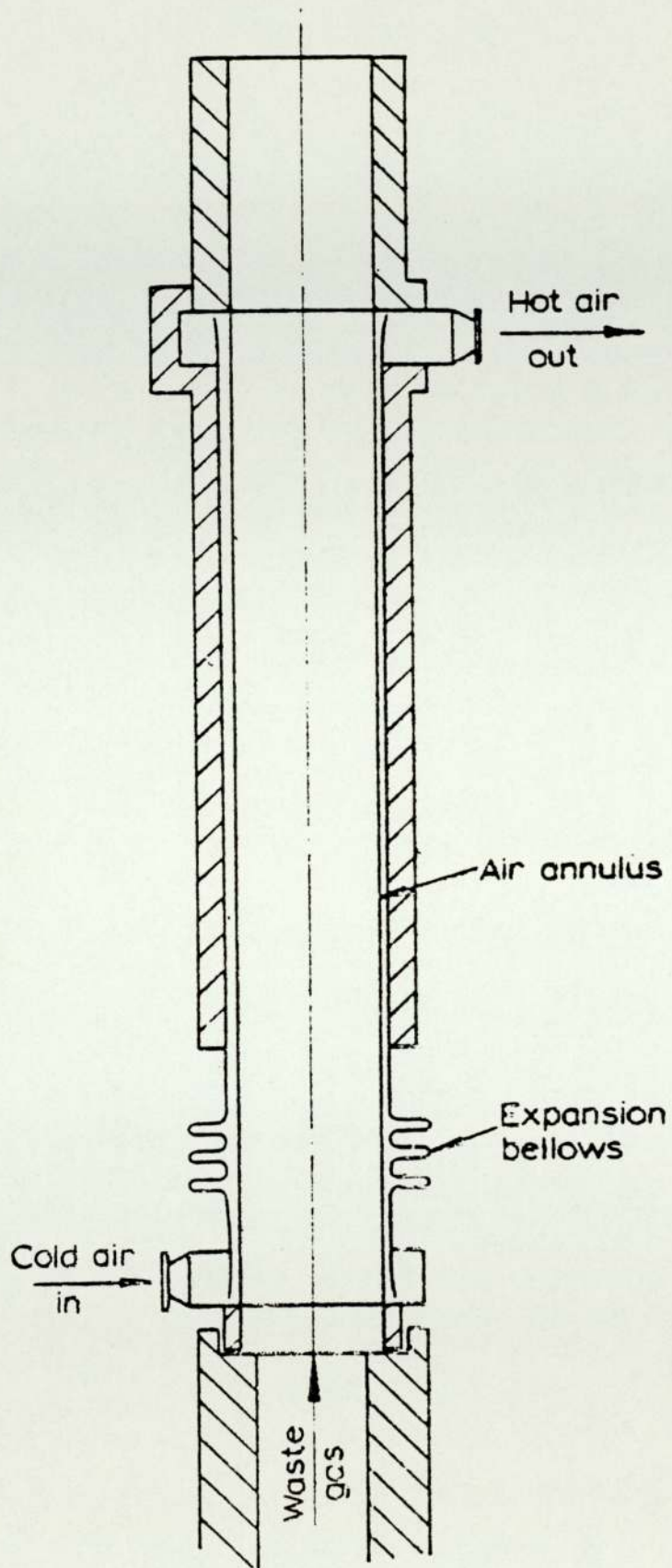


FIGURE 2.15 RADIATION RECUPERATOR

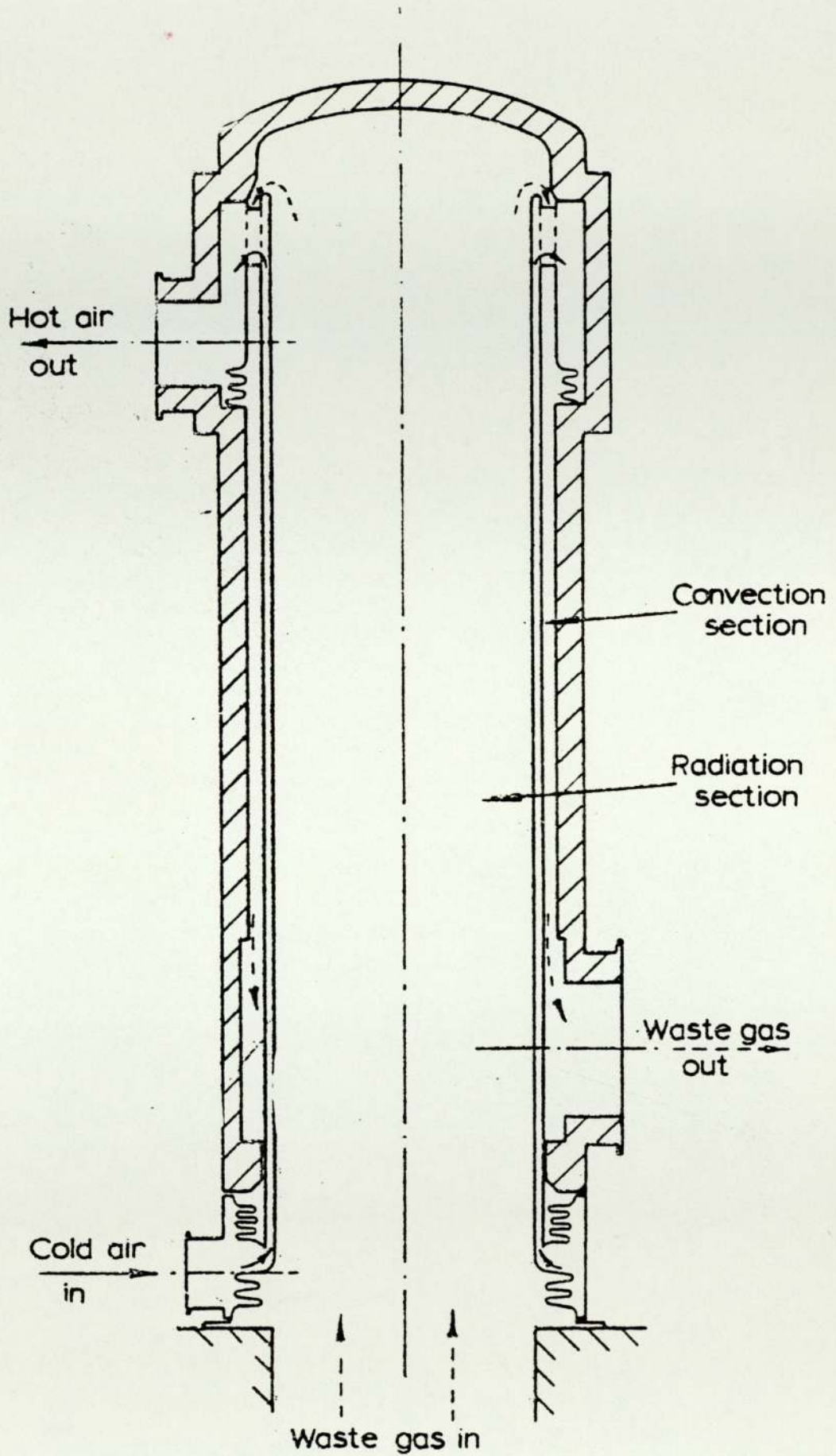


FIGURE 2.16 COMBINED CONVECTION AND RADIATION RECUPERATOR



CHAPTER 3  
ENERGY RECOVERY : NEW DEVELOPMENTS

### 3.1 Ceramic recuperator

The limitation of metallic and earlier types of ceramic recuperator has been amply discussed in Chapter 2 and were noted by Winkworth and Blundy (1972). To overcome these, the Corporate Engineering Laboratories (CEL) of the British Steel Corporation [Laws (1975), McChesney (1974), Morris (1974), Winkworth (1974) and Winkworth et al (1972)] proposed and patented a design in 1968 using long ceramic tubes which span the waste duct and are sealed into the recuperator walls using flexible ceramic seals as shown in Figures 3.1 and 3.2.

An intensive development programme was initiated to determine suitable tube and seal materials. The selection of a tube material was based on the following criteria:

- (i) High temperature strength
- (ii) High thermal shock resistance
- (iii) Low permeability
- (iv) Good thermal conductivity
- (v) Abrasion resistance
- (vi) Resistance to corrosion in furnace gases
- (vii) Reasonable dimensional accuracy in fabrication
- (viii) Low cost

The rate of heat transfer in an air-to-air heat exchanger is generally controlled by the heat transfer coefficients, therefore the requirement of high wall thermal conductivity is not critical. The choice of ceramic materials for the tubes was easily reduced to various grades of silicon carbide as only these offered the best chance of fulfilling the above specification.

The major limitation of all existing ceramic recuperators is the high rate of air leakage, requiring seal material capable of



operating at temperatures up to 900 C and flexible enough to allow for frequent expansion and contraction. A gland type seal packed with alumino-silicate ceramic fibre [Lloyds (1972)] was chosen as the seal design most likely to meet the above requirements. Ceramic fibre is available in a variety of forms and, provided a type without binder is used, retains its resilience at temperatures up to 1260 C. Laboratory tests were carried out to determine the seal life in terms of the heating and cooling cycle and to optimise on the best form of ceramic fibre. These tests indicated that on a full-scale recuperator, air leakage through seals after three years of heating and cooling cycles will be under 2 per cent.

Aerodynamic studies were undertaken to determine the best configuration and header design to minimise pressure losses on the hot-air side and to evaluate entry design to ensure uniform waste gas flow through the recuperator.

A mathematical model of a cross counter-flow recuperator was constructed to optimise on recuperator design and to carry out design studies for possible applications.

To fully evaluate the design and the predicted performance claims, the first CEL ceramic recuperator was built and commissioned on an oil-fired soaking pit at Llanwern Works in 1973. This recuperator was of four-passes, each tube bundle made up of four tubes long and eight tubes high. The preliminary performance tests showed that temperature limitations of metallic and leakage problems of earlier ceramic recuperators can be largely overcome.

To enhance air side heat transfer coefficients, the use of ceramic cruciform inserts [Myall (1975) and Myall (1976)] (see Figure 3.3) was considered and evaluated. Two types of cruciform materials were tested in the prototype ceramic recuperator at Llanwern steelworks. These were:

- (a) mullite type refractory with good thermal shock and abrasion resistance for high temperature use
- (b) High alumina castable refractory in the low temperature region.

Good agreement between predicted and measured preheats was noted. Air preheat temperatures up to 630 C have been obtained without cruciforms and an average fuel saving of 10 per cent above that obtained in an identical soaking pit operating with metallic recuperators is forecast.

The air flow leakage is determined using an oxygen probe to measure oxygen content of waste gases before and after the recuperator. No differentiation is made between air leakage from atmosphere and from combustion air. Because of a low and relatively negligible pressure differential between atmospheric and waste gases in comparison with the difference between combustion air and waste gases, it can safely be concluded that an overwhelming proportion of the air leakage is contributable to the latter. Air leakage directly to atmosphere was observed but it was not possible to quantify.

A linear relationship between air flow and percentage air leakage to the waste gas was observed as shown in Figure 3.4, and under normal pit operating conditions air losses of between 10 and 12 per cent were measured.

A hybrid system of energy recovery from waste gases using a two-pass ceramic recuperator incorporating new seal design followed by a metallic recuperator has been installed and commissioned at Normanby Park works.

The air leakage into the waste duct has been successfully reduced to under 2 per cent of the total flow at full flow conditions. The introduction of cruciform inserts has not contributed to air leakage.

An average air preheat of 665 C with a waste gas temperature of



1100 C were measured, and at turndown during soak period, of 745 C with waste gas temperature of 1100 C.

In a hybrid system capital cost recovery of the ceramic part is under two years. On the above basis, air preheats in excess of 700 C are possible at full flow conditions with a waste gas temperature at entry of 1200 C.

### 3.2 Rotary regenerator

A rotary regenerator can take one or other of the forms shown in Figure 3.5. The rotary disc type is the more widely used. The disc is the simpler and has the advantage of low production cost. In some cases, the drum type is better suited especially if the centre portion can be used to house other components. However, the difficulty in matching differences in thermal expansion and contraction of ceramic and metallic parts causes problems. Also, in the disc type, the flow area is increased by an increase in the diameter of the disc, whereas in the drum type, axial length has to be increased. Ritz originated the idea of using the rotary regenerator for air-to-air heat recovery. The design of a disc type regenerative heat exchanger has been evaluated by Hrynyszak.

In recent years, the rotary regenerator has been employed in many applications, including heating and ventilation systems, medium temperature heat recovery from gas turbines, [Winkworth and Applegate (1974), Blundy (1972)] and boiler plant waste gases. The rotary regenerator provides a very compact heat exchanger (i.e. high surface area to volume ratio) but high temperature non-uniformities cause sealing problems.

Conventional rotary regenerator matrices consist of metallic or ceramic heat storage elements. These are completely enclosed in metallic cages or baskets as shown in Figure 3.6. The seals between

the air and gas stream system are located and operate on these cages or baskets. Therefore, the maximum gas temperature is restricted to the maximum operating temperature of the cage material and the ability of the seal system to cope with the thermal distortions of the metallic cage. Cost considerations limit the choice of materials and hence the upper waste gas temperature is limited to around 1000 C.

CEL has carried out preliminary theoretical and experimental studies on rotary regenerators for high-temperature heat recovery from steelworks waste gases [Pereira(1976)]. As a result of these developments, several novel designs of rotor and sealing systems have been proposed to surpass the current limits. A high temperature test rig was under construction at CEL, which will be used to evaluate these designs.

A rotor assembly as shown in Figure 3.7, which is the subject of a BSC patent application, has been selected for further development. It is mounted in a horizontal plane and rotates about a vertical axis by a drive mechanism acting on the circumference. A counter-current heat transfer mode is achieved by passing hot gases downward and air upward through the ceramic rotor. The rotor assembly is made up from rectangular sectioned heat storage blocks supported on a metallic grid. The flow configuration is such as to give a low temperature in the lower half of the assembly where the metallic grid is positioned. Mathematical modelling studies have shown that stainless steel can be used for the support grid structures.

The selection of the matrix block material was decided on the following criteria:

- (a) High corrosion and oxidation resistance
- (b) High thermal shock resistance
- (c) Good refractory properties
- (d) Ease of fabrication into matrix blocks



The choice of materials is between the 'mullite' group of alumino-silicates, sillimanite with 50 - 70% alumina content and alumina-bonded silicon carbide. All of these have excellent thermal shock properties and are currently in use in steelworks.

In a regenerator application study on an Opposed Zone Reheating Furnace, a waste gas temperature of 1300 C would require a matrix face area of 167 m<sup>2</sup> to give an air temperature of 1100 C. Considering fabricating limits on the rotor matrix, an axial length of 0.7m is required with an air leakage allowance of 10% of total air flow. This will result in a potential fuel saving of 28 per cent, which is equivalent to fuel cost savings of £600 000 per annum. From these initial studies this project is economically viable. A programme of further studies was planned by CEL.

### 3.3 Evaporative cooling of blast furnace

The modern trend in increased size of blast furnaces has placed a heavy burden on their cooling systems. The need to maintain adequate cooling for increased furnace campaign life and to reduce maintenance cost in the face of the high cost of or shortages in water supply has led to the development and use of closed re-circulation cooling systems [Pyne (1973)]. For increased economy, the evaporative cooling of blast furnaces was developed and has been used with some success in the Soviet Union.

The earlier once-through system has been largely replaced by the open-recirculation cooling system [Schnegelsberg (1974)]. The choice is generally made on the basis of the local water supply situations. In the open re-circulation system, the make-up water can be as high as 30%, therefore, both of these rely on the continuity of water supply and shortages can lead to severe reductions in furnace campaign life. The use of untreated industrial water leads to frequent

breakdown of blast furnaces due to the failure of the cooling elements. Therefore, the development of a more reliable and efficient cooling system is an essential requirement to keep production costs to a minimum in large blast furnaces. The development and use of the closed re-circulation cooling system has reduced the need for make-up water. Also the design for more reliable cooling elements as well as chemical treatment of make-up water has enabled the campaign life of blast furnaces to be considerably prolonged. Four systems of blast furnace cooling are shown diagrammatically in Figure 3.8.

The closed re-circulation system offers many advantages over the open re-circulation system and the once-through system. They include:

- (a) the negligible make-up water requirement
- (b) the improved water-treatment is economical which improves the life of the cooling elements and lowers clean-out expenses, hence overall maintenance costs are reduced
- (c) the water supply is not critical
- (d) the current practice in blast furnace cooling system operation enables one or more cooling elements to be isolated for repairs without disturbing the operation

However, special precautions against breakdown of the cooling system are necessary to prevent large scale damage to the furnace. This is because of the lower water capacity of the closed re-circulation system.

Nearly half of the energy loss from the blast furnace is in the form of the low grade cooling water thermal energy. The recovery of this energy in useful form will represent a significant improvement in the economics of the furnace operation. The evaporative cooling of blast furnaces has been successfully developed and used in the USSR and other countries as a economically viable proposition. The pumping costs are considerably reduced by using natural circulation. The



steam produced can power a turbine to generate electricity or used to augment the steam mains.

Glazkov and Krasnozhen (1960) describe the use of the evaporative cooling system on a 1033 m<sup>3</sup> blast furnace which was first blown in November, 1957. The cooling system was divided into two zones (upper and lower), each of which consisted of six sections. Each section of the top zone had 36 coolers, whereas in the bottom zone there were between twelve and fifteen coolers each. All were plate coolers with four pipes cast in each. The columnwise sections were independently connected to an overhead steam separator tank. The installation was rated at 5 kg/s of steam at 12 atm.

Its initial operation on non-deaerated water led to the corrosion of some parts and hence the steam pressure was limited to 4 atm. No problems were encountered in the first year but in the second year the uneven thermal loading in some sections caused dry-out conditions. The change in charging procedure to compensate for this proved successful. In conclusion it was found that the system needs to be simplified and its controls centralised.

Most of the recommendations of the above report were incorporated in the installation reported upon by Zherebin et al (1966). In three years of its operation some twenty mantle coolers failed through the formation of cracks in the water inlet tube at the welded joints. A total of 39 coolers were turned off where thermal loading was a maximum and the shell in these areas was cooled by water sprays.

A typical vertical plate cooler is shown in Figure 3.9 which can be used on most of the blast furnaces with minor modifications.

For safe and reliable operation of plate coolers, they are designed to withstand furnace atmosphere without the added protection of the refractory lining. Also the spacing between cooling pipes is selected such

that in the event of a pipe failure the adjacent pipes can carry the additional thermal loading and prevent damage spreading to other coolers as well as the shell.

Evaporative cooling offers many advantages, of which some are listed below:

- (i) the use of chemically treated and deaerated water which:
  - (a) eliminates scale accumulation in the cooling tubes thus maintaining a high rate of thermal exchange
  - (b) increases the life of cooling elements because of the high heat transfer rate, so reducing maintenance cost
- (ii) the quantity of make-up water is small hence the feedwater supply piping, pumps and screening equipment can be substantially reduced in size.
- (iii) the direct use of steam eliminates cooling towers, air coolers etc.
- (iv) the natural circulation of water in the system ensures adequate cooling of the blast furnace in the event of power failure.
- (v) the experience in the USSR shows that the normal campaign life of blast furnaces can generally be doubled.
- (vi) the controlled operating temperature (evaporating temperature) ensures that furnace operation is independent of climatic changes.

Both German [Schnegelsberg (1974)] and USSR experience indicates that substantial savings are possible with the use of evaporative cooling, particularly where water shortage due to ecological, geographical or climatical reasons is prevalent. Also the savings in energy terms are sufficient to more than offset the cost of installation and operation. Therefore, the British Steel Corporation should look critically whenever faced with a decision for a major overhaul of the existing cooling system or a new blast furnace.



### 3.4 Dry-coke quenching

The dry-coke cooling system was developed by Sulzer Brothers in Switzerland in the early 1900's [Savage (1949)]. A number of plants were installed but were later abandoned as low-cost natural gas became readily available. Hence, in the majority of the coke-oven plants operating throughout the world, the coke is quenched with cold water in an open tower, consequently its energy is dissipated to the atmosphere in the form of steam and water spray.

The interest in dry-coke quenching has gathered momentum with the increase in fuel price [British Steel Corporation (1970)]. A latest report by American Waagner-Biro Co., 1975, based on studies in various countries, concludes that an average pay-off period is under four years. Therefore, the financial incentive for re-consideration is overwhelming and in the next decade or two an upsurge in the installation of dry-coke quenching plants is anticipated.

A dry-coke cooling system is shown in Figure 3.10. An inert gas circulates between the hot-coke chamber and a waste-heat boiler in which the gas is cooled. The hot coke is cooled from over 1000 C to around 200 C and its thermal energy is used to raise steam.

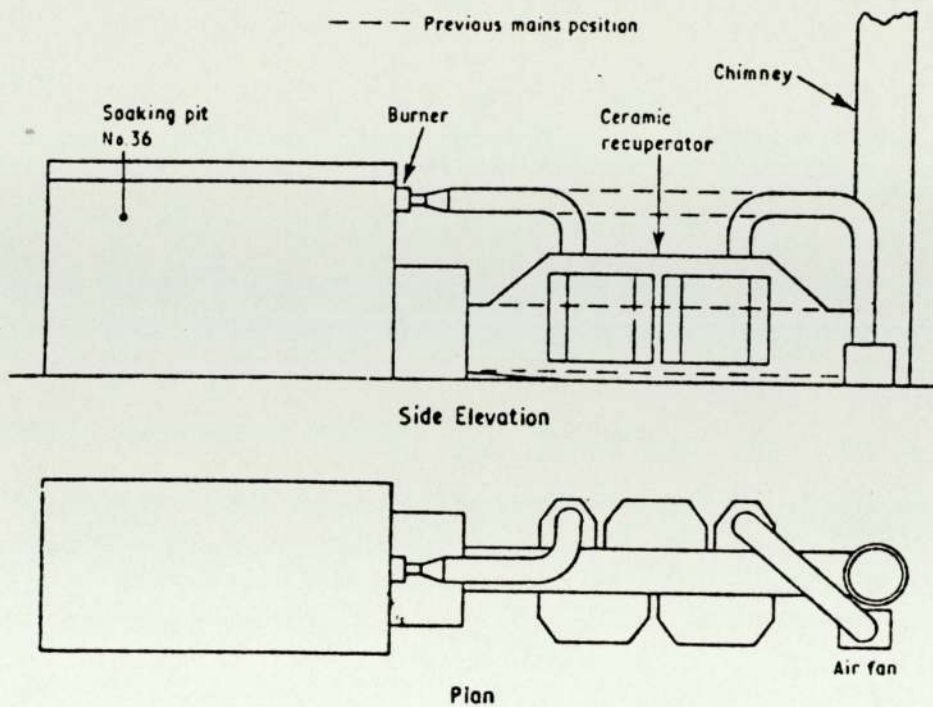


FIGURE 3.1 INSTALLATION OF PROTOTYPE CEL CERAMIC RECUPERATOR AT LLANWERN

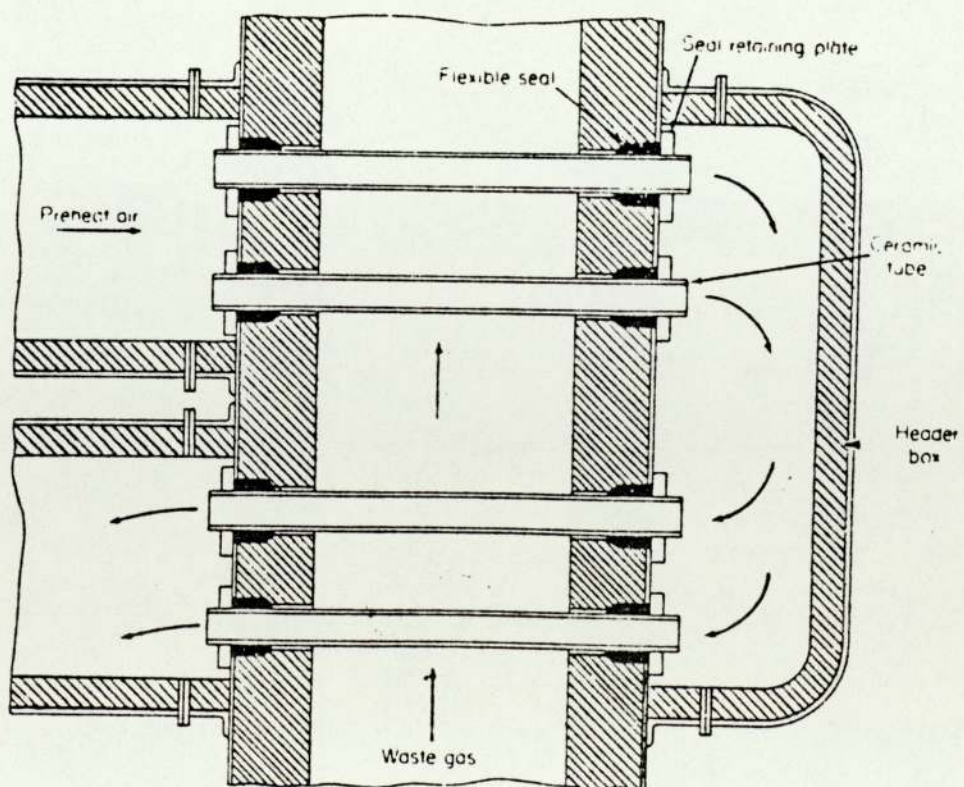


FIGURE 3.2 A CROSS-SECTION VIEW OF CERAMIC RECUPERATOR





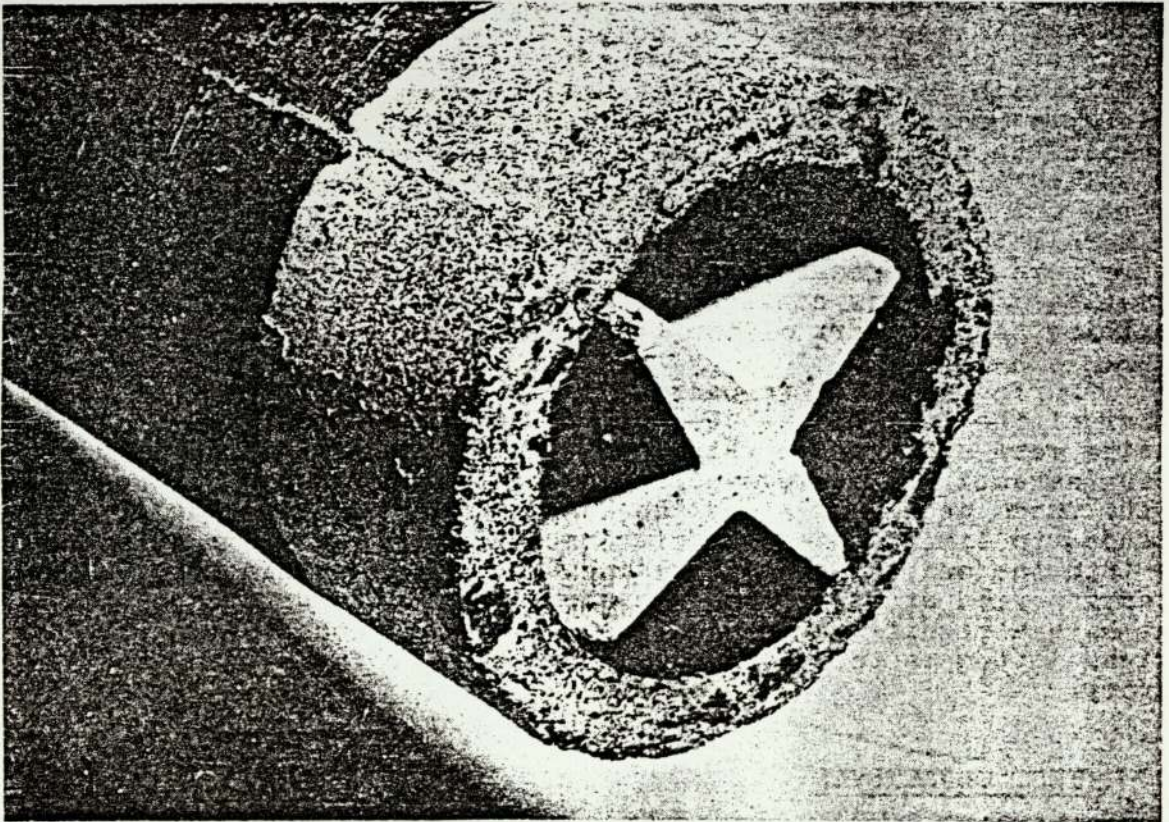


FIGURE 3.3 CERAMIC CRUCIFORM INSERT

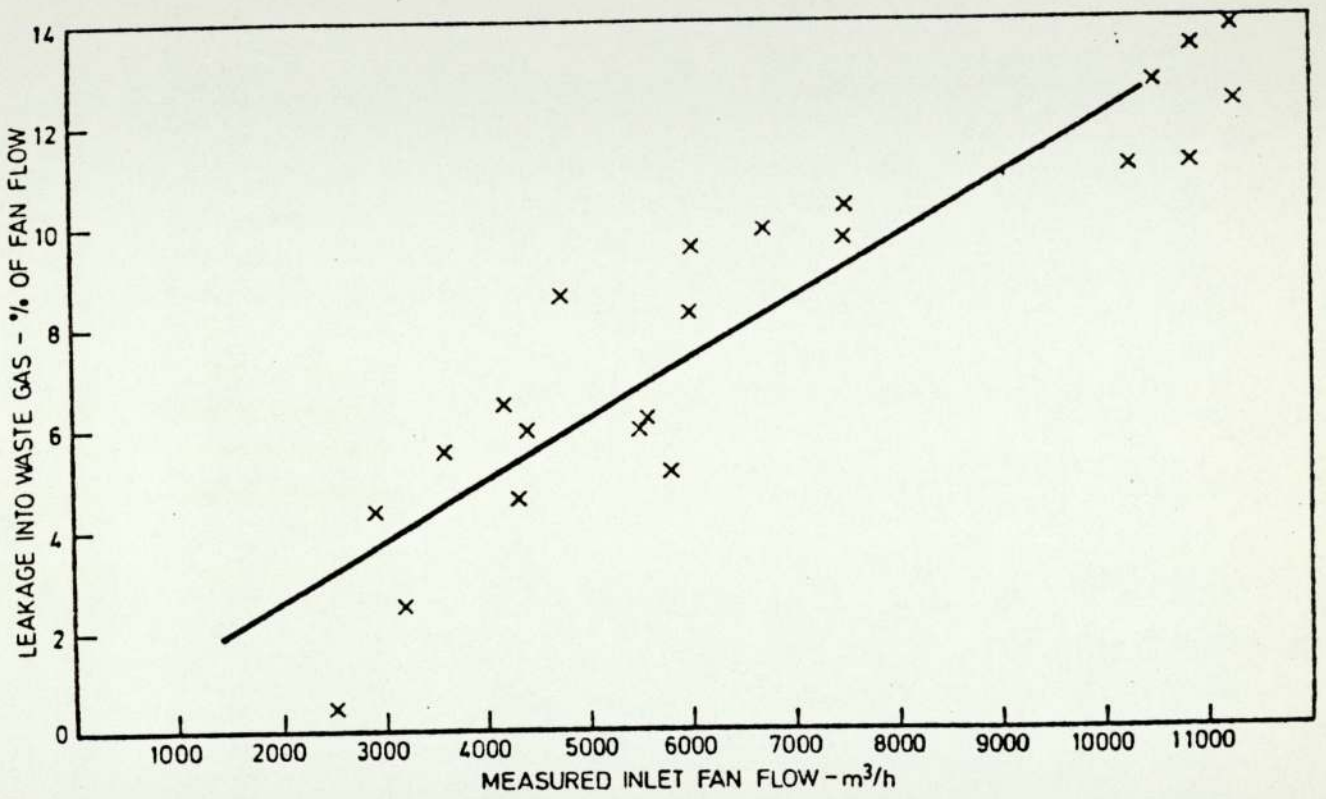
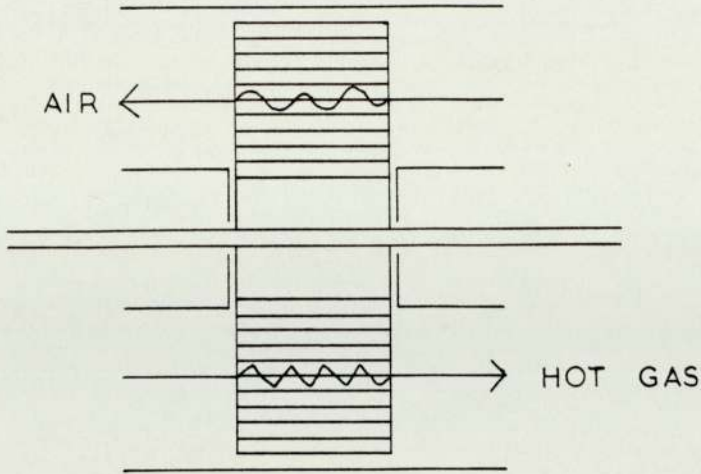
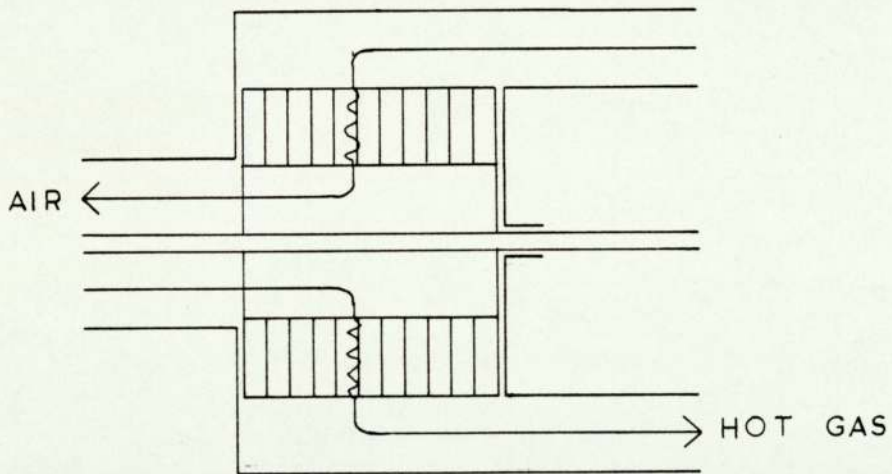


FIGURE 3.4 LEAKAGE INTO WASTE GAS v. MEASURED INLET FAN FLOW



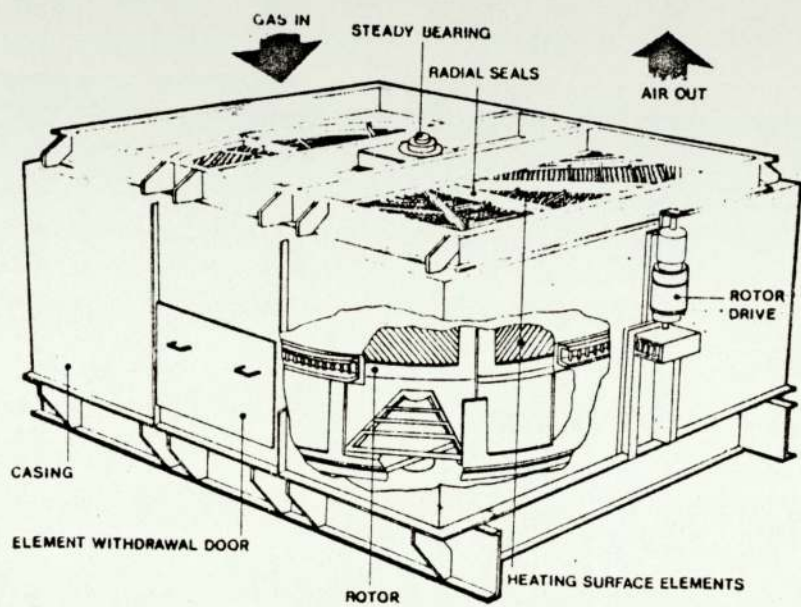


A. DISC



B. DRUM

FIGURE 3.5 TYPES OF ROTARY REGENERATORS



[SOURCE : DRUMMOND (1974)]

FIGURE 3.6 A TYPICAL METALLIC ROTARY REGENERATOR



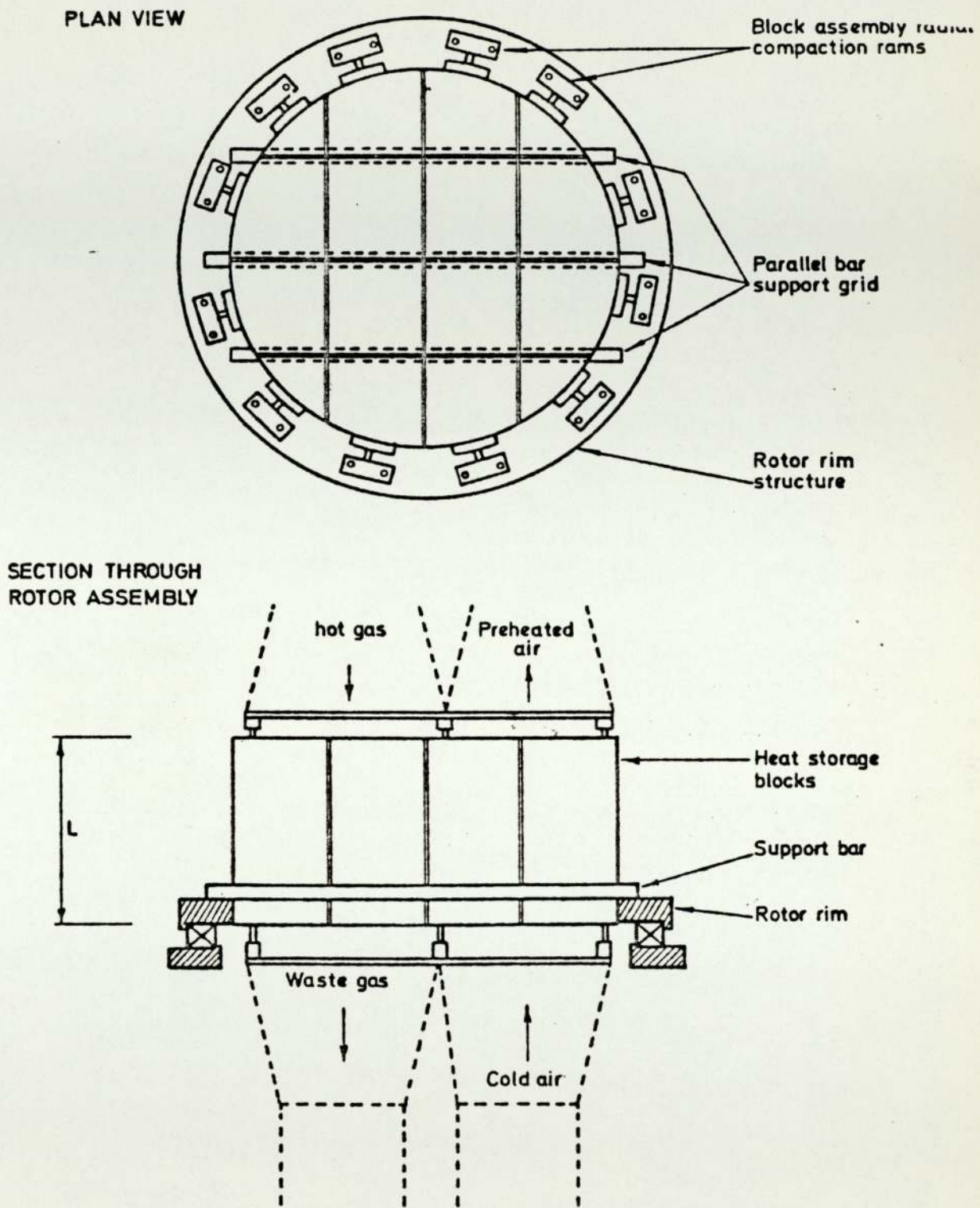
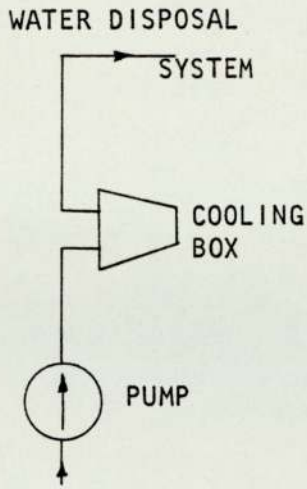
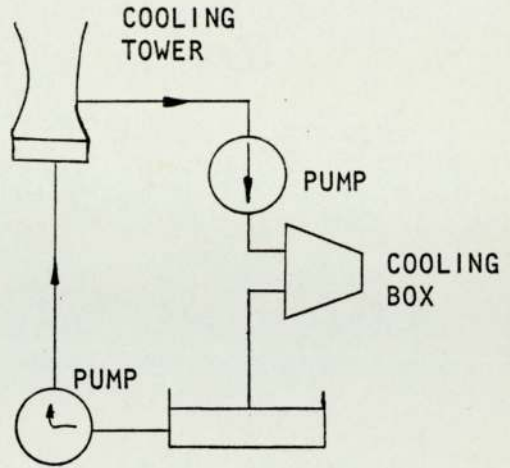


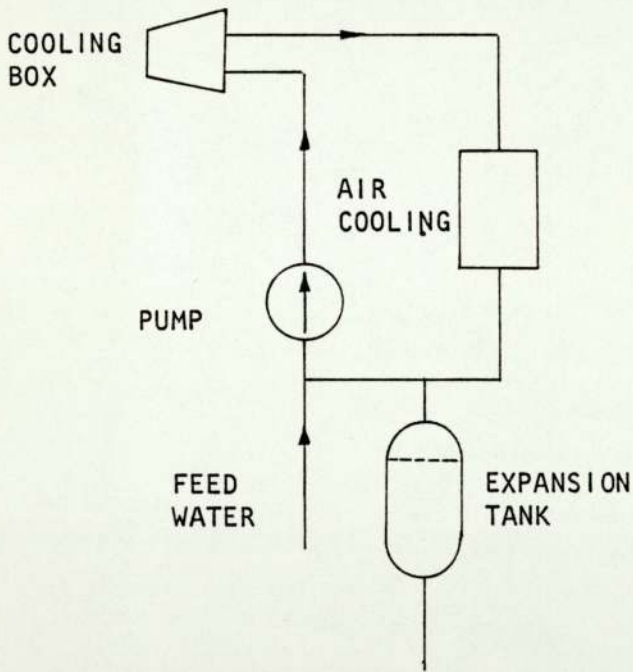
FIGURE 3.7 THE ROTOR ASSEMBLY OF CEL CERAMIC ROTARY REGENERATOR



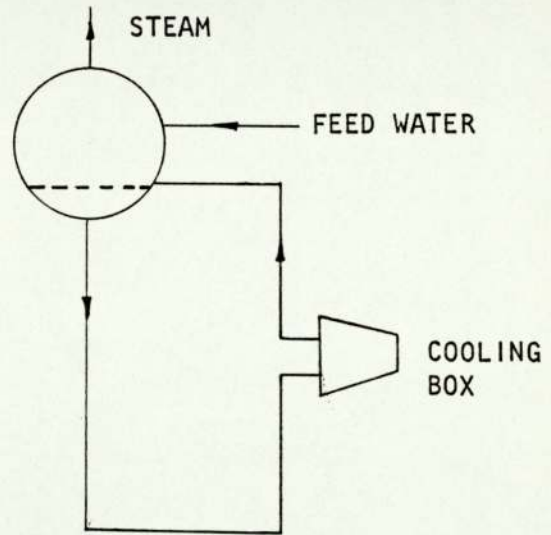
(a) ONCE-THROUGH SYSTEM



(b) OPEN RECIRCULATION SYSTEM



(c) CLOSED RECIRCULATION SYSTEM



(d) EVAPORATIVE COOLING SYSTEM

FIGURE 3.8 - Comparison of blast furnace cooling systems



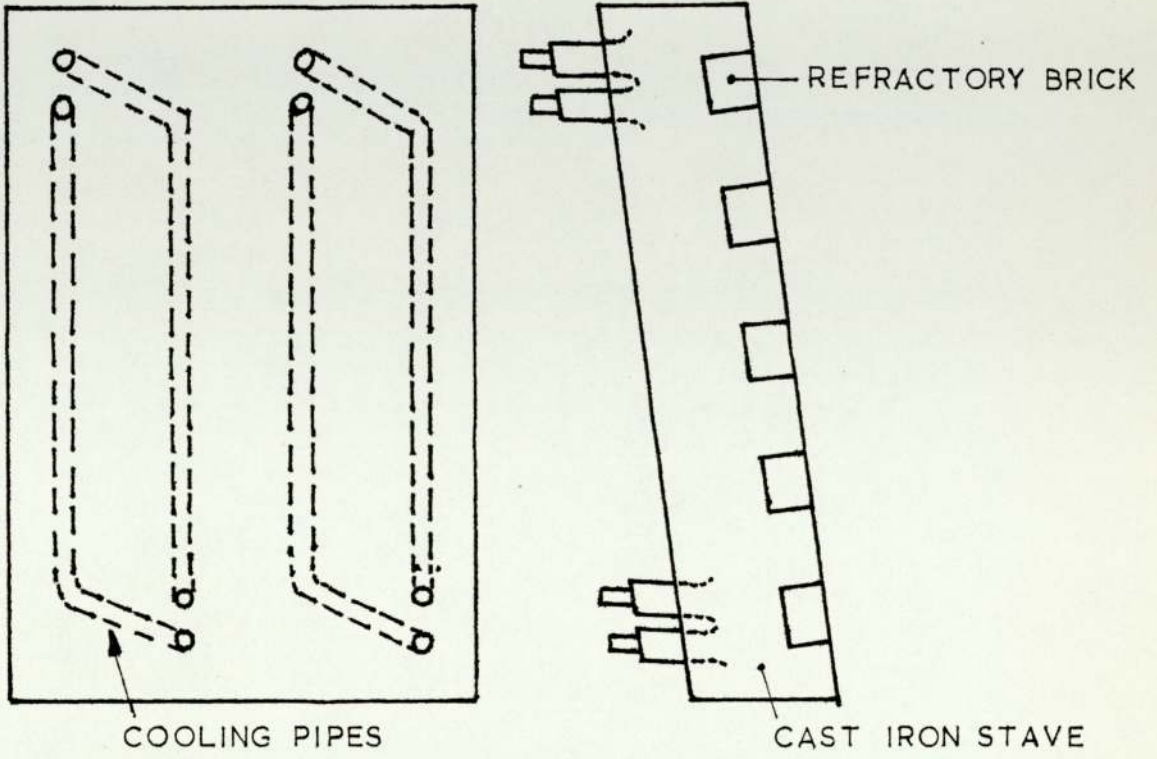


FIGURE 3.9 TYPICAL EVAPORATIVE-COOLING COOLER

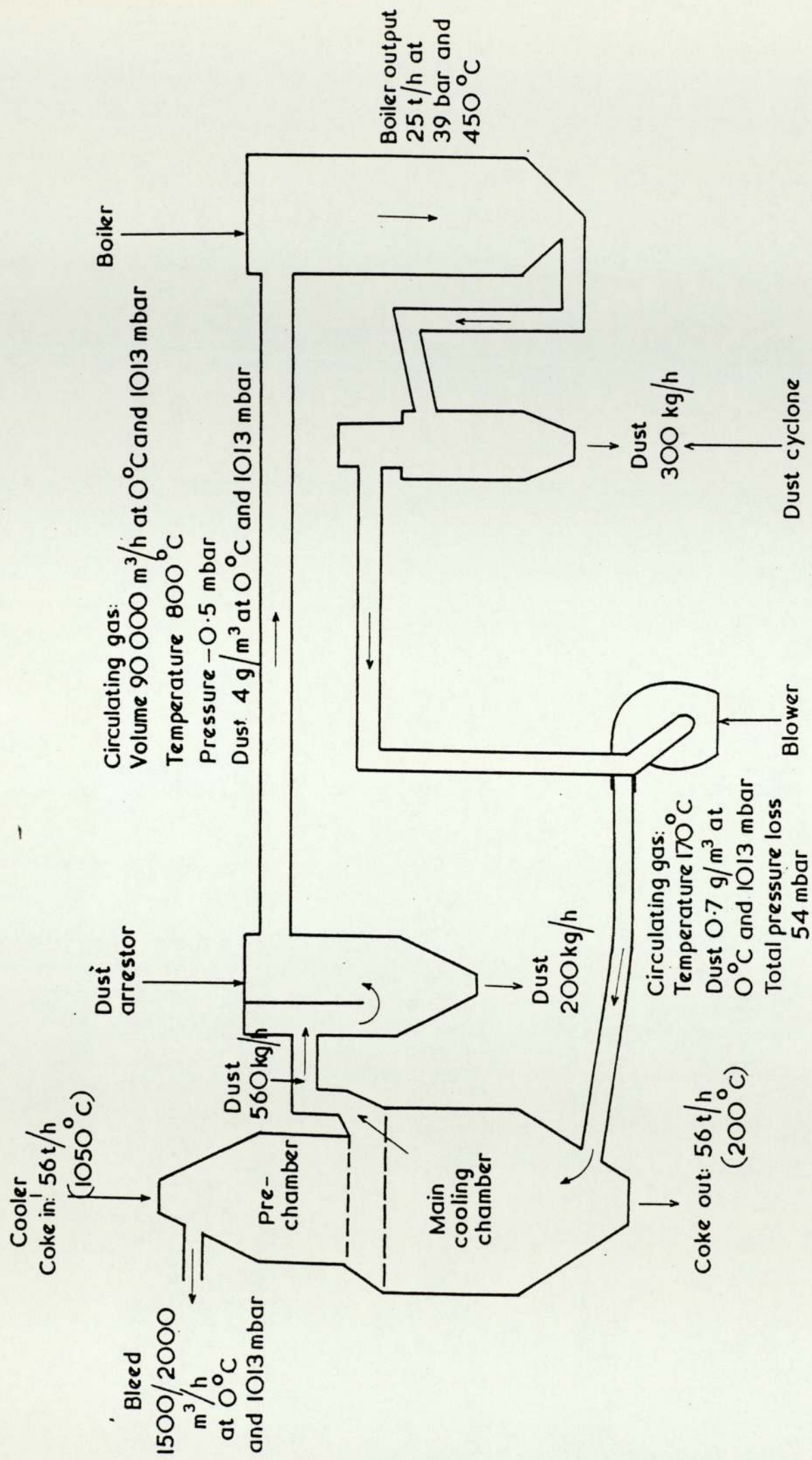


FIGURE 3.10 GIPROKOKS DRY-COOLING SYSTEM

(TYPICAL WORKING DATA)



CHAPTER 4  
ENERGY RECOVERY : NOVEL TECHNIQUES

## 4.1 Fluidised bed recuperator

A fluidised bed recuperator consists of two fluidised bed streams (waste gas and combustion air) with heat pipes spanning them. This design of an air-to-air recuperator is an attempt to use the advantageous properties of both heat pipe technology and fluidisation (see Appendix I) to recover thermal energy from high temperature gases or combustion products to preheat combustion air required within the primary combustion process.

In all current heat exchangers, a common wall is introduced between the two streams to transfer energy and to reduce cross contamination. But the proneness of numerous joints to crack and open-out increases leakage with usage. The use of heat pipes eliminates the common heat transfer area hence cross contamination. Also the high rate of axial heat transfer insures that the surface temperature difference between evaporator and condenser sections is low.

Other major shortcomings of the present air-to-air heat exchangers are:

- (i) poor rate of heat transfer between fluid and surface
- (ii) the need for air dilution of high temperature gases especially in metallic recuperators, to enable the use of cheap manufacturing materials and to prolong their working life.

Both of these problems can be overcome by the use of fluidised bed techniques at the expense of using 'high grade' mechanical/electrical energy to power air compressors or suction pumps. The rapid mixing of particles in the gas fluidised bed leads to equalisation of bed temperature, hence a uniform temperature front is presented to the heat exchange surface. The improved rate of exchange associated with the fluidised bed technique leads to a compact heat



exchanger and hopefully lower capital expenditure should be required for similar thermal conditions. But the cost of heat pipes needs to be considered.

The limitations imposed by the fluidisation technique severely restrict the design of recuperator. The essential requirements are upward flow of fluid at a rate limited by the minimum fluidising velocity and the terminal velocity. Also the heat pipe axis must be horizontal. This reduces the possible configuration of a fluidised bed recuperator to that shown in Figure 4.1.

#### 4.2 Fluidised bed regenerator

The need to combine two new and relatively little known technologies in the fluidised bed recuperator requires a substantial research programme for its development. The use of particle exchange by pneumatic transport eliminates heat pipes and so reduces the research programme to one technology. The fluidised bed regenerator is an attempt towards this end and also to eliminate the restrictions placed by the use of heat pipes on the operating temperature range.

The fluidised bed regenerator can take one of the two configurations shown in Figure 4.2. The first type is an adaptation of the fluidised bed recuperator. The method of heat exchange between two beds is changed from the use of heat pipes to pneumatic transport of solid particles. An air lock for each particle conveyancing system is provided to reduce cross contamination of the streams. In the second type only one air fluidised bed is necessary. The thermal energy from hot gases is transferred to the particles as they fall under gravity through the upward moving hot gas stream. This eliminates the need for a fluidised bed in the hot gas stream and pressure drop across the free falling cloud of particles is sufficiently low to make a natural draught system feasible. A more detailed description

of each type of fluidised bed regenerator is given under the appropriately named headings.

The principle of a moving bed regenerator has been considered before [Dul and Schneller et. al. (1974)] and two designs are shown in Figure 4.3. These employ fixed bed systems where particles are fed under gravity from hot to cold fixed-bed and returned via mechanical means. The air and waste gases slowly percolate through their respective beds. The rate of particle flow is controlled by a central nozzle.

#### 4.2.1 F-B Regenerator - first type

Figure 4.2(a) shows a simple single stage fluidised bed regenerator. The bed in stream 'A' is fluidised by hot gases and, due to the existence of a temperature difference, the particles are heated to a temperature dependent on their respective residence times. However the rapid mixing of the particles in the bed insures that a uniform temperature of the bed is attained. These particles are fed under gravity through an air lock to the pneumatic conveyancing system on to the bed in stream 'B'. The particles impart their thermal energy to the cold stream of air employed to fluidise the particles. Then they are returned via a similar system to the bed in stream 'A', thus completing the cycle. Under ideal conditions if the residence time is long enough and there are no heat losses through the container walls, the bed temperature and the temperature of gases leaving the bed will reach a state of equilibrium dependent upon the relative thermal capacities and mass flow rates of particles and fluidising medium i.e:

For bed 'A'

$$\dot{m}_g C_{pg} (T_{gi} - T_{go}) = \dot{m}_s C_{ps} (T_{so} - T_{si}) \quad (1)$$

for ideal and steady conditions  $T_{go} = T_{so}$



Similarly for bed 'B'

$$\dot{m}_a C_{pa} (T_{ao} - T_{ai}) = \dot{m}_s C_{ps} (T_{si} - T_{so}) \quad (2)$$

for ideal and steady conditions  $T_{ao} = T_{so}$

For single stage fluidised beds

$$(T_{so})_A = (T_{si})_B \text{ and vice versa}$$

Therefore, the above equations reduce to

$$(T_{ao} - T_{ai}) = (T_{gi} - T_{ai}) / \left[ 1 + \frac{\dot{m}_a C_{pa}}{\dot{m}_g C_{pg}} + \frac{\dot{m}_a C_{pa}}{\dot{m}_s C_{ps}} \right] \quad (3)$$

From the above it can be concluded that the maximum air preheat is limited by the mass flow rate of particles, which in turn requires expenditure of power. Therefore, a compromise will be necessary. For soaking pit applications, where a 2:1 ratio of gas:air mass flow rate is required for gas (BF)-fired pits, the maximum air preheat is limited to midway between entry gas and air temperatures provided the thermal capacity of the circulating particles is similar to that of waste gas. It will be shown that the rapid mixing of the particles in the fluidised bed restricts the air preheat. Equation (3) above was derived using the assumption of perfect mixing in a shallow fluidised bed, the solution of which readily confirms the maximum value of air preheat. One method of approaching the more effective counter-current arrangement is by a multi-stage fluidised bed which is considered below.

### Multi-stage fluidised-bed regenerator

Two adjacent multi-stage fluidised beds are placed in hot waste gas and combustion air streams. The solid particles are fed into the upper stage of each bed and slowly make their way down, under gravity to the lower stage from which they are taken out through an air-lock

and pneumatically conveyed to the upper stage of the adjacent bed, thus establishing a circulatory path of solid particles as shown in Figure 4.4. A major disadvantage of fluidisation is the high pressure drop associated with it. A multi-stage fluidised bed will further aggravate this situation because of the need to have many distributor plates to separate the stages. However, to investigate the possibility of using multi-stage fluidised bed regenerators, a simple mathematical model was developed. This was based on steady state conditions and that uniform temperatures are quickly established in the fluidised bed. The following assumptions were made.

1. For thermal equilibrium:

at every stage, the average temperatures of exit gas and solids are equal and constant. This implies that:

- (a) particles are thoroughly mixed
- (b) particle residence time and gas flow path produces uniform conditions
- (c) bubble formation is negligible
- (d) mass feed rate of particles is constant throughout the system

2. No heat losses:

- (a) from bed to atmosphere
- (b) no radiation from bed walls to the gas or vice versa
- (c) from solid particles to the pneumatic medium
- (d) steady temperatures are attained
- (e) no conduction through bed wall between stages

3. Gas and air entry conditions remain unchanged

4. 'Air-locks' are 100% efficient

These simplifying assumptions are used to obtain a very rough and highly optimistic solution to the problem. Therefore, a further indepth study is warranted, only if the results are more than promising.



In all fluidised bed heat exchanger designs, where heat is transferred to an immersed surface or by circulation of particles to a secondary cooler bed, it is usually assumed that the fluidised bed is at a constant and uniform temperature equal to the gas exit temperature. Also, a state of 'perfect' mixing is assumed for a gas-fluidised bed. Based on this assumption of perfect mixing, a mathematical approach was adopted to determine the limitations of isothermal conditions in the fluidised bed.

Various stages of development of the mathematical model and the results are shown in APPENDIX I. It can be concluded that, in practice where heat losses through the container wall are negligible, the temperature difference between the fluidising medium and the bed particles is expected to be well under four percent of the highest temperature difference in the system. Therefore the assumption of an isothermal condition in each stage is valid.

#### **4.2.2 Fluidised bed regenerator - second type**

The fluidised bed regenerator of the first type has the disadvantage of requiring high pressure systems or large induction fans to fluidise the multi-stage system. Hence, the applicability of such a system in the iron and steel industry is very much in doubt, because waste gases having pressures well in excess of atmospheric are rarely, if ever, encountered. However, to compete with and to replace established equipment, any new system must more than match it. It is not sufficient to eradicate some disadvantages of the existing system whilst introducing new and unforeseen difficulties. It has been predicted that high air preheats are possible with the multi-stage fluidised bed regenerator, but the complex nature of the fluidisation system is likely to hamper its adaptation even when fully developed. A method which may simplify the system and yet retain the

advantageous properties of fluidisation is a falling cloud of dense particles in the rising stream of air [Howard (1977)]. The heat transfer between air stream and particle is based on a similar principle to that in the fluidised bed system but without the inherent disadvantage of high pressure drop common in a fluidised bed and across the distributor plate. The application of such a system to a soaking pit or reheating furnace waste gases, laden with dust particles is shown diagrammatically in Figure 4.2(b). A very brief experimental study was conducted using simple equipment by Howard et. al. (1977) and some agreement between theoretical predictions and experimental data on heat transfer coefficients was obtained.

The heating rates for particles of various sizes has been analysed for the fluidised bed regenerator of the first type in Appendix I and are equally applicable to the present discussion. The particle residence time for attaining temperatures approaching those of combustion products, is in the region of 1 to 10 seconds depending on the size and material. Particles under free fall conditions will quickly reach their terminal velocity relative to the surrounding medium. Therefore, the height of the falling cloud heat exchanger will depend on the characteristics of the particles, fluidising medium and heat exchange effectiveness required. Therefore changes in the flow conditions will drastically alter the effectiveness of the heat exchanger.

## **Discussion and conclusions**

The use of fluidisation techniques for an air-to-air heat exchanger has been evaluated and shows that high air preheats are possible. However, the factors which will almost certainly limit the use of fluidisation in the iron and steel industry are numerous, and include the following:



1. All industrial furnaces used in the iron and steel industry operate at or near ambient pressures. To meet high pressure requirements of the fluidised bed and the associated distributor plate the use of a forced circulation system is necessary. This will invariably increase operating costs and will further complicate the overall system.
2. The reliability of heat transfer data, used in the design of a falling cloud system to even within 50% is questionable, because the test data from laboratory models is scattered and is difficult to correlate accurately [Howard and Sanderson (1977)]. This implies that Item 3 below must be given priority to evaluate the performance of and design full scale equipment.
3. The inherent difficulty of using test data from a laboratory model for the design of a practical system requires a solution. Two solutions are possible:
  - (a) Install an assembly of small fluidised beds
  - (b) Experiment with a large fluidised bed to optimise its performance

Both solutions are highly capital intensive and the short term application of a fluidised bed is ruled out.

The erosion of high temperature particles subjected to impact in the falling cloud system may require an extensive replacement of material, thus increasing running cost. The selection of heat transfer material for both types of regenerators is critical for the successful operation of the heat exchangers.

The ideal material should have:

- (a) high temperature strength
- (b) high heat capacity
- (c) a particle shape such as to give high surface area/volume ratio
- (d) high shatter strength and low rates of agglomeration at maximum working temperatures and pressures

(e) high thermal conductivity

(f) uniform particle size

Although the application of fluidised bed heat exchangers in the iron and steel industry is severely restricted due to the inherent low pressure operations, Müller (1967) considered their use with ceramic spheres or molten salt droplets to preheat air in the combined MHD-steam power plant. The system consisted of chambers fitted with baffles or retarders to prolong the particle residence time in the system. The hot-gas chamber is placed vertically above the cold-gas chamber and they are connected by a transfer system and a system for returning the heat transfer medium from lower to upper chambers.

Nicholls (1975) considered the use of fluidised bed regenerators for Brayton cycles. A high pressure deep fluidised bed is placed prior to the heat source in an open cycle turbine system and a low pressure deep fluidised bed is placed in the exhaust line, the two fluidised beds being interconnected by hot and cold solid particle transfer lines.

Whereas Muller made no attempt to compare his system with other comparable systems for preheating air, Nicholls compared his system with a shell and tube heat exchanger for the same duty and concluded that a reduction in total volume by a factor of 2 to 3 is possible with high operating temperature capabilities.

It is generally accepted that rapid mixing of particles promotes isothermal conditions in the shallow gas fluidised bed and this assumption was used to develop the mathematical model for the multi-stage fluidised bed regenerator. But Nicholls considers a deep bed and assumes that the particle temperature is height dependent, and gives a very optimistic solution and high air preheats are forecast.

In the regenerative fluidised bed system considered above the temperature of the particles in the cold return line is high and non-



productive. It can be likened to reactant currents and voltages in the electrical system, as it merely loads the system. Therefore, a reduction in this temperature will increase the overall rate of energy recovery by the introduction of heat transfer surfaces to heat water, produce steam or boil refrigerants for low temperature turbine application. However, a drop in air preheat temperature is inevitable from equation 2. A possible configuration for a combined steam and air-to-air heat exchanger is shown in Figure 4.4.

The complexity and unpredictability of the fluidised bed system requires extensive research for the successful design of primary and the large amount of auxiliary equipment. The design of a regenerator system will require the solution of the following problems:

1. Design of air-tight seals capable of working at temperatures in excess of 1200 C
2. Design of solid transfer lines
3. Design of distributor plate
4. Selection of heat transfer particles
5. Design of fluidised beds

Items 1 and 4 are similar problems to those encountered in the development of the ceramic recuperator and rotary regenerator and hence can be quickly solved as the working materials will be similar. The complexity of the system and non-availability of applicable experimental data for the design of large fluidised beds imply that the costs are likely to be excessive. Also, the prospect of its use in the iron and steel industry is remote. Therefore, further study of the fluidised bed system was not continued.

#### 4.3 Refrigerant turbine cycle

All industrial processes, where thermal energy is produced to raise the temperature of a material, invariably exhaust thermal energy

at a temperature higher than the desired material temperature. This represents a large proportion of the total energy supplied to the system. However, in most metal manufacturing processes, energy recovery equipment is incorporated to improve its energy utilisation. A further increase in the size of energy recovery equipment on existing lines may not be cost effective therefore, to improve energy recovery, other methods may be considered. A method of converting low grade thermal energy to mechanical or electrical is to use refrigerant turbines capable of operating at relatively low temperatures. Other thermal processes also exhaust energy at temperatures just above 100 C in the form of steam, process gas or process solids etc. The economics will be governed by the method of energy recovery adopted and the usefulness of the energy in the recovered form.

The refrigerant turbine cycle is similar to a steam cycle but organic fluids are used in place of steam. The use of such fluids offers the following advantages over the steam power cycle.

1. The properties of some are such that dry saturated vapour expands into the superheated region. Therefore, the problem of blade erosion, common in steam turbines, is eliminated
2. A single stage turbine can be used for the same power output because the enthalpy drop during expansion is low. The reduction in turbine cost is considerable
3. At usual condenser temperatures, the vapour pressure is close to atmospheric, hence the air entrainment is reduced or even eradicated
4. The low specific volume of organic fluids generally results in compact heat exchange and auxiliary equipment.
5. Most organic fluids have low critical temperatures, therefore super-critical operation is possible
6. Non-corrosive with common turbine blade materials, therefore no new materials are needed.



The major disadvantage of a refrigerant power plant is the initial cost of working and make-up fluid. Other disadvantages include:

1. Low cycle efficiency in comparison with the steam cycle over the same temperature range, if this were possible.
2. A de-superheater is required prior to the condenser
3. All refrigerants are toxic, if exposure period and concentrations are high

A refrigerant power cycle is shown in Figure 4.5. The turbine and associated equipment has been developed in Japan, and is commercially available from I.H.I. Refrigerant 11 is used and is capable of developing 490 kW of electrical power using process gases or steam as the heat source. [Sega (1975)]

To optimise the power recovery, the selection of a suitable refrigerant is critical. The desirable properties of refrigerant for power cycles are as follows:

- (a) The critical temperature of refrigerant should be above ambient and the possibility of using both sub-critical and super-critical
- (b) Refrigerant pressure must be sufficient to drive the turbine and not too high to avoid using expensive materials
- (c) Low specific volume for compact equipment
- (d) Non-toxic and non-flammable
- (e) High stability at working temperatures
- (f) Low cost
- (g) High cycle efficiency

On consideration of factors (a), (b) and (c) a list was compiled of all refrigerants which meet these criteria and is given in Figure 4.6. Further investigation into stability, flammability and toxicity of the refrigerants reduces the list to R-11, R-113 and R-114. Although R-216 was another possibility, and has higher stability than both R-11 and R-114 [Snider (1967)], it is not commercially available. Therefore cost is likely to be high.

The thermodynamic properties of the three remaining refrigerants is given in Figure 4.7. The specific volume of these refrigerants is similar and therefore equipment of similar size is expected but for the differences in their heat transfer properties.

The next stage in the selection of the refrigerants was to evaluate the order of Rankine cycle efficiency for these refrigerants. A simple procedure was adopted. The Rankine cycle is shown on a p-h chart of R-113 in Figure 4.8 where,

- 1 → 2 isentropic compression of fluid from  $p_1$  to  $p_2$
- 2 → 3 constant pressure heating to dry saturated line or superheated region
- 3 → 4 isentropic expansion of dry vapour from  $p_2$  to  $p_1$
- 4 → 1 constant pressure de-superheating and condensation

Using usual heat and work transfer equations, the thermal efficiency can be evaluated.

The relative Rankine thermal efficiencies up to critical pressure for R11, R113 and R114 are plotted in Figure 4.9 and show that R11 and R113 are comparable whereas R114 has lower efficiency by 2.5 per cent at its critical pressure. Similarly, the plot of boiling load (Figure 4.10) leads to the conclusion that on thermal and physical properties R113 has slight edge on R11. However, the relative cheapness and availability of R11 leads to its final selection.

#### 4.3.1 Application of refrigerant turbine to recover energy from blast furnace stoves No. 1, 2, 3, 4 and 5 at Port Talbot works

Total gas mass flow rate	=	130.4 kg/s
Exhaust gas temperature	=	270°C
Total energy loss above ambient condition (15°C)	=	34.3 MW

Using refrigerant 11 and let  $P_{sat} = 27.6$  bar and  $T_{sat} = 170^\circ\text{C}$ .



Figure 4.9 gives Rankine efficiency = 22.6% and assume turbine isentropic efficiency of 85% and pinch-point (minimum thermal separation between gas and refrigerant temperature) approach of zero.

The maximum power generated is 2.58 MW.

#### 4.3.2 Conclusions and recommendations

The exercise of energy recovery from combustion products of blast furnace stoves has shown that sufficient thermal energy is available for a refrigerant turbine of 2-3 MW rating. A saving in annual energy consumption of  $20 \times 10^6$  kWh is forecast.

A thorough refrigerant selection procedure has been followed to reduce the choice to R11, R113 and R114 and finally R11 was selected on the basis of availability and relative cheapness.

Initial development of refrigerant turbine has rested on the I.H.I. engineers of Japan. Although further development of the turbine and associated equipment is outside the scope of the British Steel Corporation, the possibility of its usage is highlighted in the event of its commercial availability in appropriate electrical rating and widespread acceptance.

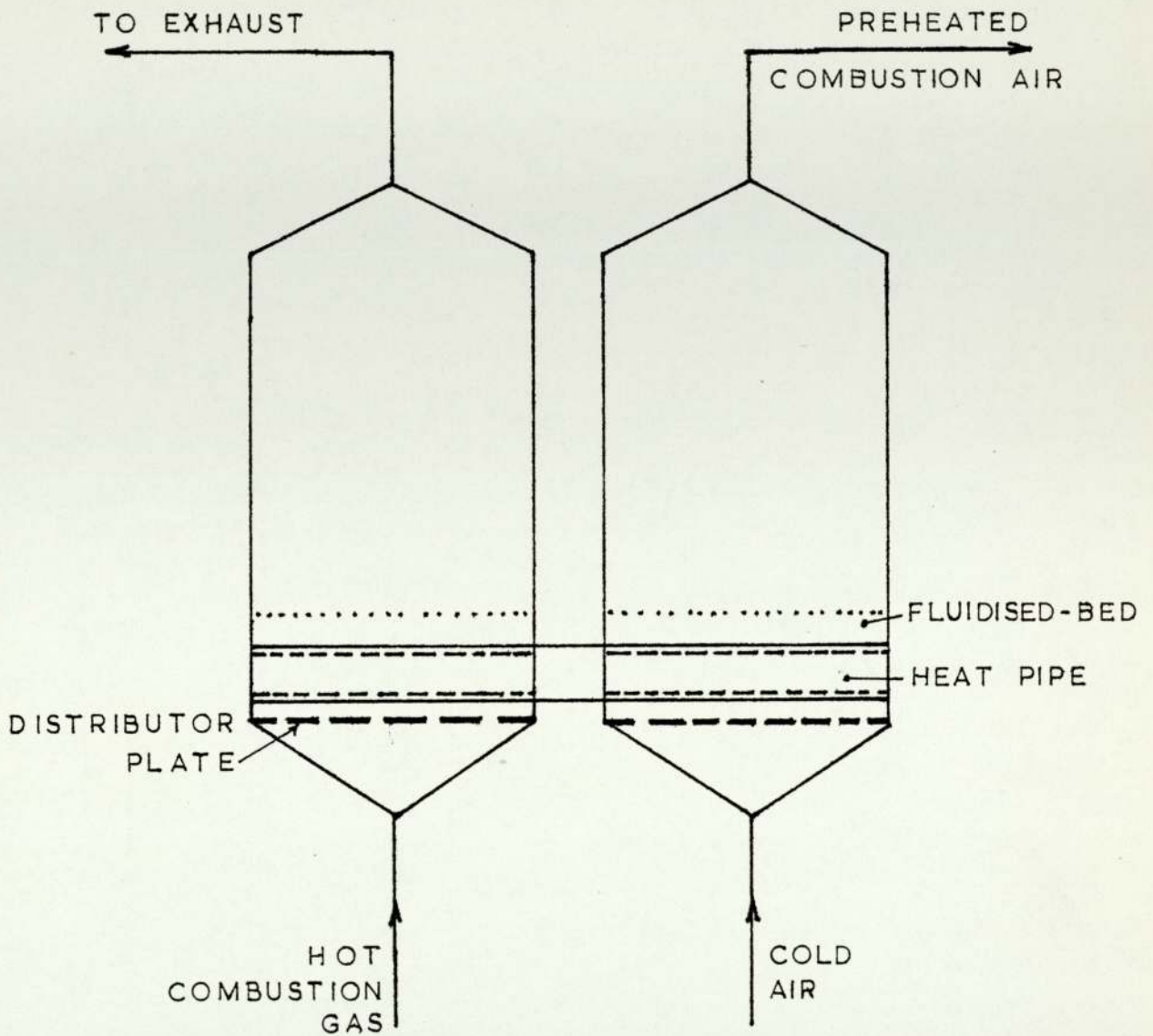
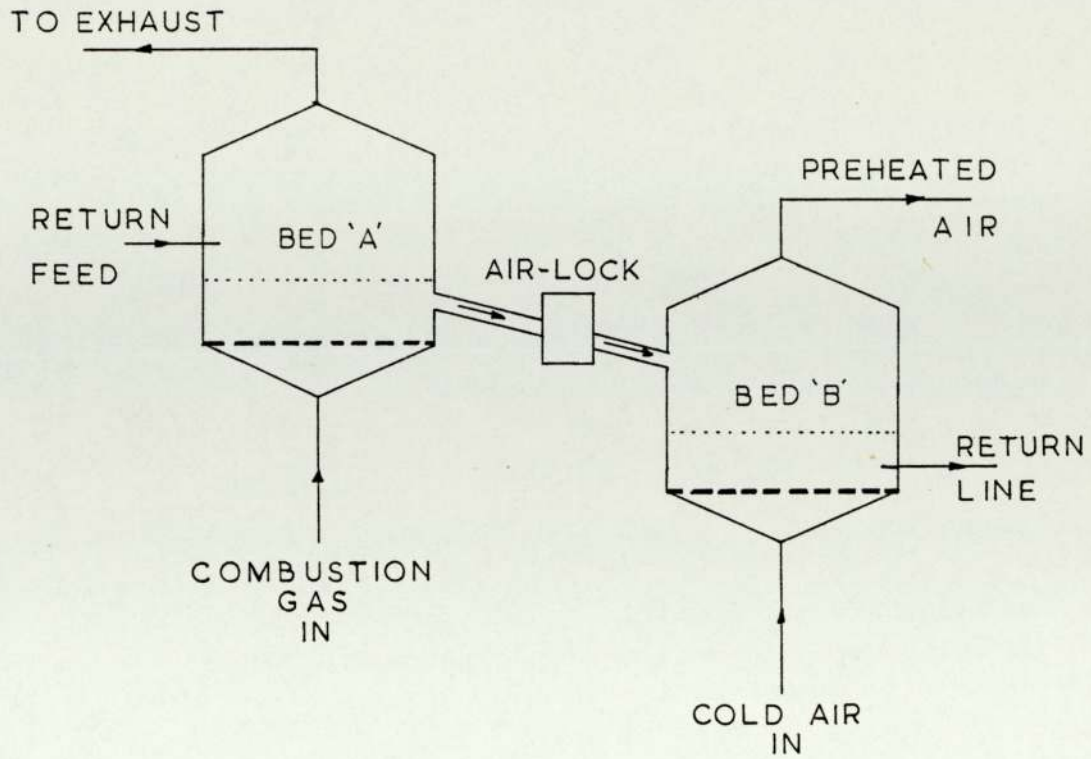


FIGURE 4.1 FLUIDISED-BED RECUPERATOR





[a] FLUIDISED-BED REGENERATOR - FIRST TYPE

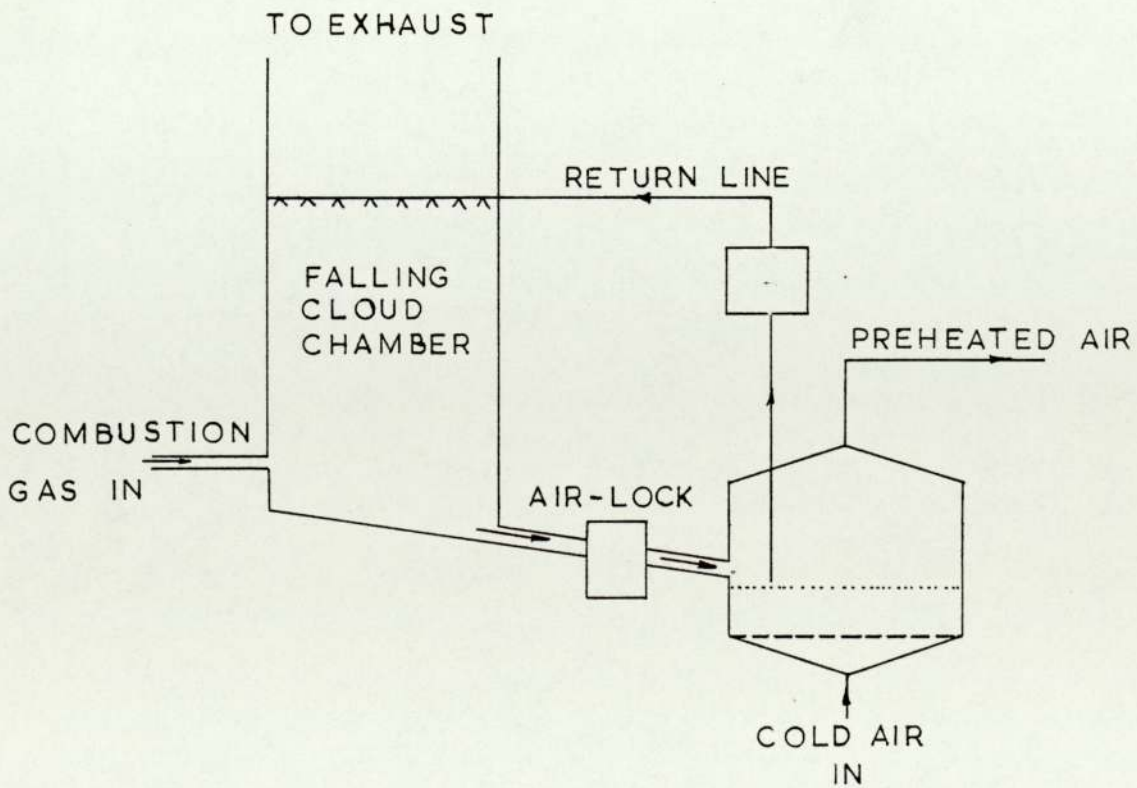
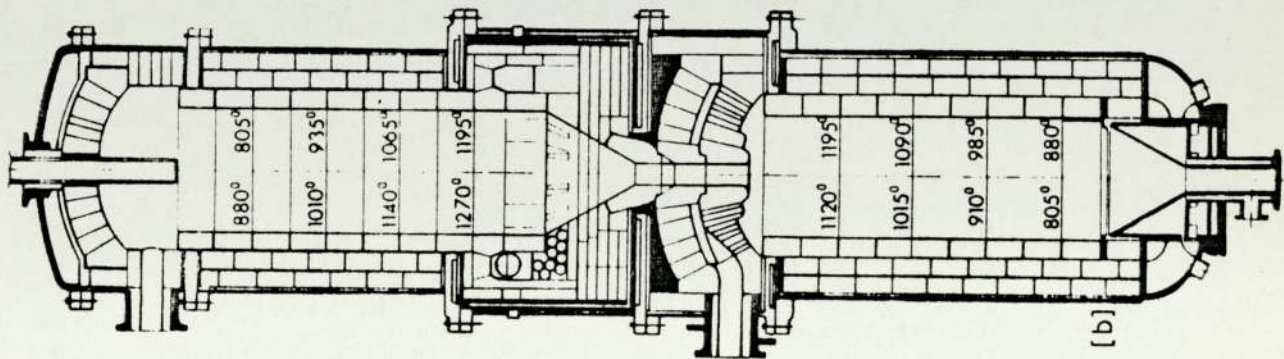
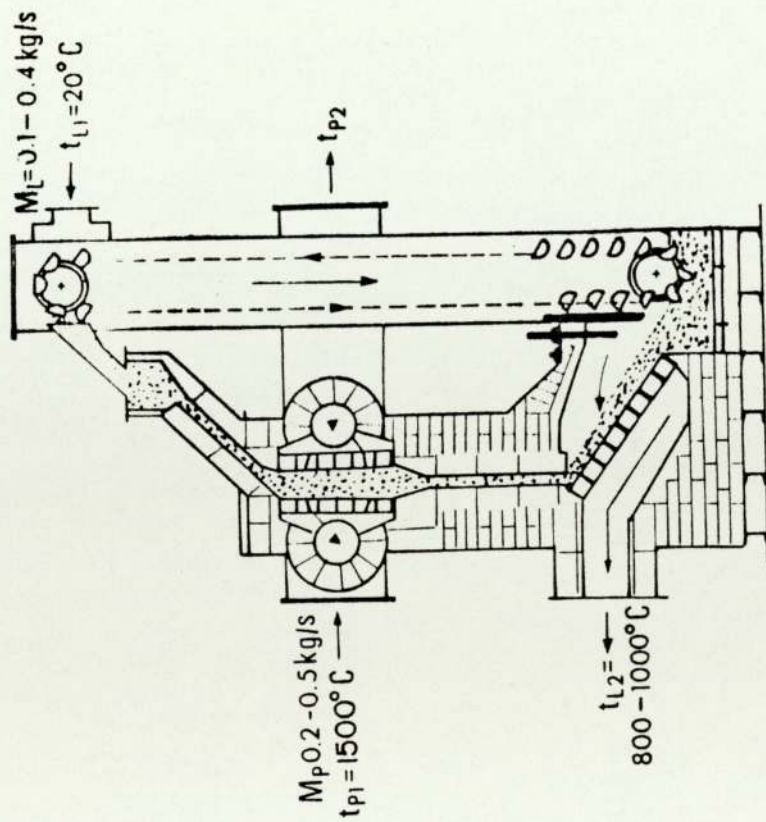


FIGURE 4.2 [b] FLUIDISED-BED REGENERATOR - SECOND TYPE



[SOURCE : Du1 (1974)]



[SOURCE : Schneller and Hlavačka (1974)]

FIGURE 4.3 MOVING BED REGENERATOR DESIGNS



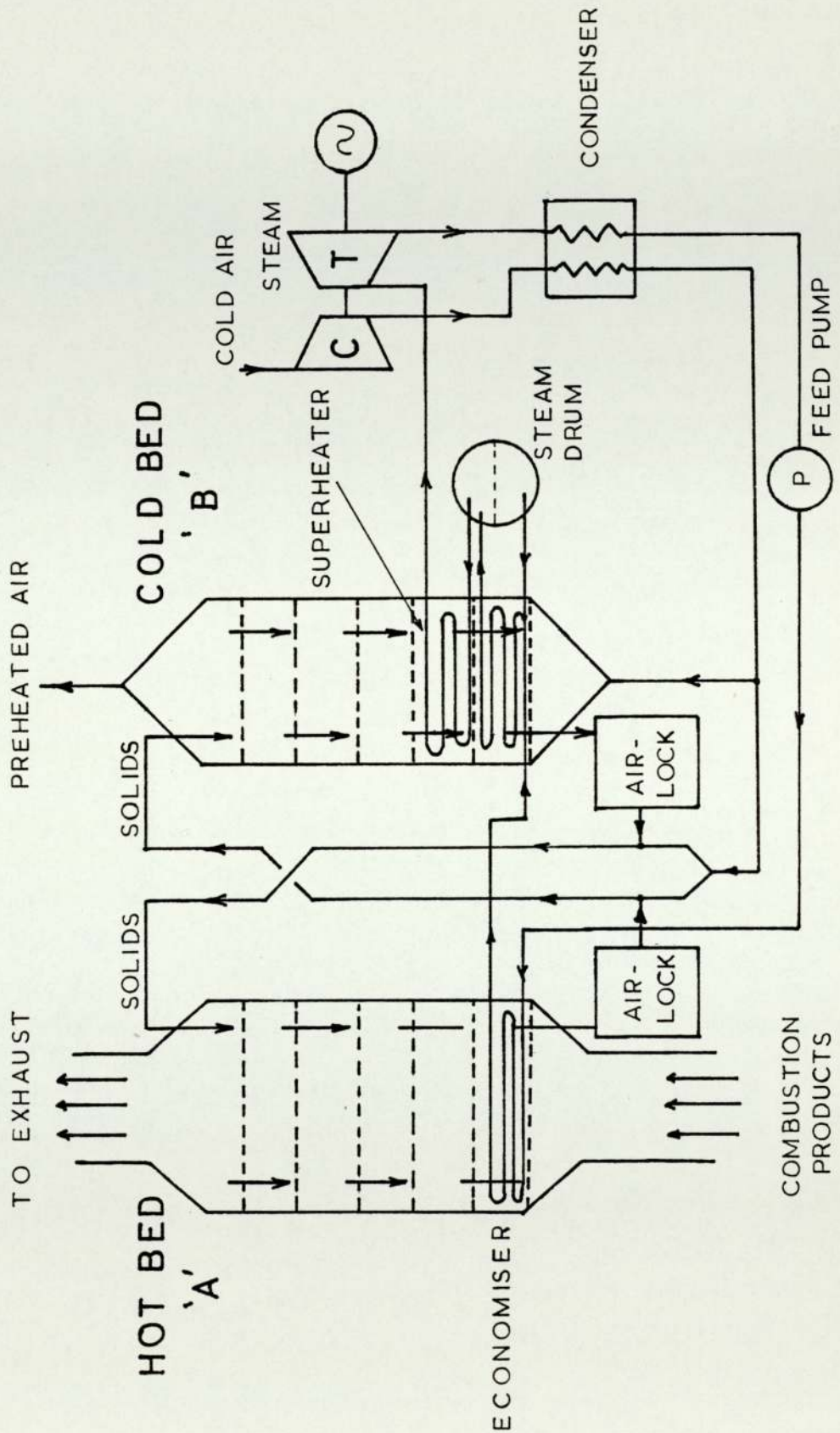


FIGURE 4.4 MULTI-STAGE FLUIDISED-BED REGENERATOR WITH TURBO-GENERATOR

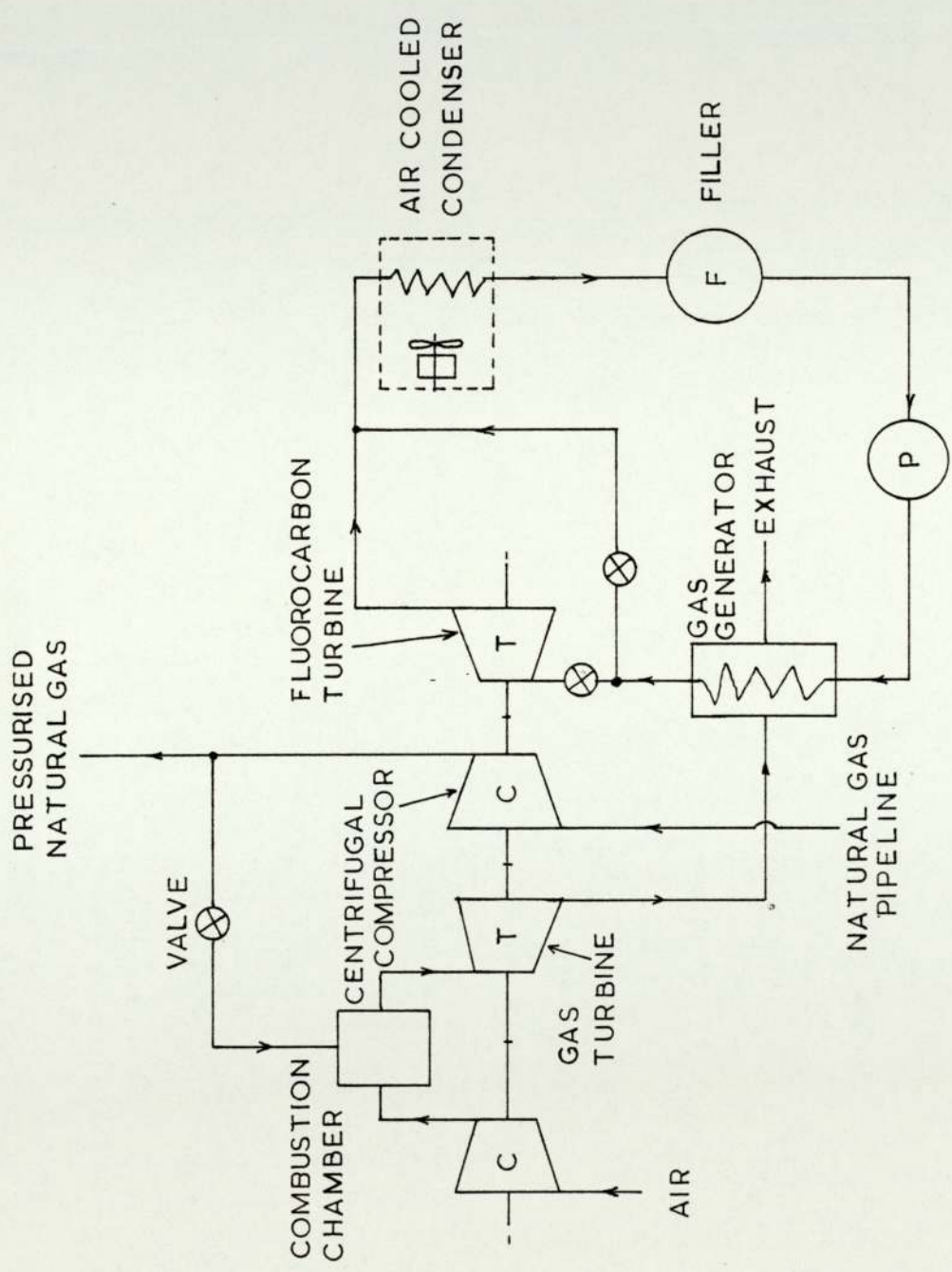


FIGURE 4.5 COMBINED CYCLE GAS-FIRED TURBINE ( for gas compression use )



Refrigerant No.	TEMPERATURES (°C)				PRESSURE (BAR)		Toxicity Classification*	*Underwriters' Laboratories Classification of comparative hazard to life of gases and vapours [ASHRAE (1972)]	
	Critical	Gas Generator	Condenser	Gas Generator	Gas Generator	Condenser		Group	Definition
11	198	171	37.8	29.7	1.07	5a	4	Gases or vapours which in concentrations of about 2 to 2.5% for durations of exposure of about 2 hours are lethal or produce serious injury	
12	112	82.2	37.8	24.1	6.82	6	4-5	Appear to classify as somewhat less toxic than Group 4. Much less toxic than Group 4 but somewhat more toxic than Group 5 e.g. R-113	
21	178.5	149	37.8	32.5	2.76	4-5	5a	Gases or vapours much less toxic than Group 4 but more toxic than Group 6	
113	214.1	149	37.8	12.1	0.92	4-5	5b	Gases or vapours which would classify as either Group 5a or Group 6	
114	145.7	121.1	37.8	21.0	3.16	6	6	Gases or vapours which in concentrations up to at least 20% by volume for durations of exposure of about 2 hours do not appear to produce injury	
216	180	149	37.8	16.25	1.09				
C318	115.3	93.3	37.8	18.0	4.65				

Figure 4.6 - List of refrigerants considered for power turbine cycle

Figure 4.7 - Critical thermodynamic properties of refrigerants  
R-11, R-113 and R-114

Property \ Refrigerant No.	R-11	R-113	R-114
Molecular Weight	137.4	187.4	170.9
Critical temp. (°C)	198.0	214.1	145.7
Critical Pressure (bar)	44.1	34.2	32.6
Critical Specific Volume (m <sup>3</sup> /g)	$1.8 \times 10^{-3}$	$1.74 \times 10^{-3}$	$1.72 \times 10^{-3}$
Boiling Point at one Bar (°C)	23.8	47.6	3.8



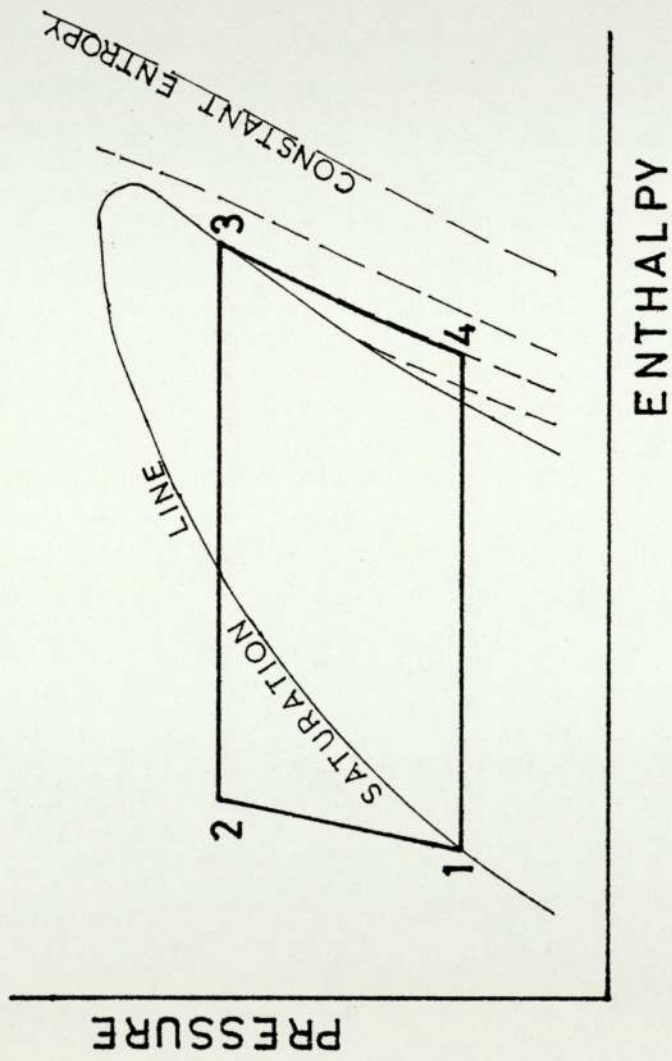
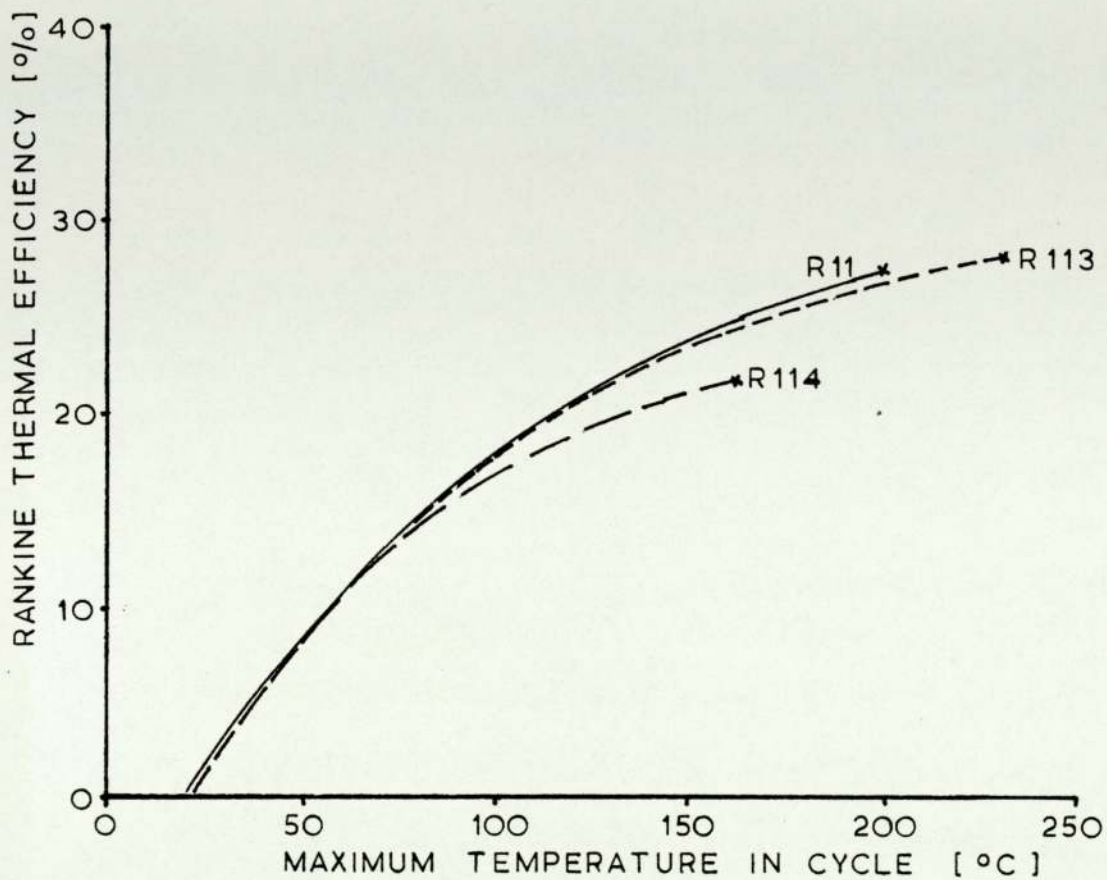


FIGURE 4.8 RANKINE CYCLE ON P-H CHART OF R-113



Note:

- R11 Expansion to saturation line
- - - - R113 Expansion from saturation line
- R114 Expansion from saturation line

FIGURE 4.9 RANKINE THERMAL EFFICIENCY UP TO CRITICAL PRESSURE FOR R11, R113 AND R114



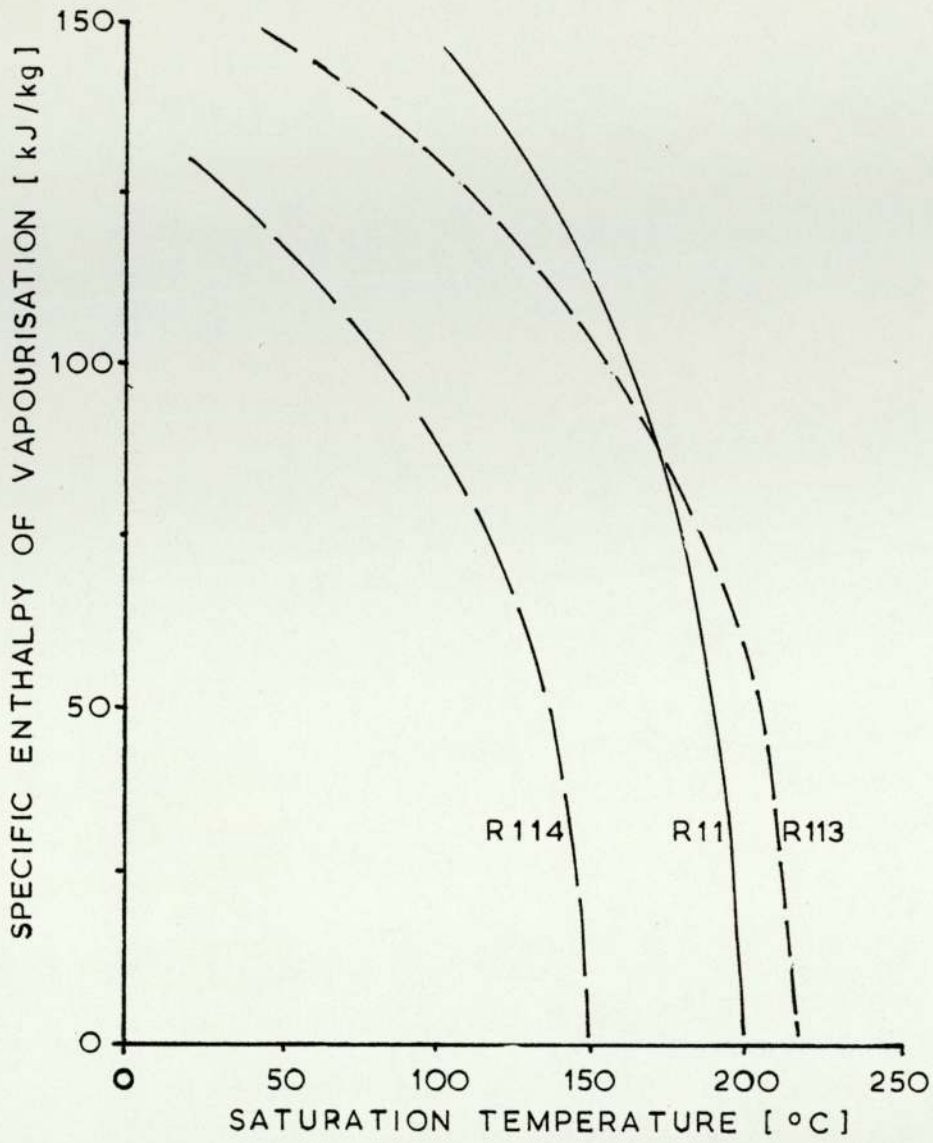


FIGURE 4.10 SPECIFIC ENTHALPY OF VAPOURISATION AT CONSTANT PRESSURE FOR R11, R113 AND R114

## CHAPTER 5

### THEORETICAL AND ECONOMIC FEASIBILITY OF SLAB COOLING



## 5.1 Introduction

A vast quantity of thermal energy is continuously wasted in air cooling of hot slabs between slab and hot strip mills. The cooling of slabs is necessary to detect and rectify any surface imperfections and to ease production scheduling problems. Any requirement which necessitates cooling and reheating of products at an intermediate stage invariably requires extra expenditure of energy and is not economically desirable. To reduce or eradicate this problem, a number of solutions are possible. Each solution requires an improvement in production scheduling and the development of surface detection and corrective techniques at temperatures in excess of  $800^{\circ}\text{C}$ . These solutions can be categorised into short or long-term depending on the stage of development and economics of the above techniques.

### (a) Short-term

There are two possibilities:

- (i) to use a continuous system of counter-current flow of slabs to preheat 'corrected' slabs prior to their entry into a reheating furnace. This requires that the slab mill and hot strip mill are in simultaneous and continuous operation.
- (ii) to recover thermal energy in a secondary medium for use elsewhere within or outside the iron and steelworks.

### (b) Long-term

These require the attainment of a 'perfect' surface (i.e. a surface having a low or negligible incidence of imperfections) or the development of an automated system of detection and rectification of surface imperfections (e.g. surface impurities, slag inclusions, micro and macro-surface cracks etc) at temperatures in excess of  $800^{\circ}\text{C}$ .

Again, two possibilities are discussed:

- (i) An improvement in production technique to reduce waiting time between rolling operations. Furthermore, a system of retaining thermal energy in the slabs to iron-out any deficiencies in the scheduling technique is necessary. The introduction of both of these solutions leads to a reduction in energy and storage requirements.
- (ii) The ultimate goal of any system analysis is to reduce the overall cost per unit produced. Any reduction in the number of processes or steps to obtain the desired product without significantly affecting the remaining processes results in the same. Therefore the use of a reliable and continuous scheduling technique together with the elimination of surface imperfections is the desired solution.

A sister study [Girvan and McKie (1975)] considered b(i) and a preliminary estimate concludes that significant net savings in energy can be achieved. A 'tea-cosy' effect was considered for retaining thermal energy in the slabs but it assumes that a 'perfect' surface is attained and that production scheduling is significantly improved.

An immediate and more reliable solution for reducing overall energy cost is discussed in this report and was postulated in a(ii). A preliminary theoretical study was sufficiently encouraging to continue the evaluation to the experimental stage. An experimental rig was designed and constructed to verify and improve on the theoretical analysis and is discussed in Chapter 6. The remainder of this chapter is concerned with a preliminary feasibility study of a slab cooling - energy recovery system.

## 5.2 Hot slab details

### 5.2.1 Slab size

Basically slabs are produced in four lengths:



1. Short (or  $\frac{1}{4}$ ) 3.6m to 4.0m
2. Medium (or  $\frac{1}{2}$ ) 5.3m to 6.1m
3. Intermediate (or  $\frac{3}{4}$ ) 6.7m to 7.7m
4. Long (or 1) 8.0m to 9.3m

The available data for Llanwern Steelworks in South Wales suggest that the slab width varies between 750mm and 1500mm and its thickness from 150mm to 250mm. Figure 5.1 shows the frequency and relative sizes of slabs produced during a typical week (week ending 19.12.75) at the above integrated iron and steelworks. The following size was selected as the average:

1.26m x 0.2m x 9.0m long and 10 slabs per hour.

#### 5.2.2 Physical properties of mild steel

- (i) Thermal conductivity,  $k_s = \frac{1000}{157.5 - 0.0538T - 65709.5/T}$  [W/mk]
- (ii) Mass density,  $\rho_s = 7800$  [kg/m<sup>3</sup>]
- (iii) specific heat,  $Cp_s = 650$  [J/kgK]
- (iv) emissivity,  $\epsilon = 0.78$  to  $0.85$

The emissivity of hot slabs was investigated using a simple 'gun' type radiation pyrometer. A method recommended in the accompanying booklet was used; however due to high inaccuracy of the device the results cannot be wholly relied upon. From the experiments conducted it can be ascertained that because of fast initiation and growth of the oxide layer on the metal surface at these high temperatures, the emissivity was close to 1.0.

### 5.3 The energy recovery system

There are a large number of possible configurations of an energy recovery system. The permutations and combinations of the list given below will serve as an indication of the range available.

- (i) Physical movement of slab in the system?
  - (a) continuous
  - (b) intermittent
  - (c) static
- (ii) Which slab?
  - (a) selective
  - (b) non-selective
- (iii) Energy recovery - how?
  - (a) slab-to-slab e.g. preheating of cold slabs
  - (b) water heating
  - (c) steam production
- (iv) Heat exchanger design?
  - (a) tube arrangement
  - (b) separate compartments or one integral unit
  - (c) structural details e.g. entrance, internal and exit
  - (d) economiser/boiler/superheater arrangement
  - (e) intermittent or continuous water/steam flow to optimise energy recovery

The overall energy recovery system will be governed by the alternatives selected. But for this study the following configuration was selected to give as wide a range as possible of interchangeable parameters.

A 'sandwich' type of infrastructure for steam production by recovery of thermal energy in cooling of hot slabs is shown in Figure 5.2.

The slabs are placed between cooling water/steam pipes on a moving/static platform/rollers to give continuous/intermittent/batch or coke oven type operation.

A computer program was developed, based on the above system, to evaluate its thermal performance and the heat transfer equations used are given in Appendix II.



## 5.4 Criteria for optimisation of slab cooling system

Three possibilities are discussed below:

- 5.4.1 The first criterion is that the rate of energy recovery from slabs is a maximum. This requires that the slab temperature throughout the system is as great as possible. This criterion holds when the system is adiabatic therefore requiring infinite slab velocity through the system. However, a practical optimisation procedure is to compare the marginal cost of an energy recovery system and the price of recovered energy. The maximum economic size is reached when these are equal and further recovery of energy is un-economic.
- 5.4.2 The second criterion is based on the attainment of a maximum total energy recovery. This state is reached when slabs are cooled to ambient conditions and requires infinite time and size of a continuous system. This is economically undesirable. A refinement on this principle is to equate cost of system to price of recovered energy.
- 5.4.3 A more desirable method of optimisation is to evaluate the energy recovery from all economically and technically feasible angles i.e. rate and number of slabs cooled, lowest slab temperature, rate and total energy recovered and the system of recovery. However, the non-availability of appropriate data severely limits this approach. The following parameters require a more detailed consideration for a satisfactory and reliable outcome.
- (a) More information is required on slab size, their production and waiting time between processes as well as any anticipated changes in these in the future. The analysis of this will reduce the options available for selection of an optimum size of heat exchangers or the mix of heat exchanger sizes. The top priority is to maximise energy recovery as well as

maximising the operating time of heat exchangers with due consideration of economics.

- (b) The optimum number and size of heat exchangers. This is influenced by energy price, distribution of slab sizes and the rate of slab production.
- (c) The optimum thermal cycle is governed by the rate of total energy recovery per slab and hence the minimum slab temperature.
- (d) The details of local energy demands and requirements.

When all these parameters are considered and optimised, a multi-dimensional plot of the economically desirable system is obtained and the final choice will depend on local parameters.

In all of the above methods of energy recovery, the availability of reliable economic data is of profound importance. The information on capital expenditure on novel heat exchangers and auxiliary equipment, future changes in energy price and running costs are not readily available. A simple solution to overcome some of these problems is considered in the next section.

## 5.5 Capital investment appraisal

Energy recovery equipment manufacturers are reluctant to handout information on cost breakdown of their equipment which could be used for novel or unproven heat exchanger design. They are unwilling to discuss their accounting practice, when tendering for a new type of heat exchange equipment, generally because it is based on opinions and past experience which cannot be easily quantified. Faced with these difficulties, a reverse approach was adopted for the economic analysis of the system under consideration in this chapter. This was based on the assumption that the rate of and the total energy recovery can be accurately predicted and a practical system can be designed and built. Hence using a



simple investment appraisal technique, it is possible to evaluate the maximum expenditure on heat exchange equipment which can be economically justified.

#### Economic analysis - assumptions

The following assumptions were made in arriving at the final results:

- (a) An initial investment of £50,000 for experimental and feasibility study and detail design of the system. One year was allowed for this exercise.
- (b) The remainder of investment in the plant, commissioning and trial studies was envisaged in the second year.
- (c) The training of plant operators was envisaged to be £10,000 in the second year.
- (d) The plant maintenance cost per annum was assumed to be a fixed percentage of the initial investment.
- (e) Energy price per kWh of steam was assumed to be 0.5 pence.
- (f) Plant life was 15 years, at the end of which the plant is scrapped and 15 percent of its initial cost is recovered.
- (g) All expenditure and revenue were discounted to the first year. The labour and maintenance costs and energy price were assumed to increase annually by a fixed rate.

#### 5.6 Heat exchanger design - assumptions

Theoretical equations used in the slab cooling - energy recovery system are given in Appendix II. The following assumptions were made in the analysis:

1. Temperature of the cooling surfaces is a constant and the maximum for given steam plant operating conditions. For example:

Cooling surface temperature

300 C

Steam level

40 bar - dry saturated or 30 bar  
with 16K superheat.

Cooling surface temperature

500 C

Steam level

Superheated steam at 140 bar  
and 425 C.

2. Initial slab temperature is 1100°C.
3. 80 per cent of the total energy incident on the cooling surfaces is recovered.
4. The first 15 minutes are allowed for transferring the hot slabs from primary mills to the energy recovery plant. During this part of the cycle some 30 percent of the recoverable energy is dissipated to the atmosphere.
5. The plant is operational for 5000 hours per annum i.e. 57 percent utility rate. Hence under 70 percent of the slabs available are processed through the system.
6. The maintenance cost per annum is assumed to be between 5 and 10 percent of the maximum investment predicted by the model i.e. if £2 million is invested then a maintenance cost of between £100,000 and £200,000 is assumed for every year of its operation.

## 5.7 Discussion and results

### 5.7.1 Theoretical accuracy of the mathematical model

#### (a) The energy recovery system

All three modes of heat transfer are taken account of in the model, see Figure 5.3. The accuracy of simulating heat transfer by radiation is governed by the accuracy of the product of view factor and emissivity which is difficult to predict accurately from the data available. A simple experiment was conducted to determine the emissivity of bright drawn mild steel at temperatures between 500 and 1200°C. Within the limitations of the instrument used, the emissivity was determined to be close to 1.0. In assuming a value of 0.8 in the model a reasonable precaution is taken for its



variation from steel to steel and at different temperature levels.

It is difficult to ascertain the role played by convective currents and direct conduction in transferring thermal energy. Since both of these modes account for a small proportion of the total energy exchange, any inaccuracies are unlikely to greatly influence the overall results.

In assuming the temperature of the cooling surfaces to be constant, the mathematical model is simplified and the accuracy is reduced. But to avoid any undue optimism, the maximum surface temperature obtainable under certain steam plant operating conditions are assumed to be prevalent throughout the system.

All other things being equal, the main assumptions tend to err on the pessimistic solution and hence this model under-estimates the real potential of the system as a whole. Yet despite these assumptions the results are very encouraging.

Design shortcomings or limitations of the structural members may inhibit full use of the system. These and other practical limitations are difficult to predict without resorting to experiments.

(b) Appraisal of capital investment

This model is based on discounted cash flow [Alfred (1971)] for capital investment appraisal. Under this form of economic analysis due account is taken of inflation. Apart from inherent shortcomings of the thermal system other inaccuracies are governed by the degree of accuracy to which future cash flows can be predicted and continued consistency of a given rate of inflation (i.e. discounting factor).

The possibility of mild steel slabs plastically deforming under their own weight when placed on their side and subjected to high temperatures was considered. However, creep strength of mild steel and alloy steel [Dern (1961)] is able to withstand internal stresses so imposed.

### 5.7.2 Results

The output from the "SLAB COOLING" computer program was in the form of:

- (a) the rate at which slabs are cooled,
- (b) the total energy extracted from the slab after a given time interval, and
- (c) the surface, centre and intermediate temperatures for the same time interval.

As mentioned earlier the slabs are air cooled whilst in transit from the primary mill stands to the energy recovery system. In the first 15 minutes of cooling some 98 MJ/m<sup>2</sup> surface area of thermal energy is dissipated to the atmosphere; see Figures 5.4 and 5.5. In the subsequent 180 minutes (i.e. the length of time it spends in the energy recovery system) the internal thermal energy is further depleted by 210 MJ/m<sup>2</sup> whilst its temperature drops to around 480 C; see Figure 5.4.

Given that only 210 MJ/m<sup>2</sup> is recovered from the slab and the cycle time is limited to three hours, the economic analysis was instituted. And only 10 slabs per hour are processed for a period of 5000 hours per annum through the system. Based on these assumptions the output from the economic model was in the form of the maximum possible investment which the system can sustain and yet remain economically viable.

Figure 5.6 shows that when the maintenance cost per annum is 5 per cent of the total capital investment and for zero rate of inflation up to £2.35 million can be invested. Any lesser amount will contribute



to increased rate of return on the investment. If however the inflation rate increases to say 20 per cent the level of investment feasible becomes £3.34m to break even with inflation. Again a lower level of investment will yield a net return on investment.

Figure 5.7 shows the consequences of increased maintenance cost (i.e. 10 per cent of investment). At zero inflation an investment of £1.6m is recoverable. Again lower investment or increased inflation yields a net return on the investment.

A minimum of 30 cubicles are required, occupying a total ground area of the order of  $140\text{m}^2$  and 1.5m high to process ten slabs per hour on a three hour cooling cycle.

## 5.8 Conclusions of preliminary theoretical study

The outputs from the mathematical model suggest that an investment of around £2m is a highly desirable proposition and would yield a net return on this investment. When these results are viewed against the pessimistic assumptions made in arriving at these conclusions the whole situation appears even more promising.

The system has not been optimised to the maximum due to the non-availability of economic data on the marginal or total cost of such a unit. This estimate can only be assessed after a preliminary design study has been conducted and elemental costs analysed. Once this data is available it may be possible to extend the cycle time and the number of slabs processed.

This study shows that the energy recovery system postulated here is technically and economically feasible and on initial assessment appears highly promising. Therefore it was decided to design a scaled model of the system and to conduct experiments to verify the theoretical model used.

(a) Slab length : 3.6m to 7.7m

Width (mm)	THICKNESS (mm)			
	152-179	180-204	205-229	230-254
750- 880	-	-	15	7
881-1010	-	10	85	19
1011-1135	-	3	15	10
1136-1260	-	25	4	9
1261-1390	60	50	12	30
1391-1525	-	-	8	2

TOTAL = 364

(b) Slab length : 8.0m to 9.3m

Width (mm)	THICKNESS (mm)			
	152-179	180-204	205-229	230-254
750- 880	25	24	107	91
881-1010	15	23	42	171
1011-1135	23	7	143	171
1136-1260	2	1	72	8
1261-1390	22	40	81	43
1391-1525	-	-	12	7

TOTAL = 1109

Figure 5.1 - Slab production data for week ending 19.12.75 at Llawern  
Iron and Steel Works



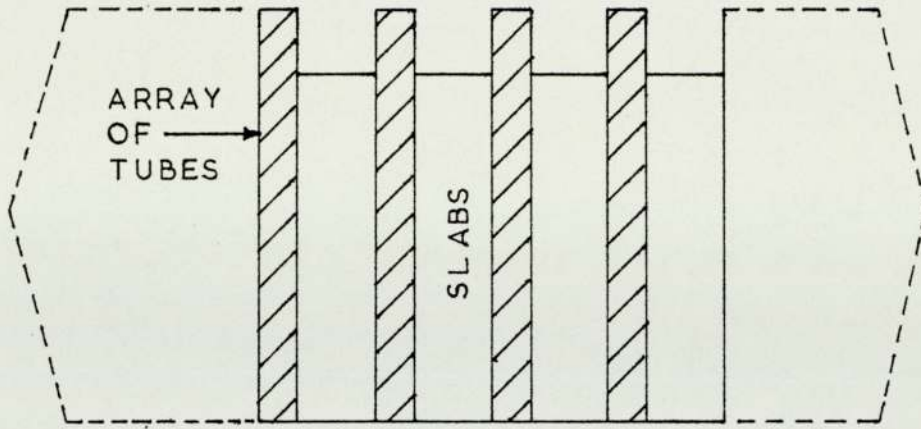


FIGURE 5.2 AN ARRANGEMENT FOR SLAB COOLING

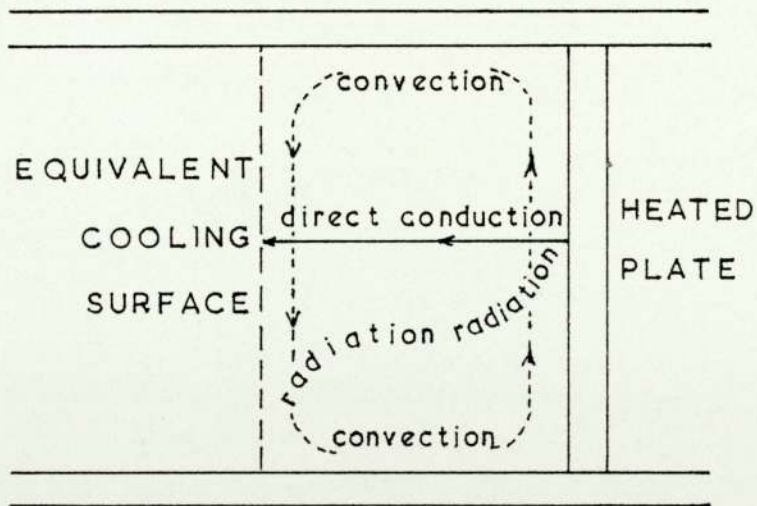


FIGURE 5.3 THREE MODES OF HEAT TRANSFER IN SLAB COOLING

ENERGY RECOVERY - COOLING OF HOT RECTANGULAR SLABS

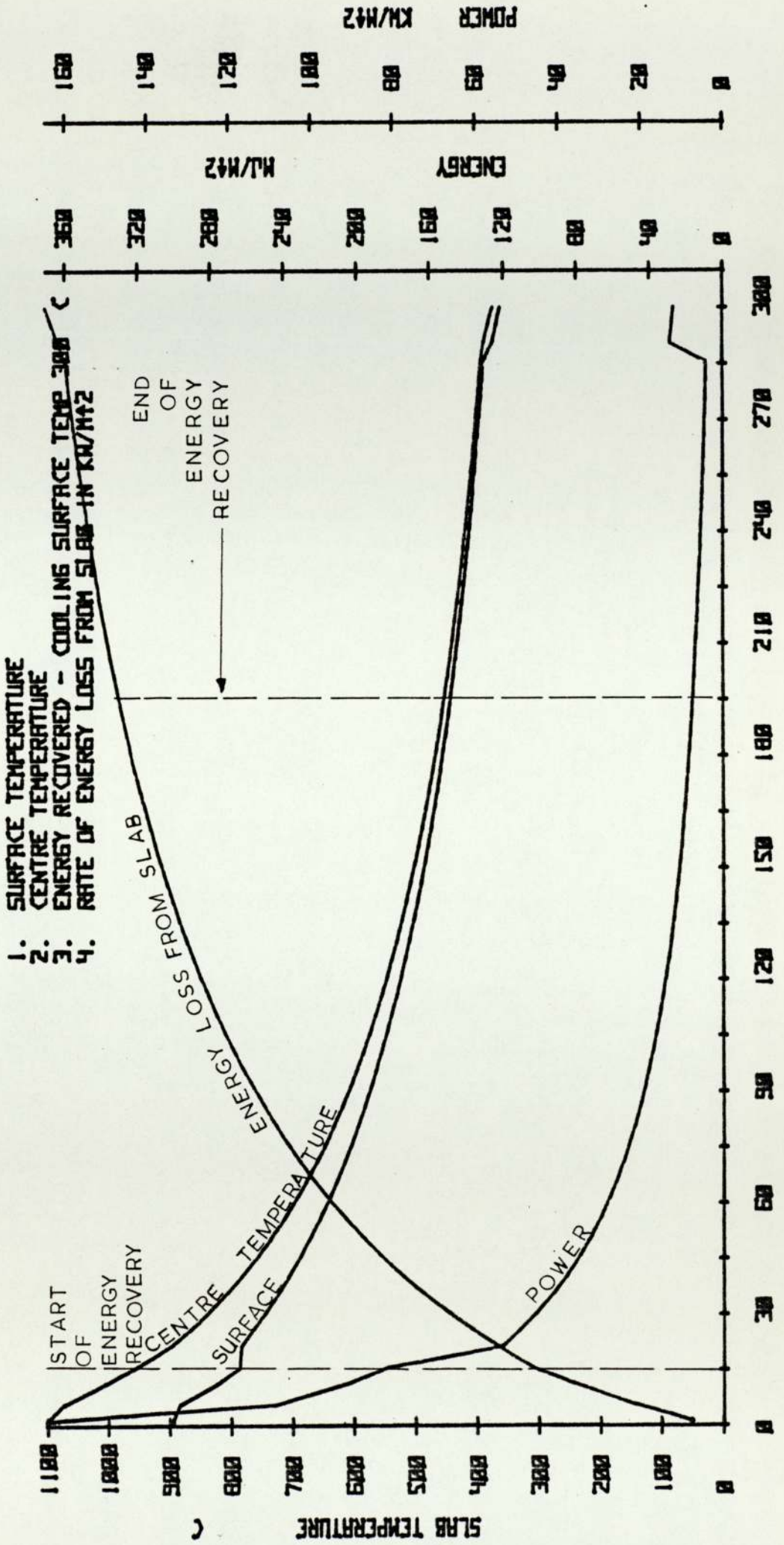


FIGURE 5.4 SLAB COOLING WITH COLD SURFACE AT 300 C





5000 HOURS OF OPERATION PER ANNUM  
 MAINTENANCE COST PER ANNUM IS 5% OF ORIGINAL INVESTMENT  
 STEAM PRICED AT 0.5 PENCE PER kWh

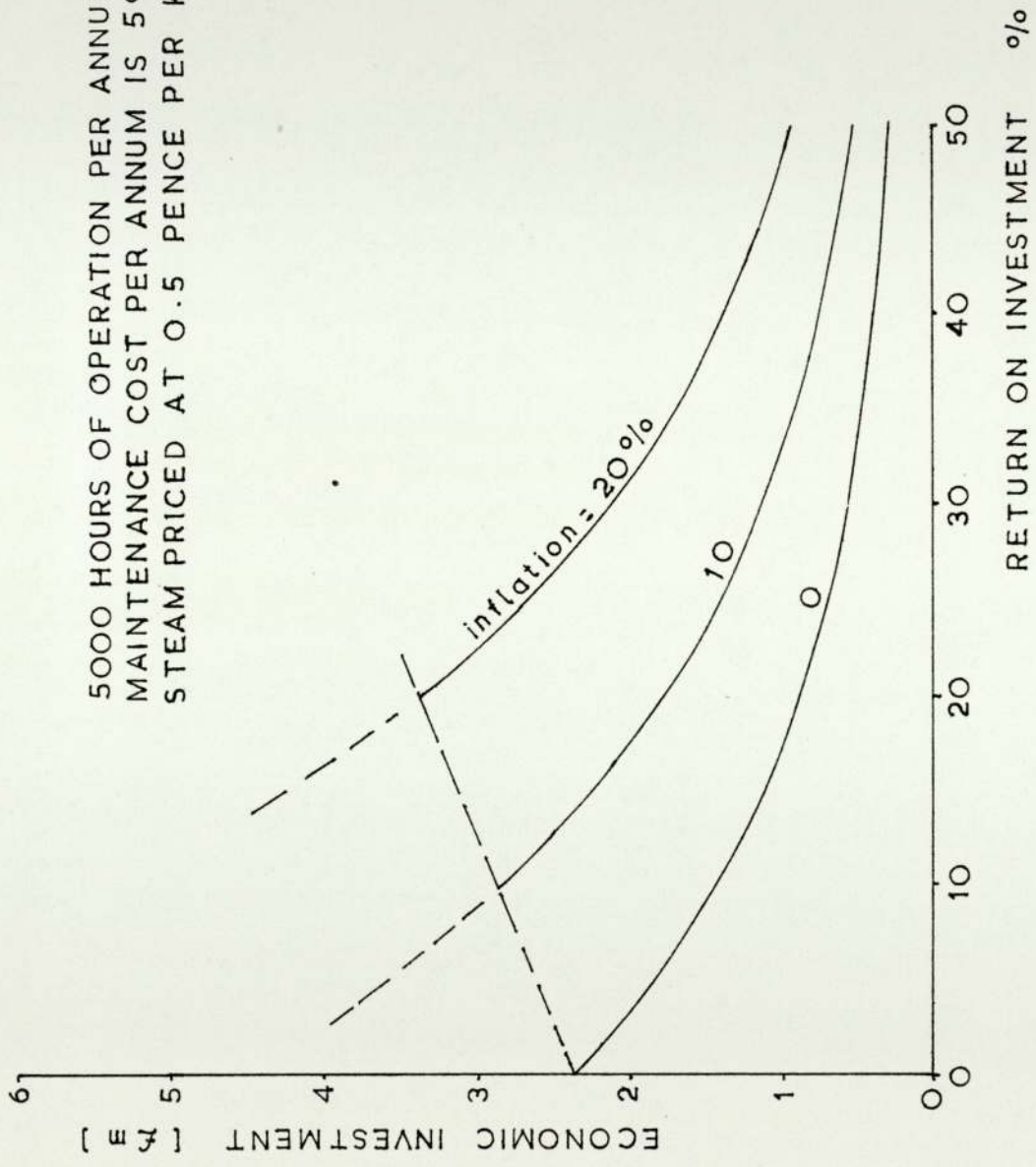


FIGURE 5.6 ECONOMIC INVESTMENT IN SLAB COOLING WITH 5% MAINTENANCE COST



5000 HOURS OF OPERATION PER ANNUM  
 MAINTENANCE COST PER ANNUM IS 10% OF ORIGINAL INVESTMENT  
 STEAM PRICED AT 0.5 PENCE PER kWh

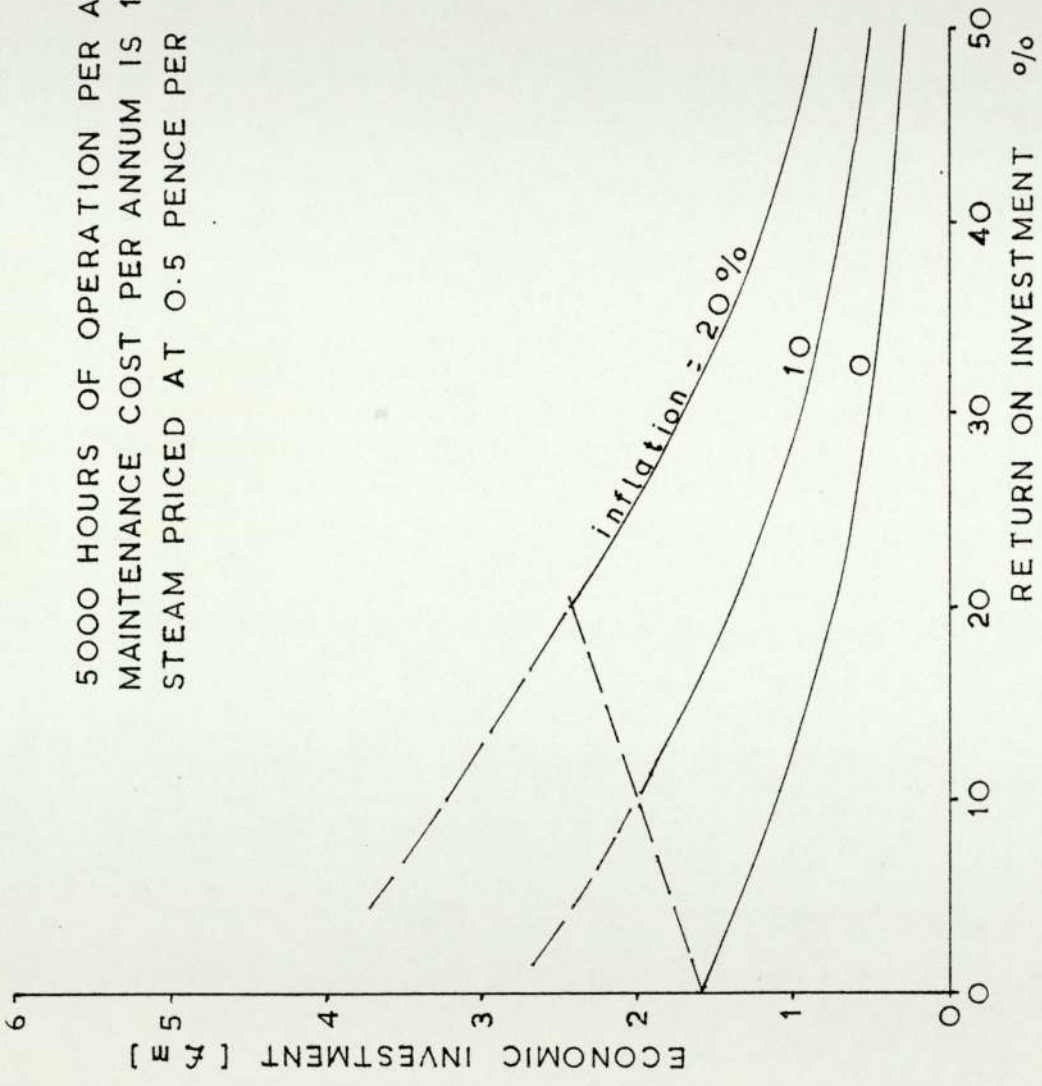


FIGURE 5.7 ECONOMIC INVESTMENT IN SLAB COOLING WITH 10% MAINTENANCE COST

## CHAPTER 6

### DESIGN OF AN EXPERIMENTAL RIG FOR SLAB COOLING



The preliminary technical and economic feasibility study of slab cooling concludes that the system is a viable proposition provided the assumptions inherent in the model hold good. To investigate the validity of the heat transfer data, an experimental rig was designed and built. A system incorporating a heat exchanger sandwiched between two electrically heated mild steel plates was employed and is shown in Figure 6.1. The following design parameters were incorporated in the system.

- (a) The heat exchanger can be rotated to give both horizontal and vertical tube arrangements.
- (b) The steam drum is lined with flow diverters to act as a steam/water separator as shown in Figure 6.2.
- (c) A water feedback system controls the water level in the heat exchanger.
- (d) Independently heated mild steel plates simulate various conditions of cooling.
- (e) Water flowmeters measure both the total flow rate and flow distribution through the heat exchanger.
- (f) Ceramic spacers vary the distance between hot plates and cooling tubes.

Although the rig was designed for high pressure and boiling operation, the need to use an existing installation of rubber/plastic pipes, water pump etc., meant that the maximum temperature was restricted to around 75°C.

Various sections of the experimental rigs are described in detail below.

## 6.1 Plate heaters

A structure of castable refractory, known as Monocast 114/27 is mounted in a steel cage with three roller bearings to facilitate assembly and removal of the heat exchanger and refractory spacers is shown in Figure 6.3. Four Silit heating elements type ED 15.9 mm x 305 mm x 810 mm shown in Figure 6.4 are electrically connected in series or 2 x 2 series -

parallel to a single phase variable transformer of 100A x 240V rating. The front open face of the refractory block is lined with a 10 mm thick rolled mild steel plate to represent a hot slab surface. Three Cr-Al thermocouples measuring 3.2 mm x 1.0 m, mineral insulated and inconel sheathed are embedded into the mild steel plate from its rear (Figure 6.5) to measure non-uniformities in the surface temperature.

## 6.2 Heat exchanger

The heat exchanger comprises a number of 9.5 mm OD x 6.4 mm ID copper tubes positioned in Sindanyo spacers and connected to an inlet header and the steam drum using Enot connectors as shown in Figure 6.6. Three rows of copper tubes are arranged in an equi-lateral triangular pitch of 19 mm. The steam drum is lined with flow diverters acting as a steam/water separator (Figure 6.2). An outlet pipe from the steam drum is connected at its uppermost position to reduce the likelihood of an air trap. The water circuit is shown diagrammatically in Figure 6.7. Water is pumped from a header tank through the heat exchanger via flowmeters, then returning to the header tank.

The heat exchanger is mounted between the two plate heaters and is rigidly fixed to the centre of a steel bench as shown in Figure 6.1.

The water temperature is measured using calibrated mercury in glass thermometers and Cr.Ni-Al.Ni thermocouples suitably positioned in the water circuit. To measure the flow distribution in the heat exchanger a few copper tubes are installed with tappings which in turn are connected through two flow switches to an inclined inverted U-tube water manometer as shown in Figures 6.8 and 6.9 respectively.

The water circuit was purged of trapped air prior to commencement of all experiments by maintaining the water flow rate at a maximum until



no air bubbles were observed from the steam drum/outlet header. A short length of water pipe connected to the outlet header is made of clear flexible plastic to allow observation of water flow. Furthermore, every precaution was taken to ensure that no air entered the water circuit whilst conducting experiments.

#### Heat exchanger calculations

As mentioned earlier, the experimental rig was designed for boiling operation and hence the calculations were based on two-phase flow conditions. The following design parameters were decided upon in determining the number and size of tubes.

Steam flow velocity	=	15 m/s (for turbulent flow)
Heating load (max)	=	20 kW
Operating pressure	=	1.01 bar
Inlet water condition	=	100°C, saturated liquid
∴ mass flow rate of steam	=	$8.86 \times 10^{-3}$ kg/s
volumetric flow rate of steam	=	$1.48 \times 10^{-3}$ m <sup>3</sup> /s

This is equivalent to 0.53 litres per minute of water flow rate.

To meet the above steam conditions, the number and size of tubes were calculated as below:

8 tubes, tube diameter	=	12.5 mm
32 tubes, tube diameter	=	6.3 mm

Hence thirty-two standard copper tubes measuring 9.5 mm OD x 6.4 mm ID were chosen.

### 6.3 Selection of heating elements

Two methods of heating the plates were considered. Firstly, hairpin elements made from strips of Brightray - S (an 80/20 nickel/chromium alloy) capable of continuous operation up to a maximum

temperature of  $1150^{\circ}\text{C}$  were considered. However, for a heating load of 10 kW per heater, the required length of strip was over 80 metres, which proved difficult to incorporate into the plate heater measuring 0.3 m x 0.3 m.

Secondly, various sizes of Silit heating elements were considered. Silit heating elements comprise a mixture of ceramic and metallic materials having low electrical resistivity and are capable of continuous operation up to  $1500^{\circ}\text{C}$ . The choice of heating element was restricted due to their non-availability at short notice to 15.9 mm diameter x 305 mm hot zone length each capable of delivering a heating load of over 3 kW at  $1200^{\circ}\text{C}$ .

Four Silit heating elements per heater were installed as recommended by the manufacturer using a highly resistant pure asbestos string.

#### 6.4 Convective vs radiative heat transfer

To evaluate the relative importance of convection and radiation, a shield with varying gap was placed between the hot plate and the heat exchanger. The heat transfer via radiation is controlled by increasing or reducing the gap in the shield and hence allow measurement of convective transfer to proceed. A flow visualisation experiment was planned to investigate the possibility of the shield obstructing the convection path.



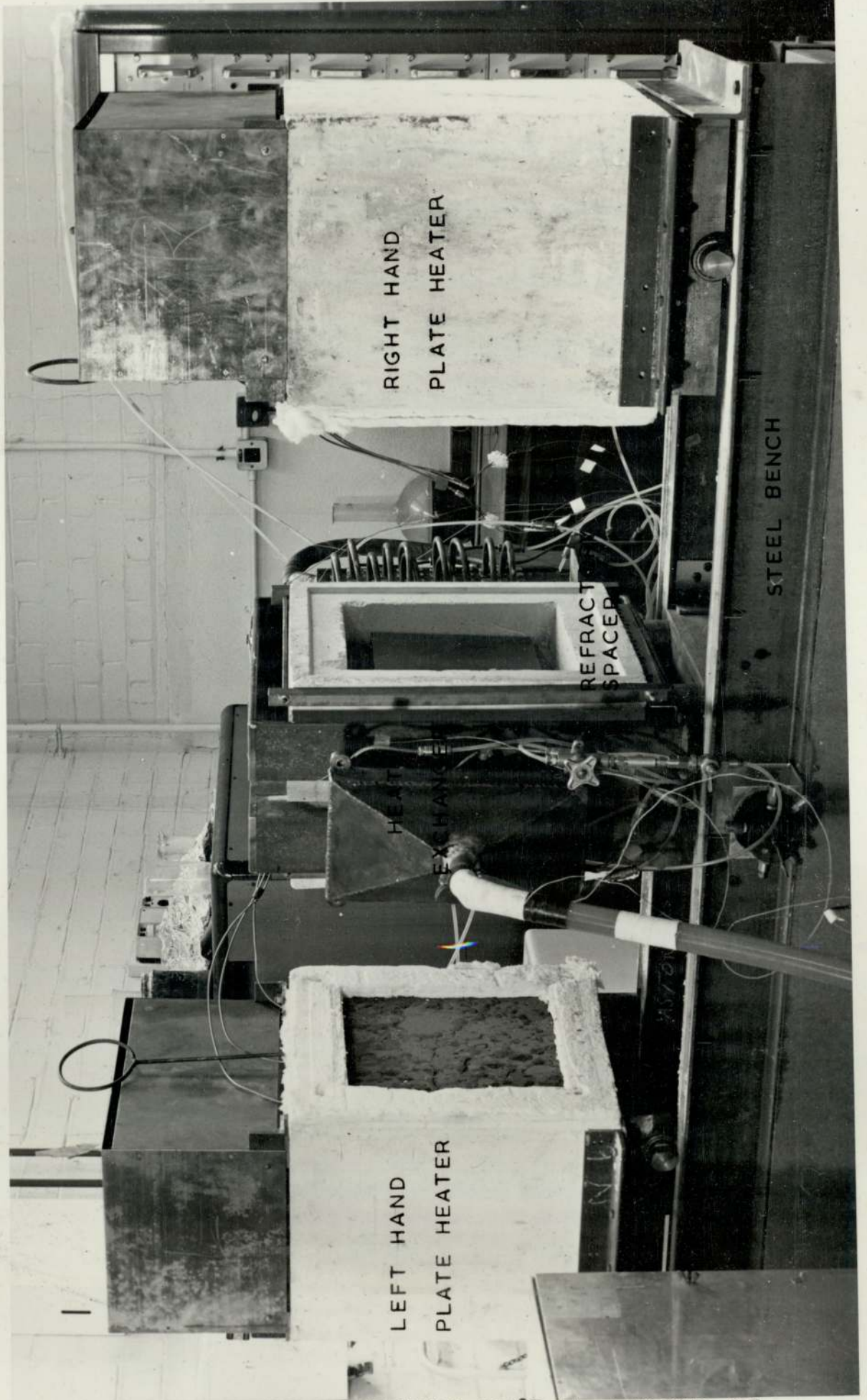


FIGURE 6.1 PHOTOGRAPH SHOWING OVERALL LAYOUT OF SLAB COOLING EXPERIMENTAL RIG

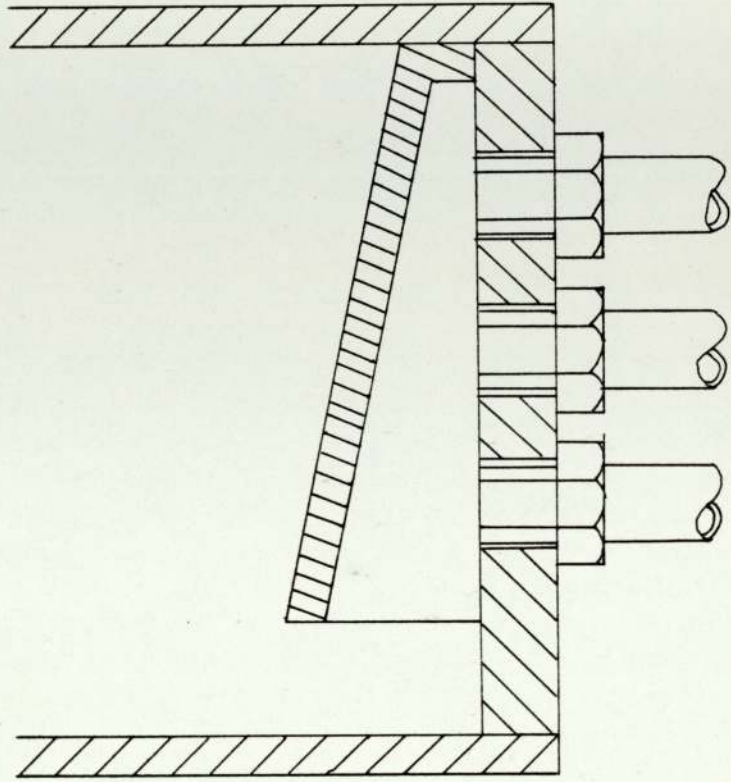
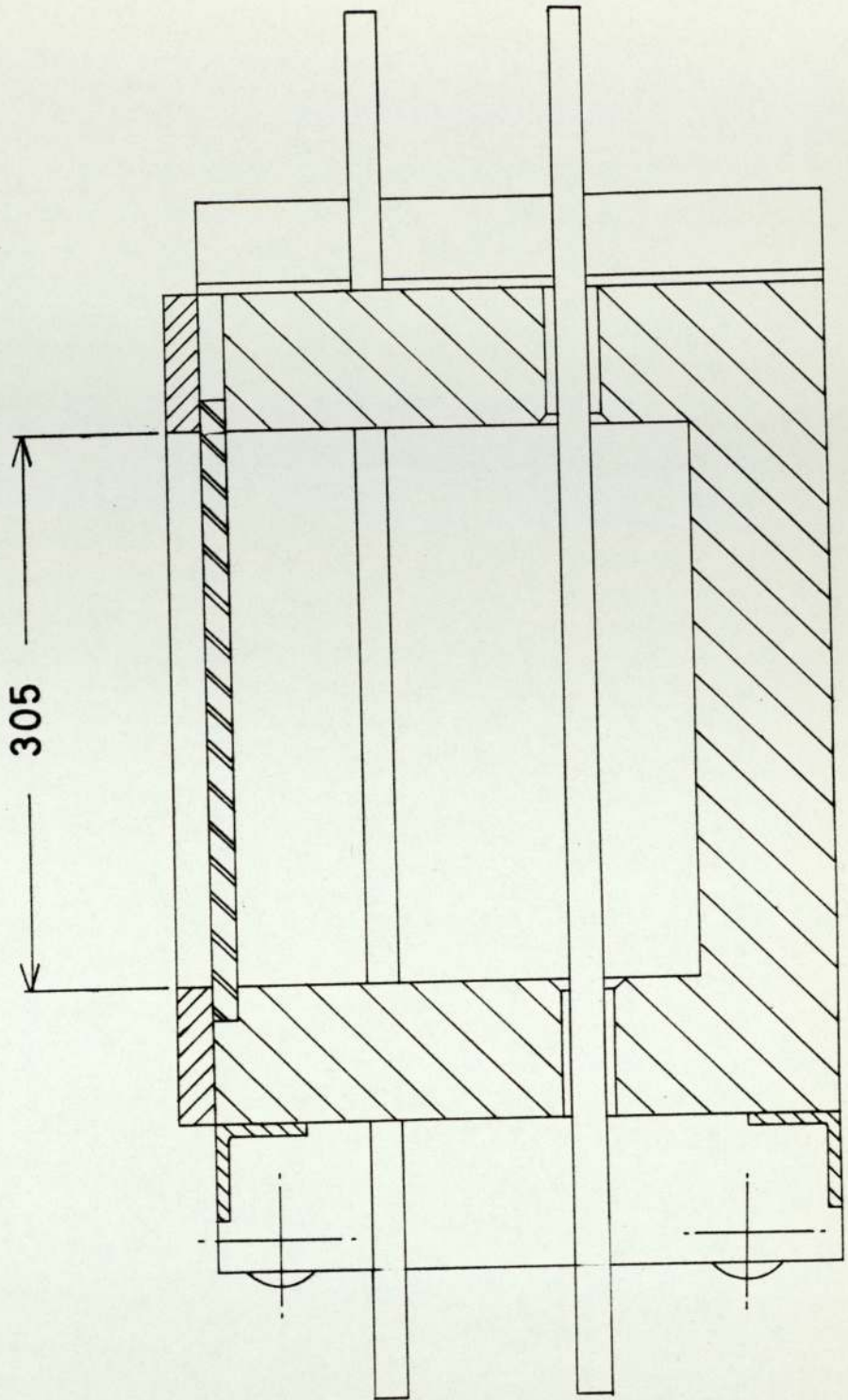


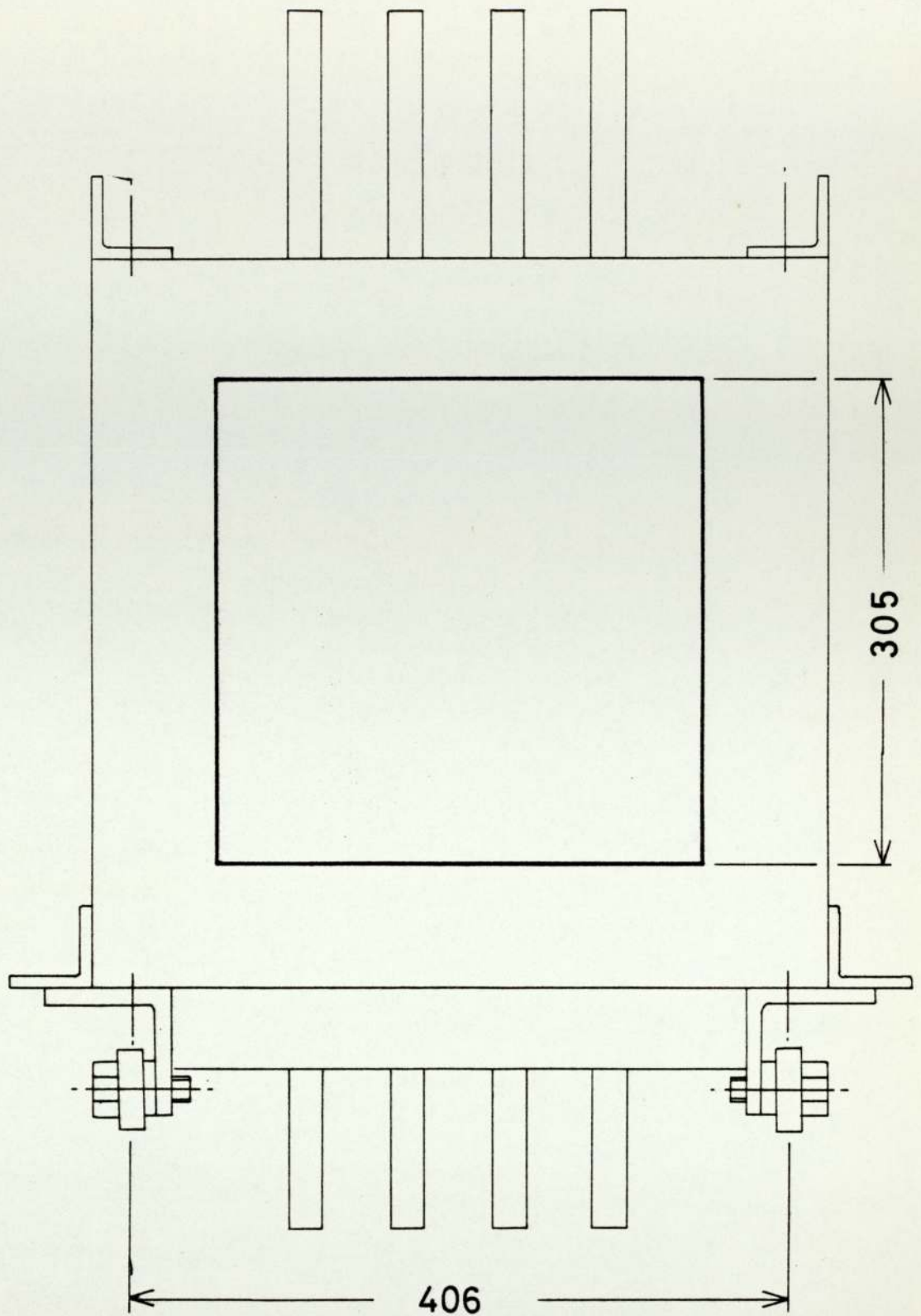
FIGURE 6.2 STEAM / WATER SEPARATING TECHNIQUE





SIDE ELEVATION

FIGURE 6.3a PLATE HEATER  
(SIDE ELEVATION)



FRONT ELEVATION

FIGURE 6.3b PLATE HEATER  
(FRONT ELEVATION)



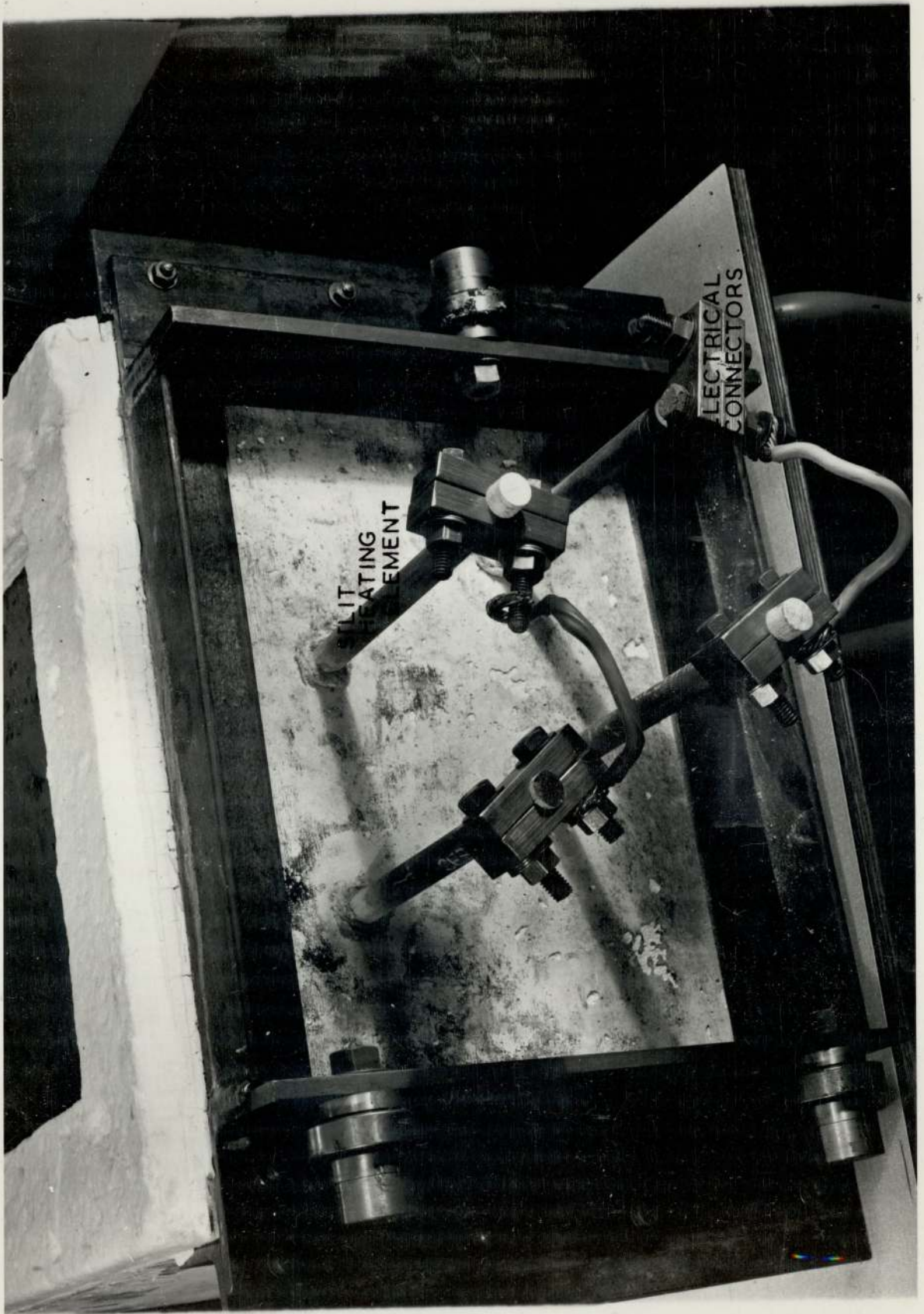


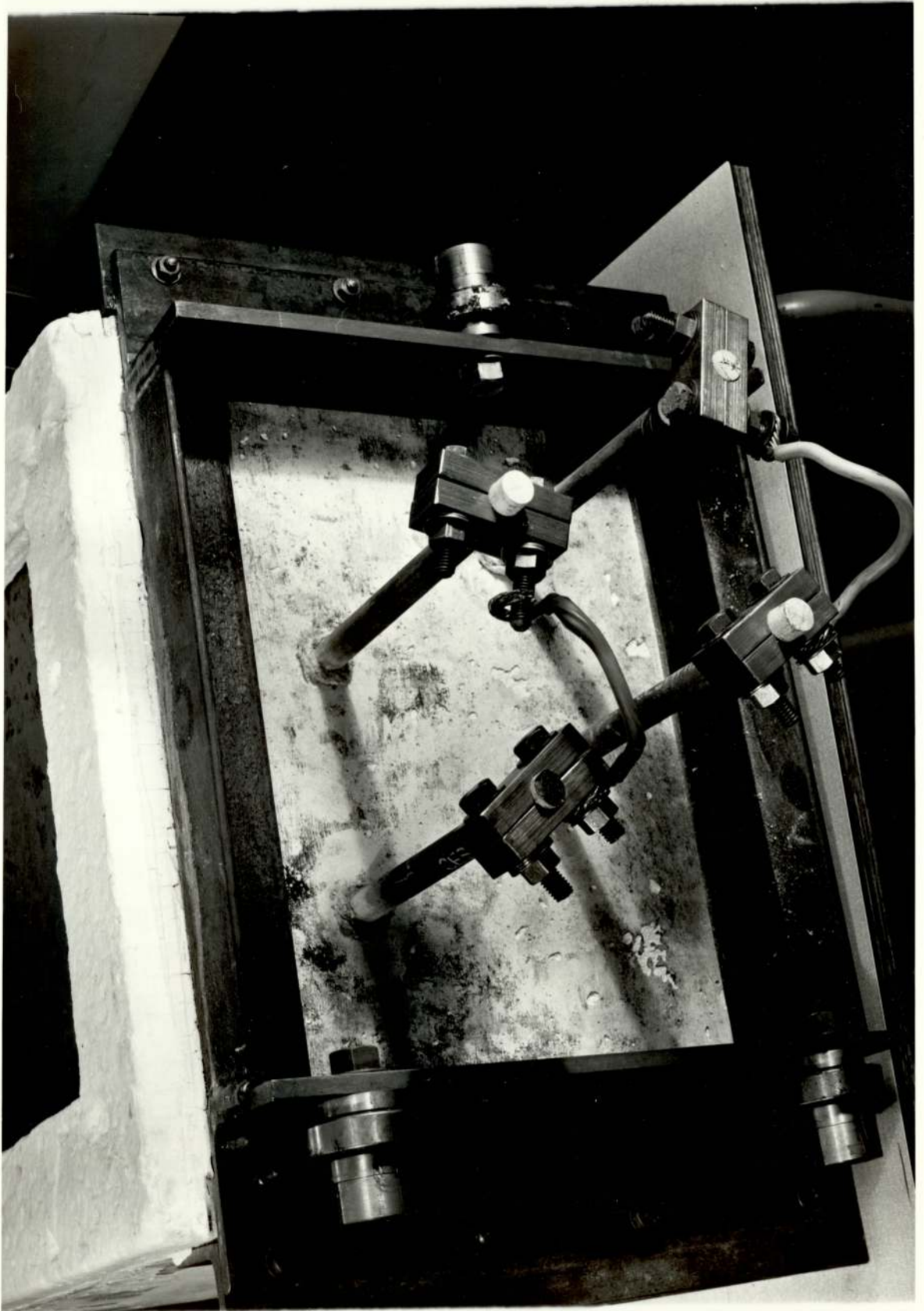
FIGURE 6.4 PHOTOGRAPH OF BASE OF A PLATE HEATER SHOWING DETAILS OF SILIT HEATING ELEMENTS

SILIT  
HEATING  
ELEMENT

ELECTRICAL  
CONNECTORS

FIGURE 6.4 PHOTOGRAPH OF BASE OF A PLATE HEATER SHOWING  
DETAILS OF SILIT HEATING ELEMENTS





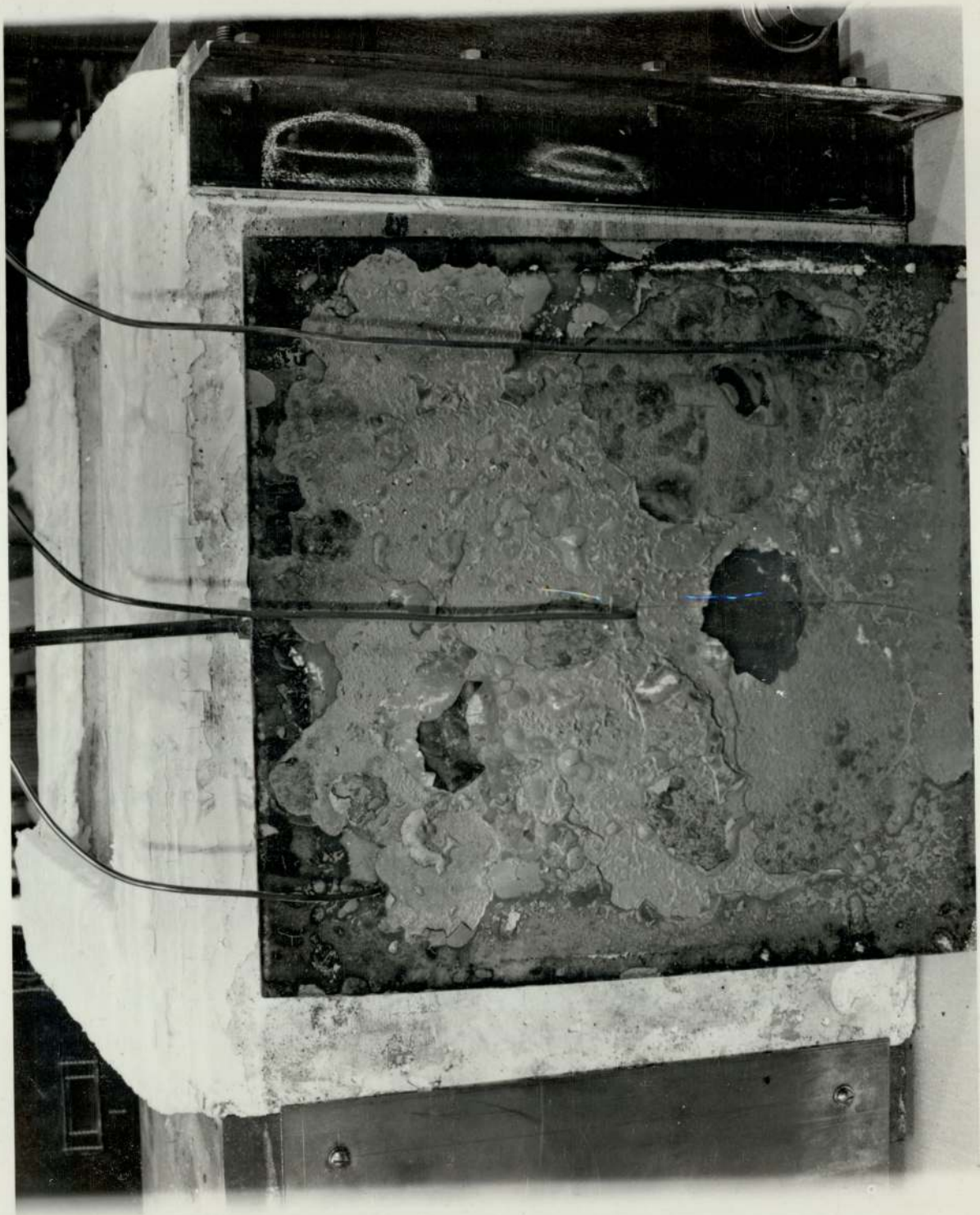
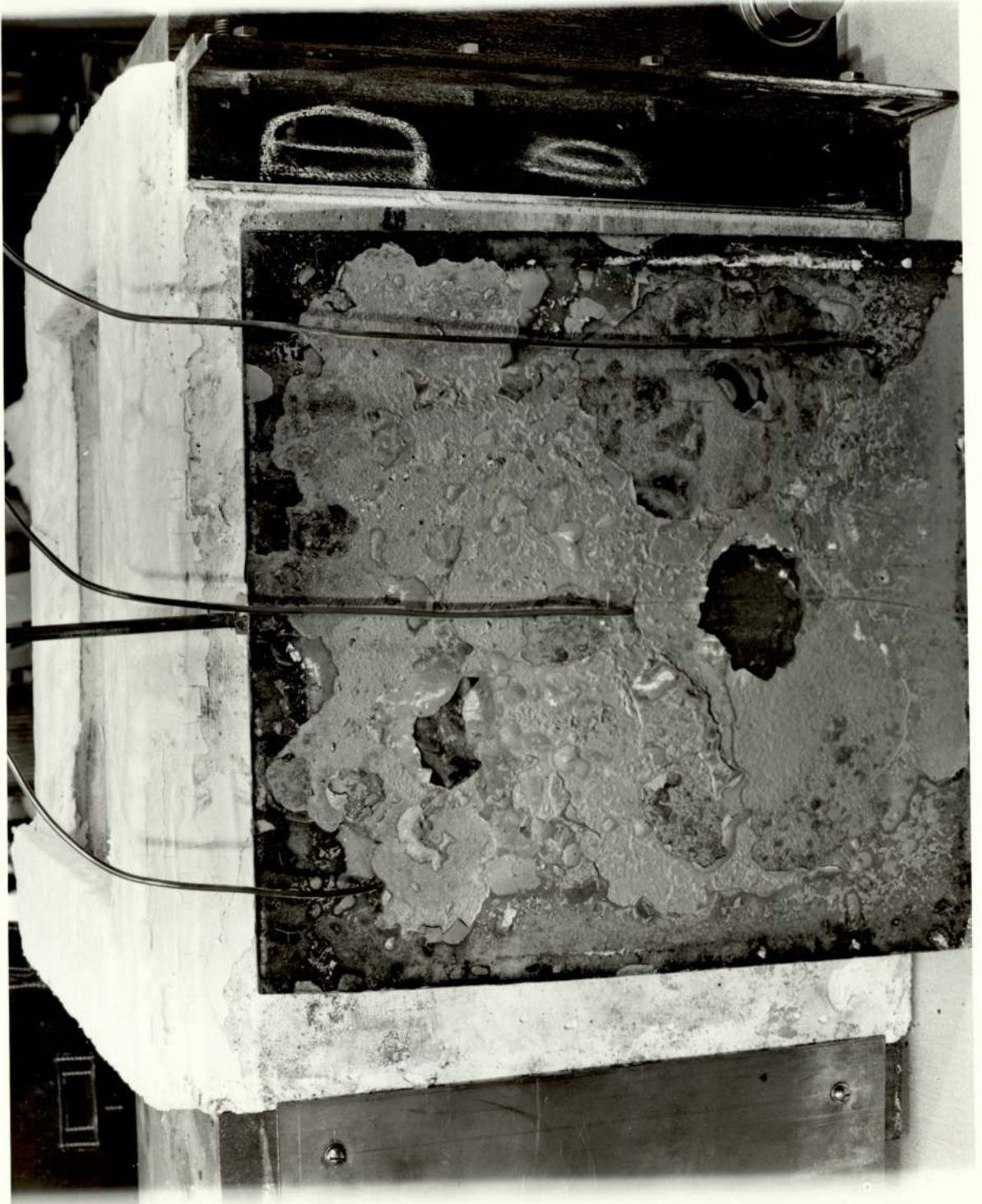


FIGURE 6.5 PHOTOGRAPH OF REAR OF A MILD STEEL PLATE  
WITH EMBEDDED THERMOCOUPLES



FIGURE 6.5 PHOTOGRAPH OF REAR OF A MILD STEEL PLATE  
WITH EMBEDDED THERMOCOUPLES





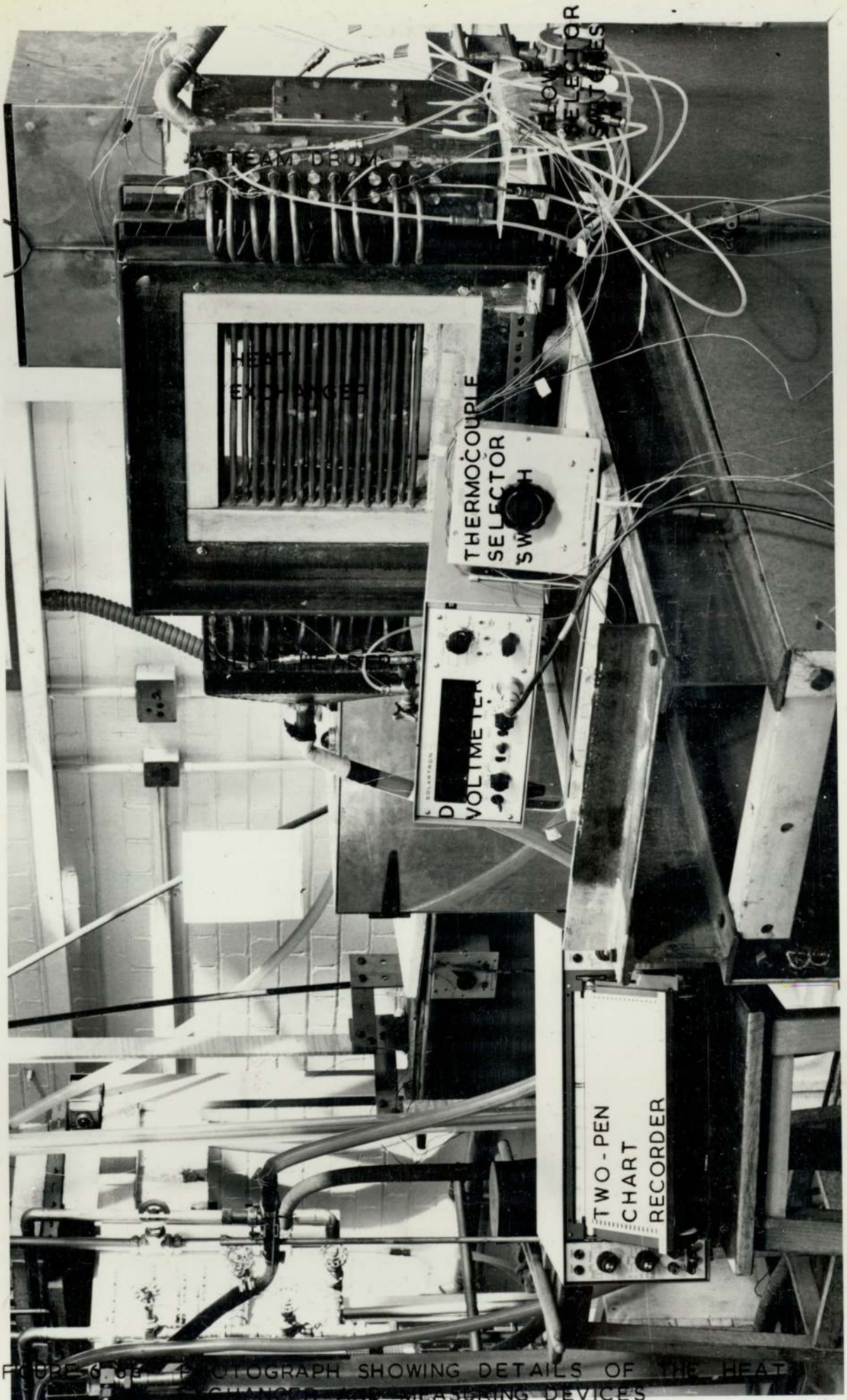


FIGURE 6.69 PHOTOGRAPH SHOWING DETAILS OF THE HEAT EXCHANGER AND MEASURING DEVICES

STEAM DRUM

FLOW  
SELECTOR  
SWITCHES

HEAT  
EXCHANGER

THERMOCOUPLE  
SELECTOR  
SWITCH

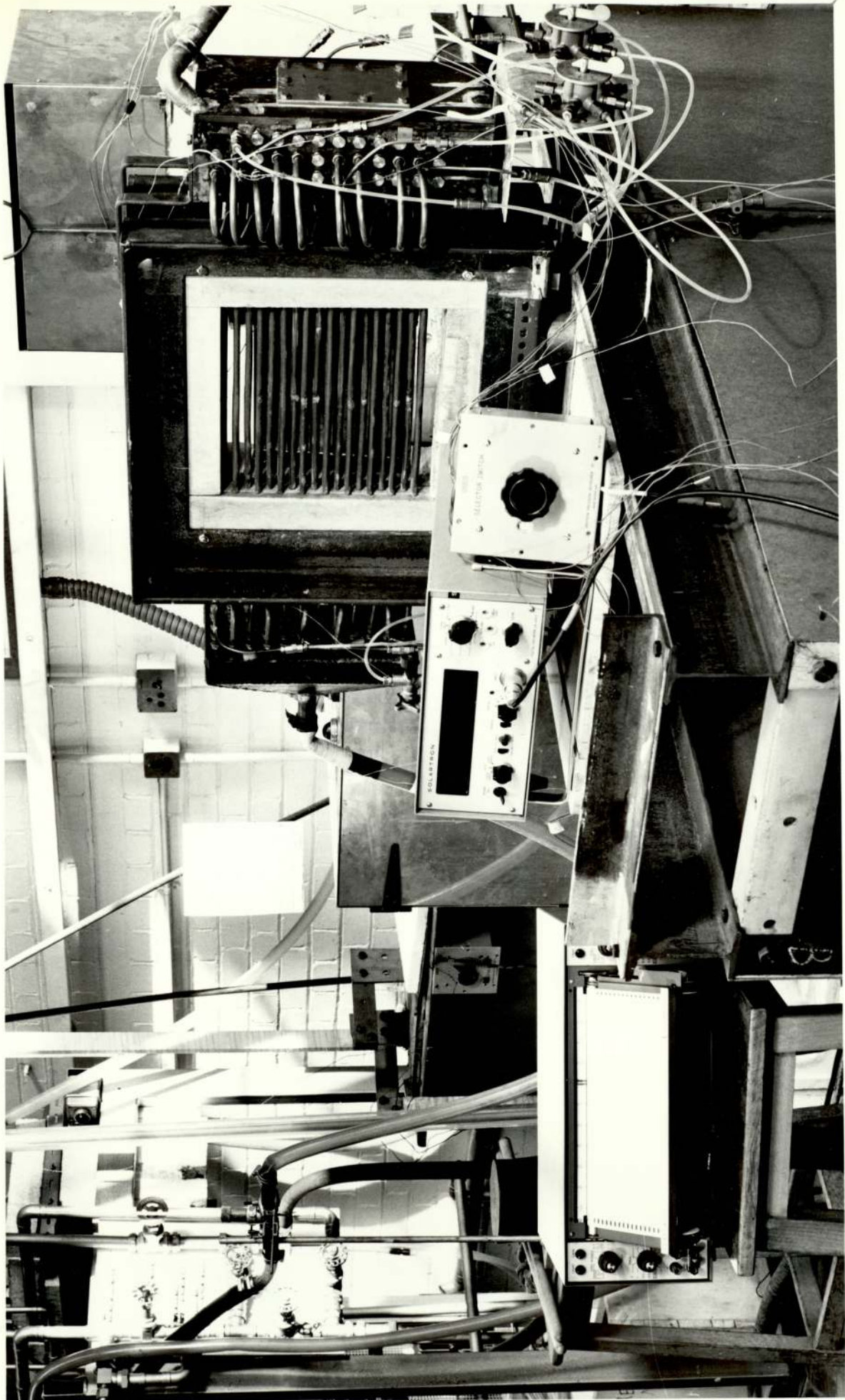
INLET HEADER

DIGITAL  
VOLTMETER

TWO-PEN  
CHART  
RECORDER

FIGURE 6.6a PHOTOGRAPH SHOWING DETAILS OF THE HEAT EXCHANGER AND MEASURING DEVICES







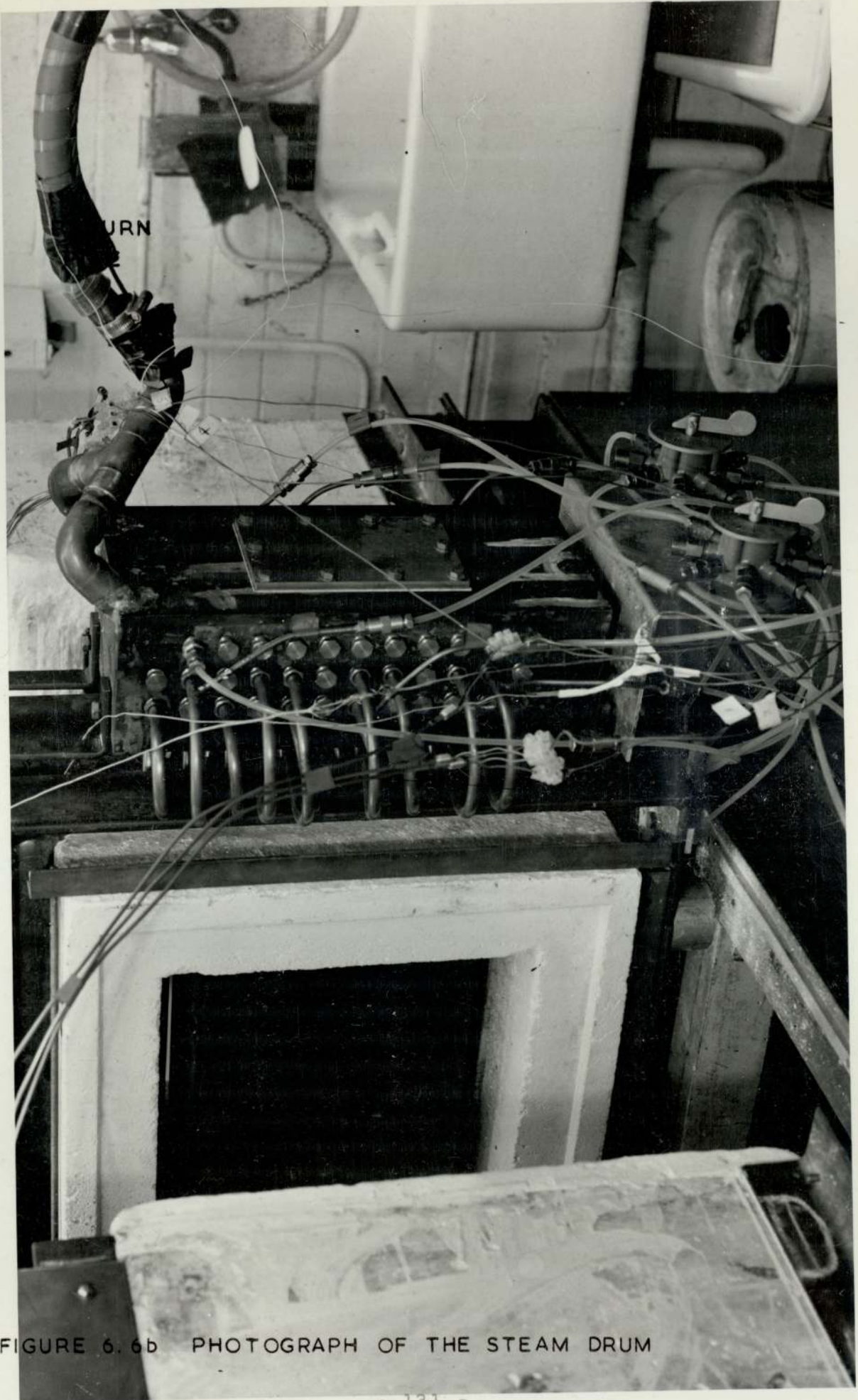
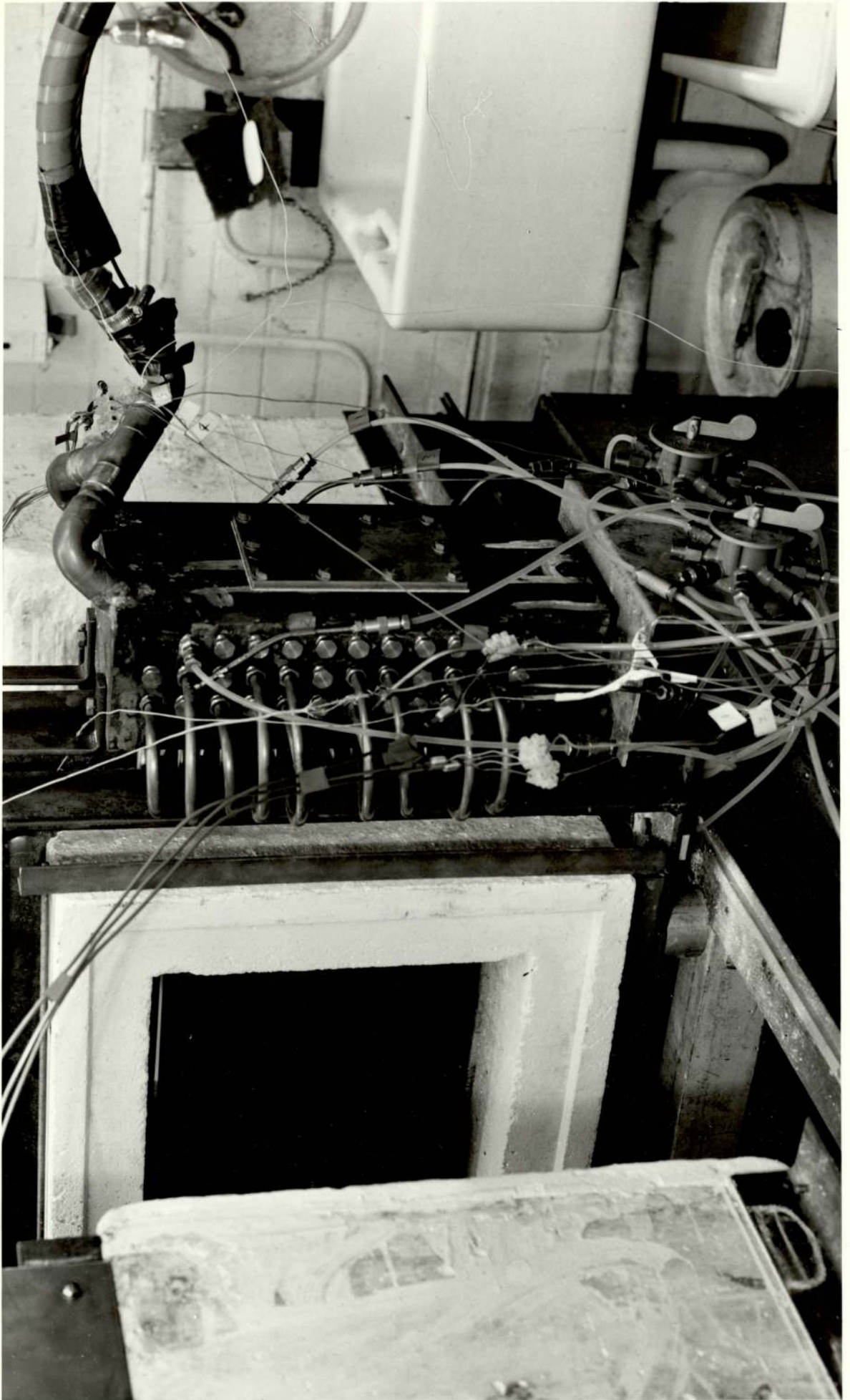


FIGURE 6.6b PHOTOGRAPH OF THE STEAM DRUM



RETURN  
PIPE

FIGURE 6.6b PHOTOGRAPH OF THE STEAM DRUM





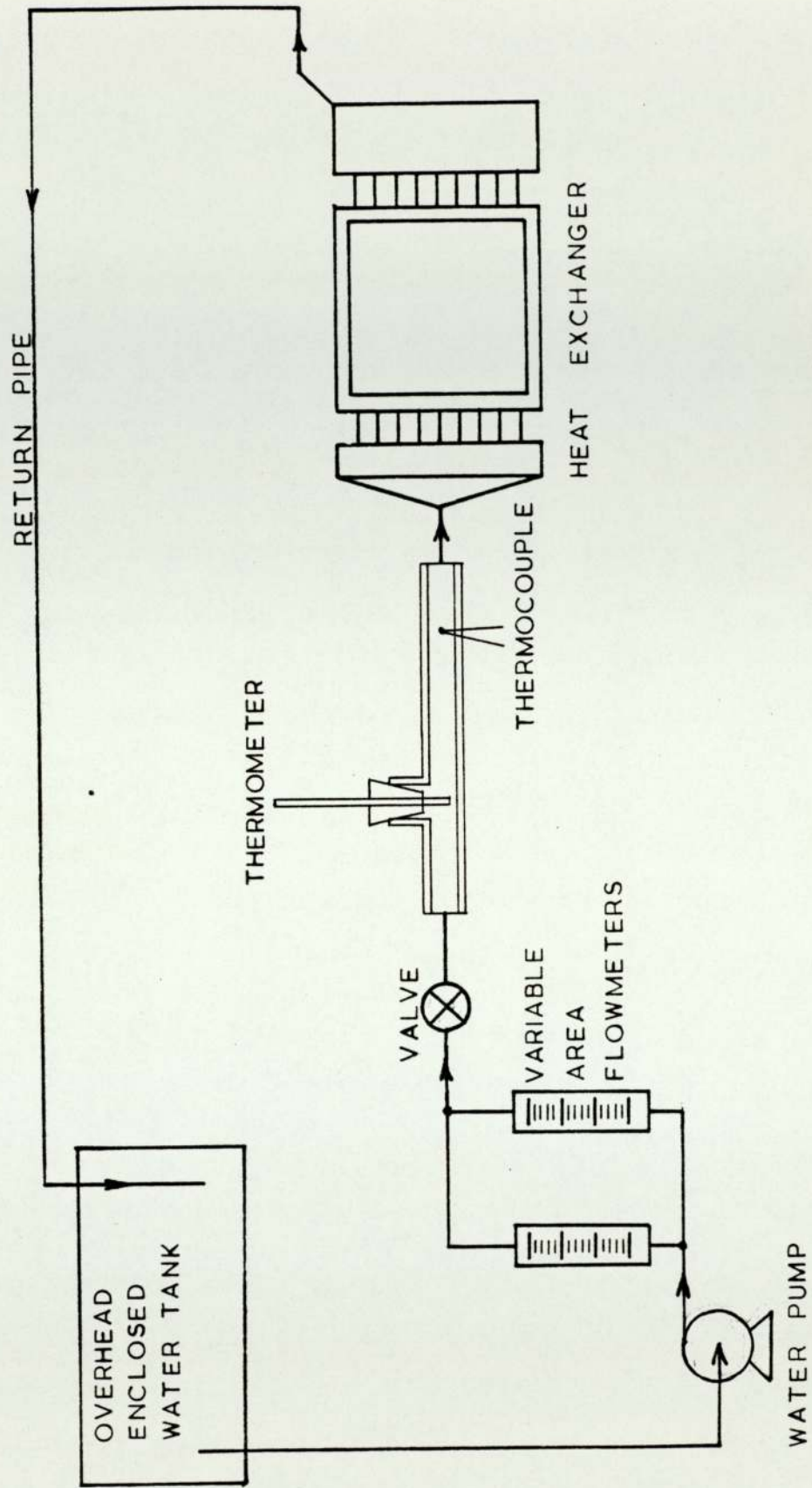


FIGURE 6.7 PICTORIAL DIAGRAM OF THE WATER CIRCUIT

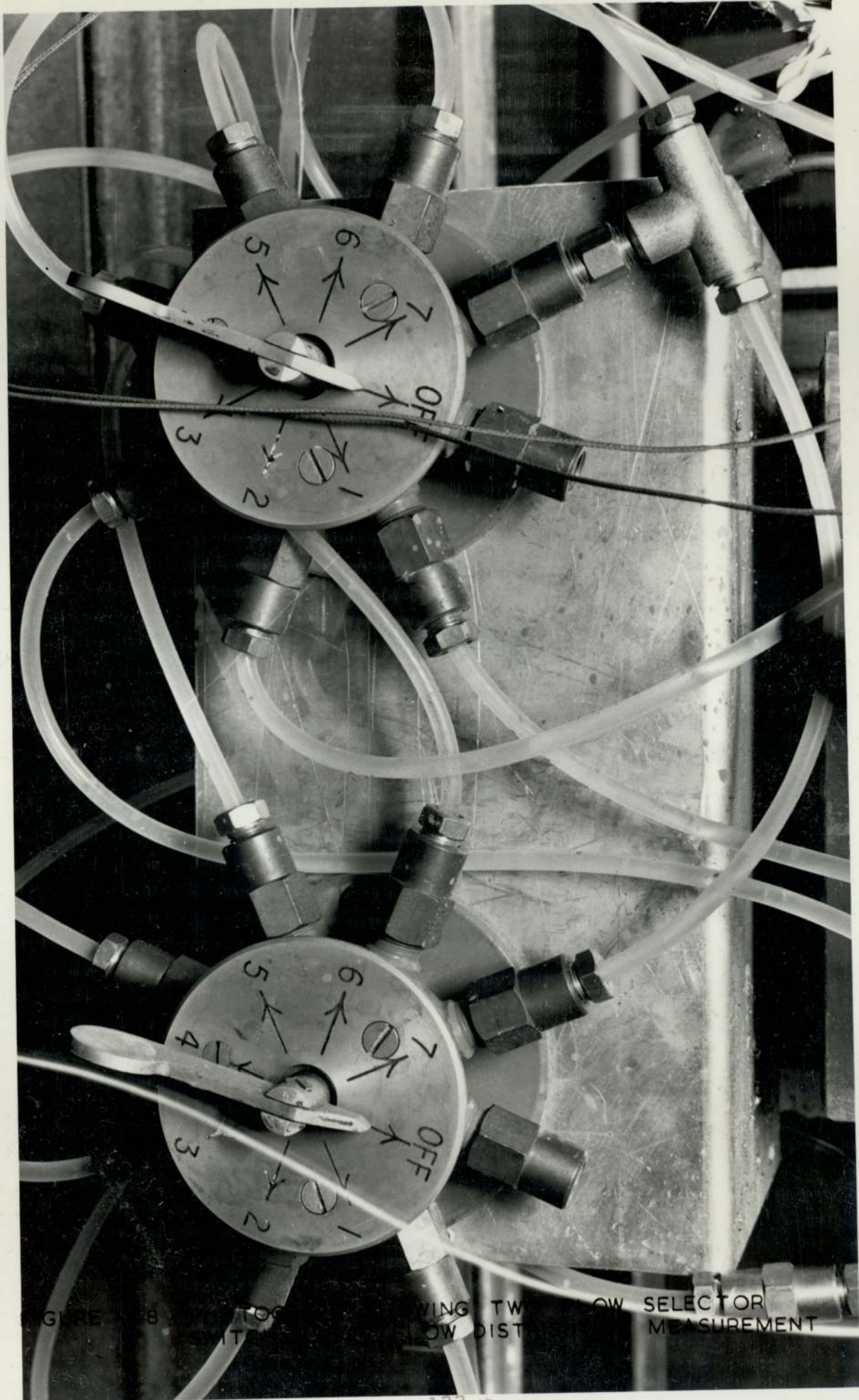


FIGURE 8

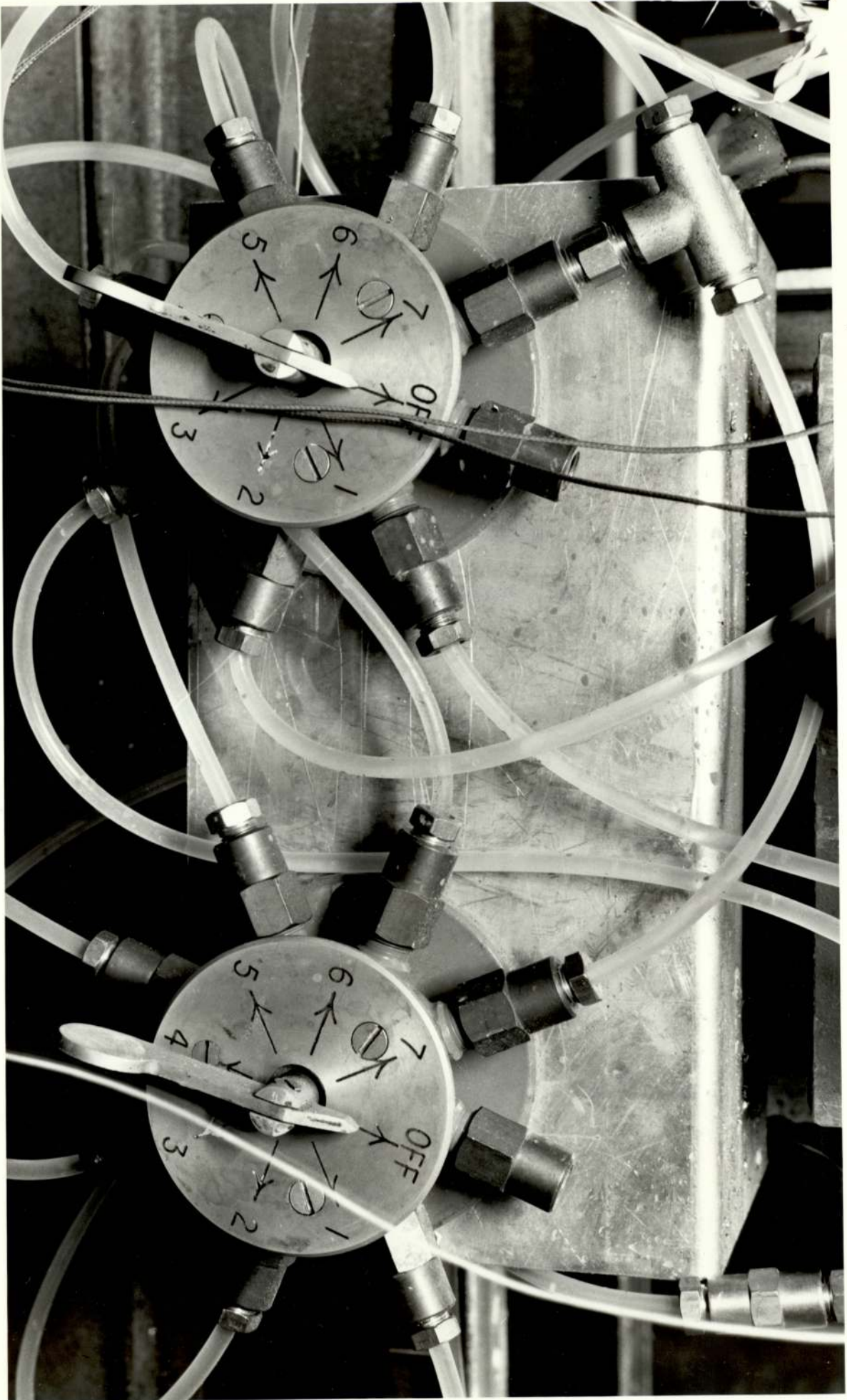
FLOW SELECTOR

LOW DIST

LOW SELECTOR MEASUREMENT



FIGURE 6.8 PHOTOGRAPH SHOWING TWO FLOW SELECTOR SWITCHES FOR FLOW DISTRIBUTION MEASUREMENT





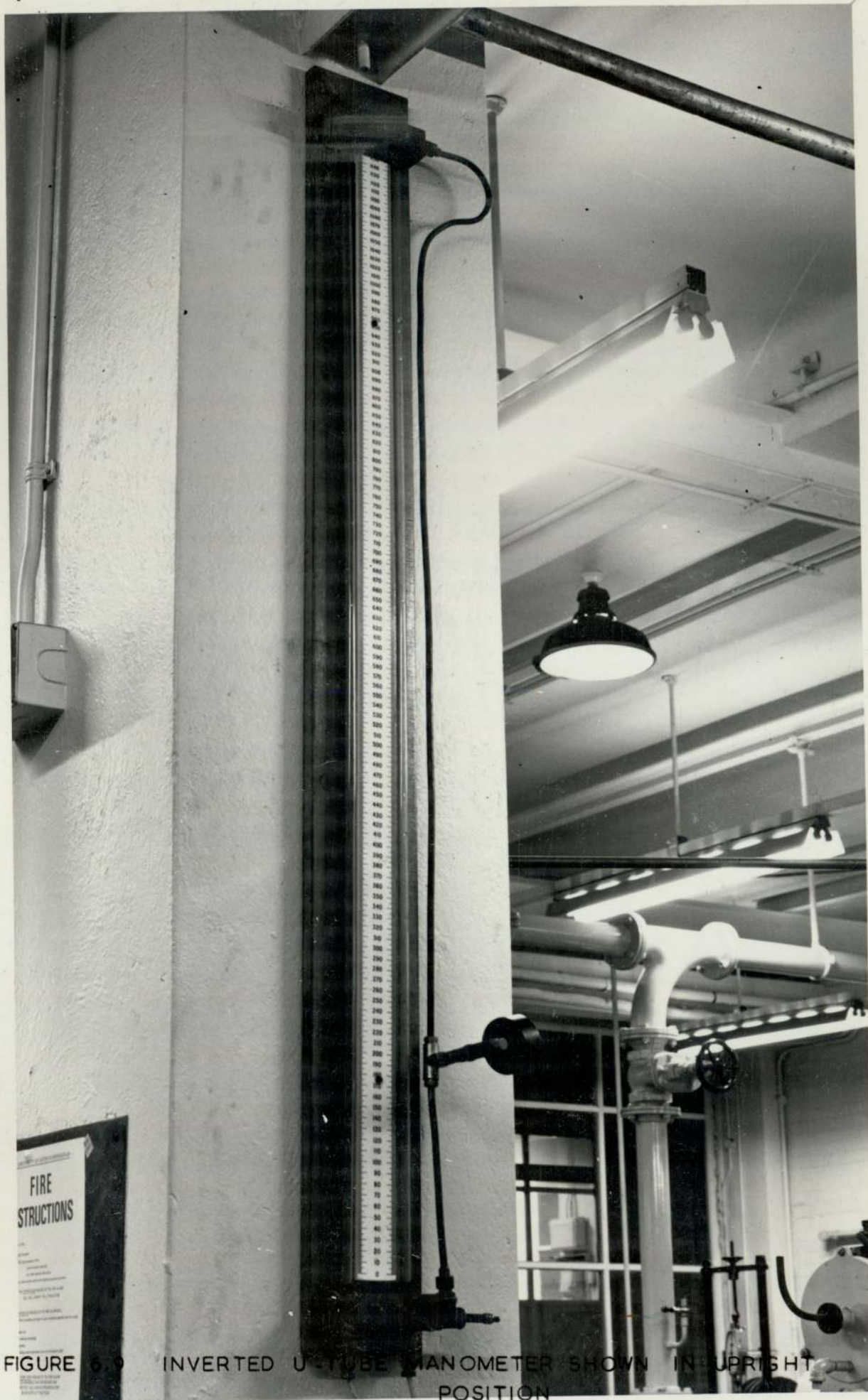


FIGURE 6.9 INVERTED U-TUBE MANOMETER SHOWN IN UPRIGHT POSITION

FIGURE 6.9 INVERTED U-TUBE MANOMETER SHOWN IN UPRIGHT POSITION





CHAPTER 7  
RESULTS AND DISCUSSION ON SLAB COOLING



This chapter is divided into three sections. The first explains the water flow measurement technique employed to obtain the flow distribution in the heat exchanger. The results of the experiments are presented and discussed. The second section gives the calculation procedure employed for the analysis of the tests. Finally, in the third section the results are presented and discussed.

## 7.1 Water flow measurements

### (a) Flow characteristics of a straight and formed tube

In a water-tube heat exchanger, particularly a boiler, uniform flow distribution is desirable to prevent burnout and maintain turbulent flow throughout. Towards this aim a simple system was devised to determine the degree of uniformity of flow distribution. The pressure drop across one metre of plain and formed copper tube was measured using an inclined water U-tube manometer over a range of flow rates. A plot of pressure drop and Reynolds number is shown in Figure 7.1. The following relationships have been established:

#### (i) Flow characteristics of a 6.37 mm ID plain copper tube.

Laminar Region ( $Re < 2500$ )

$$\Delta P = 4.169 \times 10^{-2} [Re]^{1.07} \text{ Pa} \quad (1)$$

$$\text{where } Re = \frac{\rho \cdot u \cdot d}{\mu}$$

Turbulent Region ( $Re > 2500$ )

$$\Delta P = 1.412 \times 10^{-4} [Re]^{1.8} \text{ Pa} \quad (2)$$

#### (ii) Flow characteristics of a 6.37 mm ID formed (in a similar manner to those used in the heat exchanger) copper tube.

Laminar Region ( $Re < 2500$ )

$$\Delta P = 3.022 \times 10^{-2} [Re]^{1.2} \text{ Pa} \quad (3)$$

Turbulent Region ( $Re > 2500$ )

$$\Delta P = 1.236 \times 10^{-3} [Re]^{1.6} \text{ Pa} \quad (4)$$

The results are of a similar form to those which would be anticipated for pipe flow.

(b) Flow distribution in the heat exchanger

A number of copper tubes were installed with pressure tapings. Pressure drop measurements were taken on each tube, using an inverted U-tube manometer, for the complete range of overall water flow rates. The results were substituted in equations (3) and (4) above and the flow distribution was determined and plotted in Figure 7.2. The non-uniformity in the flow distribution was noted. To rectify this problem a new design of inlet header was tried. This consisted of a 75 mm ID pipe having 32 equally spaced holes drilled radially through it. The header was connected to the heat exchanger using rubber tubes. The flow connection was made to its base and the water flow distribution in the heat exchanger was significantly improved. However, the proneness of the rubber joints to leakage at high water flow rates and at water temperatures exceeding  $50^{\circ}\text{C}$  led to its abandonment.

Two corrective methods were considered:

- (i) Redesign of inlet header on the basis of the second design considered above.
- (ii) Incorporation of a control valve and pressure tapings for tube. A multi-tube inclined manometer to adjust the flow through each tube until uniform flow is obtained.

Both of these procedures were time consuming and costly. Since a decision was made to restrict the maximum water temperature to below  $75^{\circ}\text{C}$ , the occurrence of burnout heat fluxes was unlikely. Therefore, the original design of inlet header was used in all of the experiments.



(c) Comparison of overall water flow rates measured using direct and indirect techniques

The accuracy of the flow distribution plots was determined by comparing the overall water flow rate obtained using the variable area flowmeter and that calculated from Figure 7.2. The results are given in Figure 7.3 and show that at low flow rates the error is over 20 per cent. Since the tests were conducted at 20 and 30 litres per minute the maximum error is limited to about 11% and when compared with the variable area flowmeter of + 6% over the flow and the temperature range of interest, the results are satisfactory enough.

## 7.2 Heat exchanger cooling calculations

(a) Water temperature rise measuring techniques

As mentioned earlier three methods of measuring water temperature rise were employed.

- (i) Calibrated thermometers measuring the bulk temperature rise of the water circuit. No feed water was supplied to the water circuit whilst experiments were in progress.
- (ii) Cr.Ni Al.Ni thermocouple with cold junction in ice measuring the bulk temperature rise of the water circuit as (i) above.
- (iii) Two Cr.Ni Al.Ni thermocouples connected in opposition to measure the temperature rise across the heat exchanger. However, due to the positioning of thermocouples at some distance from inlet and outlet the accuracy was in some doubt, hence the reason for employing the techniques mentioned in (i) and (ii) above.

Initially, only thermocouples were employed to measure the water temperature in the fluid circuit but these were prone to occasional

failure and proved unreliable. A strong electrical field tended to upset the readings. An attempt was made, without success, to trace the cause of these electrical fields. Henceforth, the calibrated thermometer was installed in the fluid circuit to ensure the reliability and continuous monitoring of results.

(b) Heat losses in the water circuit

To accurately determine the energy recovered by the experimental rig it is necessary to calculate the heat losses in the water circuit. The overhead water tank in the water circuit had electrical immersion heaters installed in it to preheat the water as required. Whilst the plate heaters were switched off, a constant heating load of 2.0 kW was supplied and the water pump was switched on to give flow ranging from 10 to 40 litres per minute. The results were plotted in Figure 7.4 using the analytical equation obtained by equating heat losses to heat input as below.

$$P = hA\theta + M \cdot C_p \frac{d\theta}{dt} \quad (5)$$

where P = heating load	[W]
h = external heat transfer coefficient	[W/m <sup>2</sup> K]
A = the effective external surface area of the water circuit	[m <sup>2</sup> ]
θ = water temperature above ambient	[K]
M = total mass of water in circuit	[Kg]
C <sub>p</sub> = specific heat of water	[J/kgK]
$\frac{d\theta}{dt}$ = rate of temperature rise	[K/s]

But for natural convection with low Grashoff number

$$h = \text{a constant } (C_1) \cdot \theta^{1/4} \quad (6)$$

substituting equation (6) into equation (5) and re-arranging,

$$\frac{d\theta}{dt} = \left[ \frac{P}{M \cdot C_p} \right] - \left[ \frac{C_1 A}{M \cdot C_p} \right] \theta^{5/4} \quad (7)$$



The graph in Figure 7.4 was plotted in accordance with equation 7 above but with  $\left(\frac{d\theta}{dt}\right)$  having units of K/minute. Using a least squares fit computer program, the following values of the terms, given in square brackets, were obtained:

$$(60) \left[ \frac{P}{M.C_p} \right] = 0.2944/60 \quad (8)$$

$$(60) \left[ \frac{C_1 A}{M.C_p} \right] = 2.154 \times 10^{-3}/60 \quad (9)$$

Substituting  $P = 2000W$  and  $C_p = 4186 J/kgK$  in equation (8)

$$\therefore M = 97.5 \text{ kg}$$

This result is in good agreement with the measured water tank capacity of 90.1 litres and was used in subsequent calculations involving the energy recovered by the heat exchanger.

Good agreement between the abovementioned techniques was obtained and is shown in Figure 7.4.

### 7.3 Air cooling of a plate heater

The left hand heater was heated to over  $1200^{\circ}C$  and allowed to cool in air. The internal temperature of the heater was monitored and is plotted in Figure 7.5. Because of the rapid rate of temperature drop at operating temperature, manual control of heaters to maintain a steady temperature proved difficult. Therefore no attempt was made to obtain steady operating conditions whilst conducting experiments. Although, the experiments were conducted under transient, the analysis of results was steady state using a forward difference technique. The rapid response of the heat exchange equipment to changing environment was noted and justifies the assumption of steady state conditions by considering short time intervals.

## 7.4 Results and discussion on energy recovery

The three modes of heat transfer in the slab cooling and the appropriate equations are given in Figure 5.3 and Appendix II respectively. The comparatively small size of the experimental rig necessitates the consideration of end effects in evaluating the experimental results. An account for the end effect is taken by using an all embracing term 'losses'. For thermal equilibrium of the system, the thermal energy gained by the water circuit is equated to the effective thermal energy leaving the hot plate less 'losses'. The term losses is given in quotations so as to clarify that its value will depend on the prevailing transient conditions. In terms of mathematical equations the above statement is presented as follows:

Total rate of energy recovery by the water circuit =  
(Radiation + convection + conduction) heat transfer - 'losses'

The LHS term comprises the increase in the enthalpy of water in the fluid circuit ( $= M.C_p \frac{\Delta T_w}{\Delta t}$ ) and heat losses from the circuit ( $= C_1.A.\theta^{5/4}$ ).

$$\therefore M.C_p \frac{\Delta T_w}{\Delta t} + C_1.A.\theta^{5/4} = (k_{conv} + k_{cond}) \cdot \frac{A_{he}}{D} (T_p - T_c) + \epsilon.F.A_{he}\sigma(T_p^4 - T_c^4) - \text{'losses'} \quad (10)$$

From equations (8) and (9) above,

$$M.C_p = 4.076 \times 10^5 \text{ J/K}$$

$$C_1.A = \left( \frac{2.154 \times 10^{-3}}{60} \times 97.5 \times 4186 \right)$$

$$\therefore \underline{C_1.A = 14.652}$$

Re-arranging quotation (10) gives the rate of energy recovery via radiation,



$$M \cdot C_p \frac{\Delta T_w}{\Delta t} + C_1 \cdot A \cdot \theta^{5/4} - (K_{\text{CONV}} + K_{\text{COND}}) \frac{A_{\text{he}}}{D} (T_p - T_c) = \epsilon F A_{\text{he}} \cdot \sigma \cdot (T_p^4 - T_c^4) - \text{'losses'}$$
(11)

$\frac{\Delta T_w}{\Delta t}$  - forward difference

The results of experiments were analysed using equation (11) above and are presented graphically in Figures 7.6 to 7.12. The anticipated linear relationship between the terms on the left hand side of equation (11) and  $(T_p^4 - T_c^4)$  was employed in correlating all of the data and good agreement is evident. A difference between heating and cooling periods is observed and can be explained by noting the changing nature of the surrounding environment of the heat exchanger. At the start of the heating period the whole system is cold, therefore a significant proportion of the thermal energy from the furnace walls and the hot plate helps to raise the temperature of the structure and so depressing the effective rate of energy recovery. As the temperature of the structure rises above the water temperature a secondary but solid path of heat transfer by direct conduction is created between the furnace and the heat exchanger through the thickness of the spacer and the Sindanyo lining of the heat exchanger tubes which augments the heat transfer rate. This effect is partially responsible for a relative increase in the heat transfer noted during the cooling period and is clearly shown in Figures 7.9 to 7.12. During the heating period the structural surface temperature is relatively low compared with that of the hot mild steel plate, therefore direct and reflective radiative energy significantly influences the net exchange of energy between the plate heater and the heat exchanger surface.

During the cooling period the relative thermal potential of heat exchange surfaces may change, particularly since the structure has a higher thermal storage by virtue of its mass and a lower emissivity than the heater plate. However, the plate heater and the enclosed heat

exchange chamber maintains the thermal equilibrium. As the temperature difference between surfaces is reduced the thermal conduction and radiated energy from adjacent walls to the heat exchanger tubes will increase, thus leading to an apparent high rate of heat transfer during the cooling period.

The energy data was correlated using a least squares fit technique and the results are tabulated in Figure 7.13. Equation (11) was used to evaluate the product of emissivity and view factor which is plotted against the air gap width in Figure 7.14. In Chapter 5, a simple experiment was briefly mentioned for measuring the emissivity of a rolled mild steel plate sample whilst it was heated to 1000°C. A 'gun' type radiation pyrometer was employed and an emissivity of approximately unity was obtained. The heater plates were constructed from the same material and an emissivity of unity is used.

The overall view factors between the plate heater and the heat exchanger tubes were calculated using the equation for rectangles in perpendicular planes and having one common edge given on Page 51 and Yamauti principle on Page 61 of Hottel and Sarofim (1967). By consideration of Figure 7.15 and using shorthand for  $A_1 F_{12} = \frac{(1)(2)}{(1)(2)}$ , the equations below were derived:

$$\frac{(1+2+3)(A)}{(1+3)(A+C)} = \frac{(1+3)(A+C)}{(3)(C)} - \frac{(3)(C)}{(3)(C)} \quad (12)$$

$$\frac{(1+2+3)(B+C)}{(1+2+3)(A+B+C)} = \frac{(1+2+3)(A+B+C)}{(1+2+3)(A)} - \frac{(1+2+3)(A)}{(1+2+3)(A)} \quad (13)$$

$$\frac{(r_{tb}) (B+C)}{(r_{tb}) (A+B+C)} = \frac{(r_{tb}) (A+B+C)}{(r_{tb}) (A+B)} - \frac{(r_{tb}) (A+B)}{(r_{tb}) (A+B)} + \frac{(r_{tb}) (B)}{(r_{tb}) (B)} \quad (14)$$

$$\frac{(r_{tb}) (A)}{(r_{tb}) (A+B+C)} = \frac{(r_{tb}) (A+B+C)}{(r_{tb}) (B+C)} - \frac{(r_{tb}) (B+C)}{(r_{tb}) (B+C)} \quad (15)$$

$$\frac{(r_v^1) (A)}{(r_v^1) (A+B)} = \frac{(r_v^1) (A+B)}{(r_v^{11}) (B)} - \frac{(r_v^{11}) (B)}{(r_v^{11}) (B)} \quad (16)$$

where  $r_v^1$  has common length of 0.305 metres -y  
and  $r_v^{11}$  has common length of y



$$\overline{(r_v)}(B+C) = \overline{(r_v)}(A+B+C) - \overline{(r_v)}(A) \quad (17)$$

Therefore,

$$\overline{(r)}(A) = 2 \overline{(r_{tb})}(A) - 2 \overline{(r_v)}(A) \quad (18)$$

$$\overline{(r)}(B+C) = 2 \overline{(r_{tb})}(B+C) - 2 \overline{(r_v)}(B+C) \quad (19)$$

Figure 7.15(b) simplifies the heat exchange between the hot plate and the heat exchanger such that the radiation incident on (B+C) from the hot plate is assumed to impinge directly on the heat exchanger. And, radiation incident on (B+C) from re-radiative surface ( $r_p$ ) is directed to re-radiative surface ( $r_c$ ). These assumptions give error varying from zero to a maximum of under 7% for zero shield condition. Using the above equations, overall view factors were calculated as below:

- |                                   |  |
|-----------------------------------|--|
| (i) For a complete shield         | $F_{pc} = 0.424$                           |
| (ii) For air gap width = 0.0127m  | $F_{pc} = 0.448$                           |
| (iii) For air gap width = 0.0254m | $F_{pc} = 0.459$                           |
| (iv) For air gap width = 0.038m   | $F_{pc} = 0.502$                           |
| (v) For no shield                 | $F_{pc} = 0.796$ using the above equations |
| and                               | $F_{pc} = 0.748$ actual                    |
|                                   | Error = 6.6%                               |

These view factors were used to determine the emissivity of the heat exchanger tubes and the results are tabulated in Figure 7.13. The above calculations assume the distance between the heat exchanger tubes and hot plate of 0.12m (100mm nominal) and a centrally placed shield. Figure 7.12 shows a discrepancy in emissivity from that obtained using the remaining experiments. This may be due to insufficient data points for the cooling period. Also during the flow visualisation tests, a thick layer of ash was deposited on the heat exchanger tubes. It was washed off and the tube surface subsequently cleaned with emery cloth.

It is quite possible that the experiments giving low emissivity followed it, although no record is available.

Similarly, using Yamauti principle the overall view factor between an average slab and the heat exchanger surface measuring 1.5 x 12.0m with 0.2m gap between them was calculated as below. These surfaces are represented diagrammatically in Figure 7.16.

$$\frac{(A+B+C+D)(1+2+3+4)}{(A)(1)} = 15.536$$

$$\frac{(A)(1)}{(A)(1+2+3+4)} = 9.5025$$

$$\therefore \frac{(A)(1+2+3+4)}{(A)(1+2+3+4)} = 9.5262$$

and  $F_{(A)(1+2+3+4)} = \underline{0.84}$

Therefore, provided the emissivity of heat exchanger tubes is above 0.9 then the condition analysed in the theoretical model is valid. Any reduction from this will result in a proportionately reduced rate of energy recovery or an increase in the size of slab cooling units.

The air circulation due to natural convection in an enclosed heat exchange chamber was observed. A U-shaped refractory spacer with the fourth side housing an observation panel made from Pyrex thermal glass plate was placed between the heat exchanger and one of the plate heaters. A smoke pellet was ignited and introduced into the chamber to observe the air currents. The existence of convective currents in the heated chamber was noted but its contribution to the total heat exchange was insignificant as predicted by the equations in Appendix II and on Page 63 of Spiers (1961). The dominance of the heat transfer by radiation is clearly indicated by the linear relationship obtained between the radiative heat transfer and  $(T_p^4 - T_c^4)$  plots in Figures 7.6 to 7.12 and the correspondingly minor role played by convection and direct conduction. Therefore, it is suggested that the heat exchanger design for slab cooling should



primarily concentrate on radiative considerations.

The results from the experimental rig has verified the mathematical model for slab cooling. A number of design parameters for the full-scale slab cooling system are listed below:

- (i) For an air tight heat exchange chamber with the hot and cold surface in direct visual contact, the major heat exchange is by radiation. Therefore, for simplification the heat exchanger design could be evaluated and optimised on the basis of radiation only.
- (ii) The tube arrangement should be such that it maximises the view factor and have an emissivity close to unity. A single row of closed packed tubes is recommended.
- (iii) The distance between the slabs and the cooling surfaces should be kept to a minimum.
- (iv) The structural barriers between the heat exchange surface and slabs should be kept to a minimum, preferably below 10% of the total heat transfer area.
- (v) In the slab cooling system suggested in Chapter 5, each chamber should be physically isolated from its neighbours to reduce structural thermal fatigue. However, the arrangement is not recommended for the final design.
- (vi) A fast and reliable conveyancing system, between the primary rolling mill and the slab cooler, is desirable to reduce heat losses and to optimise the total energy recovery.
- (vii) The heat exchanger elements should be capable of quick assembly and dis-assembly for repair, maintenance and replacement. Also, in future, when hot inspection for surface imperfections becomes available, the ability to convert the heat exchanger to a thermal storage unit is desirable.

In all energy recovery systems the need for flexibility in their operation is essential to balance the mismatch between the supply and the demand requirements. For example, in power generation a continuous and uniform energy source is desirable for high thermal efficiency and to ensure uninterrupted operation. In Chapter 5, a three hour slab cooling cycle was suggested, together with the physical separation of each cooling chamber. Since the slab temperature significantly influences the rate of energy available for recovery, a large variation in power output will disturb the continuity of a constant heat source. Therefore, the use of separate cooling chambers is not compatible with the power generation requirements without the installation of complex flow valves. Another possible boiler arrangement is to use pool boiling with auxiliary firing for superheating. All these suggestions introduce complexities in the boiler design.

A solution is to use a continuous train of slabs placed on a variable speed conveyor, thus giving a known thermal gradient from start to finish and a once-through boiler arrangement can be employed. The conveyor system is enclosed in a draught-free chamber. The length of the complete structure can be divided into appropriately sized short lengths of economiser, boiler and superheater sections. To reduce the overall length of the heat exchanger a number of parallel chambers separated by heating elements can be installed. It is suggested that the economiser should be divided into two sections, placed at the front and the rear of the cooler to reduce high thermal strains in the structure by presenting a low temperature front to the external environment whilst permitting entry and exit of slabs. The speed of the conveyor can be varied in accordance with the cooling cycle, slab production and steam quality and quantity requirements.

Although these proposals for a slab cooling boiler involve moulding a boiler around a slab conveyor no new advanced technologies



are proposed. Hence, it represents a short-term solution to the present production scheduling and surface imperfection problems. The conveyancing system will be similar to that currently used in the fire-zone reheating furnace. A rotary/tilting table to set up the slab for its introduction into the slab cooler is not new as these are currently employed near the primary rolling mills and in many other iron and steelwork processes. Therefore, most of the equipment is available and is currently in use by the British Steel Corporation except the boiler. The boiler itself involves radical structural modifications on present design, but few problems are anticipated.

On the author's behalf, a cost survey of conventional waste-heat and fuel-fired boilers was carried out [Taft (1979)] for a 13 MW boiler operating at a pressure of 30 bar and 14K superheat. An estimated price of a conventional shell and tube waste-heat boiler was approximately £100,000 and, with modifications for use in slab cooling, its cost is anticipated to double. These costs are only a guide and may not reflect the true cost of a slab cooling boiler. No allowances were made for the conveyancing system in the chamber, slab feed and extraction equipment, and transportation of slabs from the primary rolling mills to the slab cooler. In Chapter 5, the economic investment for a slab cooling system to process 10 slabs per hour, 5000 hour operation per annum and with maintenance cost per annum of 5% of initial capital investment was £3,000,000 assuming energy cost at 0.5 pence per kWh of steam produced. These estimates were based on the Llanwern iron and steelworks whilst operating at just over half its full-capacity and 57% of the slabs available were processed through the slab cooling system.

In December, 1979 the energy cost of one unit (kWh) of steam produced using heavy fuel oil is over one pence. Therefore, slab cooling is even more a viable-economic and practical proposition. A 13 MW system represents an annual saving of nearly £700,000 in the fuel bill at Llanwern

steelworks alone. A potential annual saving of £1,000,000 exists at Llanwern iron and steelworks in recovering energy from hot slabs for steam production. These figures, as mentioned earlier are based on slab production at Llanwern in 1975. The lack of sufficient data on current slab production and possible usage of steam so produced has hindered the decision on specifics. Therefore, all potential savings are based on the assumption that the available energy can be used economically or substitute one or more processes where brought-in fuel is used. A number of requests were made for this information but without success. Before making the final decision on size of slab cooler and location, further in depth study of local conditions is desirable.



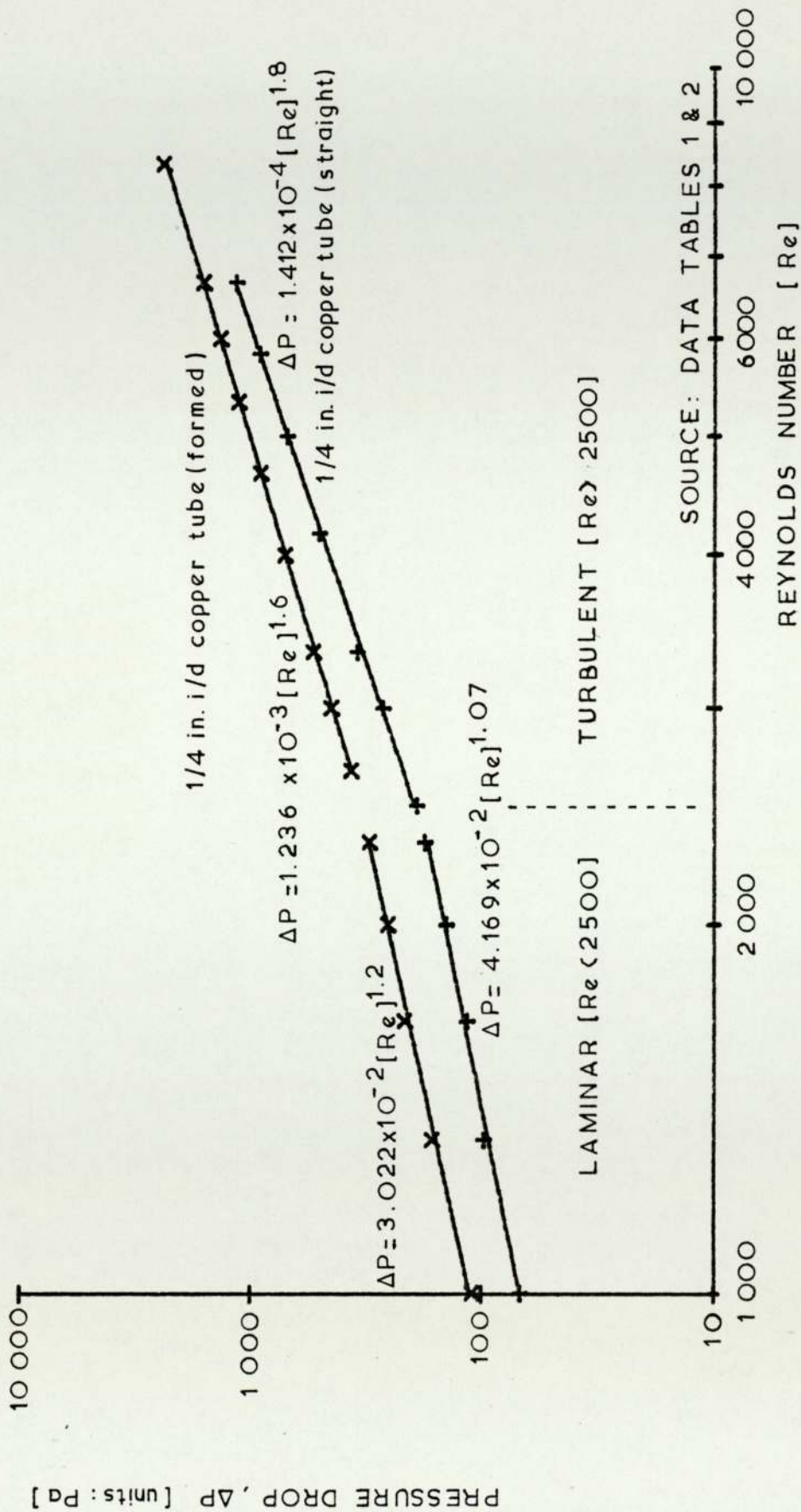
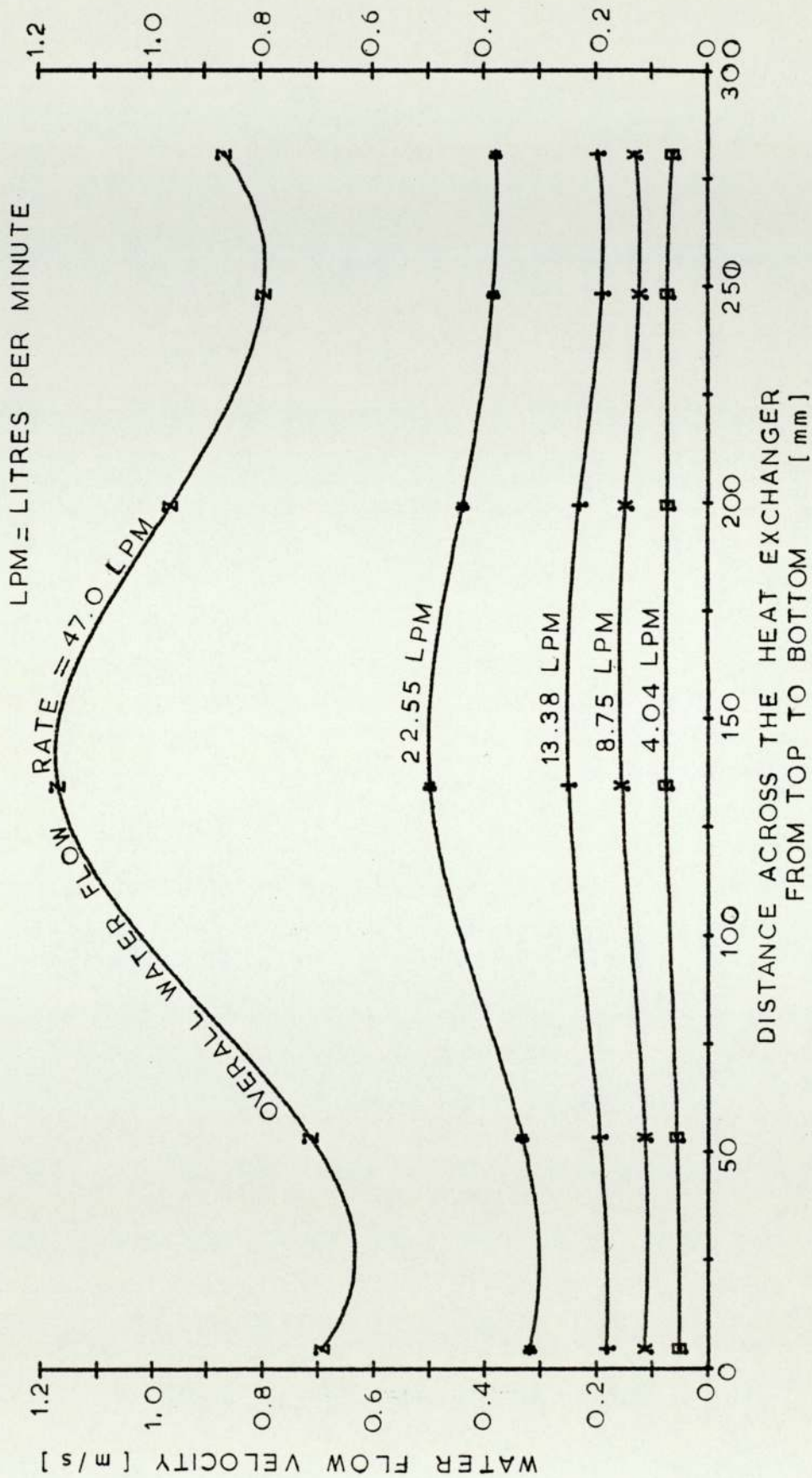


FIGURE 7.1 PRESSURE DROP ACROSS A 1m LONG COPPER TUBE (similar to those used in the heat exchanger)



SOURCE : DATA TABLE 3

FIGURE 7.2 WATER FLOW DISTRIBUTION IN THE HEAT EXCHANGER



FIGURE 7.3 - Comparison of measured and calculated overall water flow rates

Measured Water Flow Rate by a Variable Area Flowmeter (Litres/Min)	Calculated Value from Water Flow Distribution (Litres/Min)	% Error $\left[ \frac{(M-C)}{M} \times 100 \right]$
4.04	3.323	17.75
8.75	6.72	23.2
13.38	10.68	20.18
22.55	20.20	10.42
47.0	44.66	5.0

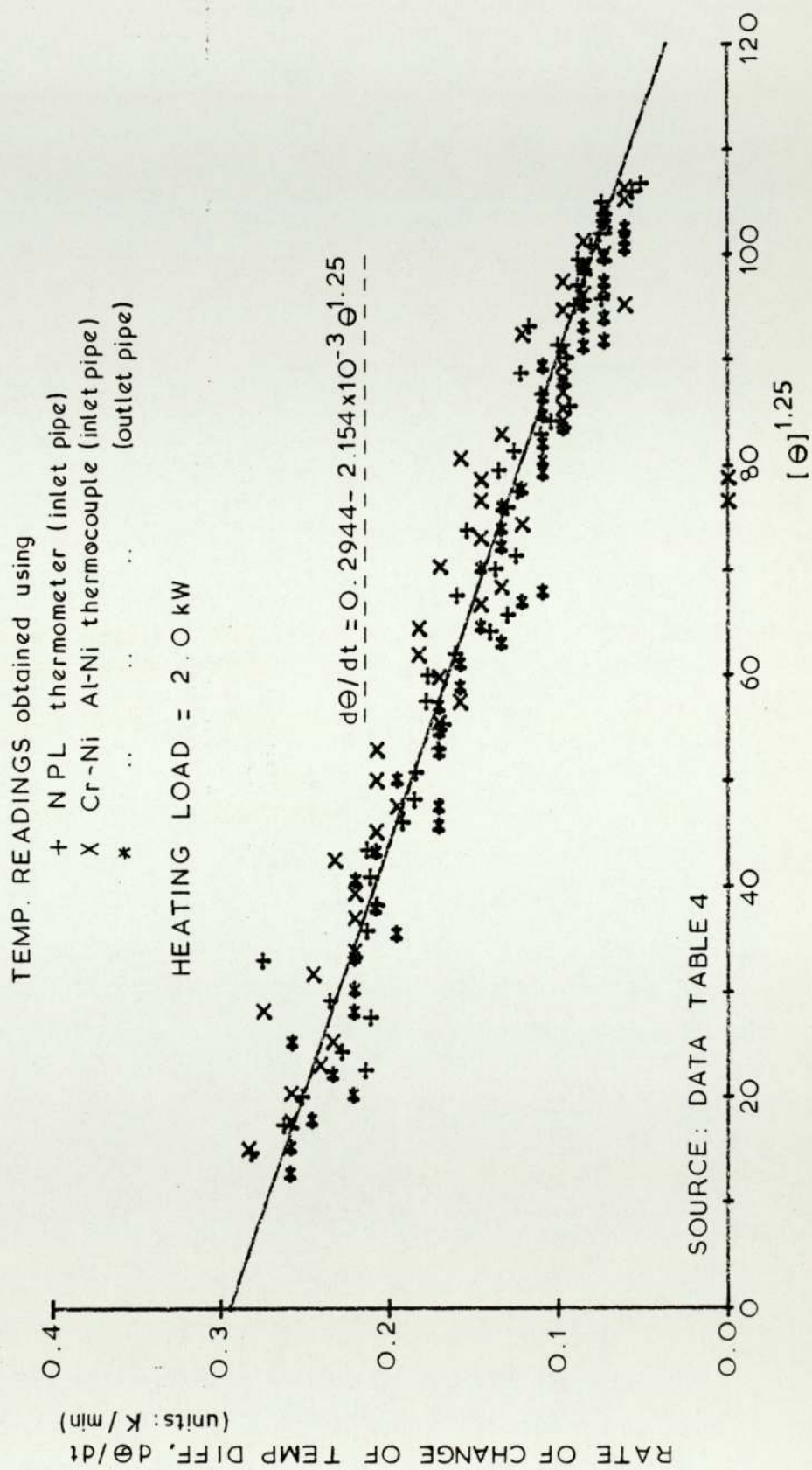


FIGURE 7.4 HEAT LOSSES VIA NATURAL CONVECTION FROM COOLING SYSTEM



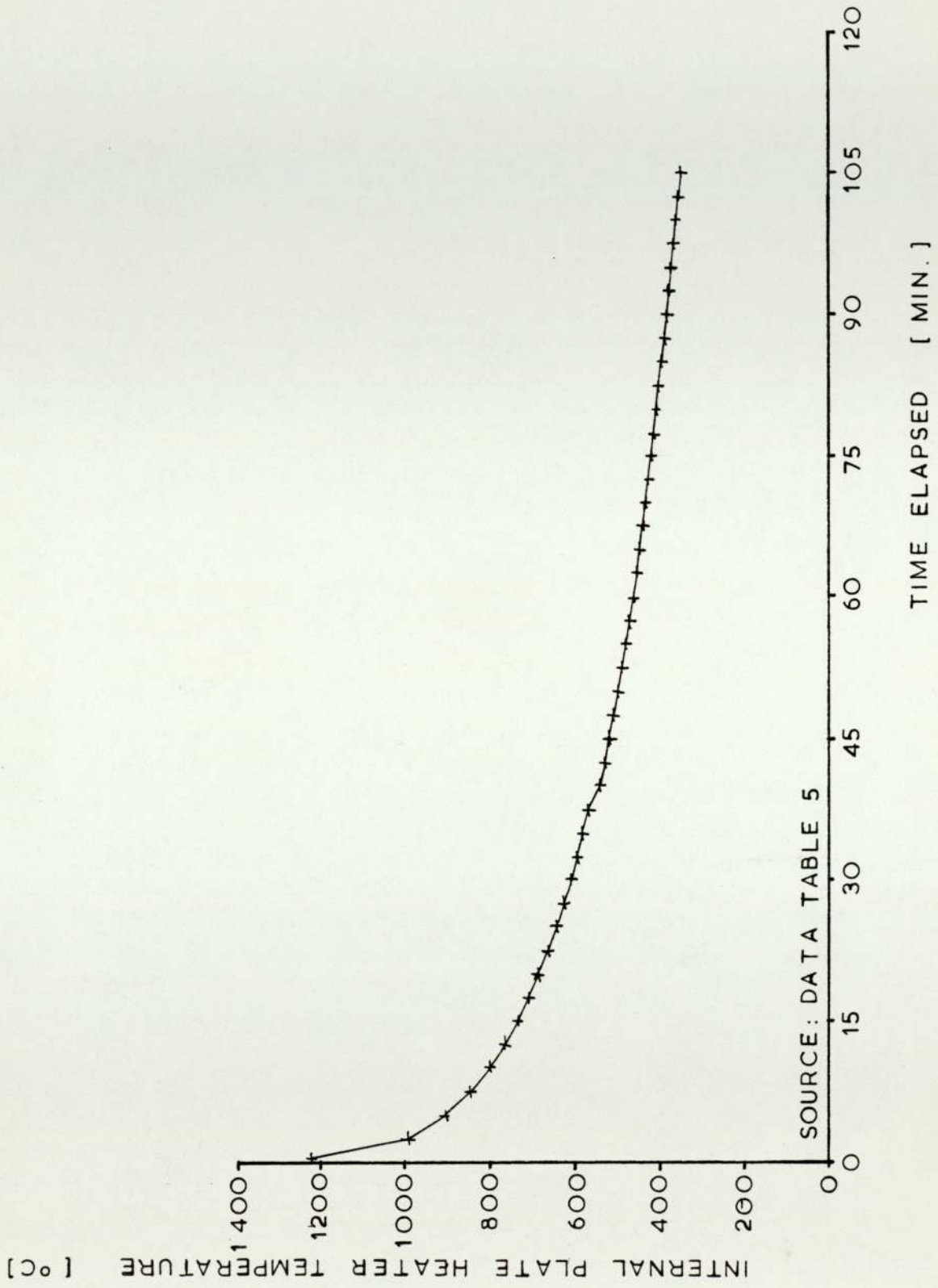


FIGURE 7.5 AIR COOLING OF A PLATE HEATER WITH ALL SIDES INSULATED USING 76mm THICK REFRACTORY

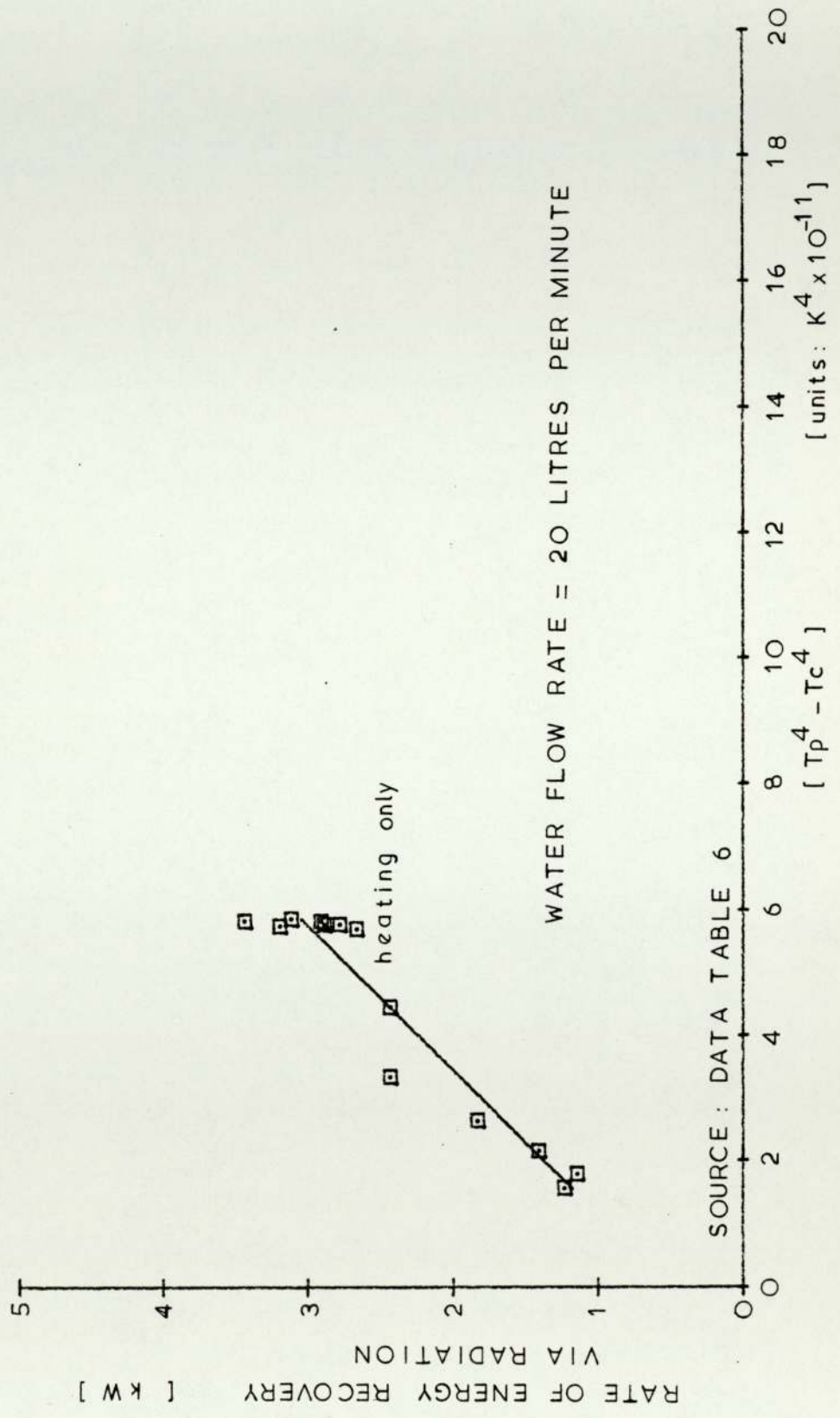


FIGURE 7.6 ENERGY RECOVERY WITH BOTH HEATERS AND NO REFLECTORS



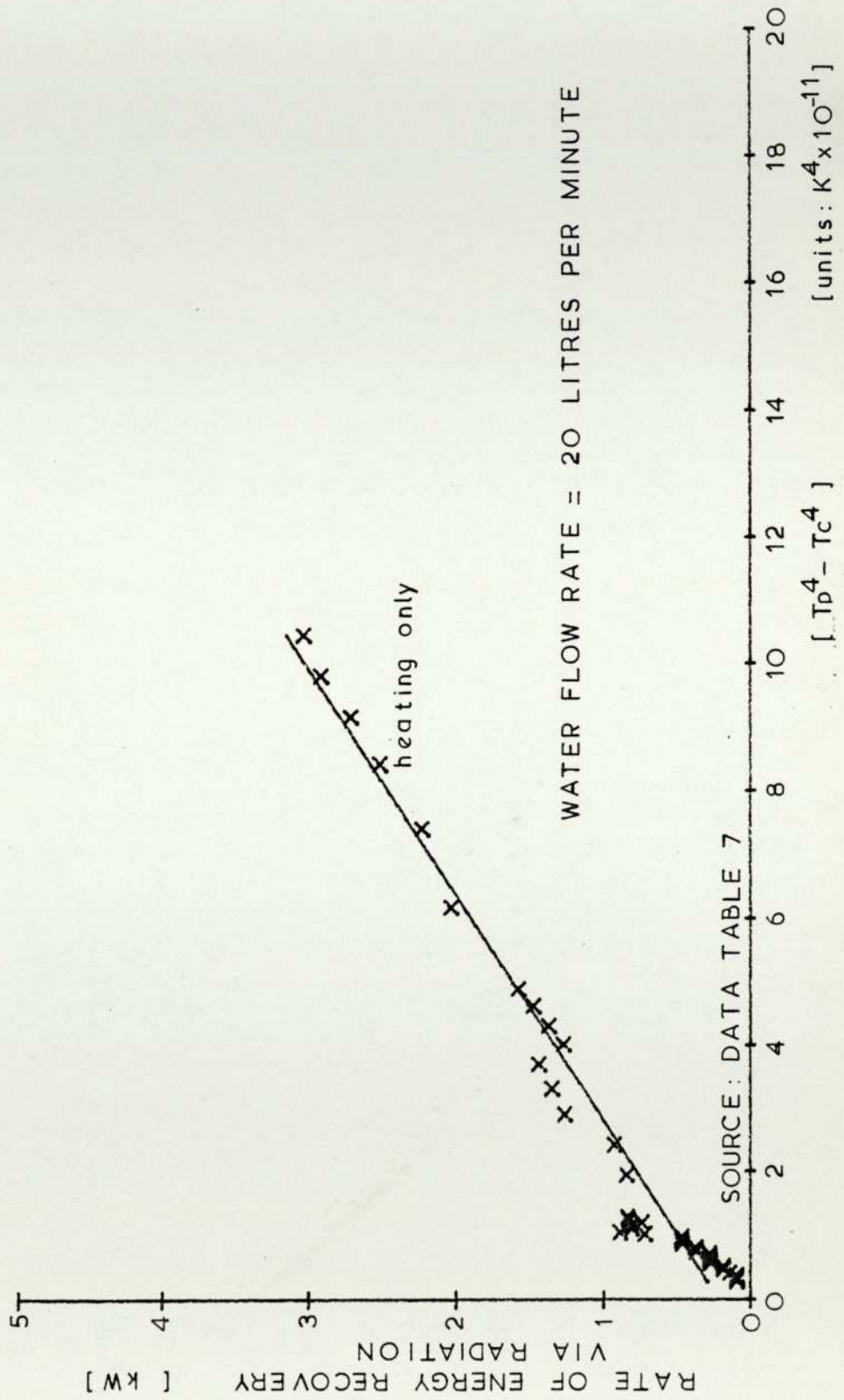


FIGURE 7.7 ENERGY RECOVERY WITH BOTH HEATERS AND AIR GAP WIDTH OF 25.4 MM

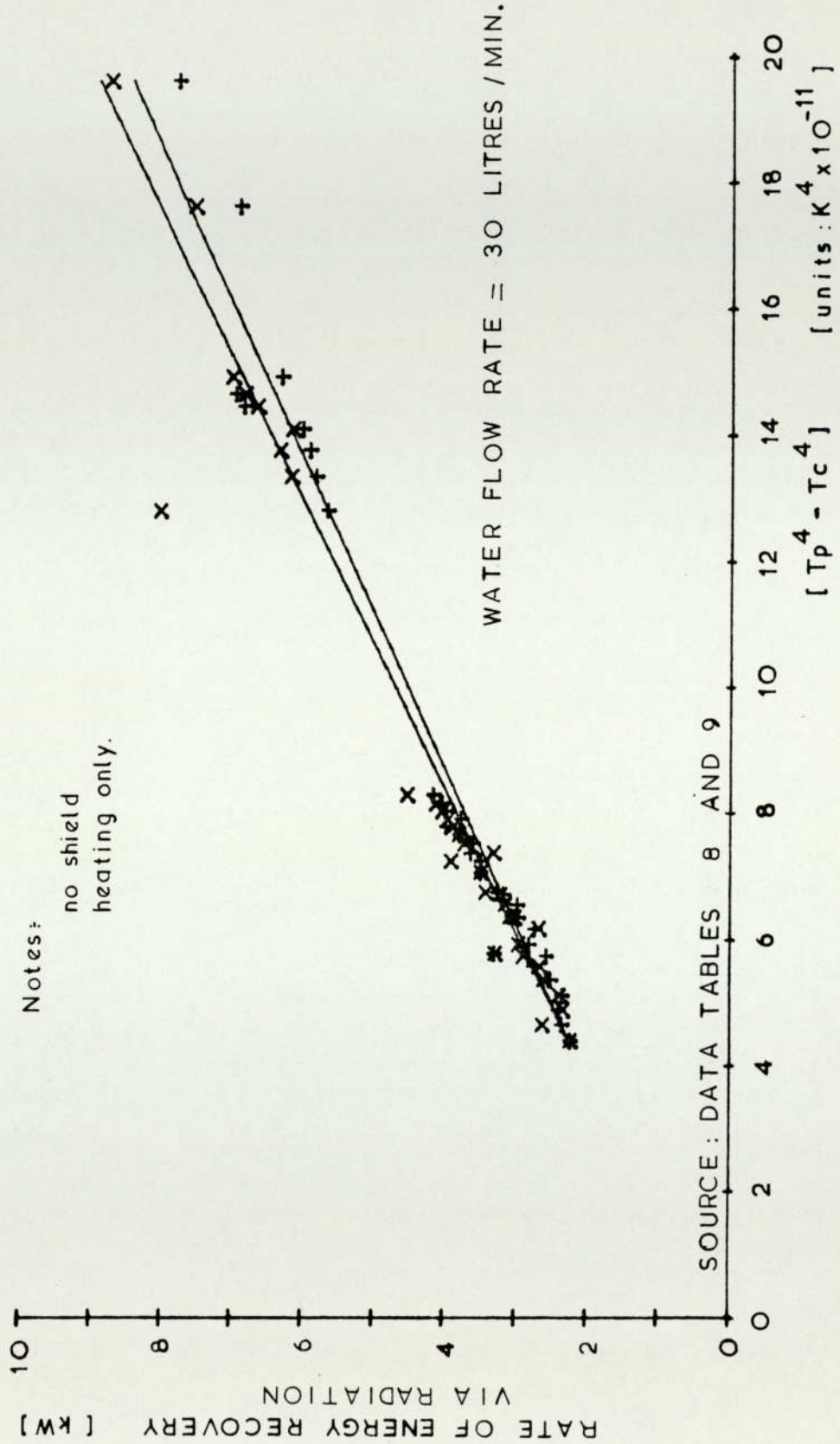


FIGURE 7.8 ENERGY RECOVERY WITH BOTH HEATERS AND NO REFLECTORS



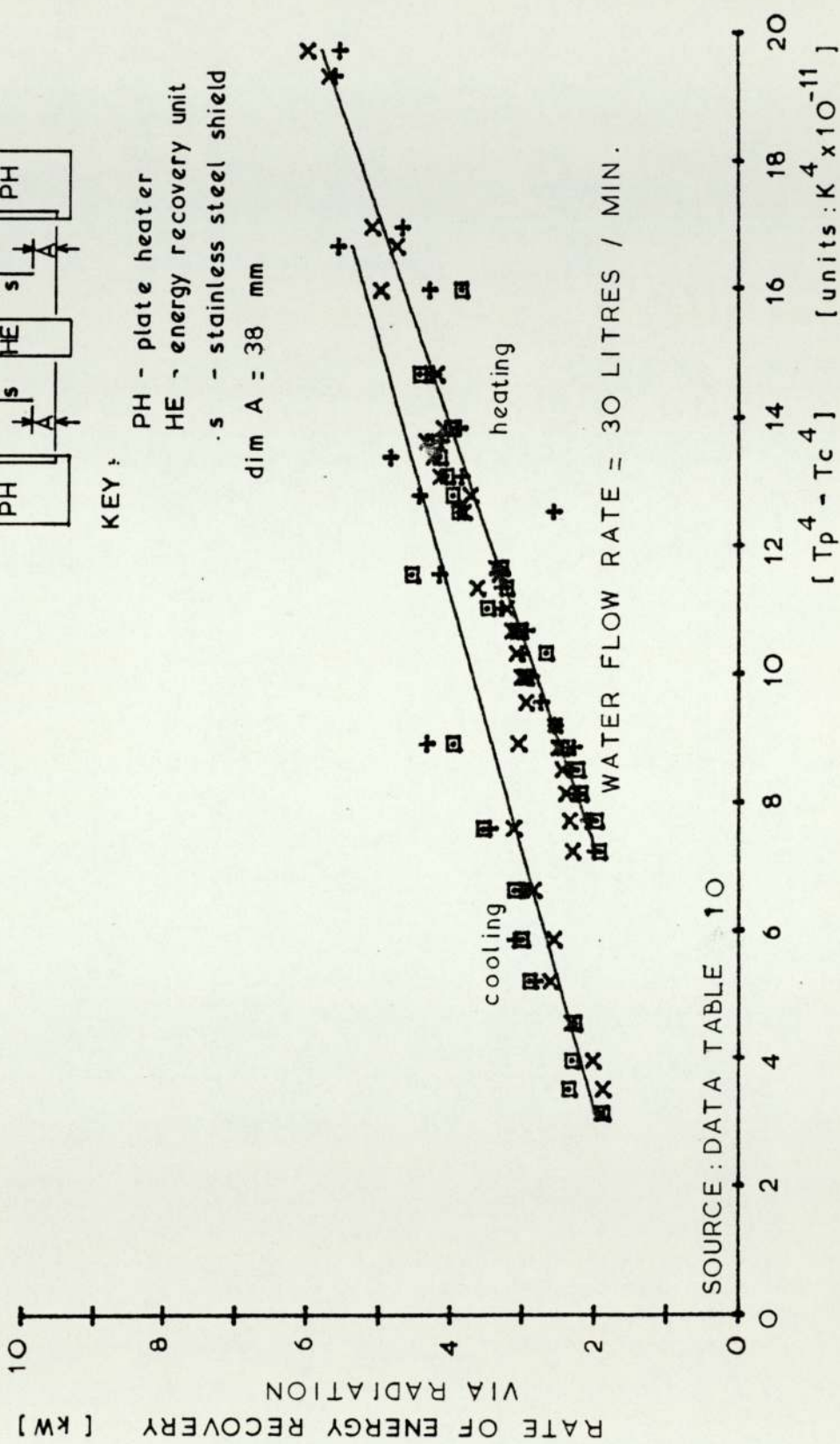
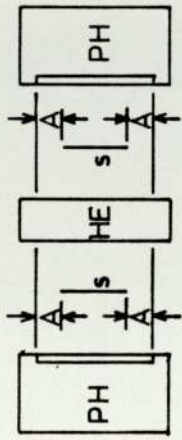


FIGURE 7.9 ENERGY RECOVERY WITH BOTH HEATERS AND AIR GAP WIDTH OF 38 mm



KEY:  
 PH - plate heater  
 HE - energy recovery unit  
 s - stainless steel shield  
 dim A = 25.4mm

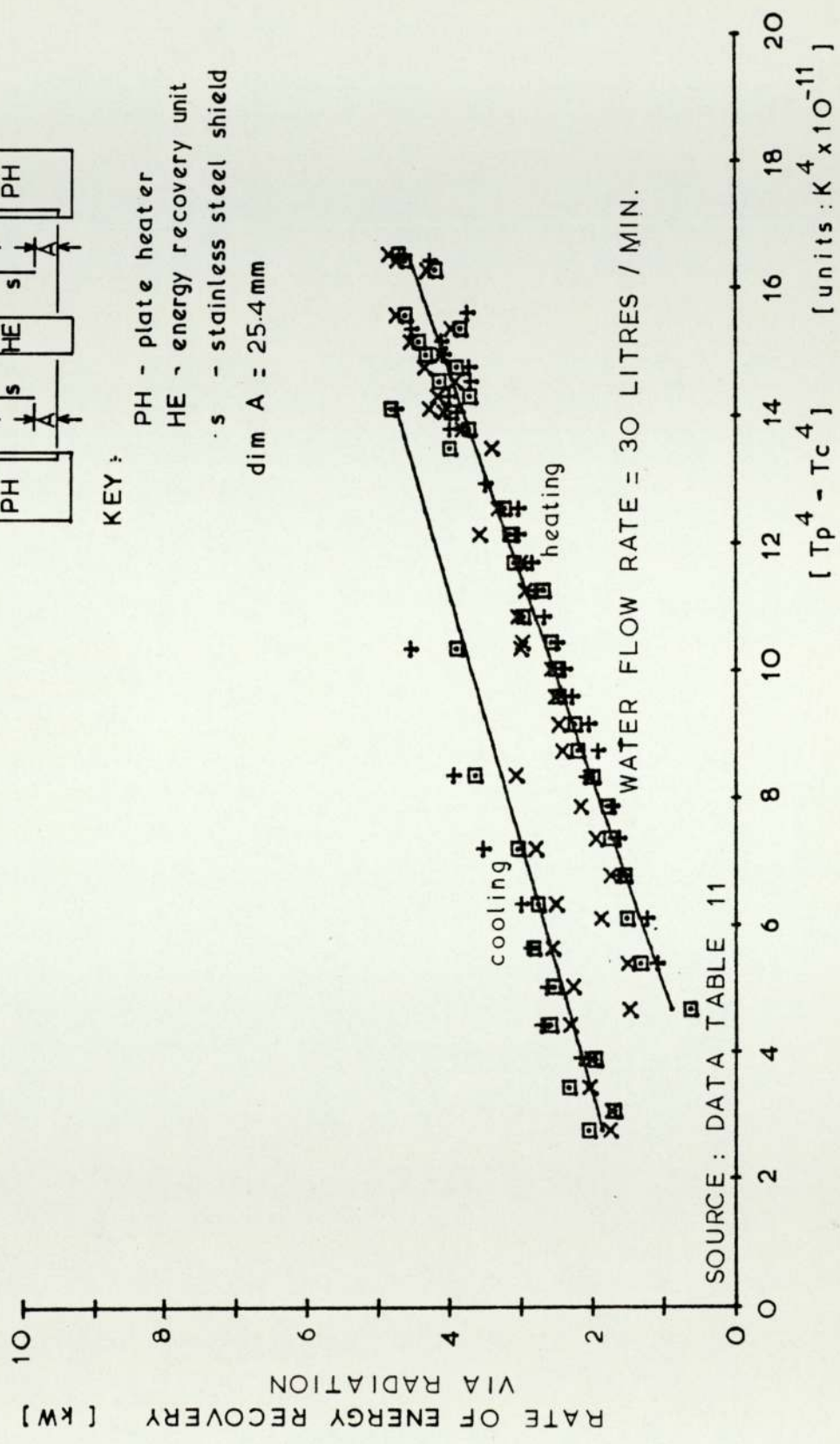
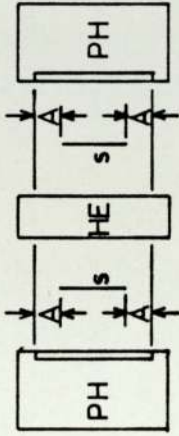


FIGURE 7.10 ENERGY RECOVERY WITH BOTH HEATERS AND AIR GAP WIDTH OF 25.4 mm





KEY :  
 PH - plate heater  
 HE - energy recovery unit  
 s - stainless steel shield  
 dim A = 19 mm

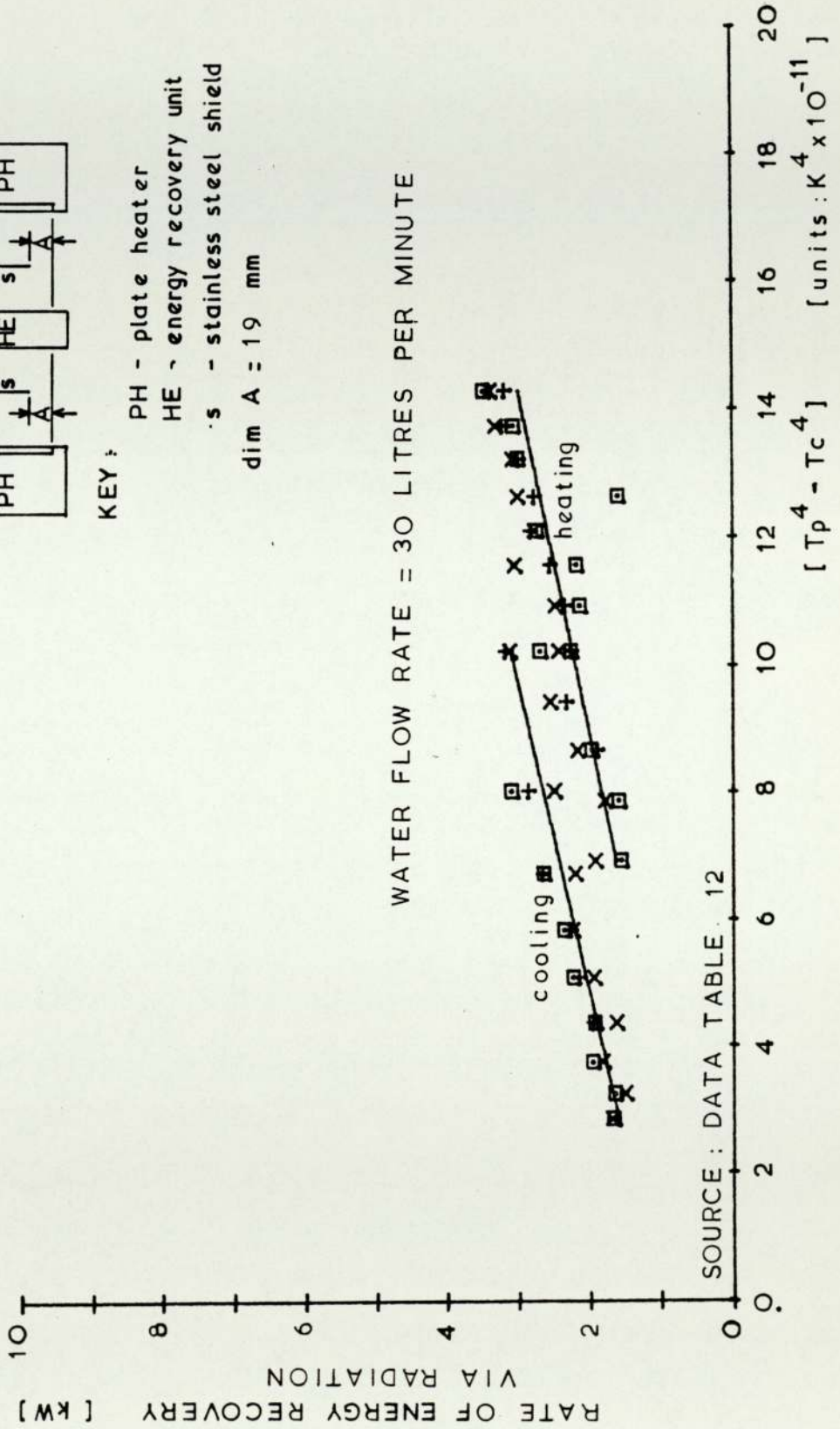


FIGURE 7.11 ENERGY RECOVERY WITH BOTH HEATERS AND AIR GAP WIDTH OF 19 mm

RATE OF ENERGY RECOVERY [ KW ]  
VIA RADIATION

10  
8  
6  
4  
2  
0

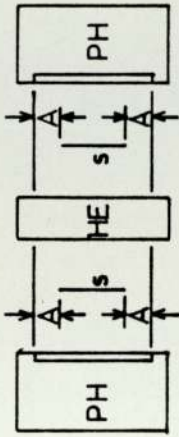
WATER FLOW RATE = 30 LITRES PER MINUTE

cooling heating

SOURCE: DATA TABLE 13

0 2 4 6 8 10 12 14 16 18 20

[  $T_p^4 - T_c^4$  ] [ units :  $K^4 \times 10^{-11}$  ]



KEY :

- PH - plate heater
  - HE - energy recovery unit
  - s - stainless steel shield
- dim A = 12.7 mm

FIGURE 7.12 ENERGY RECOVERY WITH BOTH HEATERS AND AIR GAP WIDTH OF 12.7 mm



FIGURE 7.13 - Correlations of energy recovery system and evaluation of emissivity x view factor ( $\epsilon.F$ )

Figure No.	Air Gap Width (mm)	Heating or Cooling	Correlations [ $P_R = A_1 + A_2 \times (T_p^4 - T_c^4)$ ]		Emissivity x View Factor ( $\epsilon.F$ )	Emissivity	Comments
			$A_1$	$A_2 \times 10^9$			
7.6	No Shield	Heating	514.9	4.31	0.423	.566	-
7.7	25.4	Heating	213.6	2.8	.274	.578	-
7.8	No Shield	Heating	521.5	4.05	0.40	.535	Using Calibrated Thermometer
			403.3	4.36	0.43	.575	Using Inlet Thermocouple only
7.9	38.0	Heating	-183.3	3.02	0.296	.590	-
		Cooling	1241.2	2.48	0.243	.484	-
7.10	25.4	Heating	-550.0	3.09	0.303	.639	-
		Cooling	1162.4	2.53	0.248	.523	-
7.11	19.0	Heating	373.4	1.83	0.179	.390	-
		Cooling	1027.8	2.03	0.199	.434	-
7.12	12.7	Heating	-353.3	2.64	0.259	.578	-
		Cooling	1393.1	1.60	0.157	.350	-

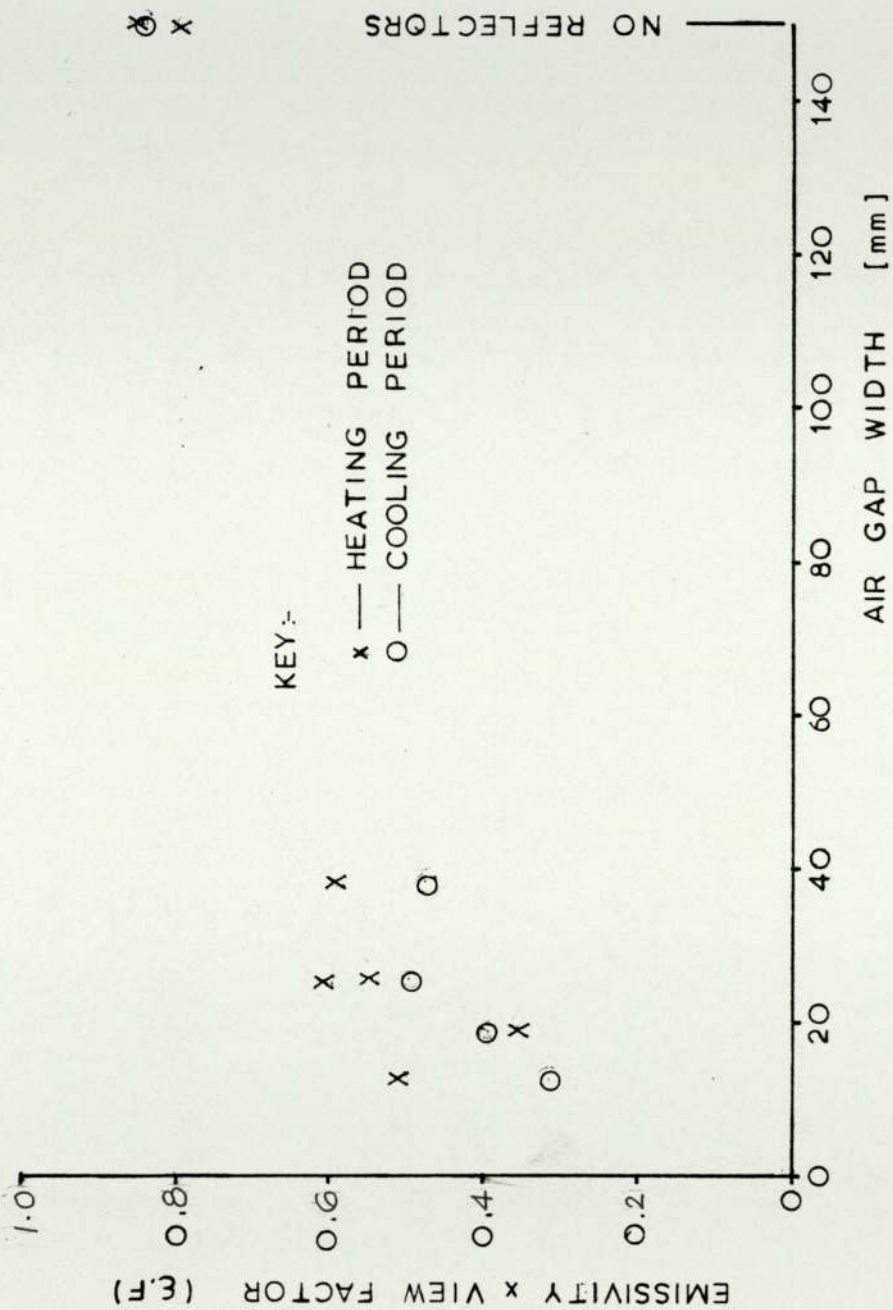


FIGURE 7.14 VARIATION OF EMISSIVITY x VIEW FACTOR WITH AIR GAP WIDTH



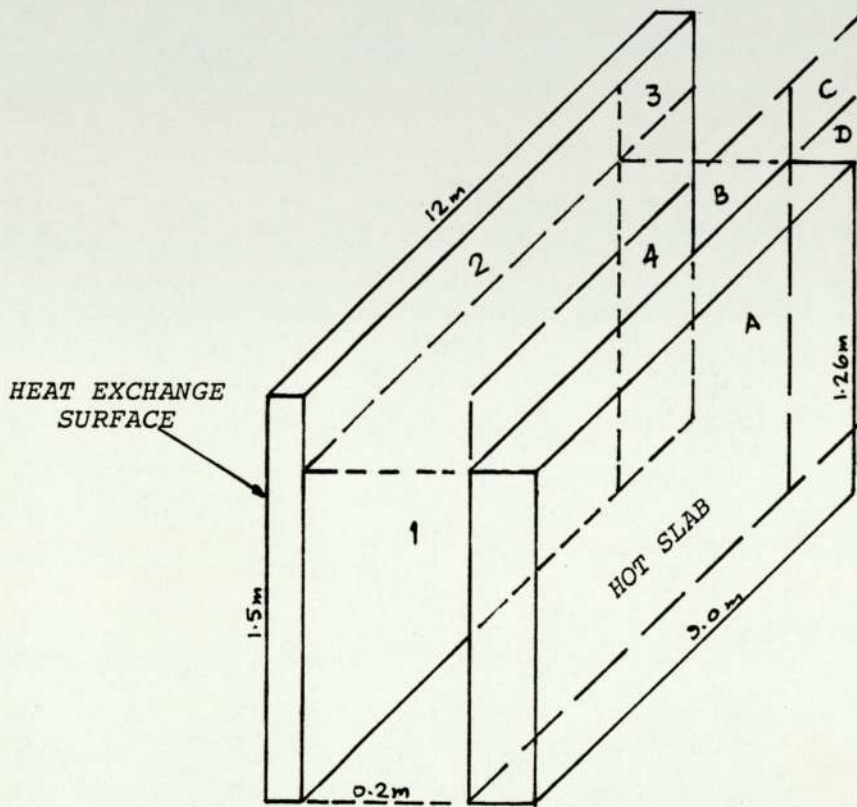
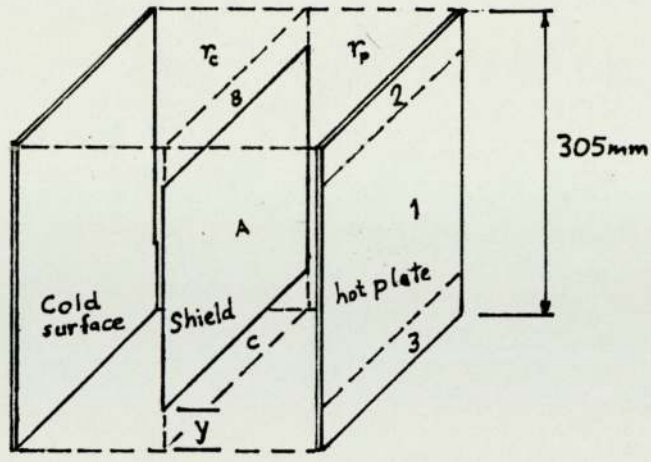
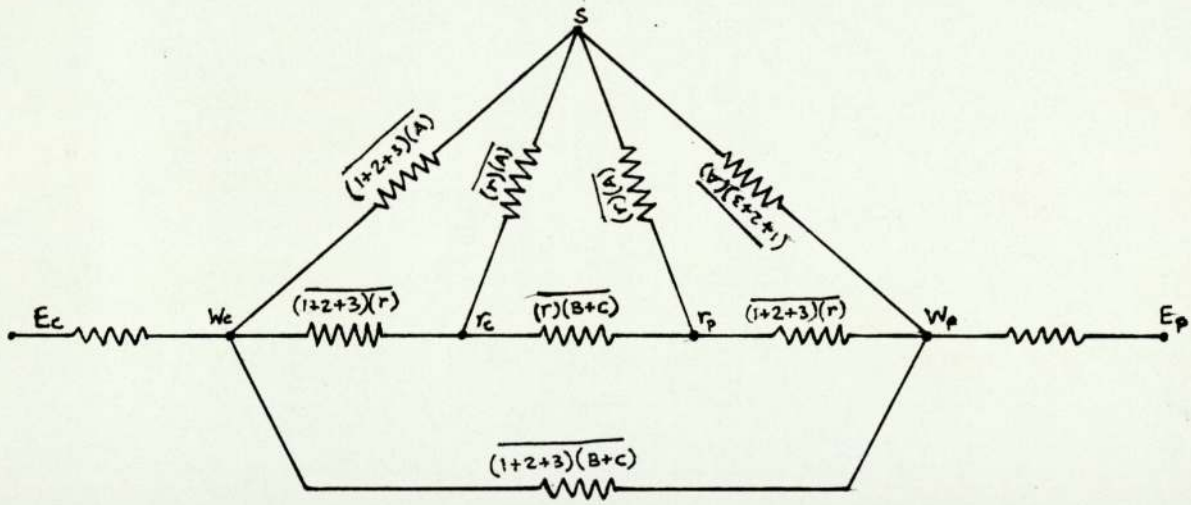


FIGURE 7.16 - Diagrammatic Representation of Slab Cooling



(a) Diagrammatic Representation of Slab Cooling



(b) Electrical Analogy of Slab Cooling

FIGURE 7.15 - Representation of radiative heat transfer in slab cooling



CHAPTER 8  
CONCLUSIONS AND RECOMMENDATIONS

This chapter is divided into two sections, namely (i) Conclusions and recommendations on slab cooling and (ii) general conclusions. The latter section concludes the earlier chapters on the world energy situation and how it relates to the British Steel Corporation and the methods of energy recovery discussed and analysed.

## 8.1 Conclusions and recommendations on slab cooling

The theoretical model on slab cooling developed in Chapter 5 was verified. The radiative heat transfer mode dominates the energy exchange in the temperature range of interest in the slab cooling system. The existence of convective currents in a circulatory motion was noted. It is concluded that in the proposed system of a sandwich-type structure, the view factor between the hot slabs and the adjacent tubes will be in excess of 0.8. Therefore, the heat exchanger can be optimised on the basis of radiative heat transfer alone. The main design parameters are identified.

Two structural layouts of the slab cooling system were considered. In conclusion, a continuous system incorporating economiser, boiler and superheater sections is compatible with an un-interrupted and constant source of thermal energy for power generation. The first proposal of 30 separate cooling chambers is appropriate for its use as a pool-boiler and for a modification at a later date into a thermal storage unit, if and when equipment for hot inspection and rectifications of surface imperfections becomes available.

On the basis of the information available for the Llanwern iron and steelworks, an annual saving in its fuel bill of £700,000 is anticipated. The capital cost of a conventional 13 MW shell and tube waste-heat boiler is around £100,000 at 1979 prices, although the boiler itself is unlikely to significantly contribute to the total cost of the slab cooling system. However, the slab cooling proposal appears a practical and economic proposition and it should be considered further with a view to implementation.



The recommendation based on the theoretical, economic and experimental study is to formulate a design for slab cooling for a particular application and location, say at Llanwern, with due consideration to the prevailing local conditions. It is proposed that future studies should be based at the iron and steelworks under review in line with BSC policy of decentralising the research programmes.

## 8.2 General conclusions

The major contribution of the present study is to bring together existing new developments and novel techniques of energy recovery in the iron and steel industry. Also, the current world energy situation and its implication to the metal manufacturers, particularly the British Steel Corporation, are discussed. The present world recession and the alarming increase in fuel price has caused a major setback to the world iron and steel industry and without government subsidies the British Steel Corporation will cease to exist in its present form.

In spite of the British Steel Corporation investment in energy recovery equipment, a large percentage of its annual fuel consumption goes to waste in one form or another. The thermal energy stored in combustion products represents a major source of high-grade waste energy. To recover the high-grade thermal energy, three proposals employing fluidisation technology were evaluated. The two methods known as fluidised-bed regenerator and recuperator are incompatible with the available source of energy, particularly as high pressures are required to fluidise the particles. The third proposal called the falling-cloud method shows some promise but requires an extensive research and development programme. An analysis of thermal equilibrium in the fluidised bed was theoretically pursued and shows that rapid mixing in shallow fluidised beds promotes uniform temperature conditions and high rates of heat transfer to the immersed heat exchange surfaces. However, a counter-current flow arrangement is sacrificed. It indicates the relative size of fluidised beds

required for high air preheats. Also, the height of the falling-cloud chamber can be evaluated to give optimised energy recovery. The applicability of the falling-cloud method to the iron and steel industry and its potential for energy recovery and pollution control are promising enough to warrant further studies.

The limitations and advantages of the low temperature turbine were discussed, and extensive study for the selection of a suitable refrigerant was conducted. In conclusion, the choice was between R-114 and R-11, but the latter was selected on the basis of its present cost. Its application to energy recovery from combustion products leaving blast furnace stores was considered and the potential saving in the fuel bill highlighted.

It is suggested that its early stage of development and small size does not warrant at present more than a passing interest in its development.

The new developments outside the British Steel Corporation on evaporative cooling of blast furnaces and dry-coke quenching should be of immediate interest and require detailed study for their implementation.



APPENDIX I

FLUID BEDS AND HEAT PIPE

## I.1 Fluidised beds

### I.1.1 Fluidisation technique

A bed of particles behaves in a fluid-like manner when the upward fluid velocity is sufficient to create drag on particles equivalent to their weight. The lowest velocity at which this phenomenon first appears is known as the minimum fluidisation velocity. In a gas fluidised bed, a further increase in the fluid velocity results in the formation of gas bubbles which carry solid particles upward in their wake and hence promote rapid mixing. At even higher velocities, a point is reached where the drag forces are such that the particles become entrained within the fluid stream and are carried from the bed. A dramatic decrease in pressure drop is noted. This velocity is called the terminal velocity.

The advantages and limitations of the technique of fluidisation are listed as follows:

#### Advantages

- (i) The smooth, liquid like behaviour of a bed of particles allows continuous automatically controlled operations with ease of handling.
- (ii) A very large surface area to particle volume ratio permits the achievement of high overall rates of heat transfer between the solid and the fluid.
- (iii) A thorough and rapid mixing of solids in gas-fluidised systems leads to nearly isothermal conditions in the bulk of the bed.
- (iv) The high rates of heat transfer between the fluidised solids and an immersed surface reduces the surface area required for a fluidised-bed heat exchanger.
- (v) The circulation of solids between two fluidised beds makes it possible to transport large quantities of thermal energy.
- (vi) It is suited to large scale operations.



## Limitations

- (i) It requires expenditure of power for fluidisation.
- (ii) The changes in mixing patterns and fluid behaviour cause problems in applying small-scale laboratory test data to large scale equipment.
- (iii) The rapid mixing of particles leads to non-uniform residence time in the bed.
- (iv) Some particles cannot be fluidised because of their tendency to degrade or agglomerate.
- (v) There is usually an upper and a lower limit to the size of particles which may be fluidised.
- (vi) Operating rates are restricted to the flow rates over which the bed may be fluidised.
- (vii) The abrasion of pipes and vessels by particles may be serious.
- (viii) The general absence of thermal gradients throughout a well mixed fluidised bed is a disadvantage where these gradients will promote higher rates of heat exchange e.g. in a counter-current heat exchanger.

The properties of fluidisation which are particularly relevant to the present study are those associated with heat transfer. The variables which affect heat transfer rate are as follows:

- (i) Properties of the fluidising gas i.e. density, viscosity, specific heat and thermal conductivity.
- (ii) Properties of the solids i.e. diameter, density, sphericity, specific heat and thermal conductivity.
- (iii) Flow conditions i.e. superficial velocity and voidage.
- (iv) Geometric properties of the system i.e. bed size, size of immersed surface, static bed height.

## Formulae for fluidisation

### Minimum fluidisation velocity

Kunii and Levenspiel (1969) have suggested a generalised formula

covering the whole range of Reynolds numbers:

$$u_{mf} = \frac{\mu}{dp \rho_g} \left( \left[ (33.7)^2 + 0.0408 dp^3 \frac{\rho_g (\rho_s - \rho_g) g}{\mu^2} \right]^{1/2} - 33.7 \right) \quad (1)$$

### Terminal velocity

For terminal velocity,  $u_t$  for spherical particles, the following correlations are given:

$$u_t = g (\rho_s - \rho_g) d_p^2 (18\mu) \text{ for } Re_p < 0.4 \quad (2)$$

$$u_t = \left( \frac{4}{225} \frac{(\rho_s - \rho_g)^2 g^2}{\rho_g \mu} \right)^{1/3} dp \text{ for } 0.4 < Re_p < 500 \quad (3)$$

$$u_t = \left( \frac{3.1g (\rho_s - \rho_g) dp}{\rho_g} \right)^{1/2} \text{ for } 500 < Re_p < 200\,000 \quad (4)$$

$$\text{where } Re_p = \rho_g \frac{U \cdot dp}{\mu}$$

### Pressure drop across fluidised bed

A good approximation for pressure drop across fluidised bed is given by:

$$\Delta p_D = W/A = (1 - \epsilon_{mf}) (\rho_s - \rho_g) L_{mf} g \quad (5)$$

The prime aspect of this study is the process of heat transfer from the fluidising medium to the immersed surface of heat pipes. Also, the rate of heat transfer from solid particles to the container wall governs the rate at which heat is lost to the surroundings. Experimental data show that there is a marked increase in heat transfer rate between fluid and solid particles beyond the minimum fluidisation velocity. The relative increase in heat transfer coefficient in relation to the fluidising velocity is shown in Figure I.1.

The experimental data on heat transfer in gas fluidised beds is divided into three divisions:

#### (a) Heat transfer between fluid and particles

Kunii and Levenspiel (1969) concluded that, of the published data,



those following a plug flow model gave a more consistent pattern, whereas measurements based on perfect gas mixing are widely scattered. The results based on the plug flow pattern were correlated by the equation:

$$Nu_p = 0.3 Re_p^{1.3} \quad (6)$$

(b) Heat transfer between particles and immersed surface  
Horizontal tubes

Vreedenberg (1960) using single water cooled horizontal tube situated 850mm above the distributor plate in a 1200mm deep bed obtained the following relationship:

For fine and light particles:

$$Re_p \frac{\rho_s}{\rho_g} < 2050$$

$$Nu_p = 0.66 Pr^{0.3} Re_p^{0.44} (d_p/d_t)^{0.56} (\rho_s/\rho_g)^{0.44} \frac{(1-\epsilon_f)^{0.44}}{(\epsilon_f)} \quad (7)$$

where  $Nu_p = \frac{h \cdot d_p}{k}$

For coarse-heavy particles:

$$Re_p \frac{\rho_s}{\rho_g} > 2550$$

$$Nu_p = 420 Pr^{0.3} Re_p^{0.3} Ar^{-0.3} (d_p/d_t)^{0.7} \quad (8)$$

Although Atkinson (1974) using shallow beds between 25 and 62mm deep, predicted a decreasing heat transfer coefficient with rising temperature in contradiction with other workers, it was not fully explained.

Vertical tubes

Wender and Cooper (1958) obtained the following relationship for vertical tubes between Reynolds numbers of  $10^{-2}$  and  $10^2$ .

$$Nu_p = 3.5 \times 10^{-4} C_R (1-\epsilon_f) Pr^{0.43} Re^{0.2} (C_{ps}/C_{pg})^{0.8} (\rho_s/\rho_g)^{0.66} \quad (9)$$

Although some discrepancy has been noted by Botterill (1975), it is not conclusive to discredit the above correlation.

The factor  $C_R$  is to allow for the effect of the non-axial

positioning of the tube and is taken directly from the work by Vreedenberg (1960) which is fully reported by Botterill (1975).

(c) Heat transfer between particles and container walls

Wen and Leva (1956) correlated data and about 95 percent of it fell within  $\pm 50$  percent of the values predicted by the equation:

$$Nu_p = 0.16 Pr^{0.4} Re_p^{0.76} (\rho_s C_{ps} / \rho_g C_{pg})^{0.4} (\eta / g \cdot d_p)^{-0.2} (Lmf)^{0.36} \quad (10)$$

where  $\eta = (u - \text{superficial velocity for uniform expansion of bed}) / u$ .

The range of vessel diameters varied from 35mm to 288mm with an average height of 90mm. Particles were of many materials including glass beads, sand, alumina, silica-gel, carborundum, coke,  $Fe_3O_4$  and  $CaCO_3$ . Also particle diameter ranged from 0.02 to 4.34mm but mainly fluidised in air.

The operating mode of heat transfer is generally temperature dependent. At temperatures below  $600^\circ C$  when radiant heat transfer can be neglected, the heat transfer to particles is by conduction. Convective transfer through gas makes a negligible contribution because of the low heat capacity of the gas. Hence to promote high rates of heat transfer, a rapid exchange of particles in the bulk of the bed and those at the immersed surface is required.

At higher temperatures radiative heat transfer begins to exert its influence. Radiative heat transfer between a gas fluidised bed and an exchange surface is given in Botterill and Sealey (1970).

The other aspect to which this study relates is the process of heat transfer from the fluidising medium to the immersed surface. However, its contribution to the overall heat transfer rate is negligible and hence it is generally not considered.



### I.1.2 Verification of assumption 1 in fluidised bed regenerator

A method of representing a continuous process by the use of a large number of discrete time intervals,  $\Delta t$  was adopted. During each time interval, the following occurs in the sequence given below:

1.  $n$  particles flow into the bed containing  $N_0$  particles
2. a perfect mixing process occurs i.e.  $n$  particles are uniformly distributed amongst  $N_0$  particles
3.  $n$  particles flow out of the bed having uniform composition of 'old' and 'new' particles.

#### (A) Start-up condition

At  $t=0$

The composition of particles leaving the bed is:

$$\left[ \frac{N_0}{(N_0 + n)} \right]_{t < 0, \text{'old'}} + \left[ \frac{n}{(N_0 + n)} \right]_{t = 0, \text{'new'}} \quad (11)$$

Therefore, the particles remaining are:

$$\left[ N_0 - \frac{n \cdot N_0}{(N_0 + n)} \right]_{t < 0, \text{'old'}} + \left[ \frac{n - n^2}{(N_0 + n)} \right]_{t = 0, \text{'new'}} \quad (12)$$

Hence the total number of particles remaining in the bed is  $N_0$ .

At  $t = \Delta t$

The composition of particles leaving the bed is:

$$\left[ \frac{(N_0 - n \cdot N_0 / (N_0 + n))}{(N_0 + n)} \right]_{t < 0} + \left[ \frac{n - n^2}{(N_0 + n)} \right]_{t = 0} + \left[ \frac{n}{(N_0 + n)} \right]_{t = \Delta t} \quad (13)$$

Hence remaining particles are:

$$N_0 \left[ 1 - \frac{n}{(N_0 + n)} \right]_{t < 0}^2 + n \left[ 1 - \frac{n}{(N_0 + n)} \right]_{t = 0}^2 + n \left[ 1 - \frac{n}{(N_0 + n)} \right]_{t = \Delta t} \quad (14)$$

Similarly, for each successive time interval the procedure is repeated. And steady state conditions are reached when  $t$  is large and

$$N_0 \left[ 1 - \frac{n}{(N_0 + n)} \right]_t^{t + \Delta t} \longrightarrow 0 \quad (15)$$

(B) Steady state condition

At any time t, the composition of bed is

$$n[X]_t + n[X]_{t-\Delta t}^2 + n[X]_{t-2\Delta t}^3 + n[X]_{t-3\Delta t}^4 + \dots \quad (16)$$

$$\text{where } [X] = [1 - n / (N_0 + n)]$$

A graph plot of bed composition and time is shown in Figure I.2. It represents the percentage of particles in the bed having a residence time greater than time, t given the mass flow rate of particles into and out of the bed is 1, 2, 5 and 10 percent of the total mass of particles present in the bed at the end of each interval.

The following table of results shown in Figure I.3 was extracted from I.2 and is an attempt to show the implications of and changes in bed composition due to the variations in the mass flow rate.

To evaluate the composition of the bed in accordance with the temperature of the particles, the next step is to consider the heat transfer rate between the fluidising medium and the bed particles.

The following relationship is given above for the heat exchange between fluid and the particles:

$$Nu_p = 0.3 Re_p^{1.3} \quad \text{equation (6)}$$

Using this relationship, Figure I.4 was plotted for particle sizes of 0.5, 1.0 and 2.0mm up to an air temperature of 1000°C. It shows that the heat transfer coefficient is almost independent of temperature, therefore it is not necessary to evaluate heating/cooling rates of particles at different air temperatures.

Using an air mass velocity of 0.35 kg/m<sup>2</sup>s [the velocity at which a bed remains fluidised at all possible air temperatures], the relationship between particle temperature and its residence time in the hot air stream was obtained and is shown in Figure I.5. The exit gas temperature of 800°C and particle inlet temperature of 20°C are assumed.



A summary of the results in tabular form is given in Figure I.6 for mild steel particles.

The analysis indicates the fluidised bed composition with changes in the solid mass flow rate and the heating rates of particles. This was combined to obtain the composition of the fluidised bed based on the temperature of the particles. Figures I.7 and I.8 shows this relationship for mass flow rates of 1 and 10 percent respectively. In a gas fluidised bed, having parameters used in the model, the particle mass flow rate is unlikely to exceed one percent of the total mass of particles in the system. Therefore, the average temperatures listed in Figure I.7 are likely to be exceeded in a real system given that the process is similar to the one assumed in the model and the assumption of perfect mixing holds good. Therefore, the difference in average temperature of particle and the outlet air temperature is unlikely to exceed four percent of the initial temperature differences, provided the heat losses through the container wall are negligible.

### I.1.3 Mathematical model of multi-stage fluidised bed regenerator

A mathematical model was developed to evaluate the operation of a multi-stage fluidised bed regenerator working between a gas inlet temperature of  $T_{gi}$  and air inlet temperature of  $T_{ai}$ . This model was modified to consider the influence of a temperature difference between bed and exit gas.

For ideal conditions (referring to Figure I.9)  $(T_{so} = T_{go} \text{ or } T_{ao})_{stage}$

Ratio of capacity rates

$$R_A = \frac{m_g \cdot C_{pg}}{m_s \cdot C_{ps}} = \frac{T_{AB} - T_{si}}{T_{gi} - T_{go}} \quad (17)$$

$$R_B = \frac{m_a \cdot C_{pa}}{m_s \cdot C_{ps}} = \frac{T_{AB} - T_{si}}{T_{ao} - T_{ai}} \quad (18)$$

Effectiveness

$$\epsilon_A = \frac{T_{gi} - T_{go}}{T_{gi} - T_{si}} = \left[ \frac{\sum_{j=1}^M R_A^j}{(R_A(1 + \sum_{j=1}^M R_A^j))} \right] = (R_A^M - 1) / (R_A^{M+1} - 1) \quad (19)$$

$$\epsilon_B = \frac{T_{ao} - T_{ai}}{T_{AB} - T_{ai}} = \left[ \frac{\sum_{j=1}^N R_B^j}{(R_B(1 + \sum_{j=1}^N R_B^j))} \right] = (R_B^N - 1) / (R_B^{N+1} - 1) \quad (20)$$

Therefore,

$$\left( \frac{T_{si} - T_{ai}}{T_{gi} - T_{ai}} \right) = [1 - R_B \cdot \epsilon_B] / [R_B \cdot \epsilon_B / R_A \cdot \epsilon_A + 1 - R_B \cdot \epsilon_B] \quad (21)$$

$$\frac{T_{ao} - T_{ai}}{T_{gi} - T_{ai}} = \epsilon_B \cdot [R_B \cdot \epsilon_B / R_A \cdot \epsilon_A + 1 - R_B \cdot \epsilon_B] \quad (22)$$

The ratios of <sup>gas to air</sup> heat capacity rates, generally encountered in the iron and steel industry are 1:1 for oil fired or natural gas fired furnaces and 2:1 for Blast Furnace gas-fired furnaces. Both conditions were considered and evaluated. The results are shown in Figures I.10 and I.11 respectively. It can also be appreciated that a higher mass flow rate of particles in the system results in a lower temperature difference between the beds. An optimum rate of mass transfer between beds can be determined if the cost of transportation is known as each increase in the rate of solid circulation results in a reduced rate of improvement in air preheat. This phenomenon is shown in Figure I.12 where a single-stage fluidised bed regenerator is considered for systems in which either  $R_A$  or  $R_B$  is equal to unity over a wide range of  $R_B/R_A$  ratios.

Modified for temperature difference,  $\theta$  between bed and exit gas

The 'new' effectiveness,  $\epsilon_{A1} = \frac{T_{gi} - T_{go}}{T_{gi} - T_{si}}$

hence,  $\epsilon_{A1} = \epsilon_A [1 - \theta / (T_{gi} - T_{si})]$  (23)



$$\frac{(T_{gi} - T_{si})}{T_{gi} - T_{ai}} = \left[ \frac{(R_B \cdot \epsilon_B / R_A \cdot \epsilon_A)}{(R_B \cdot \epsilon_B / R_A \cdot \epsilon_A + 1 - R_B \cdot \epsilon_B)} \right] \quad (24)$$

and

$$\frac{(T_{ao} - T_{ai})}{T_{gi} - T_{ai}} = \left[ \frac{\epsilon_B}{(R_B \cdot \epsilon_B / R_A \cdot \epsilon_A + 1 - R_B \cdot \epsilon_B)} \right] \quad (25)$$

Similarly,

$$\epsilon_{B1} = \epsilon_B \left[ 1 + \theta / (T_{AB} - T_{ai}) \right] \quad (26)$$

where

$$(T_{AB} - T_{ai}) = \frac{\sum_{j=1}^N R^j}{1 + \sum_{j=1}^N R^j} \left[ T_{gi} - T_{si} - \theta \right] + (T_{si} - T_{ai}) \quad (27)$$

and

$$|T_{AB} - T_{ai}|_{\theta} = |T_{AB} - T_{ai}|_{\theta=0} - \frac{\theta \sum_{j=1}^N R^j}{1 + \sum_{j=1}^N R^j} \quad (28)$$

Figure I.13 shows the effect of temperature difference between fluidising medium and the particles, on air preheat for a multi-stage system with  $R_A = 2 \cdot R_B = 1.0$

### Power requirement for fluidisation

The prime disadvantage of the fluidisation technique is the power required to overcome the high pressure drop across the fluidised bed and the distributor plate. Therefore, the power requirement will govern the economic number of stages per bed.

Figure I.14 gives details of pressures around a fluidised bed system and the power required to drive it is as below:

$$W_{sa} = W_{si} / \eta = \left[ \frac{\gamma}{\gamma - 1} \cdot P_2 V_2 \cdot \left( 1 - \left( \frac{P_1}{P_2} \right)^{\frac{\gamma - 1}{\gamma}} \right) \right] / \eta \quad (29)$$

where,

- $\eta = 0.55 - 0.75$  for a turbo-blower
- $= 0.6 - 0.8$  for a Roots blower
- $= 0.8 - 0.9$  for an axial blower or a two stage reciprocating compressor

## I.2 Heat pipe

The heat pipe is a device having high thermal conductance. Heat fluxes as high as  $150 \text{ MW/m}^2$  have been measured with lithium as the working fluid at temperatures of  $1500^\circ\text{C}$ . It transfers heat by boiling a fluid at one point and condensing it at another, the liquid is returned to the evaporator section by capillary action through a wick structure. The capillary forces enable the circulation resistance due to friction, changes in momentum and gravity to be overcome and hence the pipe can operate with evaporator at the bottom or top.

The thermal output is limited by certain considerations, which include:

- (i) the vapour velocity cannot exceed sonic velocity
- (ii) the need to avoid liquid entrainment by vapour which starves the evaporator of liquid
- (iii) film boiling should be avoided, due to the poor heat transfer coefficient obtained
- (iv) the rate of circulation of fluid obtainable is limited

These limits are shown graphically in Figure I.15.

For optimum heat pipe operation the selection of compatible working fluid, wick structure and material of manufacture is of utmost importance. A brief list of the prime requirements are given below. The choice of working fluid is restricted by the operating temperature of the device, various fluids and the relevant data for their selection are given in Figure I.16.

For the selection of the working fluid, the prime requirements are as follows:

- (i) compatibility with wick and wall materials
- (ii) good thermal stability
- (iii) wettability of wick and wall materials
- (iv) vapour pressures should neither be too high or low over the operating temperature range



- (v) high latent heat
- (vi) high thermal conductivity
- (vii) low liquid and vapour viscosities
- (viii) high surface tension
- (ix) acceptable freezing or pouring point

The prime functions of the wick or capillary structure is to generate capillary pressure to transport the working fluid from condenser to evaporator, and to distribute the liquid around the evaporator section, indeed to all areas where heat is likely to be received.

The theoretical considerations of the heat pipe, and detailed procedure for selecting the working fluid and the wick structure are given by Chisholm (1971) and fluid characteristics are given in Figure I.16.

The broad areas of application of heat pipe technology are given below:

- (a) Separation of heat source and sink
- (b) Temperature flattening
- (c) Heat flux transformation
- (d) Temperature control
- (e) Thermal diodes and switches

An air-to-air heat exchanger for an air conditioning system designed and built by Q-dot Corporation (Figure I.17) uses a similar principle to that of a fluidised bed recuperator with the exception of the fluidised bed.

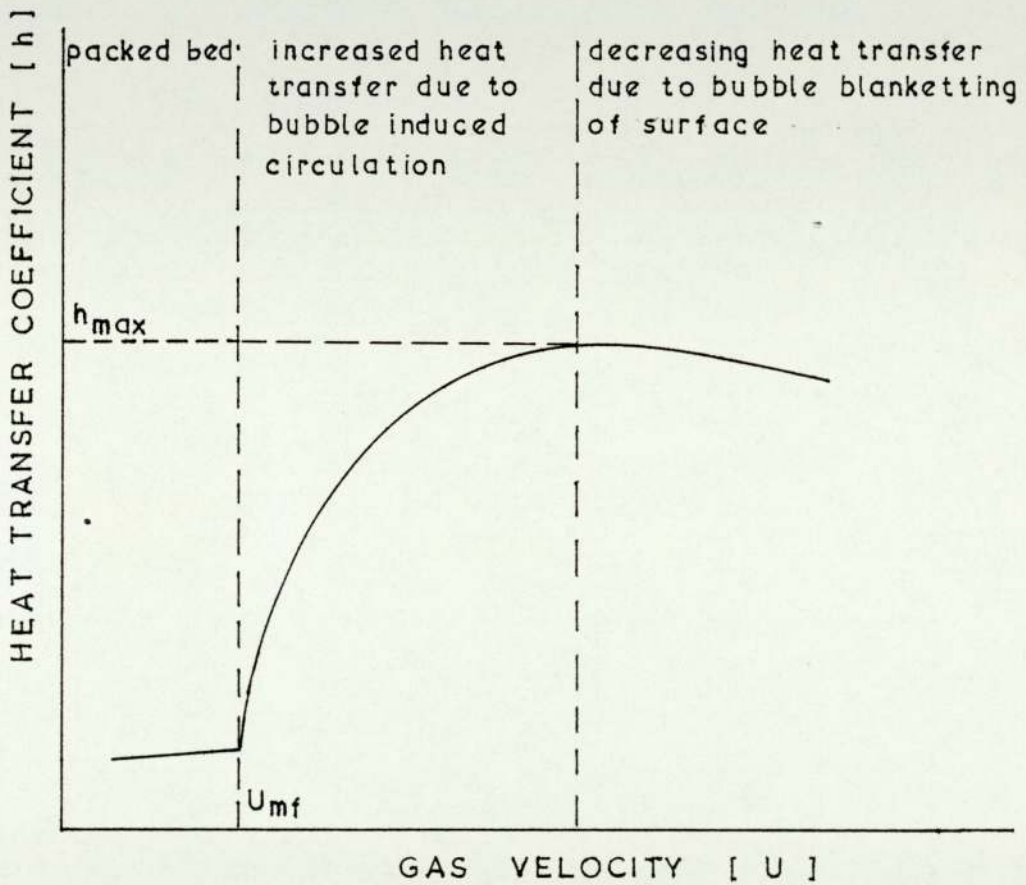


FIGURE 1.1 TYPICAL RELATIONSHIP BETWEEN HEAT TRANSFER COEFFICIENT AND GAS VELOCITY



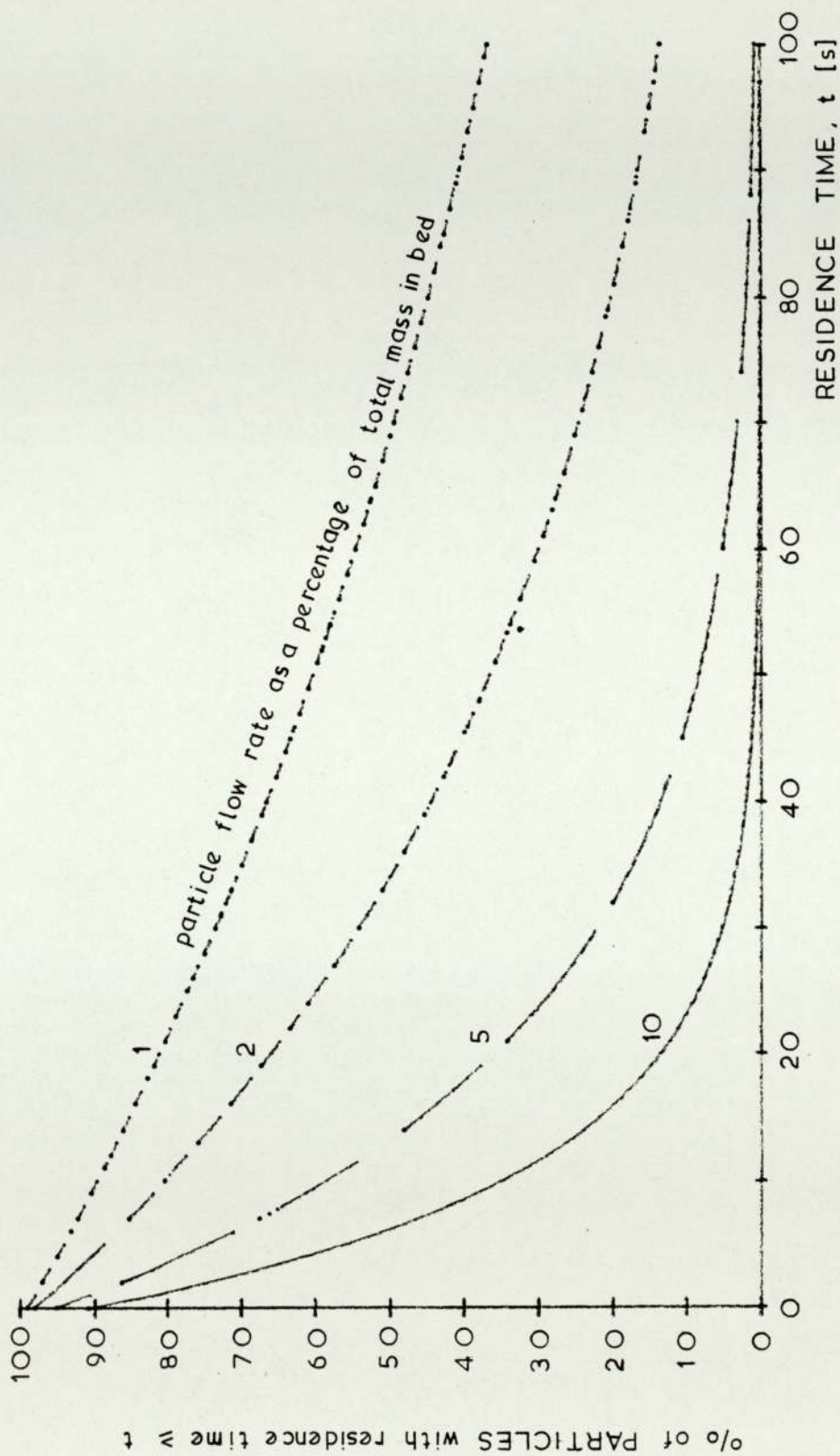


FIGURE I.2 FLUID-BED COMPOSITION in terms of particle residence time

Figure I.3 - Percentage of particles with residence time,  
 $t < 100\Delta t$  for various flow rates

$n/N_0$	% of particles with residence time $t < 100\Delta t$	Average residence time
0.10	0.00	$10\Delta t$
0.05	0.72	$20\Delta t$
0.02	13.2	$50\Delta t$
0.01	36.6	$100\Delta t$

Source : Figure I.2



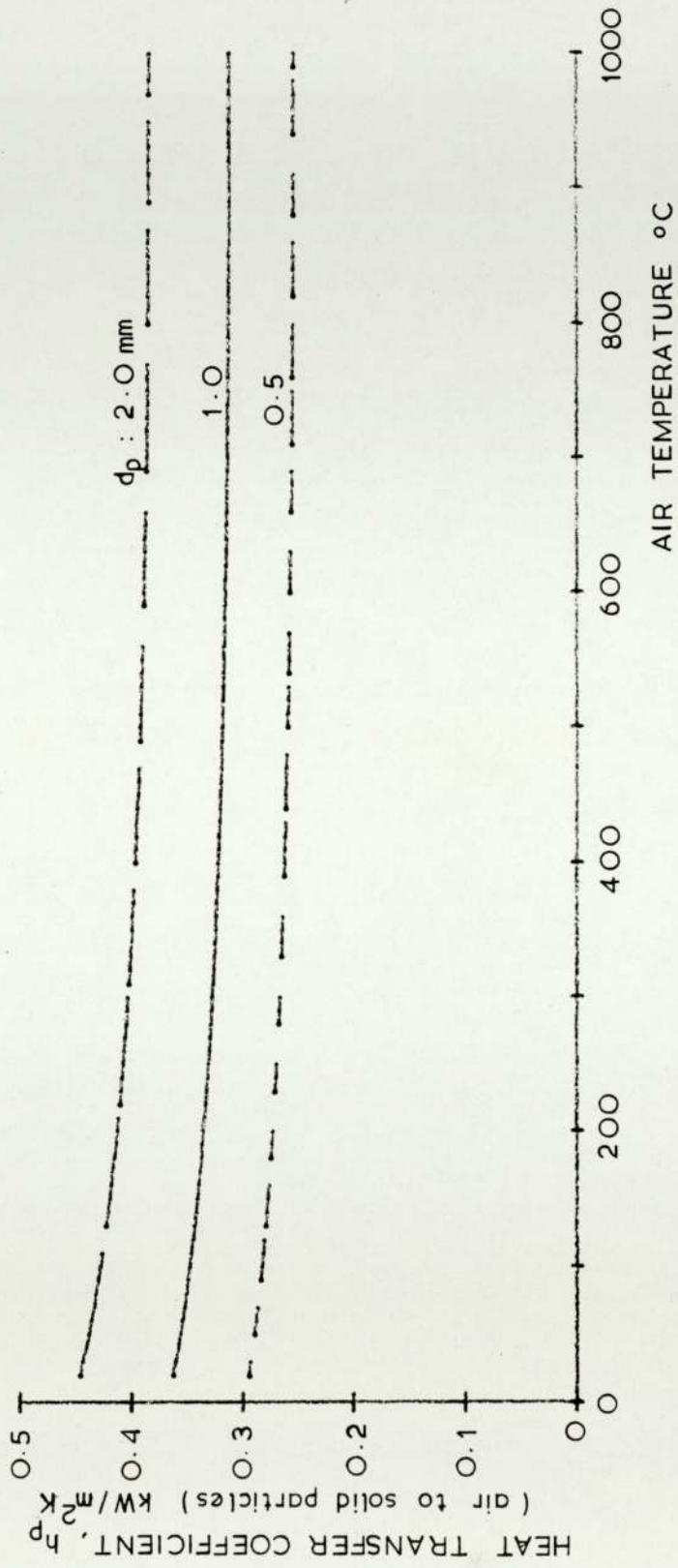


FIGURE I.4 HEAT TRANSFER CHARACTERISTICS- mild steel particles fluidised at air mass velocity :  $0.35 \text{ kg/m}^2\text{s}$

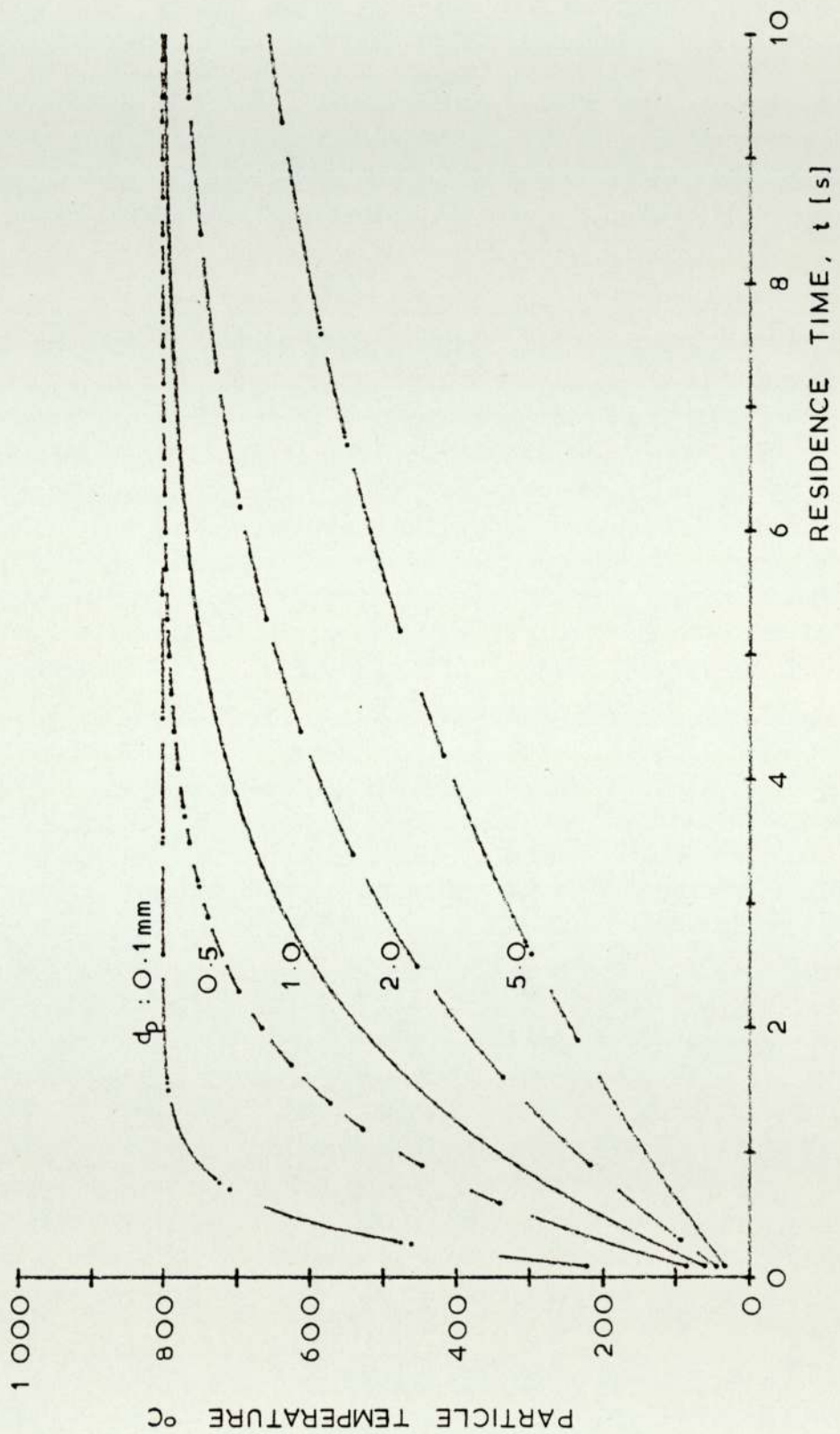


FIGURE I.5 HEATING CHARACTERISTICS OF MILD STEEL PARTICLES with air temp: 800 °C and mass vel : 0.35 kg/m<sup>2</sup>s



Figure I.6 - Minimum residence time to reach temperature, T

Particle Dia. mm	TIME TO REACH (seconds)				
	700°C	740°C	780°C	790°C	795°C
0.1	0.7	0.9	1.2	1.5	1.7
0.5	2.4	2.9	4.2	5.0	5.8
1.0	3.9	4.9	6.9	8.2	9.6
2.0	6.4	8.0	11.4	13.5	15.6
5.0	12.2	15.2	21.7	25.8	29.9

Source : Figure I.5

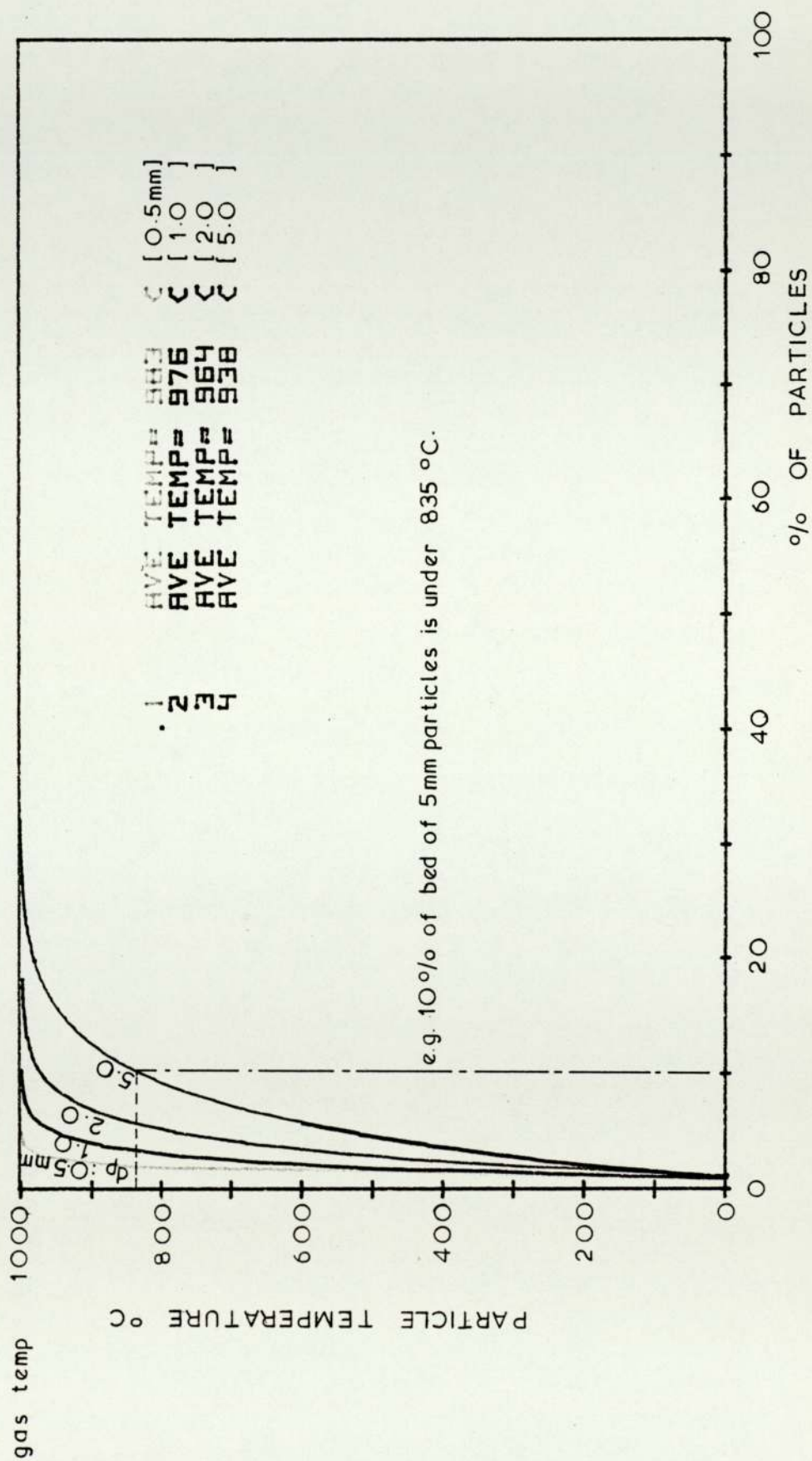


FIGURE I.7 FLUIDISED-BED COMPOSITION in terms of PARTICLE TEMPERATURE  
(where mass flow rate is 1% of total mass in bed)



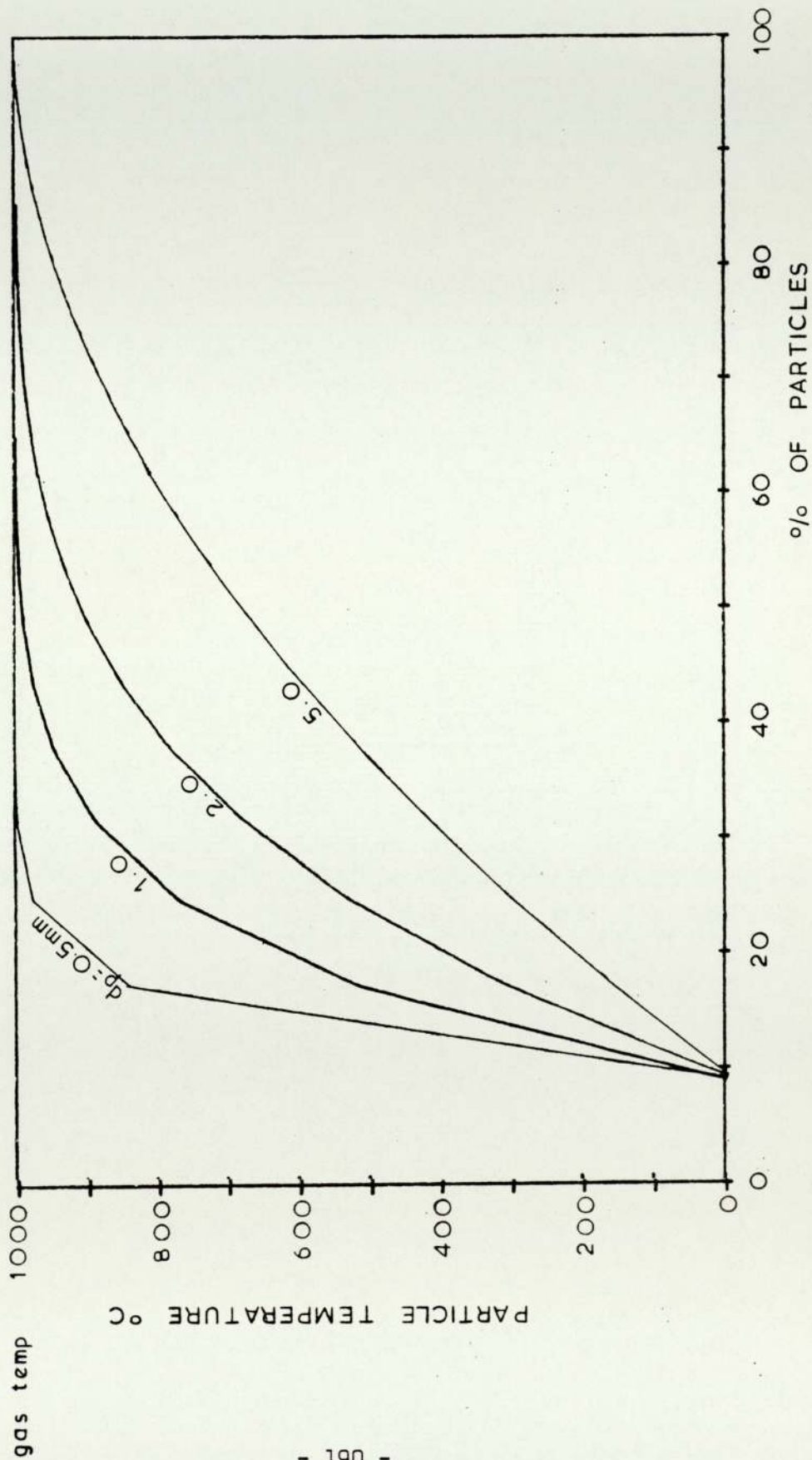


FIGURE I.8 FLUIDISED-BED COMPOSITION in terms of PARTICLE TEMPERATURE  
 (where mass flow rate is 10% of total mass in bed)

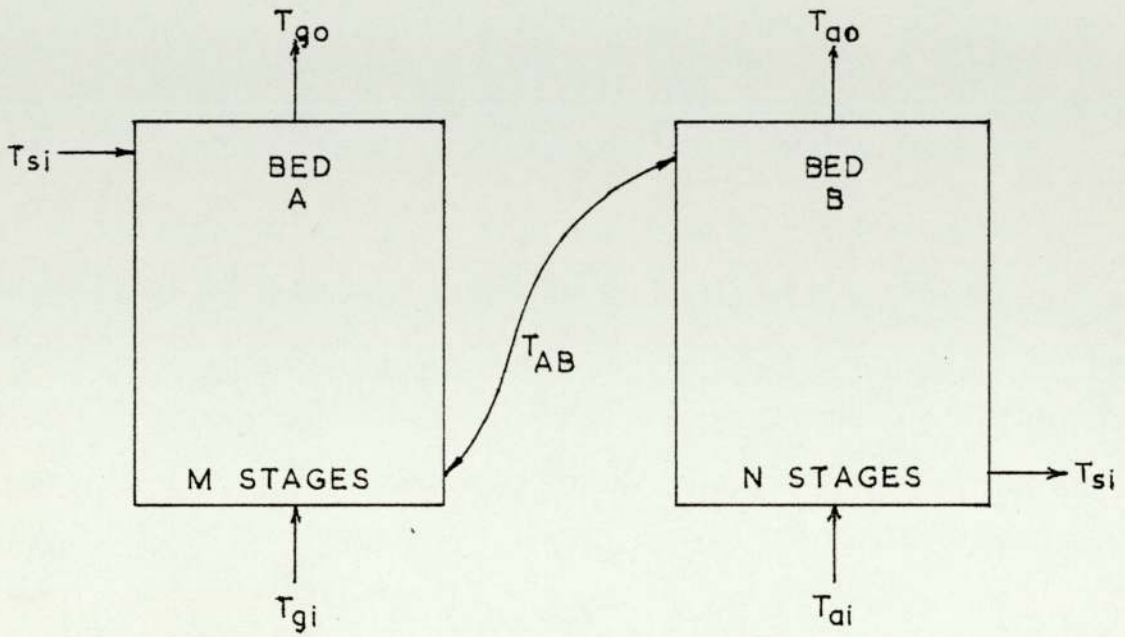


FIGURE I.9 BLOCK DIAGRAM OF MULTISTAGE FLUIDISED BED REGENERATOR



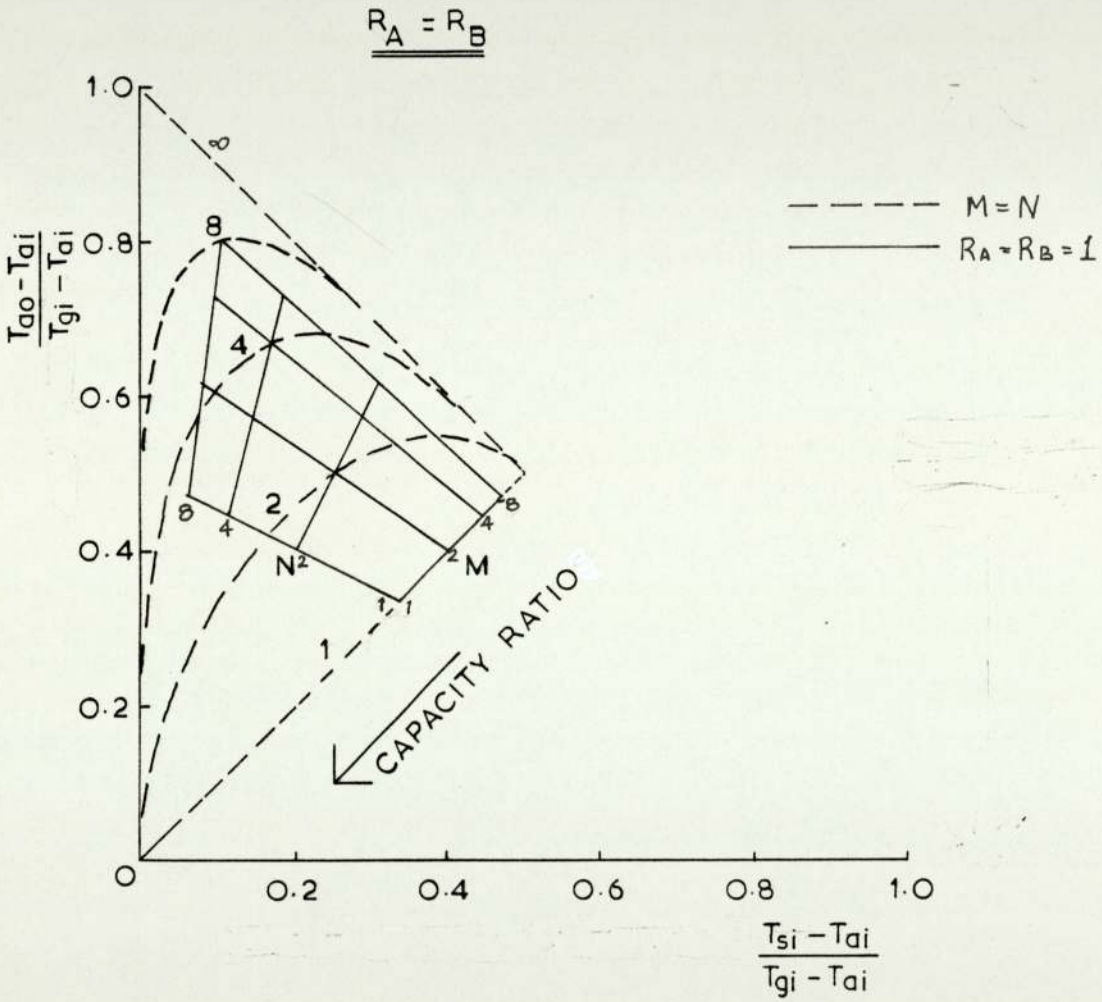


FIGURE I.10 AIR PREHEAT CHART FLUIDISED-BED REGENERATOR  
[  $R_A = R_B$  ]

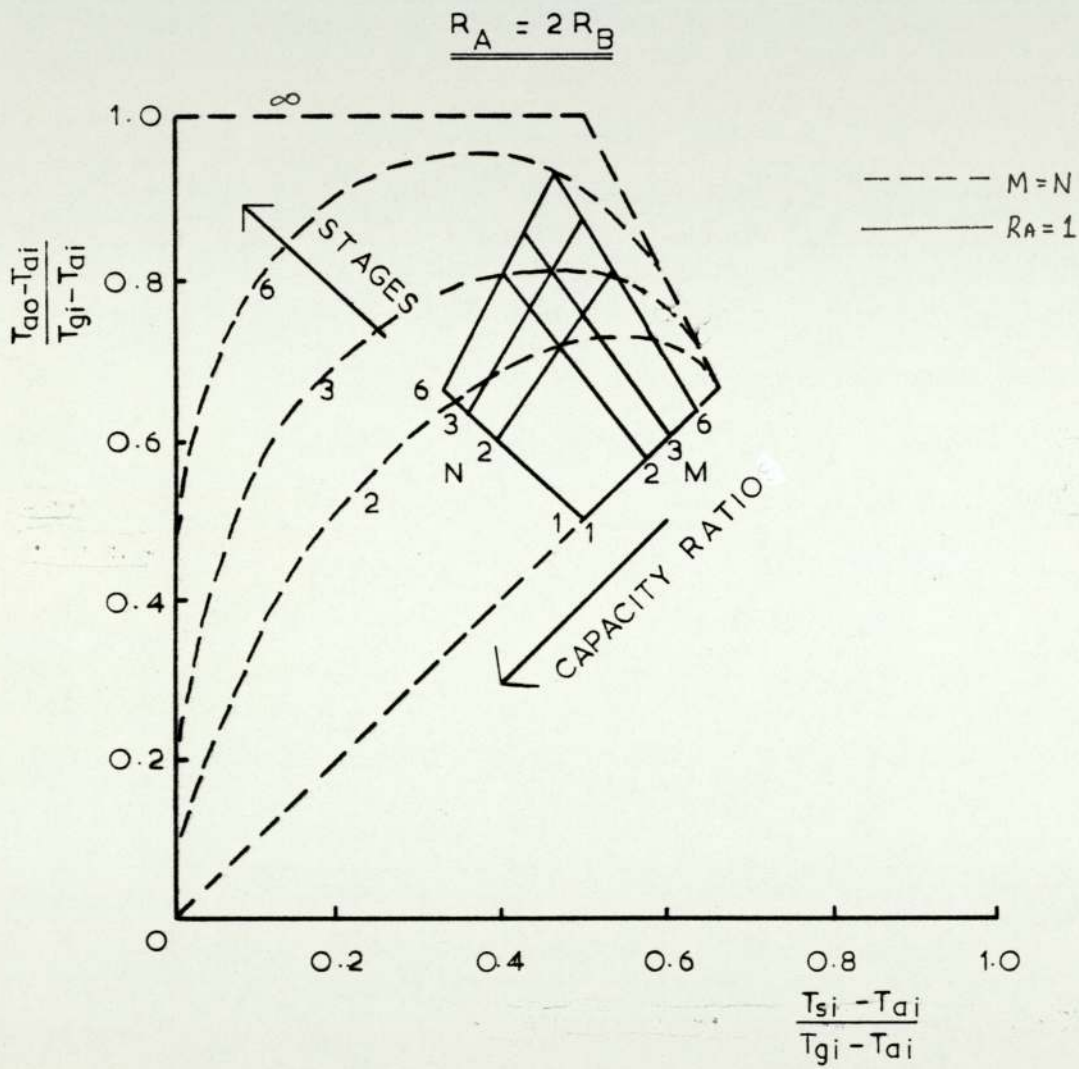


FIGURE I.11 AIR PREHEAT CHART FOR FLUIDISED-BED  
REGENERATOR [ $R_A = 2R_B$ ]

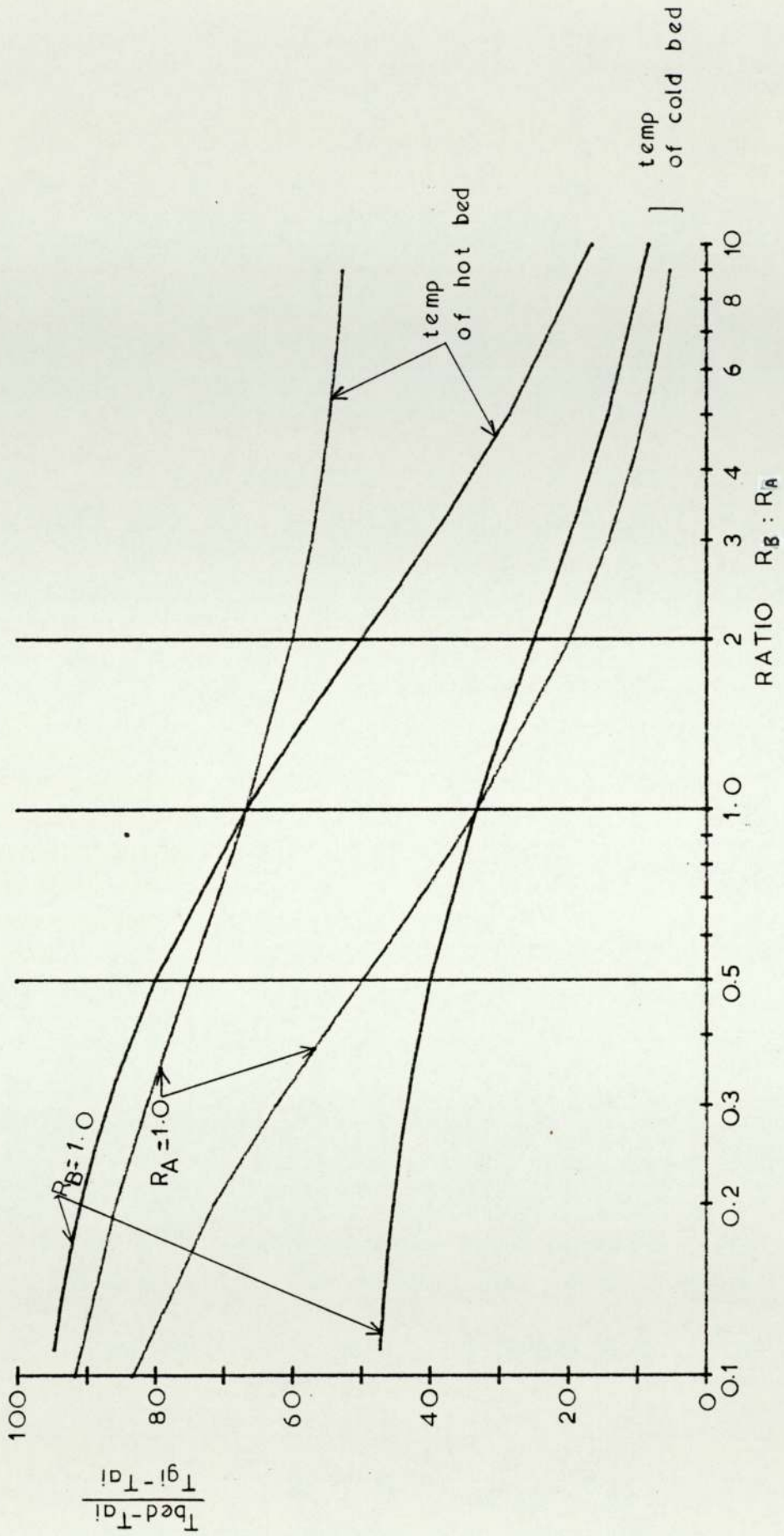


FIGURE I.12 SINGLE STAGE FLUIDISED-BED REGENERATOR-EFFECT OF RATIO OF  $R_B : R_A$



Figure I.13 - Prediction of maximum air preheat for a multi-stage fluidised bed regenerator ( $T_{gi} = 1200^{\circ}\text{C}$ )

Temperature diff. $^{\circ}\text{C}$ $\theta$	AIR PREHEAT $^{\circ}\text{C}$		
	Number of stages in each bed		
	1	2	3
0	590	953	1081
2	587	945	1069
5	583	935	1050
10	577	916	1018
20	561	878	952
30	547	839	881

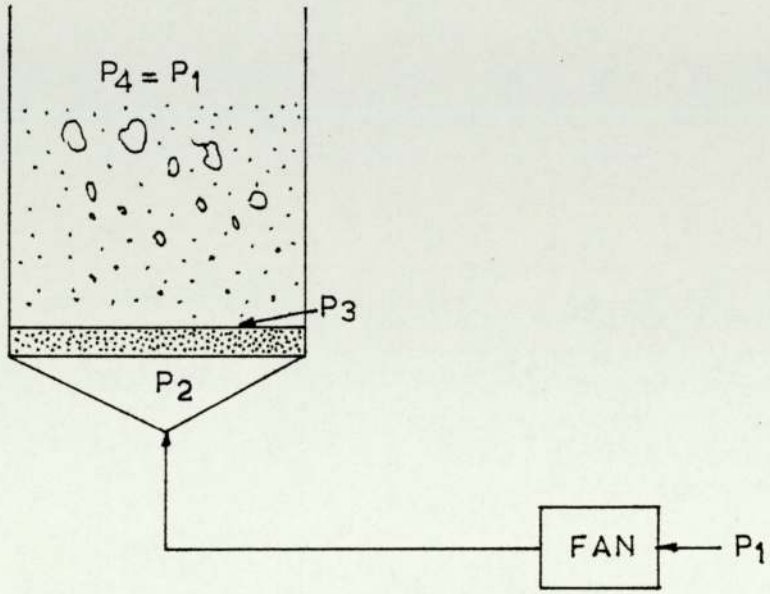
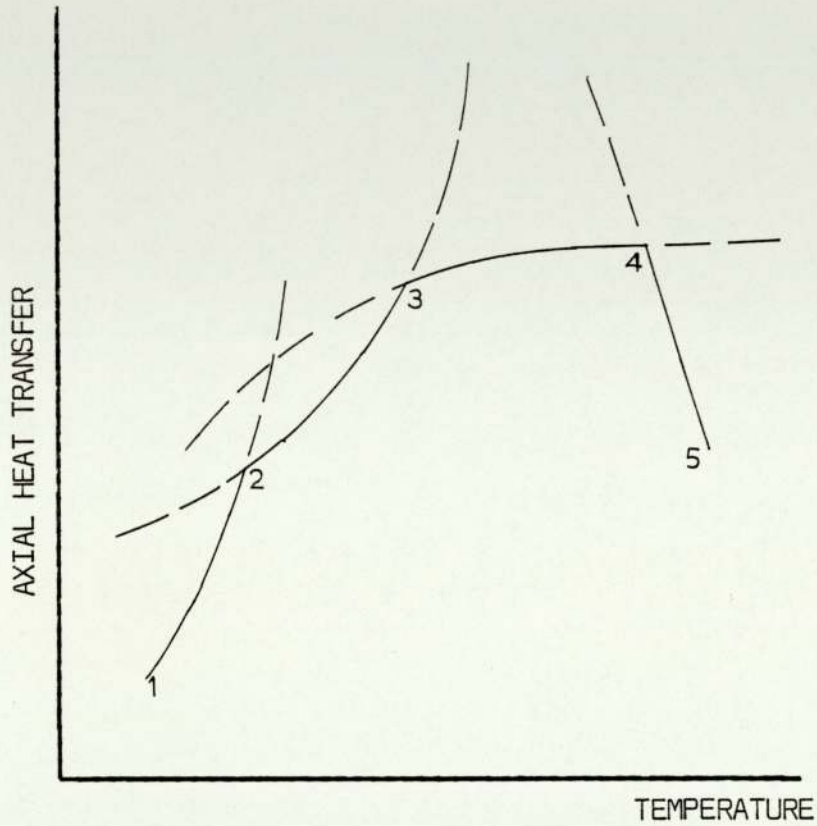


FIGURE I.14 PRESSURE DISTRIBUTION AROUND FLUIDISED-BED SYSTEM



HEAT TRANSFER LIMITS:

- |       |               |
|-------|---------------|
| 1 — 2 | SONIC         |
| 2 — 3 | ENTRAINMENT   |
| 3 — 4 | CIRCULATION   |
| 4 — 5 | BYLINK (FILM) |

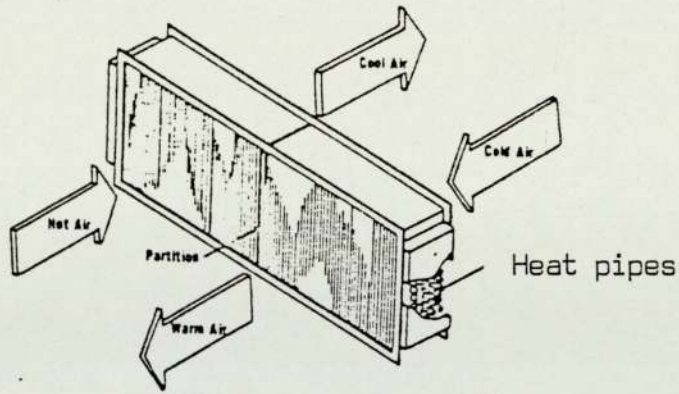
Figure I.15 Heat pipe operation envelope



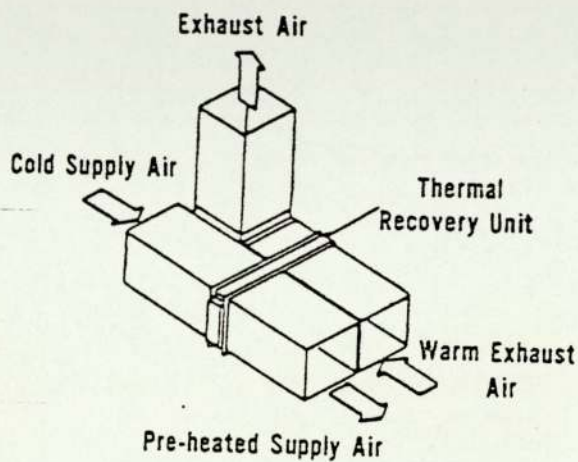
Figure I.16 - Fluid characteristics for heat pipe applications

Characteristic	FLUID				
	Mercury	Potassium (K3)	Sodium (K3)	Lithium	Silver
Practical temperature range	190 to > 550°C	400 to > 800°C	500 to > 900°C	900 to > 1500°C	1500 to > 2000°C
Axial heat flux (watts/cm <sup>2</sup> )	-	5670 at 750°C (K3)	9070 at 850°C (K3)	1950 at 1250°C	4000
Sonic limit Fig. 1.6 (kW/cm <sup>2</sup> )	25.5 at 360°C	36.6 at 700°C	94.2 at 900°C	143.8 at 1300°C	-
Surface heat flux (watts/cm <sup>2</sup> )	180	>180 at 750°C	>222 at 760°C	>207 at 1250°C	410
Liquid transport factor (kW/cm <sup>2</sup> ) equation 4.1	1.65 x 10 <sup>5</sup> at 360°C	5.8 x 10 <sup>4</sup> at 730°C	2.4 x 10 <sup>5</sup> at 730°C	-	7 x 10 <sup>5</sup> at 1200°C
Wick and shell materials	Stainless steel +0.02% Magnesium +0.001% Titanium	Nickel, Stainless steel	Nickel, Hastelloy-X Stainless steel	TZM, Niobium 1% Zirconium	Tantalum + 5% Tungsten
Typical lifetime (hours)	>16,900 hr. at 340°C	>24,500 hr. at 600°C	>20,000 hr. at 715°C	>10,000 hr. at 1500°C	-
Melting point	-38.9°C	62.3°C	97.5°C	186°C	960°C
Critical properties	1950 K	-	1963 K	2473 K	-

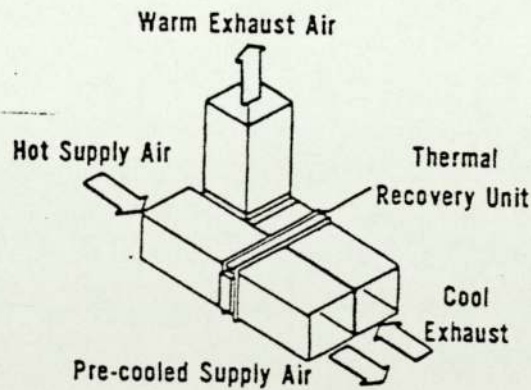
References are as given in The Heat Pipe by D. Chisholm.



(a) Q-DOT HEAT EXCHANGER



WINTER OPERATION



SUMMER OPERATION

(b) HEAT EXCHANGER INSTALLED IN THE AIR CONDITIONING UNIT

[SOURCE : Deyoe (1973)]

Figure I.17 Q-Dot heat exchanger and its application

APPENDIX II  
SLAB COOLING - THERMAL DESIGN



II.1 One dimensional transient conduction with cooling at surface by radiation and convection

For explanation of terms used in this appendix refer to Figure II.1.

The slope  $-\frac{dT}{dx}$  at plane a-b is approximately

$$= \frac{(T_4 - T_3)}{\Delta x}$$

and at plane c-d  $= \frac{(T_3 - T_2)}{\Delta x}$

Therefore, heat balance at plane 3 is:

$$k_m \cdot A \cdot \frac{(T_4 - T_3)}{\Delta x} - k_m \cdot A \cdot \frac{(T_3 - T_2)}{\Delta x} = A \cdot \Delta x \cdot \rho \cdot C_p \cdot \frac{(T_3^1 - T_3)}{\Delta t} \quad (1)$$

where  $T_3^1$  is new temperature at plane 3 after elapse of a finite time increment,  $\Delta t$  [McAdams (1954)]. But,

$$\frac{k_m}{\rho C_p} = \alpha \quad \text{thermal diffusivity}$$

and  $\frac{\alpha \Delta t}{\Delta x^2} = Fo$  Fourier number

Then equation (1) leads to

$$T_n^1 = Fo (T_{n+1} + T_{n-1}) + T_n (1 - 2 Fo)$$

At surface,

$$\begin{aligned} -\sigma \cdot F \cdot \epsilon \cdot A \cdot (T_1^4 - T_c^4) - h \cdot A \cdot (T_1 - T_\infty) + k_m A \frac{(T_2 - T_1)}{\Delta x} \\ = A \cdot \Delta x \cdot \rho \cdot C_p \cdot \frac{(T_1^1 - T_1)}{2\Delta t} \end{aligned}$$

The above equation reduces to,

$$T_1^1 = 2Fo (T_2 + Bi T_\infty) + T_1 (1 - 2Fo(1 + Bi)) - 2PFo(T_1^4 - T_c^4) \quad (2)$$

where  $P = \sigma \cdot F \cdot \epsilon \frac{\Delta x}{k_m}$

and  $Bi = \frac{h \cdot \Delta x}{k_m}$  Biot number

## II.2 Heat transfer : General equations

### II.2.1 Natural convection : vertical plate

$$Gr = (\ell^3 g \beta \Delta T \rho^2 / \mu^3)_f \quad \text{Grashoff number}$$

$$Pr = (C_p \mu / k)_f \quad \text{Prandtl number}$$

$$Nu = C (Gr Pr)^m = \frac{h\ell}{k} \quad \text{Nusselt number}$$

where for laminar flow,

$$10^4 < Gr Pr < 10^9, \quad C = 0.59 \text{ and } m = \frac{1}{4}$$

for turbulent flow,

$$10^9 < Gr Pr < 10^{12}, \quad C = 0.129 \text{ and } m = 1/3$$

$$\text{for } \beta = 1/T_\infty$$

$$T_f = (T_s + T_\infty) / 2 ; \quad \Delta T = (T_s - T_\infty)$$

$\ell$  = plate height

For air these equations reduce to,

$$\text{For laminar flow } h_m = 1.417 \times 10^{-3} (\Delta T / \ell)^{\frac{1}{4}} \quad (3)$$

$$\text{For turbulent flow } h_m = 1.312 \times 10^{-3} (\Delta T)^{1/3} \quad (4)$$

where  $h_m$  is the mean heat transfer coefficient.

### II.2.2 Free convection in enclosed spaces between vertical walls

$$\frac{ke}{k} = 1.0 \quad \text{for } Gr_D < 2000 \quad \text{_____} \quad (5)$$

$$\frac{ke}{k} = 0.18 Gr_D^{\frac{3}{4}} (\ell/D)^{-1/9} \quad \text{_____} \quad (6)$$

for  $20\,000 < Gr_D < 200\,000$

$$\frac{ke}{k} = 0.065 Gr_D^{1/3} (\ell/D)^{-1/9} \quad \text{_____} \quad (7)$$

for  $200\,000 < Gr_D < 11\,000\,000$

where  $ke$  = effective thermal conductivity as defined by,

$$\frac{q}{A} = ke \frac{(T_1 - T_2)}{D}$$

[Holman (1963)]

### II.3 Simulated heat exchanger

Radiative and convective heat transfer assuming air gap is sealed.

Heat balance at the surface,

$$\begin{aligned}
 k_m \cdot A \cdot \frac{(T_2 - T_1)}{\Delta x} - \sigma F \epsilon A (T_1^4 - T_c^4) - k_e \cdot A \cdot \frac{(T_1 - T_c)}{D} \\
 = A \cdot \Delta x \rho C_p \frac{(T_1^1 - T_1)}{2\Delta t} \quad \text{-----} \quad (8)
 \end{aligned}$$

hence,

$$T_1^1 = 2Fo ((T_2 - T_1) - (\sigma F \epsilon \frac{\Delta x}{k_m}) (T_1^4 - T_c^4) - \frac{(k_e)}{(k_m)} \frac{(\Delta x)}{D} (T_1 - T_c)) + T_1 \quad (9)$$



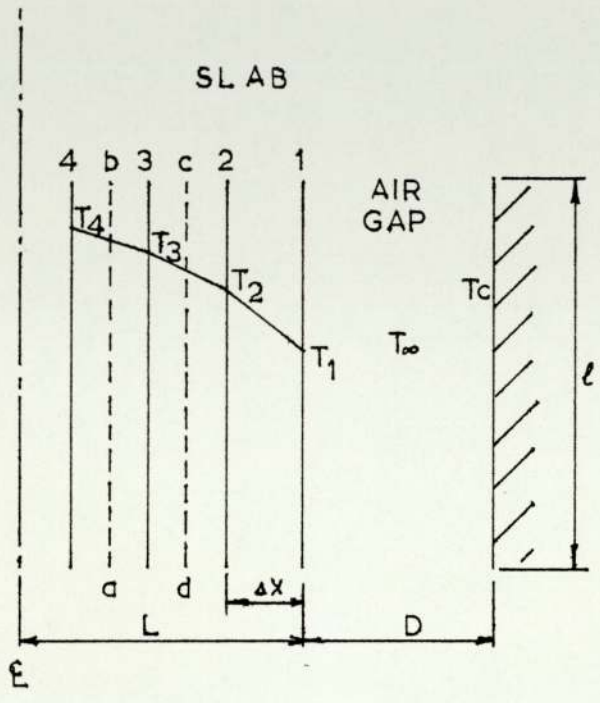


FIGURE II .1 MATHEMATICAL MODEL FOR SLAB COOLING

APPENDIX III  
TABLE OF RESULTS

TABLE 1

Pressure drop across a 6.35 mm I.D. x 0.9 m plain copper tube

WATER FLOW RATE (LITRES/MINUTE)	PRESSURE DROP MEASURED USING AN INVERTED U-TUBE MANOMETER INCLINED AT 30 DEGREES (mm H <sub>2</sub> O)
0.0	4.0
0.30	18.0
0.40	24.0
0.50	27.5
0.60	33.0
0.70	40.0
0.75	43.0
0.90	58.5
1.00	74.5
1.25	106.5
1.50	188.0
2.00	236.0



TABLE 2

Pressure drop across a 6.35 mm I.D. x 1.0 m formed copper tube

WATER FLOW RATE (LITRES/MINUTE)	PRESSURE DROP MEASURED USING AN INVERTED U-TUBE MANOMETER INCLINED AT 30 DEGREES (mm H <sub>2</sub> O)
0.0	0.0
0.3	22.5
0.4	33.5
0.5	44.0
0.6	52.0
0.7	62.5
0.8	75.0
0.9	91.0
1.0	108.5
1.2	143.5
1.4	183.0
1.6	227.0
1.8	271.5
2.0	320.0
2.5	474.0

TABLE 3

Flow distribution in the heat exchanger

OVERALL WATER FLOW RATE (LITRES/MIN)	PRESSURE DROP MEASURED USING AN INVERTED U-TUBE MANOMETER INCLINED AT 30 DEGREES (mm H <sub>2</sub> O)					
	PRESSURE TAPPING NUMBERS					
	1	2	3	4	5	6
0.00	0.0	0.0	0.0	0.0	0.0	0.0
4.04 *	6.3	7.0	10.0	9.5	9.5	8.0
6.4	11.0	10.5	15.5	11.5	13.0	12.0
8.75 *	16.5	16.5	24.0	22.5	18.0	19.5
11.08	22.5	25.5	34.5	30.0	24.0	22.5
13.38 *	29.0	31.5	42.5	38.5	30.5	32.0
15.68	35.0	40.0	58.0	45.5	42.0	43.0
17.98	40.0	42.0	71.0	63.5	50.0	52.0
20.27	41.0	45.0	81.0	62.5	60.0	63.0
22.55 *	57.0	60.0	100.0	83.5	71.0	70.0
24.85	67.0	78.0	118.0	86.5	82.0	86.0
27.15	75.0	83.0	144.0	124.5	110.0	98.0
31.84	88.0	95.0	190.0	149.5	115.0	133.0
36.64	115.0	120.0	254.0	194.5	145.0	163.0
41.65	142.0	152.0	317.0	236.5	178.0	206.0
47.00 *	169.0	177.0	390.0	287.5	211.0	242.0

\* EXPERIMENTS PLOTTED

TABLE 4

Heat losses from the water circuit with heating load = 2 kW  
and overall water rate of 30 litres per minute

TIME ELAPSED (MINUTES)	AMBIENT AIR TEMPERATURE °C	WATER TEMPERATURE		THERMOMETER °C
		Cr-Al THERMOCOUPLES INLET(mV)	OUTLET(mV)	
0	18.3	0.905	0.870	-
5	18.41	0.976	0.940	-
10	18.45	1.035	1.000	25.73
15	18.54	1.095	1.050	27.17
20	18.7	1.15	1.105	28.55
25	18.75	1.20	1.155	29.80
30	18.92	1.255	1.205	31.07
35	19.05	1.298	1.245	31.94
40	19.10	1.35	1.30	33.35
45	19.14	1.41	1.35	34.05
50	19.25	1.45	1.39	35.70
55	19.25	1.50	1.44	36.80
60	19.33	1.54	1.48	37.83
65	19.35	1.59	1.52	38.87
70	19.45	1.635	1.565	39.94
75	19.53	1.675	1.61	41.00
80	19.60	1.715	1.65	41.86
85	19.65	1.76	1.68	42.85
90	19.70	1.80	1.72	43.70
95	19.72	1.83	1.76	44.56
100	19.75	1.865	1.79	45.38
105	19.85	1.90	1.83	46.34
110	19.94	1.94	1.86	47.15
115	20.00	1.975	1.895	47.95
120	20.05	2.00	1.925	48.55
125	20.11	2.03	1.95	49.25
130	20.16	2.07	1.985	50.15
135	20.20	2.09	2.00	50.62
140	20.15	2.12	2.03	51.40
145	20.18	2.15	2.06	52.16
150	20.20	2.12	2.085	52.70
155	20.22	-	2.115	53.40
160	20.26	-	2.14	54.05
165	20.35	2.215	2.165	54.66
170	20.45	2.235	2.185	55.15
175	20.52	2.255	2.21	55.70
180	20.52	2.275	2.23	56.08
185	20.60	2.295	2.25	56.80
190	20.65	2.315	2.275	57.30

contd.



TABLE 4 (Contd.)

195	20.70	2.335	2.295	57.75
200	20.66	2.355	2.315	58.30
207	20.65	2.385	2.34	58.92
210	20.73	2.395	2.35	59.20
215	20.78	2.41	2.37	59.66
220	20.87	2.43	2.385	60.08
225	20.83	2.45	2.40	60.50
230	20.89	2.465	2.42	60.96
235	20.86	2.48	2.43	61.30
240	20.90	2.50	2.45	61.71
245	20.97	2.51	2.465	62.03
250	21.05	2.53	2.48	62.44
255	21.05	2.54	2.49	62.77
260	21.05	2.555	2.505	63.00
265	21.10	2.565	2.515	63.28
270	21.10	2.58	2.53	63.55

TABLE 5

Atmospheric cooling of a plate heater with all sides  
insulated using 76 mm thick refractory

TIME ELAPSED (MINUTES)	INTERNAL ATMOSPHERIC TEMPERATURE USING A Cr-Al THERMOCOUPLE (mV)
0.5	48.75
2.5	40.00
5.0	36.50
7.5	34.1
10.0	32.2
12.5	30.8
15.0	29.5
17.5	28.5
20.0	27.5
22.5	26.5
25.0	25.7
27.5	24.9
30.0	24.2
32.5	23.5
35.0	23.0
37.5	22.4
40.0	21.8
42.5	21.3
45.0	20.8
47.5	20.4
50.0	20.0
52.5	19.5
55.0	19.1
57.5	18.7
60.0	18.4
62.5	18.0
65.0	17.6
67.5	17.4
70.0	17.1
72.5	16.8
75.0	16.5
77.5	16.25
80.0	16.0
82.5	15.7
85.0	15.5
87.5	15.2
90.0	14.85
92.5	14.6
95.0	14.4
97.5	14.2
100.0	14.0
105.0	13.5

TABLE 6

Energy recovery data with both heaters 'on' using  
a 100 mm spacer and no reflector

WATER FLOW RATE = 20 LITRES PER MINUTE  
ATMOSPHERIC TEMPERATURE = 29°C

TIME ELAPSED (MIN.)	LEFT HAND HEATER (mV)			INLET WATER TEMPERATURE ABOVE 0°C. (mV)
	4	5	6	
0	22.75	24.4	23.7	1.36
5	22.8	24.5	23.8	1.38
10	22.9	24.5	23.8	1.41
15	22.9	24.5	23.8	1.44
20	22.95	24.6	23.9	1.47
25	22.92	24.6	23.9	1.49
30	22.98	24.7	23.95	1.52
(HEATER SWITCHED 'OFF')				
35	20.87	21.72	21.77	1.52
40	18.63	18.99	19.62	1.52
(WATER TEMPERATURE THERMOCOUPLE DAMAGED)				
				WATER TEMPERATURE RISE ACROSS HEAT EXCHANGER (mV)
45	16.77	16.96	17.77	0.052
50	15.32	15.50	16.30	0.04
55	14.04	14.22	14.92	0.0325
60	13.15	13.37	14.07	0.035

(NOTE: Right hand heater supplied with similar electrical power)



TABLE 7

Energy recovery data with both heaters 'on' using a 100 mm spacer and a reflector leaving 25.4 mm gap at top and bottom

WATER FLOW RATE = 20 LITRES PER MINUTE  
 ATMOSPHERIC AIR TEMPERATURE = 23°C

TIME ELAPSED (MIN.)	LEFT HAND HEATER (mV)			INLET WATER TEMPERATURE ABOVE AMBIENT (mV)
	4	5	6	
(ELECTRICAL LOAD = 120V)				
60	5.77	6.70	6.60	0.09
65	6.14	7.09	6.99	0.10
70	6.51	7.48	7.38	0.11
75	6.94	7.93	7.83	0.13
80	7.12	8.12	8.01	0.13
85	7.40	8.41	8.31	0.14
90	7.97	8.70	8.60	0.15
95	7.93	8.96	8.87	0.16
100	8.16	9.20	9.11	0.17
105	8.37	9.42	9.34	0.18
110	8.59	9.65	9.56	0.20
115	8.81	9.89	9.80	0.21
120	9.01	10.10	10.01	0.23
125	9.20	10.30	10.22	0.25
130	9.39	10.49	10.41	0.27
140	9.74	10.87	10.79	0.30
150	10.06	11.19	11.12	0.33
160	10.35	11.51	11.44	0.33?
170	10.60	11.77	11.71	0.28?
180	10.73	11.94	11.84	0.28?
190	11.06	12.23	12.16	0.32?
200	11.31	12.47	12.41	0.37
210	11.51	12.68	12.63	0.42
220	11.66	12.84	12.81	0.45
230	11.78	12.96	12.94	0.49
240	11.93	13.12	13.10	0.52
(ELECTRICAL LOAD = 160V)				
300	19.68	21.62	21.05	0.58
310	20.28	22.21	21.64	0.67
320	20.88	22.81	22.26	0.78
330	21.38	23.3	22.74	0.87
340	23.4	25.7	24.7	1.01
350	25.2	27.4	26.4	1.15
360	26.5	28.7	27.8	1.30
370	27.4	29.4	28.6	1.45
380	28.2	30.1	29.2	1.60
390	28.8	30.8	29.9	1.76

(NOTE: Right hand heater supplied with similar electrical power)

TABLE 8

Energy recovery data using 100 mm spacers and no reflectors

WATER FLOW RATE = 30 LITRES PER MINUTE

TIME ELAPSED (MIN.)	RIGHT HAND HEATER			LEFT HAND HEATER			INLET TEMP. (mV)	OUTLET TEMP. (mV)	INLET TEMP. THERMOMETER (°C)
	1	2 (mV)	3	4	5 (mV)	6			
(ELECTRICAL LOAD = 100V x 59.2A PER HEATER)									
0	21.66	24.45	21.59	20.29	22.67	21.49	1.05	1.23	29.88
5	22.25	25.00	22.26	20.92	23.10	22.10	1.09	1.29	31.37
10	22.78	25.50	22.86	21.48	23.60	22.61	1.14	1.36	32.91
15	23.20	26.00	23.30	21.99	24.10	23.00	1.19	1.42	34.45
20	23.70	26.40	23.80	22.47	24.50	23.40	1.23	1.48	35.91
25	24.2	26.85	24.30	22.95	24.90	23.90	1.28	1.545	37.45
30	24.5	27.20	24.70	23.30	25.30	24.30	1.335	1.61	39.12
35	24.90	27.40	25.00	23.60	25.50	24.60	1.38	1.68	40.62
40	25.20	27.70	25.40	24.00	25.80	24.90	1.43	1.75	42.25
45	25.60	28.10	25.80	24.30	26.20	25.30	1.48	1.81	43.78
50	25.90	28.40	26.10	24.70	26.50	25.60	1.53	1.88	45.49
55	26.20	28.70	26.40	25.00	26.80	25.90	1.58	1.95	47.10
60	26.50	28.90	26.70	25.30	26.90	26.20	1.67	2.02	48.80
(RIGHT HAND HEATER ACCIDENTALLY SWITCHED OFF FOR THREE MINUTES)									
65	24.30	25.30	24.90	25.50	27.10	26.30	1.71	2.09	50.54
70	25.40	27.70	25.70	25.60	27.20	26.50	1.77	2.15	51.99
75	26.30	28.80	26.50	25.80	27.30	26.60	1.82	2.22	53.60
80	27.00	29.40	27.10	26.00	27.50	26.80	1.86	2.29	55.33
85	27.30	29.60	27.50	26.20	27.70	27.00	1.93	2.37	57.00
90	27.50	29.80	27.70	26.40	27.80	27.20	1.95	2.43	58.72
95	27.8	30.0	27.9	26.6	28.0	27.3	2.035	2.50	60.36
100	28.0	30.2	28.1	26.75	28.2	27.5	2.07	2.57	62.08
105	28.2	30.4	28.3	26.9	28.3	27.65	2.12	2.64	63.88
(INLET THERMOCOUPLE CHANGED - ORIGINAL SUSPECT)									
110	28.3	30.6	28.5	27.1	28.4	27.8	2.65	2.71	65.47
115	28.5	30.7	28.7	27.2	28.6	27.9	2.72	2.78	67.15
120	28.6	30.9	28.8	27.4	28.8	28.1	2.79	2.85	68.82
125	28.8	31.1	29.0	27.6	28.9	28.3	2.86	2.93	70.52
(WATER CIRCUIT TEMPERATURE REDUCED - ELECTRICAL LOAD = 120V x 67.5A)									
145	32.9	35.6	32.85	31.7	33.1	32.3	1.52	1.62	38.67
150	33.5	36.0	33.5	32.35	33.6	32.9	1.68	1.84	42.39
155	34.0	36.4	34.0	32.9	34.0	33.5	1.83	2.00	46.12
160	34.4	36.7	34.3	33.4	34.4	33.9	1.99	2.16	49.80
(N.P.L. THERMOMETER DAMAGED - FLOW STOPPED FOR TWO MINUTES)									
165	34.6	36.9	34.6	33.8	34.7	34.3	2.145	2.31	53.44
170	34.8	37.1	34.9	34.2	35.1	34.7	2.31	2.47	57.55
175	35.0	37.2	35.1	34.5	35.2	34.9	2.48	2.63	61.61
180	35.2	37.4	35.3	34.8	35.5	35.1	2.63	2.79	65.08
(ELECTRICAL LOAD = 140V x 77A PER HEATER)									
185	37.0	39.7	36.9	36.6	37.7	37.0	2.78	2.96	68.85
190	38.3	40.9	38.2	37.8	39.0	38.4	2.96	3.16	73.10



TABLE 9

Energy recovery data using 100 mm spacers and no reflectors

WATER FLOW RATE = 30 LITRES PER MINUTE

TIME ELAPSED (MIN.)	RIGHT HAND HEATER			LEFT HAND HEATER			INLET TEMP.	TEMPERATURE RISE a/c HE
	1	2	3	4	5	6		
(ELECTRICAL LOAD = 150V x 17A PER HEATER)								
0	12.11	14.12	12.28	11.03	12.71	12.07	1.08	0.07
5	12.65	14.68	12.86	11.61	13.29	12.66	1.14	0.08
10	13.17	15.20	13.42	12.16	13.85	13.24	1.125	0.08
15	13.65	15.69	13.92	12.66	14.34	13.74	1.14	0.09
(ELECTRICAL LOAD = 180V x 23A PER HEATER)								
20	14.98	17.67	15.14	14.19	16.33	15.32	1.15	0.115
25	16.43	19.25	16.46	15.68	17.98	16.80	1.18	0.135
30	17.58	20.39	17.58	16.88	19.17	18.01	1.215	0.165
35	18.51	21.23	18.52	17.85	20.06	18.97	1.25	0.165
40	19.23	21.90	19.275	18.62	20.75	19.73	1.30	0.205
45	19.89	22.53	19.98	19.32	21.40	20.43	1.34	0.235
50	20.48	23.15	20.60	19.95	21.98	21.05	1.38	0.265
55	21.02	23.65	21.16	20.49	22.46	21.57	1.43	0.295
60	21.45	24.05	21.63	20.90	22.80	21.97	1.47	0.305
65	21.84	24.40	22.05	21.28	23.20	22.34	1.52	0.335
70	22.22	24.75	22.44	21.66	23.55	22.70	1.57	0.365
75	22.52	25.00	22.75	21.98	23.80	23.05	1.62	0.375
80	22.83	25.30	23.10	22.30	24.10	23.34	1.67	0.395
85	23.70	26.40	23.80	23.15	25.00	24.15	1.72	0.425
90	24.60	27.30	24.60	23.90	25.80	24.90	1.79	0.455
95	25.30	28.00	25.30	24.55	26.40	25.50	1.87	-
100	25.80	28.45	25.85	25.0	26.80	25.95	1.89	-
105	26.25	28.90	26.30	25.50	27.20	26.40	2.02	-
110	26.7	29.30	26.80	25.90	27.60	26.80	2.04	-
(ELECTRICAL LOAD = 200V x 23.5A PER HEATER)								OUTLET TEMP.
0	27.60	29.85	27.90	27.70	29.10	28.50	1.11	1.33
5	27.70	30.00	28.00	27.80	29.25	28.60	1.20	1.425
10	27.80	30.10	28.10	27.90	29.30	28.70	1.29	1.53
15	28.00	30.20	28.20	28.10	29.40	28.80	1.38	1.63
20	28.10	30.35	28.30	28.20	29.55	28.95	1.46	1.73
25	28.20	30.45	28.40	28.30	29.65	29.05	1.54	1.83
30	28.30	30.60	28.50	28.45	29.80	29.15	1.625	1.93
35	28.40	30.70	28.60	28.55	29.90	29.25	1.70	2.025
40	28.60	30.85	28.80	28.7	30.10	29.35	1.78	2.12
(BOTH HEATERS SWITCHED 'OFF')								
45	27.00	28.10	24.40	26.80	27.60	27.50	1.85	2.10
50	24.60	25.50	25.40	24.50	25.10	25.40	1.91	2.25
55	22.45	23.20	23.60	22.37	22.48	23.30	1.97	2.32

ALL READINGS TAKEN USING Cr-Al THERMOCOUPLES IN mV



TABLE 10

Energy recovery data using 100 mm spacers and reflectors leaving  
38 mm gap at top and bottom

WATER FLOW RATE = 30 LITRES PER MINUTE

TIME ELAPSED (MIN.)	RIGHT HAND HEATER			LEFT HAND HEATER			INLET TEMP. (mV)	OUTLET TEMP. (mV)	INLET TEMP. THERMOMETER (°C)
	1	2 (mV)	3	4	5 (mV)	6			
(ELECTRICAL LOAD = 110V x 62.5A PER HEATER)									
0	26.3	29.9	26.8	24.9	27.8	26.4	1.23	1.26	30.70
5	27.0	30.5	27.6	25.7	28.5	27.2	1.28	1.32	31.98
10	27.7	31.0	28.2	26.4	29.1	27.8	1.33	1.38	33.30
15	28.3	31.5	28.7	27.0	29.45	28.4	1.385	1.44	34.67
20	28.7	32.0	29.1	27.5	29.8	28.85	1.44	1.50	36.10
25	29.1	32.4	29.6	28.0	30.25	29.2	1.50	1.56	37.45
30	29.5	32.8	30.0	28.4	30.6	29.6	1.62?	1.62	38.95
35	29.9	33.2	30.5	28.8	31.1	30.0	1.62	1.69	40.55
40	30.4	33.6	31.0	29.2	31.5	30.4	1.69	1.76	42.20
45	30.8	34.0	31.4	29.6	31.8	30.7	1.75	1.83	43.90
50	31.2	34.3	31.8	29.9	32.2	31.1	1.82	1.90	45.50
56	31.6	34.6	32.2	30.3	32.4	31.5	1.90	1.97	47.30
60	31.9	34.9	32.5	30.6	32.7	31.8	1.97	2.05	49.05
65	32.2	35.2	32.8	30.9	33.0	32.1	2.04	2.12	-
(WATER CIRCUIT TEMPERATURE REDUCED)									
75	32.7	35.6	33.4	31.5	33.5	32.7	1.08	1.215	27.75
80	33.0	35.9	33.6	31.8	33.7	32.9	1.19	1.32	29.50
85	33.2	36.1	33.9	32.10	33.9	33.2	1.30	1.42	32.55
90	33.5	36.4	34.2	32.4	34.2	33.4	1.41	1.53	35.10
95	33.7	36.7	34.4	32.6	34.4	33.7	1.52	1.64	38.30
100	33.9	36.75	34.6	32.8	34.6	33.9	1.63	1.75	40.90
105	34.1	36.9	34.8	33.0	34.8	34.1	1.73	1.85	43.15
(ELECTRICAL LOAD = 120V x 67.8A PER HEATER)									
110	35.2	38.3	35.8	34.1	36.0	35.1	1.84	1.96	45.80
115	36.2	39.2	36.7	34.8	36.7	35.9	1.93	2.07	48.30
120	36.8	39.8	37.3	35.4	37.2	36.4	2.28?	2.19	51.00
(WATER CIRCUIT TEMPERATURE REDUCED)									
135	38.1	40.9	38.6	36.6	38.2	37.5	1.135	1.20	25.80
140	38.35	41.1	38.8	36.9	38.45	37.8	1.16	1.36	29.77
145	38.6	41.4	39.1	37.15	38.7	38.0	1.465	1.525	33.60
(BOTH HEATERS SWITCHED 'OFF')									
150	34.4	35.4	35.1	32.95	33.7	33.85	1.48	1.65	37.35
155	30.6	31.5	31.6	30.3	30.3	30.75	1.60	1.73	40.00?
160	28.6	29.2	29.2	28.5	28.9	29.4	1.70	1.80	42.70
165	27.3	27.9	28.1	26.8	27.2	27.85	1.785	1.87	44.70
170	25.8	26.7	27.0	25.7	25.9	26.4	1.855	1.93	46.30
175	24.9	25.5	25.7	24.2	24.7	25.6	1.92	1.98	47.95
180	23.7	24.6	25.0	22.8	23.2	24.1	1.98	2.03	49.35
185	22.3	23.2	23.7	21.5	22.0	22.7	2.02	2.07	-
190	21.24	22.11	22.55	20.54	20.98	21.72	2.06	2.10	-
195	20.24	21.11	21.48	19.65	20.11	20.82	2.10	2.125	-
200	19.30	20.15	20.48	18.77	19.245	19.93	2.125	2.15	-



TABLE 11

Energy recovery data using 100 mm spacers and reflectors leaving  
25.4 mm gap at top and bottom

WATER FLOW RATE = 30 LITRES PER MINUTE

TIME ELAPSED (MIN.)	RIGHT HAND HEATER			LEFT HAND HEATER			INLET TEMP. (mV)	OUTLET TEMP. (mV)	INLET TEMP. THERMOMETER (°C)
	1	2 (mV)	3	4	5 (mV)	6			
(ELECTRICAL LOAD = 110V x 63.2A PER HEATER)									
0	21.7	25.6	21.8	19.93	23.4	21.62	1.09	1.09	27.51
5	23.2	27.1	23.4	21.33	24.7	22.9	1.105	1.13	28.21
10	24.6	28.3	24.8	22.6	25.8	24.2	1.14	1.17	29.00
15	25.7	29.4	26.1	23.7	26.8	25.3	1.18	1.22	30.04
20	26.8	30.2	27.1	24.6	27.7	26.3	1.22	1.265	31.07
25	27.6	30.8	28.0	25.3	28.3	27.0	1.265	1.315	32.15
30	28.3	31.4	28.6	26.0	28.9	27.7	1.31	1.37	33.47
35	28.8	32.0	29.1	26.7	29.4	28.3	1.36	1.42	34.63
40	29.3	32.5	29.6	27.2	29.7	28.8	1.415	1.48	35.85
45	29.8	33.1	30.2	27.8	30.2	29.2	1.47	1.54	37.21
50	30.3	33.5	30.8	28.2	30.7	29.6	1.53	1.60	38.61
55	30.85	34.0	31.3	28.6	31.1	30.0	1.59	1.66	40.05
60	31.3	34.4	31.8	28.9	31.5	30.4	1.65	1.73	41.58
65	31.8	34.8	32.2	29.4	31.9	30.75	1.72	1.80	43.15
70	32.2	35.2	32.7	29.8	32.2	31.2	1.78	1.865	44.71
75	32.7	35.6	33.2	30.2	32.6	31.6	1.85	1.93	46.36
80	33.1	36.0	33.6	30.6	33.0	32.0	1.92	2.01	47.96
85	33.5	36.3	34.0	31.0	33.3	32.4	1.99	2.08	49.84
(WATER CIRCUIT TEMPERATURE REDUCED)									
95	34.0	36.7	34.5	31.65	33.8	32.9	0.99	1.14	25.70
100	34.3	36.9	34.8	31.9	34.1	33.3	1.105	1.235	28.52
105	34.5	37.15	35.0	32.2	34.3	33.5	1.21	1.34	31.20
110	34.7	37.4	35.2	32.5	34.5	33.8	1.32	1.45	33.90
115	34.9	37.5	35.4	32.7	34.7	34.0	1.42	1.56	36.32
120	35.1	37.7	35.6	33.0	34.9	34.2	1.53	1.66	38.69
125	35.3	37.8	35.7	33.2	35.1	34.4	1.63	1.66	41.25
130	35.4	37.9	35.9	33.4	35.3	34.6	1.74	1.87	43.76
135	35.6	38.1	36.0	33.6	35.4	34.8	1.85	1.98	46.50
140	35.7	38.2	36.15	33.8	35.6	35.0	1.94	2.07	48.60
145	35.9	38.4	36.3	34.0	35.8	35.2	2.05	2.18	-
(WATER CIRCUIT TEMPERATURE REDUCED)									
160	36.2	38.7	36.6	34.4	36.2	35.6	1.03	1.20	26.50
165	36.3	38.8	36.75	34.6	36.3	35.8	1.15	1.32	29.50
170	36.4	38.9	36.9	34.7	36.4	35.8	1.28	1.45	32.74
175	36.5	39.0	36.9	34.8	36.4	35.9	1.41	1.58	35.94

TABLE 11 (Contd.)

(BOTH HEATERS SWITCHED 'OFF')

180	32.8	33.8	33.5	31.4	32.2	32.4	1.54	1.69	38.91
185	29.6	30.5	30.6	29.4	29.9	30.25	1.64	1.76	41.37
190	28.1	28.65	28.7	27.6	28.3	28.8	1.73	1.83	43.47
195	26.7	27.7	26.1	26.1	26.6	27.3	1.89	1.89	45.13
200	25.4	26.2	26.5	25.1	25.7	26.1	1.86	1.94	46.65
205	24.6	25.3	25.3	23.7	24.3	25.2	1.92	1.99	47.97
210	23.4	24.2	24.8	22.5	23.0	23.7	1.97	2.03	49.30
215	22.18	23.0	23.5	21.3	21.8	22.5	2.02	2.07	50.20
220	21.06	21.90	22.33	20.37	20.90	21.59	2.05	2.10	-
225	20.06	20.88	21.24	19.45	19.97	20.63	2.09	2.13	-
230	19.19	20.00	20.32	18.63	19.15	19.79	2.11	2.15	-
235	18.38	19.17	19.46	17.88	18.40	19.02	2.14	21.7	-



TABLE 12

Energy recovery data using 100 mm spacers and reflectors leaving  
19 mm gap at top and bottom

WATER FLOW RATE = 30 LITRES PER MINUTE

TIME ELAPSED (MIN.)	RIGHT HAND HEATER			LEFT HAND HEATER			INLET TEMP. (mV)	OUTLET TEMP. (mV)	INLET TEMP. THERMOMETER (°C)
	1	2 (mV)	3	4	5	6			
(ELECTRICAL LOAD = 110V x 64A PER HEATER)									
0	25.0	28.7	24.7	22.56	25.9	24.1	0.945	0.975	-
5	26.75	30.1	26.5	24.2	27.5	25.8	0.99	1.03	-
10	28.1	31.1	28.0	25.7	28.7	27.3	1.035	1.08	25.85
15	29.0	32.2	28.9	26.9	29.6	28.45	1.09	1.14	27.16
20	29.9	33.1	29.85	27.9	30.5	29.3	1.21?	1.21	28.75
25	30.9	34.0	30.8	28.7	31.3	30.0	1.27	1.275	30.26
30	31.7	34.7	31.7	29.3	32.0	30.6	1.325	1.34	31.80
35	32.45	35.3	32.4	29.8	32.5	31.2	1.38	1.42	33.45
40	33.0	35.7	33.05	30.3	32.9	31.8	1.45	1.49	35.25
45	33.6	36.2	33.6	30.8	33.3	32.2	1.485	1.565	36.97
50	34.1	36.7	34.2	31.3	33.8	32.7	1.56	1.64	38.80
55	34.5	37.1	34.7	31.8	34.2	33.2	1.635	1.72	40.74
60	34.9	37.5	35.2	32.3	34.7	33.7	1.72	1.80	42.60
(BOTH HEATERS SWITCHED 'OFF')									
65	31.4	32.2	32.0	29.6	31.0	30.8	1.78	1.87	44.41
70	28.9	29.1	29.3	27.4	28.6	28.8	1.85	1.92	45.94
75	27.05	27.6	27.9	25.9	26.3	26.9	1.905	1.96	47.29
80	25.4	26.0	26.4	24.2	25.2	25.9	1.95	2.00	48.32
85	24.5	25.1	25.25	22.72	23.3	24.25	1.99	2.03	49.24
90	22.94	23.5	24.3	21.3	21.95	22.79	2.02	2.05	49.99
95	21.56	22.24	22.88	20.1	20.71	21.49	2.05	2.075	-
100	20.35	21.03	21.57	19.01	19.59	20.33	2.07	2.09	-
105	19.28	19.95	20.44	18.06	18.61	19.32	2.09	2.11	-

TABLE 13

Energy recovery data using 100 mm spacers and reflectors leaving  
12.7 mm gap at top and bottom

WATER FLOW RATE = 30 LITRES PER MINUTE

TIME ELAPSED (MIN.)	RIGHT HAND HEATER			LEFT HAND HEATER			INLET TEMP. (mV)	OUTLET TEMP. (mV)	INLET TEMP. THERMOMETER (°C)
	1	2 (mV)	3	4	5 (mV)	6			
(ELECTRICAL LOAD = 110V x 63A PER HEATER)									
0	26.5	29.8	26.3	25.0	28.3	26.8	0.89	0.92	-
5	27.5	30.5	27.4	26.0	29.1	27.7	0.94	0.97	-
10	28.4	31.3	28.4	26.8	29.7	28.5	0.98	1.025	-
15	29.1	32.1	29.05	27.5	30.2	29.2	1.04	1.08	-
20	29.7	32.8	29.7	28.2	30.9	29.7	1.09	1.14	27.21
25	30.45	33.5	30.5	28.8	31.5	30.3	1.15	1.20	28.65
30	31.1	34.0	31.2	29.3	32.0	30.8	1.21	1.27	30.21
35	31.7	34.58	31.8	29.7	32.5	31.3	1.275	1.335	31.76
40	32.3	35.0	32.4	30.2	32.9	31.8	1.34	1.40	33.35
45	32.8	35.45	32.9	30.7	33.4	32.3	1.41	1.475	35.00
50	33.3	35.8	33.4	31.2	33.8	32.8	1.48	1.55	36.85
55	33.7	36.1	33.9	31.6	34.2	33.2	1.55	1.62	38.54
60	34.1	36.4	34.2	32.0	34.5	33.6	1.62	1.70	40.26
65	34.4	36.6	34.5	32.4	34.8	34.0	1.70	1.785	42.30
70	34.6	36.8	34.7	32.8	35.05	34.3	1.78	1.86	44.17
75	34.75	36.9	34.9	33.1	35.25	34.5	1.86	1.94	46.11
80	34.9	37.1	35.1	33.4	35.4	34.7	1.94	2.02	47.95
85	35.1	37.2	35.2	33.6	35.6	34.9	2.02	2.105	49.86
(BOTH HEATERS SWITCHED 'OFF')									
90	31.4	32.0	32.0	30.6	31.3	31.5	2.09	2.17	-
95	28.9	29.1	29.3	28.5	29.3	29.6	2.155	2.21	-
100	27.1	27.5	28.0	26.55	27.2	27.8	2.21	2.255	-
105	25.5	25.9	26.5	25.4	26.0	26.3	2.25	2.29	-
110	24.5	24.9	25.3	23.7	24.3	25.2	2.29	2.32	-

APPENDIX IV  
LIST OF REFERENCES



## LIST OF REFERENCES

1. ADAMSON, W.O.C. 'Energy use in UK Industry'  
Coal and Energy Quarterly  
Spring 1975, n4, pp.15-21
2. ALFRED, A.M. 'Appraisal of Investment Projects by  
Discounted Cash Flow' - principles  
and some short-cut techniques
3. AMERICAN WAAGNER-BIRD  
COMPANY, INC. 'Economics of Dry Coke Cooling - Based  
on a Worldwide Study, "Pay-off Time  
Below Four Years"'. (Brochure, 1975)
4. ANTONOV, V.V., et al 'Use of a Waste-Heat Boiler with Five-  
Zone Continuous Furnace in a Bar Mill'  
1973, v3, n5, pp393-396
5. APPLGATE, G. 'Heat Regeneration by Thermal Wheel'  
Conference Papers on 'Waste Heat  
Recovery'' London, 25-26 September,  
1974
6. ATKINSON, G. Ph.D. Thesis. The University of Aston  
in Birmingham, 1974.
7. BISRA REGENERATOR GROUP 'Open-Hearth Furnace Regenerators'  
Journal of the Iron and Steel Institute  
November, 1958, v190, pp254-271
8. BAAB, K.A., AND  
J.M. BLACKWOOD 'A New Interlocking Stove Checker  
Shape'. Ironmaking Proceedings. 1968,  
v27, pp47-50
9. BAAKE, R. AND  
STOLLBERG, H. Nue Hutte, 1957, v2, pp157-168
10. BEATSON, C. 'Penny-Pinching to save energy reaps a  
Handsom Bonus'. The Engineer, 22/29  
August, 1974, pp.40-41
11. BERCZYNSKI, F.A. 'Recent Improvements in Blast Furnace  
Stove Design'. Ironmaking Proceedings  
1968, v27, pp47-50
12. BLUM, H.A., LEES, B.  
AND RENDLE, L.K. 'The Prevention of Steel Stack Corrosion  
and Smut Emission with Oil-Fired Boilers'  
Journal of Institute of Fuel 1959, n4,  
pp165-171
13. BOTTERILL, J.S.M. Fluid-Bed Heat Transfer. Publ: Academic  
Press, 1975.
14. BOTTERILL, J.S.M. 'Heat Transfer to Gas-Fluidised Beds'  
Powder Technology 1970-71, v4, pp19-26
15. BOTTERILL, J.S.M. 'Progress in Fluidisation'. British  
Chemical Engineering, August 1968, v13,  
n.8.

16. BOTTERILL, J.S.M. AND BUTT, M.H.D. 'Achieving high heat transfer rates in Fluidised Beds'. British Chemical Engineering, July 1968, v13, n7, pp1000-4
17. BOTTERILL, J.S.M. AND DESAI, M. 'Limiting Factors on Gas Fluidised Bed Heat Transfer'. Powder Technology 1972, v6, pp231-38
18. BOTTERILL, J.S.M. AND SEALEY, C.J. 'Radiative Heat Transfer Between a Gas-Fluidised Bed and an Exchange Surface' British Chemical Engineering, September 1970, v15, pp1167-68
19. BRITISH STEEL CORPORATION 'Coke Plant Design'. An addendum to the report of the Coke Plant Design Study Group, 1974.
20. BROOKS, S.H. 'A Comparison of Regenerative and Recuperative Soaking Pits'. Iron and Coal Trades Review, October 1959, v179, pp457-467
21. BROWN AND MARCO Introduction to Heat Transfer. Publ: McGraw-Hill Book Co., 1951
22. BURNSIDE, W., MARSKELL, W.G. AND MILER, J.M. 'The Influence of Superheater Metal Temperature on the Acid Dew-Point of Flue Gases'. Journal of the Institute of Fuel, June 1956, v229, pp261-269
23. CARNEY, D.J., ORAVAC, J.J. AND VAN METER, E. Journal of Metallurgy, 1955, v7, pp39-50
24. CERNOCH, S. 'Thermodynamic of Waste Heat from the Combustion Products of Industrial Furnaces'. Journal of the Iron and Steel Institute, December 1969, v207, n12, pp1578-90
25. CHAPMAN, A.J. Heat Transfer 2nd Edition pp364-367
26. CHAPMAN, P.F. 'Methods of Energy Analysis'. Aspects of Energy Conversion. Proceedings of a Summer School at Lincoln College, Oxford University, July, 1975
27. CHESSHIRE, J. AND BUCKLEY, C. 'Energy Use in UK Industry'. Energy Policy, September 1976, v4, n3, pp237-254
28. CHISHOLM, D. The Heat Pipe. Publ: Mills and Boon 1971, pp123
29. COLLINS, R.D., DAWS, L.F. AND TAYLOR, J.V. BISRA Restricted Report No. SM/A/169/55 1955



30. COREY, R.C.,  
CROSS, B.J. AND  
REID W.T. 'External Corrosion of Furnace -  
Wall Tubes - II. Significance of  
Sulphate Deposits and Sulphur Tri-  
oxide in Corrosion Mechanism, 1945,  
v67, pp289-302 [part I see Reid et al  
(1945)]
31. CREASY, D.E. 'Gas Fluidisation at Pressures and  
Temperatures above Ambient'. British  
Chemical Engineering July 1971, v16,  
n7, pp605-610
32. CRELLIN, C.R. 'No. 3 Blast Furnace - Llanwern'  
Ironmaking and Steelmaking 1975,  
v2, n1, pp14-24
33. CSATHY, D. 'Evaluating Boiler Designs for Process  
Heat Recovery'. Chemical Engineering  
1967, v74, n12, pp117-124
34. DAVIDSON, J.F.,  
HARRISON, D, Editors Fluidisation Publ: Academic Press  
1971
35. DERN, J.E.: Editor Mechanical Behaviour of Materials at  
Elevated Temperatures. Publ: McGraw-Hill  
Book Co., 1961
36. DEYOE, D.P. 'Heat Recovery - Now Can the Heat Pipe  
Help?'. Ashrae Journal April 1973, v15,  
n4, pp35-38
37. DIGEST OF UK ENERGY  
STATISTICS 1976 and 1970-71
38. DRUMMOND, W.A. 'Economics of Waste Heat Recovery from  
Boiler Flue Gases'. Conference papers  
from 'Waste Heat Recovery' organised  
by the Institution of Plant Engineers,  
25-26th September 1974.
39. DUL, J. 'Performance of a Moving-Bed Heat  
Exchanger'. Heat Exchangers - Design  
and Theory Source Book by N. Afgan and  
E.V. Schlunder. Publ: Scripta Book Co.  
1974
40. EKETORP, S. AND  
BRABIA, V. 'Energy Considerations in Reduction  
Processes for Iron and Steelmaking'  
Metallurgia and Metal Forming, December  
1974, pp363-368
41. ENERGY STATISTICS A Comparison of Fuel Prices - Oil, Coal,  
Gas 1955-1970. Eurostat, Energy Special  
Number 1974
42. ESCHER, H. 'Experiences with the Escher Metallic  
Recuperator on High-Temperature Furnaces'  
Journal of the Iron and Steel Institute,  
September 1951, v169, pp39-46



43. FLUX, J.H.,  
EDWARDS, A.M. AND  
HOWARTH, H. Journal of the Iron and Steel Institute  
January 1971, v209, n1, pp19-32
44. FORSTER, V.T.,  
ARCHER, B.V. AND  
UNSWORTH, R.G. 'Development of Experimental Turbine  
Facilities for Testing Scaled Models  
in Air or Freon'. Institution of Mechan-  
ical Engineers Conference Publication 3,  
1973, pp84-93
45. FREON PRODUCT  
INFORMATION Technical Bulletins.  
B-2 Properties and Applications  
C-30 Transport Properties  
B-44 Heat Transfer Correlations
46. GABOR, J.D. 'Wall-to-Bed Heat Transfer in Fluidised  
and Packed Beds'.
47. GAS COUNCIL, THE 'A Recuperative Town Gas-Fired Furnace  
for Temperatures up to 2000°C' by  
E.A.K. Patrick and R.D. Hastie.  
The Gas Council Research Communication  
GC62, 1959
48. GIBSON, T. 'Modern Trends in Waste Heat Recovery  
Boilers'. One Day Symposium on Heat  
Transfer in Energy Conservation.  
The Institute of Chemical Engineers  
(Midlands Branch) held on 24th March  
1976 at the University of Birmingham  
Chemical Engineering Department
49. GIRVAN, E. AND  
MCKIE, R. 'Hot Slab Storage - A Technology for  
Energy Conservation'. BSC Confidential  
Report No. CEL/EP/25/75, 1975
50. GLAZKOV, P.G. AND  
KRASNOZHEN, D.E. 'Operating Experience of a Blast Furnace  
with Evaporative Cooling'. Stal in  
English, 1960, pp323-325
51. GREGSON, W. 'Waste Heat Boilers'  
Waste Heat Recovery Publ: Chapman and  
Hall Ltd., 1963
52. GUNN, D.C. 'Waste-Heat Recovery in Boilers'.  
Energy World, 1976, n24, pp2-6
53. GUPTON, P.S. AND  
KRISHER, A.S. 'Waste Heat Boiler Failures'. Chemical  
Engineering Progress, 1973, v69, n1,  
pp47-50
54. HARLOW, W.F. 'Causes of High Dew-Point Temperatures  
in Boiler Flue Gases'. Proceedings of  
the Institution of Mechanical Engineers  
1945, v151, pp293
55. HARRISON, J.L. 'Energy in the Steel Industry'. Steel  
Times, May 1975, v203, n5, pp437-438

56. HAYNES, R. Journal of the Iron and Steel Institute 1952, v170, pp149-152
57. HAZEN, F.D. 'Improved Design of Metallic Recuperator' Iron and Steel Engineer, February 1947, v24, pp59-62
58. HAZEN METTALIC RECUPERATORS Hazen Engineering Company (Brochure) 1969
59. HER MAJESTY'S STATIONARY OFFICE 'The Increased Cost of Energy - Implications for the UK Industry'. NEDO Report 1974
60. HLINKA, J.W., PUHR, F.S. AND PASCHKIS, V. 'AISE Manual for Thermal Design of Regenerators' Part I - 'Computing Manual for Open Hearth Regenerators' Part II - 'Development of the Manual'. Iron and Steel Engineer, August 1961, v38, pp59-79 & 24
61. HOLMAN, H.P. Heat Transfer 3rd Edition. Publ: McGraw-Hill Book Co. 1972
62. HOTTELL, H.C. AND SAROFIM, A.F. Radiative Transfer. Publ: McGraw-Hill Book Co. 1967
63. HOWARD, J.R. AND SANDERSON, P.R. 'Towards More Versatile Fluidised-Bed Heat Exchangers'. Applied Energy 1977, n3, pp115-125
64. HRYNISZAK, W. 'The Design of a Disc Type Regenerative Heat Exchanger Employing "Cercox" material'. Typed Notes - Date unknown (pre-1975)
65. I.H.I. JAPAN 'Report on Research, Trial Manufacturers and Applications of Freon Turbine-Driven Turbo-Refrigerating Plant'. The Japan Society of Mechanical Engineers 1968
66. ICHIKAWA, S. 'Use of Fluorocarbon Turbine in Chemical Plants'. Chemical Economy & Engineering Review October 1970, pp19-26
67. INSTITUTE OF CHEMICAL ENGINEERS - ENGINEERING PRACTICES COMMITTEE 'A Guide to Capital Cost Estimation and Notes on Project Evaluation' 1969
68. INSTITUTE OF PETROLEUM INFORMATION SERVICE Statistical Information on Estimates of World Proved Oil Reserves
69. IRON AND STEEL INDUSTRY ANNUAL STATISTICS
70. JAKOB, M. Heat Transfer VII. Publ: John Wiley & Sons 1957



71. KAY, H. 'Recuperators - Their Use and Abuse' Iron and Steel International June 1973, pp238-239
72. KRAUSE, H.H., LAVEY, A. AND REID, W.T. Trans. ASME, J.Eng. Power 1968, v90, Series A, p38
73. KUNII, D. AND LEVENSPIEL, O. Fluidisation Engineering. Publ: John Wiley and Sons Inc. 1969
74. KUNII, D., MII, T AND YOSHIDA, K. 'Temperature Effects on the Characteristics of Fluidised Beds'. Journal of Chemical Engineering of Japan 1973, v6, n1, pp100-102
75. KUNYANSKII, M. 'Waste Heat Boiler after a Limestone Kiln'. Stal in English 1969, v19, n9, pp851-853
76. LAWS, W.R. 'Reducing Fuel Costs'. Iron and Steel International April 1974, p105-113
77. LAWS, W.R. ET AL 'The Development and Testing of a Novel High-Temperature Ceramic Recuperator' Conference on Energy Recovery in Process Plants. Organised by the Institution of Mechanical Engineers, 29-31st January 1975
78. LLOYD, B.T. 'Ceramic Fibres'. Chartered Mechanical Engineer February 1972, p51.
79. LUCHTER, S. 'Power Recovery from Gas Turbines - A Review of the Limitations, and an Evaluation of the Use of "Organic" Working Fluids'. An ASME Publication No. 70-GT-113 1970
80. MATTOCKS, G.R., TURNER, D.F. AND WHALEY, H. 'Design Aspects of Glass Tank Furnace Regenerators'. Journal of the Institute of Fuel December 1966, v39, n311, pp538-548
81. MAYER, L.A. 'Why the US is in an Energy Crisis' Fortune November 1970
82. MCADAMS, W.H. Heat Transmission. Publ: McGraw-Hill, 1954
83. MCCHESENEY, H.R. 'Recovery of Heat from Metal Processing Furnaces'. Conference Papers from 'Waste Heat Recovery' organised by the Institution of Plant Engineers 25-26th September 1974
84. METALS AND MATERIALS 'The Effective use of Energy in the Metal Industries'. March 1974, v8, n3, pp165-198
85. MISRA, L.N. 'Prospects of Power Plant Cycles Using Refrigerants'. Ashrae Journal January 1972, v14, n1, pp55-59



86. MORRIS, E.J. 'Reducing Fuel Consumption of Existing Gas Fired Soaking Pits'. Confidential Report No. CEL/CE/14/74 1974
87. MULLER, P. 'Fluidised Heat Exchangers for High Temperatures'. The Brown Boveri Review October/November 1967, v54, n10/11, pp724-732
88. MYALL, M.G. 'Preliminary Performance Studies for the Incorporation of CEL Ceramic Recuperators on the Consett Works Soaking Pits'. Confidential Report No. CEL/CE/27/76 1976
89. MYALL, M.L. ET AL 'Performance Evaluation of the Llanwern Ceramic Recuperator with Cruciform Inserts'. Confidential Report No. CEL/CE/41/75 1975
90. NATIONAL ENGINEERING LABORATORIES 'Analysis, Design and Manufacture of Heat Pipes'. Course Papers Presented at NEL 19-21st June 1973
91. NICHOLLS, L.D. 'Fluidised Bed Regenerators for Brayton Cycles'. NASA Technical Memorandum No. X-71736 1975
92. OIL AND GAS JOURNAL Proved Reserves of Natural Gas - Statistical Data
93. PARKER, A. 'World Energy Resources: A Survey'. Energy Policy March 1975, v4200, pp58-66
94. PEREIRA, J.K. 'Rotary Regenerators for High-Temperature Waste Heat Recovery' BSC Confidential Report No. CEL/CE/32/76
95. POLETAVKIN, P.G., MALYUGIN, YU.S. AND GOLOVKIN, F.B. 'Results of Experimental Investigations of a High Temperature Regenerative Air Heater, with Spherical Checker Work'. Thermal Engineering, July 1972, v19, n7, pp80-85
96. PYNE, W.E. 'Fundamentals of Evaporative Stave Cooling of Furnaces'. Iron and Steel Engineer December 1973, v50, n12, pp54-57
97. RAZELOS, P., AND PASCHKIS, P. 'The Thermal Design of Blast Furnace Stove Regenerators'. Iron and Steel Engineer August 1968, v45, pp81-116
98. REAY, D.A. 'The Heat Pipe: A Review of the State of Art with Reference to Possible Applications' - Int. Res. and Dev. Co. Ltd. Research Report No. IRD70/1. January 1970.

99. REESE, J.T.,  
JONAKIN, J. AND  
CARACRISTI, V.Z. 'The Prevention of Residual Oil  
Combustion Problems by use of Low  
Excess Air and Magnesium Additive'.  
Combustion 1964, v36, n5, pp29-36
100. REID, W.T. 'Corrosion and Deposits in Combustion'  
Combustion Technology - Some Modern  
Developments. Editors : H.B. Palmer  
and J.M. Beer. Publ: 1974
101. REID, W.T.,  
COREY, R.C. AND  
CROSS, B.J. 'External Corrosion of Furnace - Wall  
Tubes-I History and Occurance'.  
Transactions ASME, Journal of Engineering  
Power 1945, v67, pp279-288. [part II  
see Corey et al (1945)]
102. RITZ, DR. 'Regerative Type Heat Exchanger'  
British Intelligence Objectives  
Sub-Committee Final Report No. 298  
1947
103. ROBINSON, C. Britain and the World Energy Crisis:  
The Outlook for the Seventies.  
Publ: Morrell January 1974
104. SAVAGE, L.H.W. AND  
BRANCKER, A.V. 'The Application of Dry-Coke Cooling  
Plants to Integrated Iron and Steel  
Works'. Journal of the Iron and Steel  
Institute February 1949, v161, pp103-117
105. SCHACK, A. 'The Theoretical Basis of Heat  
Recuperation'. Proceedings of the  
International Recuperator Conference,  
Paris, 27-28th September 1955
106. SCHNEGELSBERG, G. 'Evaporative Cooling Systems for Blast  
Furnaces'. Journal of Metals June 1974,  
v26, n6, pp19.24
107. SCHNELLER, J. AND  
HLAVACKA, V. 'High Temperature Moving Bed Regerator'  
Heat Exchangers - Design and Theory  
Source Book by N. Afgan and E.V. Schlunder  
Publ: Scripta Book Co., 1974
108. SCHOFIELD, M. 'The Regerative Gas Furnace of Siemens'  
Iron and Coal Trades Review January  
20th 1961, v182, pp143-144
109. SEGA, K. '490 kW Fluorocarbon Turbine Generator'  
Chemical Economy and Engineering Review  
March 1975, v7, n3, pp42-49
110. SEGA, K. 'Heat Recovery by Freon Turbine'  
I.H.I. Report. Pre-1974
111. SEGA, K. AND  
MIURA, T. 'Centrifugal Refrigeration Plant Driven  
by Fluorocarbon Turbine'. I.H.I.  
Engineering Review March 1969, v2,  
n2, pp12-19



112. SNIDER, K.L. 'Thermal Stability of Several Fluorocarbons'. Ashrae Journal November 1967, v9, n11, pp54-58
113. SPIERS, H.M. (Editor) Technical Data on Fuel 6th Edition, 1961. Publ: The British National Committee, World Power Conference
114. STOKER, H.S. et al Energy from Source to Use 1975
115. STREICH, H.J. AND FEELEY JR, F.G. 'Design and Operation of Process Waste-Heat Boilers'. Chemical Engineering Progress July 1972, v68, n7, pp57-63
116. SZEKELY, J. Editor 'Blast Furnace Technology' Science and Practice. Publ: 1972
117. TAFT, M. GEC Gas Turbines Limited. A private communication. December 1979
118. THRING, M.W. The Science of Flames and Furnaces Publ: Chapman and Hall, 1952
119. TIESEN, T. 'Development of Recuperative Glass Melting Furnaces'. Proc. of the first International Congress on Glass and Ceramics, Milan, September 1933.
120. TILL, J.W. Report of 44th BISRA Steelmaking Conference. May 1955
121. TRINKS, W. Industrial Furnaces vI. Publ: John Wiley and Sons, 1950
122. TRUB, I.A., et al 'Ways of using Waste-Heat Boiler Steam' Stal in English 1969, v19, n1, pp122-126
123. TUGENDHAT, G. 'Nations and their needs - World Compromise Necessary'. Financial Times, World Energy p3-4 24th September 1962
124. U.N. STATISTICAL YEARBOOK United Nations, New York, 1953, 1956 and 1974
125. UNITED STATES STEEL The Making, Shaping and Treating of Steel VIII Edition 1957
126. WEN, C.Y. AND LEVA, M. A.I.Ch.E. Journal 1956, v2, p482
127. WENDER, L. AND COOPER, G.T. A.I.Ch.E. Journal, 1958, v4, p15
128. WILLIAMS, J.N. Steam Generation. Publ: George Allen and Unwin Limited 4th Edition 1969
129. WINKWORTH, D.A. 'Design and Preliminary Evaluation of the CEL Ceramic Recuperator'. Confidential Report No. CEL/CE/25/74 1974



130. WINKWORTH, D.A. AND  
BLUNDY, R.F. 'Trends and New Developments in High  
Temperature Air Preheat Equipment'  
British Steel Corporation - Open  
Report No. PE/A/23/72
131. VREEDENBERG, H.A. Chemical Engineering Science 1960,  
v11, p274, 1958, v9, p52. J. Appl.  
Chem. (London) 1952, v2, Suppl. 1, s26
132. YAMAUTI, Z. Res. Electrotech. Lab. (Tokyo), 148,  
1924, 1927 and 250, 1929 taken from  
Hottel and Sarofim (1967)
133. YANAGIMACHI, M. 'Recent Achievement in Freon Turbine  
Studies'. Trans. Soc. Heating, Air  
Conditioning and Sanitary Engineers,  
Japan. 1968, v6, pp41-50
134. YOSHIDA, K.,  
KUNII, D. AND  
LEVENSPIEL, O. 'Heat Transfer Mechanisms between Wall  
Surface and Fluidised Bed'. International  
Journal of Heat Transfer 1969, v12,  
p529-36
135. YOSHIDA, K.,  
UENO, T. AND  
KUNII, D. 'Mechanism of Bed-Wall Heat Transfer  
in a Fluidised Bed at High Temperatures'  
Chemical Engineering Science 1974, v29,  
pp77.82
136. ZHEREBIN, B.N. et al 'Investigating Evaporative Cooling on  
a Large Blast Furnace'. Stal in English  
1966, pp175-179.